Amino Acid Transport across the Murine Blood-Brain Barrier

Dissertation

zur

Erlangung der naturwissenschaftlichen Doktorwürde (Dr. sc. nat.)

vorgelegt der

Mathematisch-naturwissenschaftlichen Fakultät

der

Universität Zürich

von

Nadine Ruderisch

aus

Deutschland

Promotionskomitee

Prof. Dr. François Verrey
Prof. Dr. Jean-Marc Fritschy
Prof. Dr. Britta Engelhardt

Zürich, 2010

„Goat net gibt's net,
so goat's net, des ka sei.“

Artur Fischer

Table of Contents

Abbreviation List.

ABC, ATP-binding cassette;
ArAA, aromatic amino acid;
ATP, adenosine triphosphate;
BBB, blood-brain barrier;
BCAA, branched-chain amino acid;
BCSFB, blood-cerebrospinal fluid barrier;
bFGF, basic fibroblast growth factor;
BMEC, brain microvascular endothelial cells;
cAMP, cyclic adenosinemonoposphate;
cGMP, cyclic guanosinemonophosphate;
CNS, central nervous system;
CO, carbon monoxide;
CSF, cerebrospinal fluid;
CVOs, circumventricular organs;
L-**D**OPA, L-3,4-dihydroxyphenylalanine / levodopa;
ECF, extracellular fluid;
GABA, γ-aminobutyric acid;
H_2S, hydrogen sulfide;
HIV, human immunodeficiency virus;
HPLC, high-pressure liquid chromatography;
HRP, horseradish peroxidase;
IQ, intelligence quotient;
ISF, interstitial fluid;
iv, intravenous;
K_m, Michaelis constant;
KO, knockout;
LC-MS, liquid chromatography-mass spectrometry;
LNAA, large neutral amino acid;
MBMECs, mouse brain microvascular endothelial cells;
mTOR, mammalian target of rapamycin
NADPH, nicotinamide adenine dinucleotide phosphate;
NMDA, N-methyl-D-aspartic acid;
NO, nitric oxide;
PBS, phosphate buffered saline;
q**P**CR, quantitative polymerase chain reaction;
m**RNA,** messenger ribonucleic acid;
SLC, solute carrier;
T_3, triiodothyronine;
T_4, thyroxine;
TCA cycle, tricarboxylic acid cycle;
TGF, transforming growth factor;
TEER, transendothelial electrical resistance;
TNF, tumor necrosis factor;
UTR, untranslated region;
V_{max}, maximal transport velocity;
WHO, World Health Organization.

1. Summary.

The brain microvascular endothelial cells (BMECs) of the blood-brain barrier (BBB) provide a diffusion barrier between blood and brain interstitial fluid (ISF). The BBB plays a role in protecting the brain from changes in the blood. Amino acid transport through the BBB is crucial for establishing and maintaining an asymmetry in amino acid concentration between blood and brain and for the distribution of drugs and diagnostic markers. Interestingly, the cerebrospinal fluid (CSF) amino acid concentration is only about 10% that of plasma, except for glutamine [1].

Characterizing the expression and localization of solute carrier (SLC) transporters is one of the first steps in understanding the mechanisms regulating BBB transendothelial transport. Our aim is to understand how the amino acid gradient is maintained by BMEC amino acid transporters.

To address this aim, we first examined which (amino acid) transporters are expressed in total at the murine BBB on the mRNA level and how their expression is affected by a short culture step [2]. By mRNA microarray analysis using freshly isolated as well as single-cultured (5 days) and co-cultured (with glial cells in non-contact) BMECs, we have shown that as much as 60% of the known amino acid transporters are expressed in BMECs. In freshly isolated, noncultured, BMECs Lat1-4F2hc is most prominently expressed, followed by the sodium-dependent amino acid transporters Taut, Snat2, Snat5, and Eaat3. Although glial coculture is often used to mimic *in vitro* the BBB *in vivo*, levels of 73% of the amino acid transporter mRNAs were strongly altered by culture. In particular, for 78% of the transporters highly expressed in noncultured BMECs down-regulation was verified by qPCR (Lat1-4F2hc, Taut, Cat-1, Xpct, Snat3, and Snat5). In contrast, y^+Lat2, xCT, and Snat1 are expressed at low levels in noncultured BMECs and are upregulated by culture.

We hypothesize that down-regulation of transporter mRNA during culture is characteristic of transporters, such as Lat1-4F2hc, mediating transendothelial amino acid transport *in vivo*. Conversely, we postulate that transporter mRNA upregulated by culture do so to serve increased cellular amino acid demands for growth.

To understand the functional organization of the BBB and the role of transporters in physiological and (neuro)pathophysiological states, many of them characterized by impaired brain amino acid concentrations, it is necessary to not only determine at the mRNA level which transporters are expressed at the BBB, but also whether the actual transporters are

expressed at the luminal and / or abluminal membranes of BMECs, and how they are regulated.

Therefore, we studied the expression of Lat1-4F2hc (Slc7a5-Slc3a2), Snat1 (Slc38a1), and Snat3 (Slc38a3) *in vivo* on mouse brain tissue sections and additionally by *in vivo* biotinylation of the mouse brain vascular lumen with subsequent Western blot analysis. By combining the results obtained by the two different approaches, we, for the first time, could show that the sodium-dependent amino acid transporter Snat3, along with the exchanger Lat1-4F2hc, is localized to both the abluminal and the luminal membranes of BMECs. Furthermore, they are subject to posttranslational modifications. For example, Snat3 expressed in the luminal membrane has been found to be highly glycosylated, suggesting the possibility that glycosylation might play a role for its luminal membrane insertion.

The finding of Snat3 present on the luminal membrane of the BBB challenges the current hypothesis that sodium-dependent amino acid transport is an exclusive feature of the abluminal membrane [1, 3-9], in a position to protect the brain from neurotoxic levels of amino acids.

We also found Snat1, another sodium-dependent transporter, localized to the luminal membrane of vascular endothelial cells, with higher expression in the bigger vessels compared to brain microvessels. Therefore, we conclude that Snat1 seems not to play a pivotal role in the differentiated endothelial cells of the BBB, which stands in agreement with the finding that Snat1-mRNA shows very low expression in noncultured BMECs [2].

Taken together, we showed expression of a high number of not characterized amino acid transporters at the BBB, as well as their differing modulation by culture, implying functional differences. We also showed the unexpected localization of secondary active transport mechanisms at the luminal membrane, facing the blood with its high amino acid levels. Therefore, to be able to better understand the BBB transportome and its role in brain amino acid homeostasis, further studies and re-thinking of current hypotheses are needed.

2. Zusammenfassung.

Mikrovasculäre Endothelzellen (BMECs) der Bluthirnschranke (BBB) bilden eine Diffusionsbarriere zwischen Blut und Interstitialflüssigkeit (ISF) des Gehirns. Die BBB schützt das Gehirn vor Veränderungen im Blut. Transport von Aminosäuren über die BBB ist ein wichtiger Schritt um die asymmetrische Aminosäurekonzentration zwischen Blut und Gehirn herzustellen und aufrechtzuerhalten. Aminosäuretransporter sind aber auch wichtig um Medikamente und diagnostische Marker im Gehirn zu verteilen. Interessanterweise ist die Aminosäurekonzentration in der Cerebrospinalflüssigkeit (CSF) nur ca. 10% die des Plasmas, mit Ausnahme von Glutamin [1].

Die Expression und Lokalisierung von "solute carrier" (SLC) Transportern zu charakterisieren ist einer der ersten Schritte um den Mechanismus zu verstehen mit dem BBB transendothelialer Transport reguliert wird. Unser Ziel ist es zu verstehen wie der bestehende Aminosäuregradient durch Aminosäuretransporter der BMECs erhalten wird.

Um dieses Ziel zu erreichen haben wir als erstes untersucht welche Transporter überhaupt in der BBB von Mäusen exprimiert sind (mRNA) und wie ihre Expression durch eine kurze Kultur der Endothelzellen beeinflusst wird [2]. Durch eine Microarray-basierte Analyse der frisch isolierten, single-kultivierten (für 5 Tage) und co-kultivierten (mit Gliazellen ohne direkten Kontakt) BMECs konnten wir zeigen dass ganze 60% der bekannten Aminosäurentransporter in BMECs exprimiert sind. In frisch isolierten, nicht-kultivierten, BMECs zeigt Lat1-4F2hc die höchste Expression, gefolgt von den Natrium-abhängigen Aminosäuretransportern Taut, Snat2, Snat5, und Eaat3. Obwohl Co-Kultur von Endothel- mit Gliazellen oft verwendet wird um *in vitro* die BBB *in vivo* nachzuahmen, wurde die Expression von 73% der Aminosäuretransporter durch die Kultur der Endothelzellen stark verändert. Es konnte durch qPCR gezeigt werden dass 78% der Transporter mit hoher Expression in nicht-kultivierten BMECs einen weit niedrigeren Expressionslevel nach der Zellkultur aufweisen (Lat1-4F2hc, Taut, Cat-1, Xpct, Snat3, and Snat5). Im Gegensatz dazu zeigen y^+Lat2, xCT, and Snat1 einen niedrigen Expressionslevel in nicht-kultivierten BMECs und eine höhere Expression nach dem Zellkulturschritt.

Unserer Hypothese folgend repräsentieren Transporter deren mRNA während der Kultur der Zellen runter-reguliert wurde solche Transporter, die *in vivo* für transendothelialen Aminosäuretransport verantwortlich sind, wie z.B. Lat1-4F2h. Im Gegensatz dazu vermuten wir dass Transporter, welche während der Kultur der Zellen hoch-reguliert wurden, dies tun um den durch das Zellwachstum erhöhten zellulären Aminosäurebedarf zu decken.

Um die funktionale Organisation der BBB und die Funktion der Transporter in physiologischen und (neuro)pathophysiologischen Bedingungen zu verstehen, welche oft durch beeinträchtigte Aminosäurekonzentrationen charakterisiert werden können, ist es wichtig neben der mRNA-Expression auch die Expression der Transporter in der luminalen und /oder abluminalen Membran der BMECs und deren Regulation zu bestimmen.

Deswegen haben wir die Expression von Lat1-4F2hc (Slc7a5-Slc3a2), Snat1 (Slc38a1), und Snat3 (Slc38a3) *in vivo* auf Gewebsschnitten von Mäusegehirnen und darüber hinaus durch *in vivo* Biotinylierung des vaskulären Lumen in Mäusegehirnen mit darauf folgender Western-Blot Analyse untersucht. Die Ergebnisse der beiden unterschiedlichen Ansätze erlaubte es uns zum ersten Mal zu zeigen dass der Natrium-abhängige Transporter Snat3, ebenso wie der Exchanger Lat1-4F2hc, auf der luminalen wie auch abluminalen Membran der BMECs lokalisiert ist. Darüber hinaus sind die Transporter Objekt posttranslationaler Modifikationen. Zum Beispiel ist luminal exprimiertes Snat3 stark glykosyliert, was die Möglichkeit eröffnet dass Glykosylierung unter Umständen für die Insertion von Snat3 in die luminale Membran wichtig ist.

Das Snat3 in der luminalen Membran der BBB zu finden ist steht im Gegensatz zu der gegenwärtige Hypothese dass Natrium-abhängiger Aminosäuretransport ausschliesslich an der abluminalen Membran stattfindet [1, 3-9], von wo aus sie das Gehirn vor neurotoxischen Aminosäureleveln schützten können.

Wir fanden auch Snat1, einen anderen Natrium-abhängigen Transporter, in der luminalen Membran von vaskulären Endothelzellen, mit einer höheren Expression in grösseren wie in Mikrovesseln. Daraus folgerten wir dass Snat1 scheinbar keine entscheidende Funktion in den differenzierten Endothelzellen der BBB zu spielen scheint, was sich mit der sehr niedrigen Snat1-mRNA Expression in nicht-kultivierten BMECs deckt [2].

Zusammengenommen haben wir gezeigt dass eine grosse Anzahl nicht-charakterisierter Aminosäuretransporter in BBB Endothelzellen exprimiert ist, und dass diese Transporter unterschiedliche Regulation durch einen Zellkulturschritt zeigen, was wiederum auf funktionelle Unterschiede schliessen lässt. Darüber hinaus haben wir überraschenderweise auch gezeigt dass sekundäraktive Transporter in der luminalen Membran lokalisiert sind, wo sie in Kontakt mit den hohen Aminosäurekonzentrationen im Blut stehen. Um das BBB Transportom und seine Funktion in der Regulation der Aminosäurehomöostase im Gehirn besser zu verstehen sind deswegen weitere Studien und ein Überdenken der gegenwärtig vorherrschenden Hypothesen erforderlich.

3. Introduction.

3.1 Progress of Neuroscience.

The human brain is the most complex tissue in the body. It mediates behaviour ranging from simple movements and sensory perception to learning and memory. It is the centre of the nervous system and the organ of mind. But still today, many of the brain's functions are poorly understood.

For a long time the heart was seen as seat of soul and intelligence, the reason why the Egyptians removed the brain during mummification and kept the heart. Still Aristotle believed that thought occurs in the heart, Hippocrates finally located all mental processes in the brain. After establishment of the significance of the brain, it took until the 1890s before Santiago Ramón y Cajal and Camillo Golgi described the brain structure and established the neuron doctrin, telling that the nervous system is made up of discrete individual cells. In the 1940s, Alan Hodgkin, Andrew Huxley, and Bernard Katz could explain that electrical activity of neurons is based on concentration gradients of ions and movement of ions through pores. This was a pivotal moment in brain science, the first realistic promise that the CNS could be understood in detail [10].

During the latter part of the 20th century neuroscience became an interdisciplinary field. This will help to be able to understand the complex structure and interactions of the brain in normal and diseased states, with the aim to develop new therapeutic drugs. It is now well accepted that the brain can not just be seen as an accumulation of different cell types and that the neurons are not THE brain cell. The role of brain research will further increase since people get older and an increase in brain related diseases, like Alzheimer's disease, is expected. The WHO estimates that neurological disorders will increase 12% from 2005 to 2030. Among neurological disorders, 55% is contributed by cerebrovascular disease [11]. The physiological importance of the brain is also mirrored by the fact that the brain receives 15% of the cardiac output and consumes 25% of blood glucose, but represents only 2% of total body weight [12].

3.2 The concept of a vascular blood-brain barrier.

The concept of a blood-brain barrier (BBB) arose at the turn of the 19th to 20th century with the experiments of Paul Ehrlich (1885), when it was discovered that after intravenously, intraventricular or intrathecal injection of compounds or dyes no central action or staining of the brain could be observed. In the beginning, microscopy pictures did not give a hint that the capillaries of the brain are special and so Edwin Ellen Goldmann (1909), an associate of Paul Ehrlich, favoured the glial barrier. He also concluded that the main route of CNS nutrition is via the choroid plexus. In consequence in the 1920`s scientist didn't see a role of the cerebral capillaries as a route of entry of nutrients and other essential substances. In 1933 Friedrich Karl Walter and Hugo Spatz made a clear distinction between the BBB and the blood-cerebrospinal fluid (CSF) barriers. Experiments showed that the flow of the CSF is inadequate to support the gas exchange of the brain, and so the capillaries as route of supply became accepted. It took until 1940 when Tore Broman finally was able to situate the barrier at the level of the endothelial cells. By 1960, the concept of a BBB was viewed with scepticism by many, since the very small extracellular space seen under the electron microscope offered an easy explanation of the barrier phenomenon. This concept, on the other hand, could not be based on the old physiological experiments. In the consequence, during the early 1960s differing views concerning the nature of the BBB existed simultaneously: the BBB as vascular barrier, the BBB being due to an absence of extracellular space, and barrier because of metabolic limitation. In 1970 Emanuel Levin demonstrated that the absence of extracellular space was based on an electron microscopic artefact. The concept of a vascular barrier was finally accepted based on the findings of Thomas Reese and Morris Karnovsky (1967), showing that tight junctions are present in every interendothelial cleft examined, closing off the paracellular diffusion space. [13]

3.3 Barriers of the brain.

The blood-brain barrier (BBB) and the blood-cerebrospinal fluid barrier (BCSFB) maintain brain homeostasis by keeping brain interstitial fluid (ISF)* within the physiological range, partially protected from fluctuations within the blood, to maintain optimal conditions for neuronal function. The BBB is localized at the level of brain vascular endothelial cells (see section 3.3.1), the BCSFB at the level of the epithelial cells of the choroid plexus, between

* interstitial fluid (ISF), non-vascular extracellular fluid (ECF); ISF was cited in the literature as ECF

blood and ventricular CSF. There is also a third barrier, the arachnoid epithelium, which limits and regulates the molecular exchange between blood and subarachnoid CSF [14] (see Figure 1A).

In vertebrates, the continuous inter-endothelial tight junctions were recognized as the morphological correlate of the BBB [15]. However, there are structures within the brain that lack an endothelial BBB and are collectively referred to as the circumventricular organs (CVOs) since they surround the ventricular system. These areas are located in the area postrema, lamina terminalis, subfornical organ, pineal gland [12, 16-17], organum vasculosum, median eminence, subcommissural organ [12, 17], posterior pituitary [12], and neurohypopphysis [16]. Capillaries within the CVOs are fenestrated, allowing free diffusion of proteins and solutes between the blood and CVOs [15]. Brain uptake rates for small solutes in these unprotected areas, representing less than 1% of the total cerebrovascular bed [18], exceed those of normal brain by 10- to 1,000-fold [17]. Neurons in the CVOs monitor hormones and other substances within the blood or secrete neuroendocrines into the blood [15]. They regulate autonomic nervous system and endocrine glands of the body [16]. A complex network of tight junctions connecting specialized ependymal cells (tanycytes) seal the CNS from the CVOs [15].

The endothelial cells of the choroid plexus also do not form a barrier and are fenestrated like those of the CVOs [15]. The choroid plexus is a villous structure that extends from the ventricular surface into the lumen of the four ventricles of the brain [15]. The choroid plexus consists of an extensive capillary network ensheathed by a single layer of epithelium, interconnected by tight junctions, forming a BCSFB [15]. Besides its barrier function, choroid plexus epithelial cells have a secretory function and produce the CSF that fills the ventricles and bathes the interstitium of the CNS [19].

3.3.1 The blood-brain barrier and the neurovascular unit.

The BBB in vertebrates, excluding elasmobranch fishes [20-21], is located within the endothelium of the brain (micro)vasculature [22] (see section 3.3 and 3.3.1.1). The brain endothelial cells stand in close contact to neighbouring brain cells via physical and biochemical communication influencing each others properties. The network of neuro-glio-vascular interactions (the so called neurovascular unit) is known to induce specific features of the BBB endothelial cells, like tightening the tight junctions and increasing the expression (and polarization) of transporters such as P-gp and GLUT1 [23] (see also Figure 6). The

neurovascular unit is a dynamic interface between the blood and the CNS that is involved in the regulation of blood flow and nutrient supply within the CNS [22], and in maintaining the neuronal microenvironment.

The cellular and acellular components of the neurovascular unit are namely brain capillary endothelial cells (see section 3.3.1.1), the basement membranes (section 3.3.1.2), pericytes that reside within the basement membrane (section 3.3.1.3), astrocyte foot processes that ensheath almost the entire brain capillary network (section 3.3.1.4), perivascular microglia (section 3.3.1.5), and neurons (section 3.3.1.6) [23-24].

In so far as neurovascular signaling underlies normal BBB homeostasis, disruption in these networks may trigger BBB dysfunction in CNS disease [23]. BBB dysfunction has been observed in the majority of neurological diseases, e.g. stroke, head injuries, neurodegenerative diseases, bacterial and viral meningitis, encephalitis, and HIV-1 infection [25]. Therefore it has been proposed that treating brain diseases like Alzheimer's disease should include in addition to neuroprotection also glioprotection and vasculoprotection (see Figure 5B) [23].

Figure 1: Barriers between blood and brain and the neurovascular unit.

A)

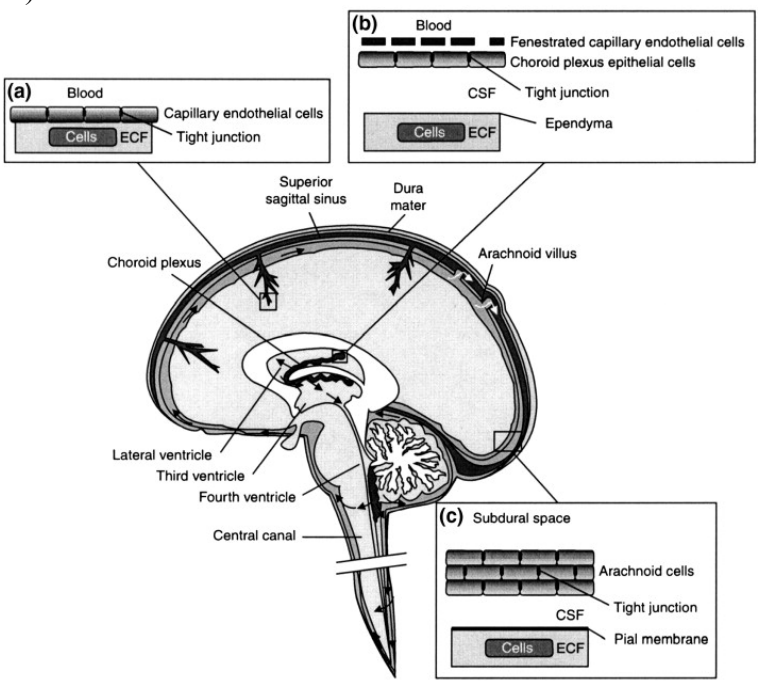

B)

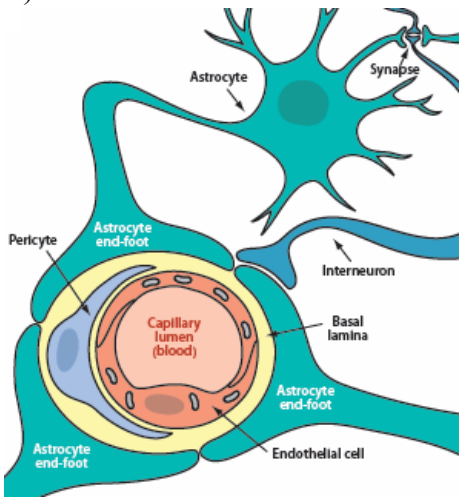

C)

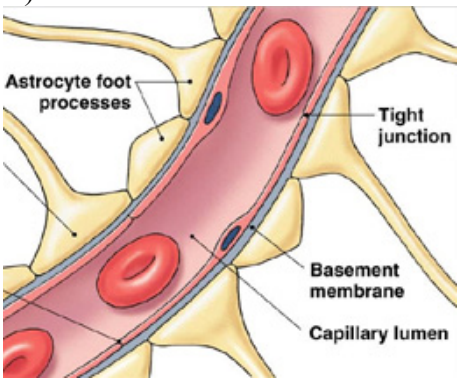

Figure legend see next page.

A) Barriers of the brain. There are three principal barrier sites between blood and brain interstitial fluid (labelled as ECF). (a) The BBB created at the level of the cerebral capillary endothelial cells by tight junction formation. It is the largest surface area for exchange and in the adult human is 12 - 18 m^2 in surface area. No brain cell is further than about 25 μm from a capillary, so once the BBB is crossed, diffusion distances to neurons and glial cell bodies are short. (b) The BCSFB lies at the choroid plexuses in the lateral, third and fourth ventricles of the brain where tight junctions are formed between the epithelial cells at the CSF-facing surface (apical) of the epithelium. (c) The arachnoid barrier. The brain is enveloped by the arachnoid membrane lying under the dura. The arachnoid is avascular but lies close to the superior sagittal sinus and is separated from it by the dura. The arachnoid is a multi-layered epithelium with tight junctions between cells of the inner layer that form an effective seal. Arachnoid villi project into the sagittal sinus through the dura and a significant amount of CSF drains into the sinus through these valve-like villi which only allow CSF movement out of the brain to blood. Source: Figure 1 from Abbott *et al.* (2009) [26]; **B)** The neurovascular unit. The mature BBB consists of close association and physical contact between endothelial cells, neurons, astrocytic endfeet, basal lamina, and pericytes. The neurovascular unit not only enables efficient cellular communication for proper brain function, such as cerebral blood flow and neurotransmission, but also drives CNS angiogenesis and barrier formation during development. Source: Figure 5a from Tam and Watts (2010) [27]; **C)** The neurovascular unit (sagittal section). Source: [28].

3.3.1.1 Endothelial cells.

Vascular system. The vascular system is diverse in structure, architecture, and physiology. An endothelium lines the entire vascular system and is composed of a monolayer of endothelial cells. In an adult, the endothelium consists of approximately 1 x 10^{13} endothelial cells forming an almost 1 kg organ [29], with a large surface of approximately 350 m^2 [30].

Vascular and neural networks share physical space, as a result of parallel anatomical distribution and development, but share also growth factors and receptors [31]. Therefore, in the adult mammalian brain angiogenesis is tightly coupled to neurogenesis [31]. In the CNS the capillaries are only about 40 μm apart [32] [33] and neuronal cell bodies are about 10 μm from the nearest capillary [14] (8-20 μm [32]), so that every neuron is virtually perfused by its own capillary [32] [33].

The principal functions of the endothelium include, in addition to it's role as a permeability barrier [29], controlling cell and nutrient trafficking [34], and the control of blood flow and blood vessel tone [29, 34]. Furthermore, the endothelium is a multifunctional paracrine and endocrine organ [29], is involved in regulation of immune responses, vasculogenesis and angiogenesis [30], as well as production of extracellular matrix components [29].

Heterogeneity. Mature cerebral capillary endothelial cells of the BBB differ from other mammalian capillary endothelial cells. Endothelial heterogeneity occurs at multiple levels, between different organs, within the same organ [20], between endothelial cells in different portions of the vascular tree [29], between macro- and microvessels, between adjacent vascular segments [20], between arterial and venous endothelial cells [20, 35], and even

between adjacent endothelial cells [30]. Cells from different individuals can vary greatly in their response to stimuli, even when obtained from the same portion of the vasculature [29].
There are different morphologic phenotypes, classified as continuous, fenestrated or discontinuous [36] (see Figure 2). Continuous endothelium lines the large vessels and forms the capillaries e.g. in the heart, lung, skeletal muscle, and brain [36-37]. Fenestrated capillaries are found within endocrine and exocrine glands, kidney and intestine [36-37], choroid plexus [36], and CVOs [22] (see section 3.3). Discontinuous endothelium is a characteristic of the liver, spleen, and bone marrow [37].
Furthermore, endothelial cells differ in size, shape, thickness, orientation with respect to the direction of blood flow, and the nature of the endothelial cell junction [34]. They are heterogeneous in gene and protein expression [34], antigenic determinants, cell surface protein expression, patterns of glycosylation, enzyme activity, and metabolic properties [37].

Determination of heterogeneity. The phenotypic heterogeneity of the endothelium is determined by a combination of genetic and environmental factors [34]. One of the important determinants of endothelial cell differentiation is the local environment, especially the interaction with surrounding cells [38]. Even small differences in expression and intracellular signaling between endothelial cells may account for large differences due to locally induced gene programs (e.g., soluble factors, cell-cell communication, synthesis and organization of matrix proteins) [34, 38]. For example, development of BBB characteristics in endothelial cells is induced by the neuroectodermal microenvironment and is not pre-determined, since non-brain vessels are able to gain BBB characteristics [22].

Functions of the BBB. Brain endothelial cells and their intercellular tight junctions form a cellular interface between the blood and the CNS. In addition to the physical permeability barrier, endothelial cells constitute a functional metabolic barrier [15]. All nutrients consumed by brain must pass this cellular barrier which at the same time protects the CNS from noxious substances in the systemic circulation [39]. Additionally, the endothelial cells affect homeostasis by adding or removing constituents from the brain interstitial space [18]. The barrier helps to keep the pools of neurotransmitters and neuroactive agents that act in the CNS and peripherally separate, so that similar agents can be used in the two systems without crosstalk [14]. Because of its large surface area (about 20 m^2 per 1.3 kg brain) and the short diffusion distance between neurons and capillaries, the endothelium has a predominant role in regulating the brain microenvironment [14].

BBB characteristics. The BBB endothelial cells differ from endothelial cells in the peripheral vasculature. Brain capillary endothelial cells are characterized by their small height, a low number of luminal caveolae [15] and cytoplasmic vesicles, a high mitochondrial content suggesting high metabolic activity [1, 22], the absence of fenestrae and an extremely low pinocytic activity inhibiting transcellular passage of molecules [15], along with specialized transport systems and complex tight junctions regulating traffic between blood and CNS [40]. Tight junctions between brain endothelial cells are the structural basis for the paracellular impermeability and high electrical resistance of the BBB endothelium [40] (see section 3.3.1.1.1). The basal lamina surrounding brain capillary endothelial cells is common with that of the perivascular astrocytic endfeet and that of the pericytes [22] (see Figure 2C and section 3.3.1.2).

There are about 400 miles of capillaries in the human brain and more than 100 billion capillaries [33] (100 million capillaries [32]). The average luminal diameter is about 4.8 μm, smaller than the diameter of an erythrocyte [18]. Endothelial cells are thin (about 0.1 μm thick), giving them a cell volume of only about 20 $\mu L/cm^3$ (1 μL/g brain) or about 0.2% of the total cell volume in brain [18, 41]. The cytoplasmic space separating the luminal (blood-facing) and abluminal (facing brain parenchyma) capillary membranes is 300-500 nm in human brain microvessels [42]. All nutrients consumed by the brain must traffic through this cellular volume and across its two membranes that have an estimated surface area of approximately 240 cm^2/cm^3 [18].

The BBB acts as anatomical as well as biochemical barrier. The metabolic barrier is maintained by expression of a high number of transport systems and enzymes [15]. Luminal and abluminal membranes of brain capillaries are biochemical, and functional, distinct [43] (see section 3.6.1.1/2; see Figure 10). This polarity is a special feature of the BBB [42]. The two membranes are characterized by asymmetric qualitative and quantitative expression differences [42]. For example, alkaline phosphatase and γ-glutamyl transpeptidase are reported as being luminal markers, whereas Na^+/K^+-ATPase and 5′-nucleotidase activities seem to be specific for the abluminal membrane [43]. Cell polarization helps to direct the transport of solutes from the luminal to the abluminal membrane and vice versa [38]. For many BBB transporters, e.g. GLUT1 (Slc2a1, see section 3.6), abluminal-luminal membrane shifts have been found, also under normal physiologic conditions [42]. But differences in the expression of GLUT1 between adjacent endothelial cells can be greater than between the luminal and abluminal membranes [42].

Figure 2: Different types of capillaries.

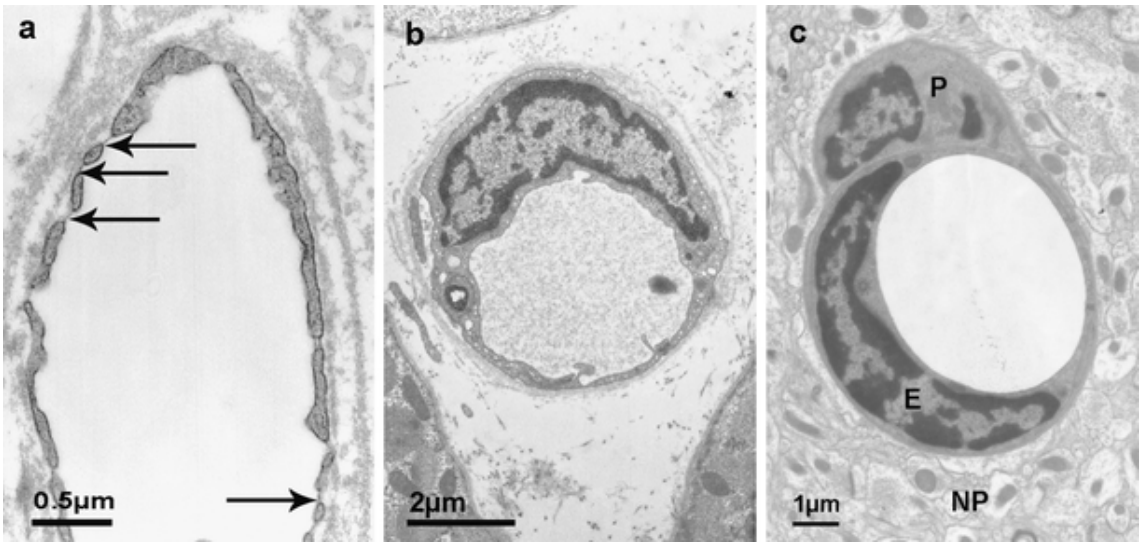

Electron micrographs of several types of blood vessels (Source: Figure 2 a, b, c from Wolburg *et al.* (2009) [22]). **a)** Fenestrated capillary of the choroid vasculature of the mouse eye. The vessel is surrounded by a thick basal lamina (arrows, some fenestration); **b)** Muscle capillary in a human biopsy. The capillary is continuous, but the space between the capillary and muscle cell is large; **c)** Brain capillary in mouse (E, endothelial cell; P, pericytes). The capillary is continuous and closely integrated within the neuropil (NP).

Localization of the BBB within the vascular tree [20]. The BBB phenotype has nearly exclusively been described in the endothelium of one particular branch of the microvascular tree, the capillary. The terms "capillaries" and "microvessels" are often used interchangeably, but the microvasculature is heterogeneous, comprised of arterioles (10-100 µm diameter), capillaries (4-10 µm), and venules (10-100 µm).

In vivo, it is known that P-gp is highly expressed in cortical capillaries, but not by intraparenchymal or meningeal arterioles and venules. Na^+/K^+-ATPase is more abundant in arteriolar endothelial cells than in capillary and venular endothelia. Furthermore, the surface biochemistry is heterogeneous and there are structural distinctions along the brain microvascular endothelium. Therefore, different branches of the brain microvasculature may respond different to specific stimuli and the BBB may actually be the function of only a specific branch of the brain microvascular tree. Another possibility is that selected aspects of the BBB are differentially expressed by specific microvascular segments, with no segment representing the BBB in its entirety.

Since *in vitro* BBB models usually represent a mixture of cells derived from different microvascular branches, together with the artefacts induced by culturing the cells (see section 3.4.2), this is probably one of the reasons why it is not possible to obtain a phenotypic, *in-vivo* like BBB model (e.g., with high TEER).

3.3.1.1.1 Tight junctions.

Endothelial (and epithelial) cells are interconnected by tight and adherens junctions [44]. Tight junctions are responsible for the polarization of the cell, separate the luminal from the abluminal membrane domain ("fence function"), and restrict the paracellular pathway between endothelial cells ("gate function") [7, 22].

The structure of the tight junction in endothelial cells of BBB capillaries has been found to be the most complex among the entire vasculature of the body [22]. The complexity of the tight junction network, the number of tight junction strands, is proposed to be logarithmically related to the transcellular electrical resistance [22]. The BBB tight junctions are highly dynamic structures and are unique among all endothelial tight junctions in that their P-face / E-face particle association ratio equals one or is slightly higher than one (1.22) [22]. This indirectly indicates a close linkage to the cytoskeleton [38]. In non-BBB endothelial cells tight junctions are almost completely associated with the E-face.

In addition, by comparing *in vivo* with *in vitro* data, the dependence of the barrier quality on the brain microenvironment, including the basal lamina, pericytes, astrocytes, and microglia, has been indicated [22]. The electrical resistance across the tight brain endothelium *in vivo* is reported to be 2,000 $\Omega \bullet cm^2$ [45] - 8,000 $\Omega \bullet cm^2$ [41, 46], in peripheral capillary endothelial cells this value is much lower, e.g. 20-30 $\Omega \bullet cm^2$ in muscle capillaries [47]. The transendothelial resistance measured in *in vitro* BBB models compared to the *in vivo* situation is much less (approximately 100-fold) [41] (see Figure 6).

The molecular components of tight junctions can be separated into different classes, the integral membrane proteins (e.g. occludin, claudins) and the adaptor proteins (e.g., ZO-1, ZO-2, ZO-3) over which the tight junctions are linked to the actin cytoskeleton [15]. Occludin and claudin family members are proteins with four transmembrane domains and two extracellular loops [22]. Occludin was the first tight junctional transmembrane molecule discovered [48]. It seems that occludin has a function in tight junction modulation via the induction of intracellular signaling rather than participating directly in the formation of tight junction strands [22-23]. In contrast, the claudins are required to establish barrier properties and are sufficient for the formation of tight junction strands [15]. At present, the claudin family contains 24 members [15], with claudin-3, claudin-12, and claudin-5 found to be expressed in the BBB. Claudin-5-deficient mice have normal tight junction morphology but exhibit size selective (<800 Da) opening of the BBB [49] (see Figure 3). In rat brain capillaries, expression of claudin-5 mRNA was found to be 751-fold greater than that of claudin-12 [50], suggesting that claudin-5 plays the key role in establishing a tight BBB.

Figure 3: The tight junctional protein claudin-5 (Cld5) is establishing a tight blood-brain barrier.

Impairment of the BBB in the Cld5$^{-/-}$ brains of 18.5-d embryos. Primary amine-reactive biotinylation reagent (443 Da) was perfused from the heart of resuscitated embryos. After 5-min incubation, sagittal frozen sections from the whole body were incubated with HRP-conjugated streptavidin. In the wild-type mouse **(a)** the reagent was completely excluded from the brain (arrow) and the spinal cord (arrowhead). In the Cld5$^{-/-}$ mouse **(a´)** the CNS showed intense peroxidase activity. Bar: 2 mm. Source: Figure 5 a, a´ from Nitta *et al.* (2003) [49].

3.3.1.2 Basement membranes.

The basement membrane at the BBB plays important roles in maintaining the capillary vessel morphology and in cell adhesion [51]. Furthermore, basement-membrane related molecules are reported to be associated with cell proliferation, extracellular proteolysis [51], and signaling properties [22]. This acellular layer separates tissue compartments, physically limits BBB permeability, and contributes to microvessel integrity and function [15].

At the level of smaller vessels (precapillary arterioles and postcapillary venules) two basement membranes can be distinguished, an endothelial cell basement membrane underlying the endothelium, and an astroglial (parenchymal) basement membrane underlying the astrocyte endfeet [15, 22]. However, in brain capillaries they fuse to form one basement membrane [15, 22]. The negatively charged basement membrane is almost as thick as the endothelial cytoplasm (in human 200 nm [42]) and is possibly involved in the movement of (charged) solutes between blood and brain extracellular fluid [52].

Endothelial and parenchymal basement membranes differ biochemically and are complex assemblies of four major glycoprotein families, namely laminins, collagen type IV isoforms, nidogens, and heparan sulphate proteoglycans [15]. Only two laminin isoforms, laminin 411 (composed of laminin α4, β1, γ1 chains) and laminin 511 (α5, β1, γ1) are found in the endothelial basal lamina [15]. In contrast, the parenchymal basement membrane contains laminin 111 (α1, β1, γ1) and laminin 211 (α2, β1, γ1) [15]. Laminin α4 and α5 are produced by brain endothelial cells, laminin α1 by leptomeningeal cells, and laminin α2 by astrocytes [15]. Collagen type IV [15] and agrin [22], an extracellular heparan sulphate proteoglycan,

have been shown to be important for structural integrity of the BBB. In another study an elevation of the TEER in *in vitro* cultured brain capillary endothelial cells by laminin and collagen type IV could be shown [53].

3.3.1.3 Pericytes.

Pericytes are the cells situated closest to the brain endothelial cells and share a common basement membrane [24] (see Figure 1B/C). Pericytes are completely surrounded by a basal lamina [22] and are located luminal to parenchymal cells [54] and abluminal to brain capillary endothelial cells, covering 20-30% of their surface [55]. There is about one pericyte for every two to four endothelial cells [56]. The distribution of pericytes and the degree of coverage of the vascular endothelium varies among different vessel types [44]. In the larger vessels (arterioles, arteries and veins), smooth muscle forms a continuous layer, replacing pericytes [14]. Pericytes form direct contacts with vascular endothelial cells *in vivo* [24] via long cytoplasmic processes along and around capillaries [44].

Function. Pericytes are thought to be local regulatory cells and important for the maintenance of homeostasis and hemostasis [54]. Reciprocal interactions between pericytes and endothelial cells play a role in angiogenesis of the nervous system, and in formation, maturation, maintenance, and regulation of normal BBB structure and function [22, 24]. Pericytes do so not only through direct contact, but also through matrix deposition and activating signals promoting endothelial cell differentiation [44]. Pericytes may also be key cells in the maintenance of the basement membrane at the BBB [51] (see section 3.3.1.2). Pericytes are multipotential stem cells in the adult brain [54], and some BBB pericytes might have the capacity to phagocytize exogenous proteins and present antigens [44]. In addition, pericytes express receptors for a number of vasoactive mediators, suggesting a role in cerebral vascular autoregulation [23]. Furthermore, pericytes have contractile capabilities and play a role in blood flow regulation by controlling the capillary diameter in response to neuronal activity [57]. Loss or injury of pericytes, leads to formation of microaneurysms and hemorrhage [23].

Pericytes-endothelial cells interactions. Due to structural proximity, bidirectional signaling between endothelial cells and pericytes [58] via direct cell-cell interaction or by release of growth factors and cytokines is possible [59].

Pericytes regulate microvascular permeability, remodelling and angiogenesis [44]. Pericyte-derived angiopoietin-1 (Ang-1) which binds to the endothelial receptor tyrosine kinase Tie-2 induces remodelling and stabilization of the vasculature and therefore decreases its permeability [60]. *In vitro* the effects of Ang-1 have been shown to occur through induction of occludin gene expression [61]. TGF-β produced by pericytes impairs the normal actin network in endothelial cells, leading to increased BBB permeability [58]. TGF-β1, however, which is likely expressed by both endothelial cells and pericytes [60], induces barrier functions by inhibiting migration and proliferation of endothelial cells and pericytes.
Platelet-derived growth factor (PDGF)-B produced by endothelial cells binds to its receptor PDGFR-β on pericytes, consequently recruiting pericytes near the endothelial cells and leading to vascular maturation [44, 60]. Pericytes migrate away from brain microvesssels in response to hypoxia or brain trauma, conditions which are associated with increased BBB permeability and disorganization of actin filaments in endothelial cells [44].
In vitro BBB models have shown significantly increased TEER values in models incorporating pericytes with endothelial cells and astrocytes, as compared to models combining only endothelial cells and astrocytes [15, 62]. This effect seems to be species dependent. Pericytes-endothelial interactions in a rat *in vitro* model showed an endothelial barrier tightening effect [24] (see Figure 6). In contrast, pericytes-endothelial interactions in a porcine *in vitro* co-culture model resulted in a decrease in barrier tightness due to increased matrix metalloproteinase (MMP)-9 secretion by the endothelial cells [59].

3.3.1.4 Astrocytes.

All vertebrates started out with a glial BBB 4-500 million years ago, and elasmobranch fishes (sharks, skates, rays) still have a glial barrier [21]. Astrocytes are the most abundant cells in the brain [63]. Anatomically, most astrocytes have stellate shapes with multiple processes [63]. Through these processes, one astrocyte can contact several neuronal synapses and cerebral blood vessels [64], making it possible to integrate signals generated from both cell types [63] (see Figure 4). The distance between the astrocyte foot process and the capillary endothelial cells and the pericytes is only 20 nm [56]. 90% [44] - >99% [39] of the abluminal surface of the cerebral microvascular endothelium is ensheated by astrocytic endfeet, a unique feature of CNS capillaries [65] (see Figure 1B/C). Astrocyte endfeet wrapping around capillary endothelial cells have a mean diameter of 4-8 μm [66]. Astrocytes each cover a territory of about 30-80 μm [66] and show a number of different morphologies, depending on

their location and association with other cell types [14]. Eight of eleven known astrocyte phenotypes specifically interact with blood vessels [14]. In the past, astrocytes were considered just glue providing physical support for neurons [63]. Today, astrocytes are known to play active roles in various brain functions [63].

Figure 4: Astrocyte processes covering vessels in 8-10 weeks old male rats.

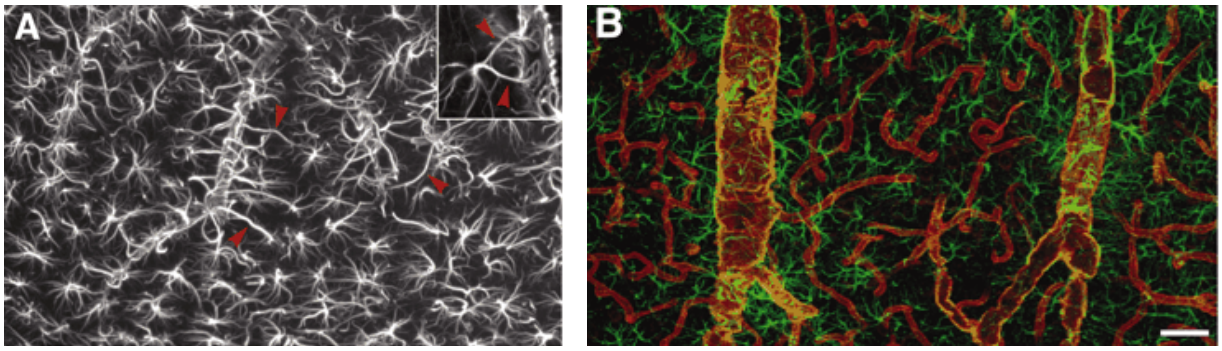

Not all vascular astrocytic endfeet processes are GFAP (glial fibrillary acidic protein) positive. **A)** GFAP immunolabeling of astrocytes in cortex. Individual astrocytes are star-shaped and distributed symmetrically, with minimal contact with neighboring astrocytes. Vascular processes differ from other processes by being straight, unbranched, and of wide diameter (red arrowheads). Inset: an astrocyte with two vascular processes; **B)** Double immunolabeling of aquaporin-4 (AQP-4; red) and GFAP (green). AQP-4 immunolabeling of astrocytes reveals that the entire network of vessels, including capillaries, is covered by astrocytic processes, albeit GFAP negative. Smaller vessels and capillaries are mostly GFAP negative but display intense AQP-4 labeling. The AQP-4 labeling reveals continuous coverage by astrocytic end feet. Source: Figure 1 A, B from Simard *et al.* (2003) [66].

Functions. It has been shown that astrocytes participate in synapse formation and function [44, 63], regulate the strength of synaptic transmission [66], and control adult neurogenesis and cerebral vascular tone [44]. Astrocytes are also involved in the maintenance and control of brain ISF's pH and ion concentrations (e.g., potassium clearance [67]), in maintaining ISF glutamate concentration low [39, 68] (see section 3.5.3.2), in nutrition of neurons [39] (e.g., glycogen stores [67]), and in the process of gliotransmission [63]. Furthermore, astrocytes function as adult neural stem cells [63].

Astrocytes are electrically nonexcitable cells that are interconnected by gap junctions allowing long-distance communication through calcium waves [66], the so called glial syncytium [67]. In cell culture, stimulation of single astrocytes resulted in expanding waves engaging >20-100 neighboring astrocytes [66]. In brain, an increase in astrocytic intracellular calcium concentrations regulates arteriole diameter [57]. Astrocytes are sensors of neuronal activity, for example responding to synaptic release of glutamate with elevations in the intracellular calcium concentration triggering the release of vasoactive compounds such as eicosanoids [64]. The calcium waves can also be transmitted to neighbouring neurons [66].

Astrocytic endfeet show a high density of AQP-4 (see Figure 4) and Kir4.1, which are involved in ion and water regulation [23], and of which the localization is dependent on the basal lamina protein agrin [14] (see section 3.3.1.2).

Astrocytes are less sensitive to glutamate excitotoxicity than neurons, they even can survive a glutamate concentration of 10 mM [67]. Ischaemic conditions are characterized by cell swelling and glutamate release in the extracellular space through reversal of glial glutamate transporters [67] (see addendum). Astrocytes showed a neuroprotective function in moderately increased extracellular glutamate concentrations but seem to amplify the damage under conditions of severe ischaemia [67].

Astrocytes show altered gene expression, hypertrophy and proliferation as response to injury, infection and degenerative diseases of the CNS, a process known as reactive astrocytosis [39].

Figure 5: Astrocytes-endothelial signaling interactions and importance of glio- and vasculoprotection.

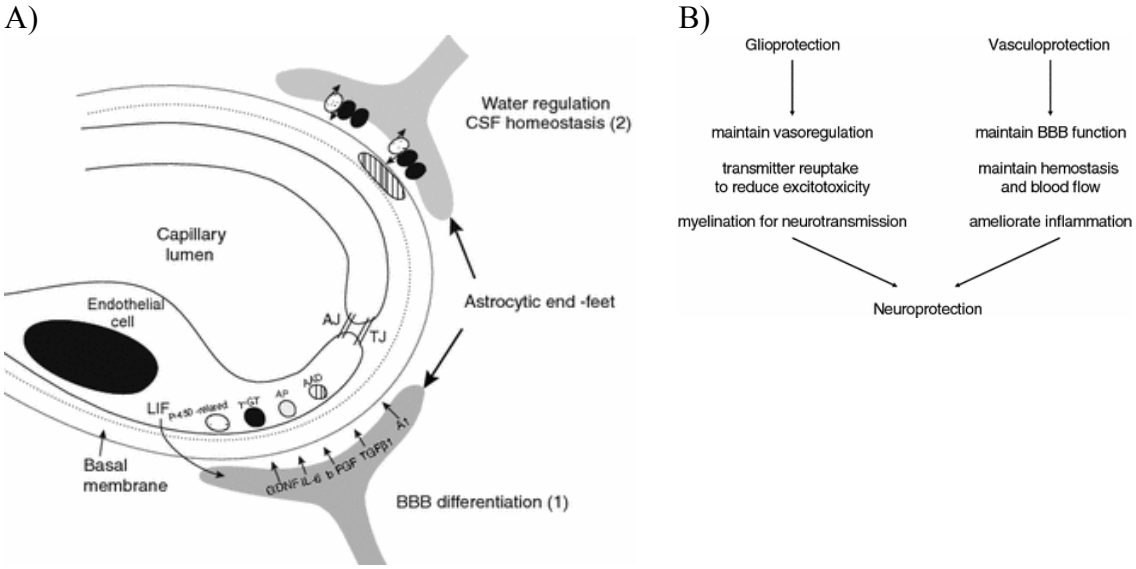

A) Astroglial-endothelial signaling interactions. Astrocytes are strongly implicated in induction of certain BBB characteristics such as tighter tight junctions, specialized enzyme systems, and polarized transporter localization (1). In addition they also play key roles in gliovascular signaling and in the regulation of brain water and electrolyte metabolism under normal and pathological conditions (2). GDNF, glial cell line-derived neurotrophic factor; IL-6, interleukin-6; bFGF, basic fibroblast growth factor; TGF-β1, transforming growth factor β1; A1, angiopoietin; LIF, leukaemia inhibitory factor; γGT, γ-glutamyl transpeptidase; AAD, aromatic acid decarboxylase; AP, alkaline phosphatase; two filled circles, AQP-4; one dashed circle, agrin; one open circle with two arrows, potassium channel Kir4.1. Source: Figure 3 from Correale and Villa (2009) [44]; **B)** Schematic for the hypothesis that true neuroprotection must be accompanied by glioprotection as well as vasculoprotection. In addition to preventing neuronal death, salvaging glial and vascular compartments should also help preserve coupling within the entire neurovascular unit that underlies functional integrity in the brain. Source: Figure 3 from Lok *et al.* (2007) [23].

Astrocytes-endothelial cells interactions. Astrocytes can be seen as mediators between endothelial cells and neuronal activity and are known to regulate BBB function [14, 25, 39, 69] (see Figure 5A). Inductive influences from astrocytes contribute to the differentiation of the specialized BBB phenotype of the brain endothelium [15], also in non-neural vascular endothelial cells [70-71]. It seems that astrocytes may play a role in barriergenesis [63], the maturation of the BBB [22, 65], rather than in angiogenesis, since the period of astrocyte differentiation coincides with that of BBB formation [63], but vessel sprouting is completed before birth [63].

Astrocytes have been reported to mediate the induction of several BBB features, for example by: (1) induction and maintenance of tight junctions, resulting in an increase of the TEER [14, 25, 44, 72]; (2) the upregulation of expression as well as polarized localization and activity of transporters (P-gp, GLUT1) [14, 44]; (3) the upregulation of expression and localization of enzyme systems [14, 44] (γ-GTP† [14, 72], alkaline phosphatase [72]); (4) the increase of neutral amino acid transport [72]; (5) an increase of Na^+/K^+-ATPase [72]; (6) the stimulation of glucose uptake [72]; (7) the correct association of endothelial cells and pericytes in tube-like structures *in vitro* [14, 72]; (8) and the modulation of endothelial differentiation [25]. Like mentioned under (4), astrocytes increase the endothelial transport of neutral amino acids, which is in the case of leucine due to increased transport efficiency [73]. Like mentioned under (6), conditioned medium from glucose-deprived astrocytes increased endothelial GLUT1 expression and glucose uptake, whereas that from normal astrocytes didn't show this effect [74].

Astrocytes secrete a large number of factors, many with matching receptors on brain endothelial cells [14] (see Table 1). Since the two cell types are separated by a basement membrane, inducing factors are likely to be small molecular weight molecules [15]. These factors, which can induce aspects of the BBB phenotype in endothelial cells *in vitro*, include TGF-β, GDNF, bFGF, and Ang-1 [14, 23, 73] (see Figure 6). For example, TGF-β1 reduces occludin gene expression in brain capillary endothelial cells [61]. Another astrocytic released factor, thrombospondin-1 (TSP-1), is known to influence both endothelial cells and neurons, for example promotes synaptogenesis and anti-angiogenesis [60]. Lee *et al.* [75] showed that SSeCKS overexpression in astrocytes triggers vessel maturation, results in tighter tight junctions and may therefore be involved in BBB barriergenesis.

Induction of the BBB phenotype is a two-way process, with endothelial cells known to enhance growth, induction and differentiation of astrocytes [14, 23]. Also the extracellular

† γ-GTP, γ -glutamyl transpeptidase

matrix is believed to contribute to the inductive communications between endothelial cells and astrocytes [14]. Astrocytic differentiation is induced by leukaemia inhibitory factor (LIF), a factor secreted by endothelial cells [14, 23, 60]. Furthermore, co-culturing astrocytes with endothelial cells results in the upregulation of antioxidative enzymes in both cell types [14, 23]. In conclusion, astrocytes upregulate the physical, transport, and metabolic barrier properties of endothelial cells, mirrored by the fact that astrocyte foot-processes facing the abluminal endothelial membrane are also polarized [42].

Table 1: Astroglial-derived factors that regulate BBB and / or epithelial barrier functions.

Barrier-disrupting factors	Barrier-inducing factors
Proinflammatory cytokines (TNF-α, IL-1β, IL-6 and MIP)	Glucocorticoids
Free radicals and nitric oxide	*S*-nitrosothiols (GSNO)
Purine nucleotides (ADP, ATP, AMP) and adenosine	Growth factors (TGFβ, basic FGF)
Platelet-activating factor, leukotrienes and prostaglandins	Neurotrophins (GDNF)
Arachidonic acid and phospholipase A2	Adrenomedullin and noradrenalin mediators
Bradykinin	Endothelin-1
Histamine	cAMP inducing mediators (VIP)
Glutamate	Secreted extracellular matrix components
Serotonin	SSeCKs/Gravin
Complement-derived peptide C3a-desArg	Regulators of membrane P-glycoprotein and toll-like receptors

Source: Table 1 from Savidge (2007) [39].

3.3.1.5 Microglia cells.

The cerebral perivascular macrophages, also named perivascular microglia, are in close contact with cerebral blood vessels [44]. They are derived from leptomeningeal mesenchymal cells or from circulating monocytes [31]. Microglia express molecules involved in antigen recognition, antigen presentation and co-stimulation [44], and can release a large number of immunoregulatory, inflammatory, and cytotoxic mediators [60]. Microglia play an essential role in the immune response and become activated in response to brain injury and immunological stimuli [76]. In the absence of pathology, the microglia are cells with small bodies and long, thin processes. During activation, microglia transform finally to a phagocytotic form. [31]

Microglia-endothelial cells interactions. Microglia are found in the perivascular space, indicating that interactions between microglia and endothelial cells play a role in BBB physiology [60]. Culture of brain capillary endothelial cells with human blood-derived macrophages has been shown to decrease paracellular permeability [44, 60]. On the other hand, microglia are a source of tumor necrosis factor (TNF)-α which is known to disrupt tight junctions [60]. In an *in vitro* BBB model in which rat brain endothelial cells were co-cultured

with microglia, Sumi *et al.* [76] showed that lipopolysaccharide (LPS) activates microglia to induce functional impairments of the endothelial barrier by producing reactive oxygen species. Oxidative stress causes BBB disruption, degradation of basement membrane proteins, and enhanced tyrosine phosphorylation of tight junction proteins [77]. Finally, microglial activation and subsequent neuroinflammation are considered to be responsible for the progression of neurodegenerative diseases like Alzheimer's- and Parkinson's disease [76].

3.3.1.6 Neurons.

Blood vessels and neurons use similar guidance cues [60] and are connected via extensive innervations [64]. In addition, astrocytes are closely located to the synaptic cleft [64]. Therefore, neuronal endings can either innervate the capillary endothelium directly or indirectly by innervating the astrocyte foot processes [23, 41]. The reciprocal interactions between blood vessels and neurons are involved in neurogenesis [23] and play essential roles for the neurovascular network and normal brain function [60]. Signaling pathways between the different cell types, the so called neurotrophic coupling, provide a specific extracellular environment for each cell type as well as for the neurovascular unit as a whole [23].

Neurons-endothelial cells interactions. The neuronal release of histamine, which transiently opens the BBB and allows the passage of growth factors and antibodies into the brain from plasma, or to sample plasma composition, is an example of direct neurovascular coupling [14, 23]. The indirect neurovascular coupling via astrocytes is exemplified by the stimulation of glucose uptake into brain via endothelial cells by histamine and ATP released by astrocytes in response to neuronal firing [14, 23] and hypoglycemic conditions [23]. Furthermore, activation of neurons in a specific brain region increases blood flow [64]. This coupling of neuronal activity to cerebral blood vessel responses is known as functional hyperemia [64], and is proposed to include a triggering of astrocyte calcium oscillations through synaptically released glutamate, which then regulates the release of vasoactive agents like nitric oxide (NO) [23] from astrocyte endfeet, leading to increased cerebrovascular blood flow [64]. Neural precursor cells (NPCs) have been shown to reduce proliferation and increase TEER of the rat BBB [78]. In addition, endothelial cells release soluble factors that stimulate proliferation of neural stem cells [23, 78] while inhibiting their differentiation [78].

3.4 Measuring transport processes across the BBB: *in vivo* and *in vitro* methods.

The lack of knowledge regarding BBB transport systems arrives mainly from the limitations of techniques available to study transport across the BBB, especially in the direction from brain to blood [79]. In addition, most of the transport studies have been performed using animal models *in vivo*, which do not enable investigation of the BBB at the cellular level [79]. Data obtained by *in vivo* methods serve as reference for *in vitro* or *in silico* data, since they have been obtained in the normal physiological brain environment. *In vitro* BBB models are commonly used to assess the permeability of new therapeutic drugs, to test their efficacy and brain penetration. A major problem in the pharmaceutical industry is that more than 98% of candidate CNS-targeting drugs show poor permeability across the BBB [80]. The development of an *in vitro* cell system that mimics the BBB *in vivo* is important to be able to understand the functional biology of the BBB and to study the direct effects of different conditions on the brain endothelium. To be valid, *in vitro* BBB models must guarantee selective permeability to molecules, high predictability and reproducibility while being fully scalable and customizable [81].

3.4.1 *In vivo* methods.

Transport polarity and its physiological significance for BBB function are difficult to study by *in vivo* techniques, since they measure at best net transendothelial flux across both membranes [82]. Thus, it is difficult to determine the individual contributions of the luminal vs. abluminal membranes. By measuring blood to brain transport, with the luminal membrane having direct access to the material injected into the vascular system, the only variables that can be measured directly are the concentration in the infusion medium and the accumulation of label in brain tissue [82].

Data interpretation is further complicated by the presence of transport systems in the choroid plexus, and the impact of endothelial cell metabolism and substrate binding on the transendothelial transport measured [82].

One important set of *in vivo* data would be measures of transport kinetics. This is very difficult, since the obtained values represent transport across two membranes in series [79] and since the artificial injection solution will mix with the plasma [82-83], therefore the measured K_m will always be higher than the actual value [83].

A promising approach is coupling of the different perfusion methods with imaging methods like autoradiography, intravital microscopy, and positron emission tomography (PET). And by using knockout (KO) animals it is possible to distinguish different transporters and their role *in vivo* [84].

Intravenous injection. To study the rate of brain penetration, the solute of interest can be administered intravenously to an animal. After, the solute concentration at different time points in brain, plasma, and CSF can be determined, reflecting their distribution between blood and brain or blood and CSF. "The method has the advantage that the system is intact, all transporters, junctional proteins, and enzymes are present at their physiological concentration, the unique architecture of the blood vessels and perivascular cells is present and undisturbed, cerebral metabolic pathways are not compromised and regulatory pathways, neuronal input, and second messenger systems have not been damaged or altered. In addition, it allows accurate incorporation of exchange and contributions of CSF and choroid plexus pathways." [85] On the other hand, the *in vivo* BBB is a very complex system and it can be difficult to determine the role of the single components. Also only limited control of the plasma levels of e.g. amino acids is possible, which makes it difficult to study the role of single transporters. The situation is further complicated by metabolism occurring in the liver and other organs. [85]

In situ perfusion. Contrary to the intravenous injection method, in the *in situ* perfusion method the animal's blood is replaced by a vascular perfusion fluid. The advantage of this method is that the solute concentration in the perfusion fluid can be altered over a large range. It is possible to characterize saturable transport, plasma protein binding and the effects of substances like hormones. Furthermore, artefacts due to metabolism in other organs are minimized since the solutes enter brain directly. On the other hand, as for the intravenous injection method, it can be difficult to determine the role of the individual components of the *in vivo* BBB. [85]

Brain efflux index. Microinjection of radioactive labeled substances and a non-permeable reference substance, e.g. inulin, directly into the brain of the animal can be used to study mechanisms of brain to blood efflux. The ratio of test substance to inulin in brain and blood is determined at different time points and expressed as brain efflux index (BEI) value. The BEI value of a solute tells how much of it is transported from brain to blood and how much is

remaining in brain. A disadvantage of this technique is that BBB damage from needle tract injections may alter BBB transport or blood flow. [85]

Intracerebral microdialysis. To perform microdialysis experiments, a semipermeable membrane with a catheter inside is implanted into the brain. Substances can be either perfused over the catheter, administered orally or intravenously. By using this method it is possible to sample the perfusate continuously, to gather concentration-time profiles, and to compare brain uptake or efflux in different brain regions. Advantages of intracerebral microdialysis include the possibility to determine the brain interstitial fluid (ISF) concentrations and to study the kinetics of solute exchange between plasma and brain ISF. Disadvantages of this technique are due to damage of the BBB and brain cell membranes due to microdialysis probe insertion which can cause overestimation of transport rates, especially for polar substances. [85]

Isolated brain capillaries. The major advantage of this method is the close similarity to *in vivo* conditions, but it also allows studying molecular events underlying endothelial cell function [84]. By using isolated microvessels it is possible to control the external substrate concentration, and to measure mainly transport from the abluminal to the luminal side [84]. But since both membranes face the compound [84], it is still difficult to distinguish the contribution of the single membranes [82]. Furthermore it is difficult to distinguish whether the substrate has actually entered the endothelial cells or is membrane bound or retained in the lumen of the capillary [82]. In addition, cells in isolated microvessels are leaky and depleted in ATP (only 5-10% of the normal cellular concentration [86]), therefore not metabolically normal [82, 86]. But the cells are still able to sustain active amino acid transport and maintain the concentration gradients of amino acids between the capillary lumen and the medium [86].

Isolated membrane vesicles. Betz *et al.* (1980) [43] for the first time isolated brain microvessel membrane vesicles. Vesicles can be used to analyse the transport properties, including the kinetics [79, 82] of luminal and abluminal membranes of the BBB separately [85] and to study the expression and activity of specific transport systems, as well as their polarized function under different conditions [85]. Vesicle studies have the advantage that conditions on both sides can be controlled, that vesicles have almost no internal metabolism eliminating the need to work with substrate analogues, that binding controls can be included, and that more studies can be performed than with intact tissues [82]. Vesicle studies have the disadvantage of working with unpure fractions, with luminal and abluminal membrane-RICH

fractions [79], distinguished based on unspecific marker proteins [87]. Therefore, corrections must be made for contamination. Further, the isolation procedure may alter the characteristics and regulation of transporters [85].

3.4.2 *In vitro* models.

In general, by performing *in vivo* studies, one cannot distinguish between different functions of the luminal and abluminal membrane in the transendothelial transport process [1]. *In vitro* models may not represent an intact *in vivo* system, e.g. the permeability of endothelial cells *in vitro* is generally greater than *in vivo* [88], but they can be used to estimate luminal to abluminal or abluminal to luminal transport. *In vitro* cell cultures have many advantages, including suitability for studying molecular mechanisms of transport in detail, and the opportunity to use human tissues, and to minimize animal studies [88]. *In vitro* models can be used to manipulate experimental conditions [88], to determine and influence BBB permeability, and to examine the effect of various normal and pathological conditions on the BBB [84]. To be valid, *in vitro* models need to fulfil a number of criteria, e.g. display a restrictive paracellular pathway [89], complex tight junctions and a "physiological relevant morphology", the functional expression of the BBB transportome, as well as a good screening capacity [84]. Youdim *et al*. [90] also mention that often underestimated physiologically relevant *in vitro* conditions can affect permeation of compounds, e.g. pH (at luminal membrane ~7.4; at abluminal membrane ~7.33), serum protein concentration (blood ~6-8% of plasma, w/v; ISF and CSF ≤1/200 of the concentration in plasma), and cellular retention. Disadvantages of using *in vitro* models include that transport [2, 80, 88] and metabolic properties of cultured cells can vary depending on whether the cells are primary cultures, passaged cell lines, or transformed cell lines [88]. Cell properties also vary depending on the number of times the cells have been passaged, and the heterogeneity of the cell line [80, 88]. It is reported that endothelial cell cultures derived from populations of larger brain microvessels (>112 μm) grow quicker than cells from capillaries. Therefore, cultures derived from mixtures of brain microvascular endothelial cells might actually represent cultures of larger cells (see also section 3.3.1.1). [20] With serial cell passage *in vitro* conditions affect the dedifferentiating process and enhance the loss of BBB characteristics [25]. Even the properties of an individual cell line may vary depending on seeding density, stage of confluency and cellular differentiation, and on the presence or absence of essential nutrients, growth factors, or associated cells [88]. Brain endothelial cells, for example, lose the BBB

phenotype in cultures in the absence of cross-talk with other members of the neurovascular unit (see section 3.3.1 and Figure 6).

Figure 6: Transendothelial electrical resistance (TEER) and endothelial permeability coefficient for sodium fluorescein (Na-F P_e) of different rat BBB *in vitro* models.

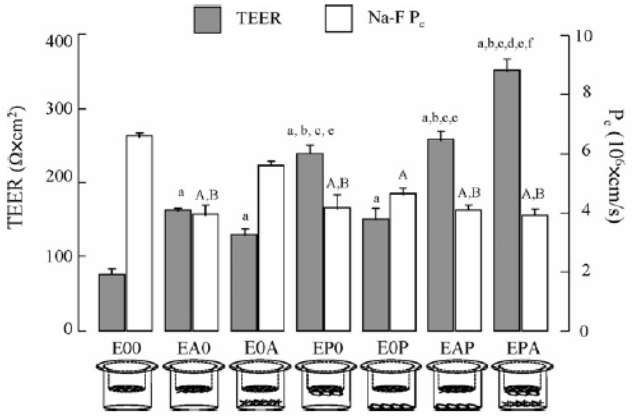

TEER expressed as Ω•cm^2, Na-F P_e, expressed in 10^{-6} cm/s. All data are presented as means ± S.E.M (n = 8). Statistically significant differences ($P < 0.05$) in TEER are indicated compared to E00 (a), EA0 (b), E0A (c), EP0 (d), E0P (e) and EAP (f), whereas these in P_e are indicated compared to E00 (A) and E0A (B), respectively. E, brain endothelial cells; A, astrocytes; P, pericytes; E00, endothelial cell monolayer; EA0, astrocyte-endothelial contact co-culture; E0A, astrocyte-endothelial non-contact co-culture; EP0, pericytes-endothelial contact co-culture; E0P, pericytes-endothelial non-contact co-culture; EAP / EPA, triple co-culture models. Source: Figure 4 from Nakagawa *et al.* (2009) [24].

Primary or low passage brain capillary endothelial cell culture. Primary cell cultures of freshly isolated cells retain many of the morphological and biochemical properties characterizing the BBB *in vivo*, including polarized expression of enzymes, transporters, and receptors, and complex tight junctions [84, 88]. Due to brain size and availability, bovine and porcine tissues have been the preferred source for brain endothelial cells, with almost as high TEER values as obtained *in vivo* [84]. Human material is, due to ethical reasons and due to constraints in obtaining large and fresh quantities, usually not an option [85]. But due to species specific differences in the transportome it remains an important source for the study of particular brain diseases and accurate prediction of drug permeability [84]. Rat *in vitro* models are of special interest since rats have extensively been used in *in vivo* studies, whereas mouse *in vitro* models offer the possibility to work with knockout and disease models [84].

The neurovascular unit has an important function in establishing BBB properties (see section 3.3.1) and therefore several approaches to mimic this influence have been used [25]. The first approach is to co-culture brain endothelial cells with primary astrocytes or glial cells (astrocytes, oligodendrocytes and microglia) [85] (see section 3.3.1.4 and Figure 6). For this purpose, the Transwell system, a bi-dimensional diffusion system where cells are cultured in contact or non-contact (on the bottom of the well), can be used [85]. A disadvantage of the

Transwell system is the irregular patterns of cell adhesion ("edge effect") which may impede the measurement of BBB permeability [25]. Another option is to use astrocyte-conditioned media, harvested from growing astrocyte cultures [25]. A third approach to mimic *in vitro* the tight *in vivo* BBB endothelium is to substitute the tissue culture medium with different factors like cAMP, and glucocorticoids, or by growing the cells on an extracellular matrix. A lack of laminin (see section 3.3.1.2), and of luminal flow (see under "three dimensional BBB models"), has been shown to lead to an increased cell cycle rate and to cause endothelial cells to "pile up in a multilayer fashion" [25].

Immortalised brain endothelial cell lines. The advantage of using immortalized cell lines is to work with a relatively consistent system [84]. On the other hand, they generally fail to generate a sufficiently restrictive paracellular barrier [89]. Also gene expression differs from that *in vivo* (b.End5) [2], and the transport function was shown to be affected, with 20% of *in vivo* glucose transport being retained (TM-BBB) [80]. The rat RBE4 cell line is the most extensively characterized immortalized brain endothelial cell line and retains the expression of many typical endothelial markers. The same is true for human cell lines such as SV-HCEC or hCMEC/D3 [84]. A murine brain endothelial cell line (cEND) is reported to form tight monolayers under influence of hydrocortisone [84].

Cell lines of non-cerebral origin. All cell lines that meet at least some of the criteria of an *in vitro* BBB permeability model can be used. The epithelial cell lines from the intestine (Caco-2) and the kidney (MDCK), as well as the ECV304 cell line, a clone of human bladder carcinoma, are currently used. These cells differ in morphology, cell-cell junctions, and gene expression compared to BBB endothelial cells. Furthermore, they lack expression of endothelial specific proteins like the vascular endothelial adherens junction protein (VE-cadherin) and the platelet-endothelial cell adhesion molecule (PECAM). [84]

Three-dimensional BBB models. Endothelial cells *in vivo* are long-lived cells which are continuously exposed to shear stress [85]. Intraluminal flow is important to maintain the BBB phenotype and is known to affect endothelial signalling pathways [89], cell differentiation, tight junction formation, and to induce metabolic changes and mitotic arrest [81]. The dynamic *in vitro* BBB model (DIV-BBB) is comprised of a hollow fibre tube that allows to co-culture brain endothelial cells (intraluminally) and glial cells (extraluminally) under flow [84]. DIV-BBBs enable maintenance of *in vivo*-like conditions, such as shear stress (4

dyn/cm^2), oxygen and glucose homeostasis [81]. Furthermore, they reduce the unstirred water layer (UWL) on the luminal side to physiological values and therefore enable measurement of *in vivo*-like permeability (passive transport)[90].

Brain slices. By using brain slices it is theoretically possible to examine the interactions between the different brain cells similar to the *in vivo* situation [85], especially the role of neuronal modulation on the BBB [84].

3.5 Role of amino acids for brain function.

3.5.1 General aspects of brain energy metabolism.

The total cerebral resting metabolic rate in adults is ~20% of the whole body metabolism, about 0.25 kcal/min [68]. Approximately 75% of the energy consumed by brain is related to signaling, the remaining 25% serves to maintain cellular activities like protein synthesis, protein degradation, and nucleotide turnover [68]. Since the brain cannot store glucose, it is dependent on a continuous supply of oxygen and energy-yielding substrates via the circulation [68]. Astrocytes account for 20% of the oxidative glucose metabolism in the human brain cortex, and are in a position to control the microenvironment of brain by transmitting signals and buffering metabolism [91] (see section 3.3.1.4). Most of the metabolic pathways in the brain are similar to those in other tissues [68]. However, the situation in the brain is more complex due to the fact that metabolism in the brain is highly compartmentalized [68]. This implies differential cellular and subcellular distribution of transporters, enzymes and metabolic pathways, requiring a coordinated function of the different cell types with intercellular trafficking of metabolites between them [91].

The rate and pathways of cerebral metabolism changes during development, starting at a high level and plateauing after maturation [68]. Glucose is essential for the developing brain and is also the most important energy-yielding substrate used by the adult brain. The brain has a respiratory quotient of 0.97, indicating that it depends almost exclusively on carbohydrate oxidation. [68] There exist large regional variations in brain glucose metabolism at rest, affected by local brain activation, suggesting a strong link between energy metabolism and brain function. [68] In addition, substrates other than glucose can provide energy for brain cells (e.g. glutamate, glutamine, lactate, fatty acids, ketone bodies). Newborns tend to be hypoglycemic but become ketotic when they begin to nurse. [68] Lactate has a special role as a readily available source of energy during the immediate postnatal period, but can also be

used in the adult human brain and is formed under both aerobic and anaerobic conditions (e.g., astrocyte-neuron lactate shuttle, see section 3.5.3). Glycogen, which is present at only low levels in brain, mainly in astrocytes [67, 92], is the only fuel store endogenous to the brain that can provide significant amounts of energy in periods during which the supply of glucose does not meet the metabolic demand [68]. Furthermore, phosphocreatine has a role in maintaining ATP levels in brain [68].

3.5.2 Amino acids in brain function and nutrition.

The brain requires continuous supply of amino acids to sustain normal cerebral development and function [93]. Amino acids play a role as building blocks of proteins and peptides and in nutrient metabolism. While the brain requires over 20 separate amino acids for normal development and function, only approximately half can be synthesized within the CNS [93] (see Table 3). Because of variations in their side chains, amino acids have different biochemical properties and functions (see Table 3). The most important gluconeogenic amino acids in humans are alanine and glutamine, accounting for 50-70% of gluconeogenesis from amino acids [94]. Along with proteinogenic amino acids, ornithine, citrulline, taurine and β-alanine also play important roles in cell metabolism [95]. Additionally, D-amino acids are present in high concentrations and fulfil specific biological functions [96]. D-serine, for example, is synthesized and metabolized endogenously and plays a role in excitatory amino acid metabolism, being a co-agonist of the NMDA receptor [96]. D-aspartate is involved in development and endocrine function [96].

The brain is dependent on a constant supply of amino acids from the periphery, but does itself not play an important quantitative role in the interorgan flux of amino acids [97]. The availability of amino acids is determined by the rate at which they appear in the plasma and the rate at which they disappear through conversion to other amino acids, breakdown, excretion, and incorporation into proteins. It was also shown that an increase in the brain content of a nonessential amino acid like glutamine can be used to promote uptake of an essential amino acid like tryptophan [98] (see section 3.6.1.1). Furthermore, the supply of essential amino acids via the plasma shows consistent fluctuations during the day, with lowest values at 12 a.m. and peaks between 4 a.m. and 8 a.m. [99].

On a molar basis, oxidation of amino acids is less efficient for ATP production than oxidation of fat and glucose. The efficiency of energy transfer from amino acids to ATP ranges from 29% for methionine to 59% for isoleucine [95]. Though not used primarily for cerebral

energy metabolism [93], amino acids can be used as carbon source and be funnelled into the TCA cycle via transamination and decarboxylation (see section 3.5.3.1). As an example, the malate-aspartate shuttle was shown to be essential to brain glucose metabolism [100].

The oxidation of amino acids by the brain for energy requires the disposal of generated ammonia [68]. The CNS lacks a complete urea cycle, therefore glutamine synthesis is the only way by which CNS cells can recycle ammonia [98]. Glutamine is not a ligand of any known neurotransmitter receptor and therefore can be viewed as a non-toxic ammonia carrier between the different CNS compartments [98].

The need of amino acids for proper brain function varies throughout development. The rapidly growing brain of an immature animal synthesizes protein at a high rate and therefore requires more amino acids from the blood than an adult brain [101]. Additionally, mouse brain utilizes ketone bodies to form amino acids [100]. Yudkoff *et al.* [100] examined the relationship between ketosis and brain amino acid metabolism in mice fed a ketogenic diet, a diet used in the management of epilepsy in children. The anti-epileptic effect of this diet is possibly due to reduced brain aspartate formation from glutamate which might then favour the synthesis of γ-aminobutyric acid (GABA) [100] (see section 3.5.3).

Amino acids play a role in the regulation of several pathways involved in gene expression and cell signaling. Regulation of gene expression by amino acids can occur at any step of transcription, translation, and post-translational modifications. Amino acids are important in cellular signalling via mTOR, cAMP, and cGMP activation pathways, as well as in generation of NO, CO, and H_2S, and therefore in endothelial function and blood flow [95].

Furthermore, amino acids participate in the regulation of cerebral osmotic and anionic balance [93] and the cellular redox state, with glutathione being the major anti-oxidant in cells [95] (see Table 3). Amino acids are also involved in hormone synthesis and secretion, e.g., insulin secretion is stimulated by glutamine, leucine, and arginine, and tyrosine is a precursor for the synthesis of epinephrine and dopamine. Furthermore, amino acids play a role in immune function and health (e.g., T-cell proliferation, B-cell maturation, and antibody production), a role which is impaired in protein deficiency [95] (see Table 3).

3.5.3 Amino acids and neurotransmission.

The three major categories of substances that act as neurotransmitters are amino acids, peptides and monoamines [102]. It was not until the 1960s and 70s that this function of amino acids was identified [13]. Amino acids can be precursors for neurotransmitters like for

serotonin, dopamine, norepinephrine and histamine, or can be neurotransmitters or neuromodulators themselves (glutamate, aspartate, glycine and GABA) [93] (see Table 3). Although there are many neurotransmitters in the CNS, the peripheral nervous system has essentially only two, acetylcholine and norepinephrine [102]. All of the known amino-acid neurotransmitters are nonessential amino acids [102].

Glutamate is the most common neurotransmitter in brain and is, like aspartate, an excitatory neurotransmitter [102] (see section 3.5.3.1), while GABA is the major inhibitory neurotransmitter of the brain, occurring in 30-40% of all synapses [102]. Another, vertebrate specific, inhibitory neurotransmitter is glycine [102]. Brain function represents a dynamic balance between excitatory and inhibitory neuronal signaling, integrated in time and location within the brain [68, 103], responsible e.g. for sensory perception, motor control, and cognition [103].

Glutamate is also known to couple energy metabolism and synaptic activity, namely via induction of glucose uptake into astrocytes [104]. In response, astrocytes release lactate, the preferred energy substrate of activated neurons, and converse glutamate to glutamine [104] (see also section 3.5.3.2).

The monoamine neurotransmitter serotonin in brain represents 1-2% of body's serotonin and is synthesized from, and is therefore largely dependent on, tryptophan transported across the BBB [102] (see also section 3.5.3.3 and 3.6.1.1). In general, the synthesis of neurotransmitters in mammalian brain responds rapidly to changes in precursor availability. It has been shown that brain serotonin concentration can be increased up to 10-fold by a tryptophan-supplemented diet [102].

3.5.3.1 Glutamate/GABA-glutamine cycle.

Glutamate. In the vertebrate CNS, the nonessential amino acid glutamate functions as the predominant excitatory neurotransmitter (see section 3.5.3). 90% of the synapses in the brain utilize either glutamate or GABA as neurotransmitters [68]. Glutamate plays a critical role in synaptic maintenance and plasticity, and further contributes to learning and memory [17]. Glutamate metabolism is closely linked to the TCA cycle. The oxidation of glutamate to oxalacetate yields 12 ATP per molecule of glutamate [7]. Therefore, under hypoglycaemic conditions, the brain mobilizes glutamate as a fuel (see section 3.5.1). Under normal conditions, most free glutamate in brain is derived from glutamine and TCA cycle intermediates, but also from recycling of brain proteins [17]. Furthermore, glutamate is the

most abundant free amino acid in the brain (10,000-12,000 μmol/L [7]). However, in comparison to the levels in plasma (50-100 μmol/L [7]) and intracellular (~12,000 μmol/L [1]), the glutamate concentration in the ISF is very low (0.5-2 μmol/L [7]). The concentration of glutamate (<0.4 μmol/L [17]) and aspartate in CSF is lower than that of any other amino acid group [7]. The low ISF concentration is essential for optimal brain function [7], to maximize the signal-to-noise-ratio upon the synaptic glutamate release and to minimize the risk of excitotoxicity [105]. If ISF glutamate rises, nerve cells may be damaged due to overexcitation which is thought to play an important role in the neural damage that occurs in diseases such as trauma, stroke, epilepsy and hypoglycaemia [17]. Plasma glutamate concentrations fluctuate during the day as a result of changes in diet, metabolism and protein turnover [17] (see section 3.5.2). The BBB helps to protect the brain from these changes by limiting the passive influx of glutamate (and other polar solutes) to a level <1% of that occurring at the blood vessels of most other tissues [17] (see also section 3.5.4.1). In the brain, glutamate exists in two separate metabolic compartments located in astrocytes and neurons (see section 3.5.3.2). This compartmentation is almost absent at birth and develops in parallel with glial cells [7].

Glutamate-glutamine cycle. The best characterized example for compartmentation (see section 3.5.1) in brain is the glutamate-glutamine cycle, which couples brain energy metabolism directly to excitatory and inhibitory neurotransmission [106-107]. Glutamine is the most abundant α-amino acid in the body [106], cannot cause excitotoxicity [102] (see section 3.5.2), and flat glutamine gradients ensure controlled movement between the different CNS compartments [98] (see Table 2 and Table 3). In contrast, glutamate exhibits a very large gradient between the intracellular space and the ISF (5,000- to 10,000-fold), with low ISF concentrations [17] (see section 3.5.3.1).

During neurotransmission, nerve impulses trigger the calcium-dependent presynaptic release of glutamate [7]. Glutamate can then either bind and activate postsynaptic glutamate receptors [7] and is directly reabsorbed into neurons, or is taken up into astrocytes [91, 102]. In the latter case, conversion of glutamate to glutamine occurs, which is then transferred back to neurons for re-conversion into glutamate [91, 102] (see Figure 7). Enzymes and amino acid transporters involved in this cycle show differential distribution, with glutamine synthetase being astrocyte-specific and phosphate activated glutaminase being neuronal-specific [68]. SNAT3 (see section 3.6.1.3.2) exports glutamine from astrocytes and SNAT1 (see section 3.6.1.3.1) mediates neuronal glutamine uptake [106]. The glutamate-glutamine cycle does not

operate in a stoichiometric fashion [68]. One reason for this fact is that in astrocytes not all glutamate is converted into glutamine, there is also glutamate metabolism [68], and glutamine can be oxidized for energy [68]. Because the cycle is not stoichiometric, glutamatergic and GABAergic neurons cannot refill their neurotransmitter pools unless precursors are received from surrounding astrocytes [68].

The cycle also operates between GABAergic neurons and astrocytes and is important to maintain the GABA pool [68].

There is evidence for a glutamate-glutamine cycle inside the BBB endothelial cells [1]. This is based on the fact that endothelial cells show glutaminase activity and that the two membranes of the BBB show a polarized expression of transporters. The intracellular glutamate concentration can be increased by either sodium-dependent glutamate transport from the ISF across the abluminal membrane, or by conversion of glutamine to glutamate via glutaminase. When the intracellular glutamate concentration is higher than in plasma, facilitative transport of glutamate across the luminal membrane into blood occurs [1]. Therefore the BBB endothelial cells may play an important role in clearing the ISF of glutamate to prevent neurotoxic levels.

Figure 7: The glutamate-glutamine cycle between astrocytes and neurons.

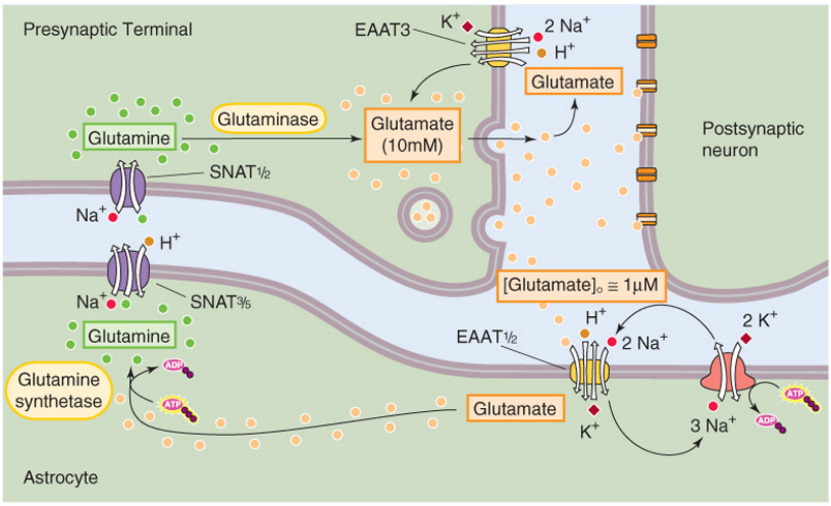

Schematic diagram of glutamate-glutamine cycles [12]. In glutamatergic neurons, glutamate and GABA (γ-aminobutyric acid) are synthesized from glucose or glutamine, which neurons themselves cannot make. Neurotransmitters released in the synaptic cleft can then interact with receptor sites. To terminate this effect, transport to astrocytes is performed with higher affinity than to neuron cells. In astrocytes there is a higher glutamine synthetase activity and glutamate and GABA are metabolized to glutamine, which has no neurotransmitter effects and can be recycled to neurons to form glutamate (in excitatory neurons) or GABA (in inhibitory neurons). [108-109]

3.5.3.2 Branched-chain (BCAA) and large neutral amino acids (LNAA).

Unlike glutamate and aspartate, lysine, arginine, and the LNAAs (except histidine; see Table 3) are essential amino acids [17]. Phenylalanine, leucine, tyrosine, tryptophan, threonine, isoleucine, valine, methionine, and histidine belong to the group of the LNAAs, whereas alanine, serine, and cysteine are small NAAs. Amino acids are further divided into BCAAs (valine, leucine, and isoleucine) and aromatic amino acids (ArAAs; phenylalanine, tryptophan, and tyrosine). [110]

BCAA uptake at the BBB exceeds that of all other amino acids. It is also reported that the uptake of valine [111], respective leucine [105], is more rapid than that of other amino acids. BCAAs participate in protein synthesis and energy production, e.g. leucine can be oxidized for energy via conversion to 3-hydroxybutyrate [68]. Furthermore, neurons can buffer excessive ISF glutamate concentrations via leucine and therefore prevent excitotoxicity [105]. The proposed BCAA shuttle between astrocytes and neurons is via transamination connected to the glutamate-glutamine cycle (see section 3.5.3.1), and 30-50% of all α-amino groups of brain glutamate and glutamine are derived from leucine [105, 112]. It has been suggested that the plasma concentrations of BCAAs may influence brain function and affect appetite, physical and mental fatigue, mental performance, physical endurance, sleep, hormonal function, blood pressure, and affective state [1] (see also section 3.5.5). BCAAs influence brain function by modifying LNAA and ArAA transport at the BBB [113], the transport of which is shared and competitive [113] (see also section 3.6.1.1). Consequently, when plasma BCAA concentrations rise they impair the entry of ArAAs, therefore implying brain synthesis of serotonin, which directly depends on the availability of tryptophan [1] (see section 3.5.3). Additionally, the synthesis and release of catecholamines (from tyrosine and phenylalanine) is reduced by reduced brain ArAA concentrations [113]. The functional effects of such changes in the neurochemical homeostasis include altered hormonal function, blood pressure, and affective state [113].

3.5.4 Different amino acid concentrations in brain ISF, CSF, and plasma.

The brain is divided into several fluid compartments with distinct properties, including the intracellular compartments, the interstitial fluid (ISF) surrounding the brain cells, the cerebrospinal fluid (CSF), and the plasma facing the lumen of the brain vasculature. This different compartments stand in constant exchange with each other.

The BBB protects the brain cells from fluctuations in the plasma amino acid concentration and determines the brain content of essential amino acids [1]. With an intact BBB, amino acids with transmitter functions have little access to the brain from blood, and there is evidence for a net efflux from the brain of glutamate and aspartate also under physiological conditions [114].

The brain ISF is a complex, dynamic microenvironment, which can buffer changes and is influenced by secretion and uptake of brain cells, homeostatic mechanisms of blood and CSF, and it is the main medium of communication between neurons [115]. Any solutes that do cross the BBB and enter the brain ISF will diffuse into the CSF and end up in the blood, therefore keeping their brain value low [116]. Once within brain ISF, solutes can move into adjacent brain areas via intercellular diffusion or via flow along the Virchow-Robin spaces [17]. The contribution of brain ISF to CSF has been estimated as 10-60% [26]. The ISF in human (~15% of total brain volume) has about twice the volume of the CSF (250-300 ml), but the rate of formation is only one-tenth of that of CSF (0.2 µl/g/min in rat). [116] The entire CSF volume is turned over completely every 4-5 h [117].

Glutamine is the dominant amino acid in the ISF, while aspartate and glutamate show the lowest concentration [115]. A concentration gradient exists between plasma and both CSF and brain ISF, and also between CSF and ISF [115], as shown in Table 2. Amino acid concentrations in the ISF are reported to be about one third the levels in CSF [115]. Amino acid levels also show several qualitative differences between these compartments [115]. ISF and CSF are formed by different tissues, the BBB and the BCSFB, respectively [26, 116, 118], which could be one explanation for the existing amino acid gradients between CSF and ISF, which also show intersubject variability [118]. The concentration of some amino acids is also influenced by their metabolism in the endothelial cells [114] and by the sink effect of brain cells [118-119]. If they take up a given amino acid at a constant rate, its ISF concentration could be lower than that in the constantly renewed CSF [118]. On the other hand, in localized regions cells may release amino acids leading to higher ISF concentrations [118]. Taken together, the CSF can not be taken as equivalent to the brain ISF [116], even if there is no anatomical barrier separating CSF and ISF [117]. Roettger and Goldfinger [118] suggested that such a barrier may be due to the ependymal surfaces and / or the toruosity within the ISF diffusion paths. To summarize, the concentration of amino acids on the abluminal side of the BBB is not directly known [119]. But since the normal direction of flow is from the brain ISF towards the CSF [116], the composition of ISF and CSF is considered to be similar [1, 118] and CSF amino acid concentration values are used as representative [119].

Table 2: Concentration ratios of amino acids and other biochemicals between different brain compartments.

		Plasma / CSF	Plasma / ISF	CSF / ISF	Tissue / ISF
Aspartate	[114]	5.8	19.9	3.4	2111‡
Glutamate	[114]	14.0	55.0	3.9	4069‡
Serine	[114]	4.0	10.0	2.5	42*
Glutamine	[114]	1.6	4.3	2.7	26*
Arginine	[114]	7.0	32.9	4.7	13*
Taurine	[114]	5.4	15.7	2.9	409°
Alanine	[114]	5.0	55.8	11.1	92*
GABA	[114]	-	-	-	2600‡
Total free amino acids	[119]	4.3			
Sodium	[119]	0.9			
Potassium	[119]	1.4			
Chloride	[119]	0.8			
Calcium	[119]	1.8			
Magnesium	[119]	0.7			
Glucose	[119]	1.3			
Protein	[119]	256.2			

There is a concentration gradient between plasma and both CSF and ISF, between CSF and ISF, and between intracellular pools and ISF (tissue / ISF). Amino acid concentrations in the ISF are about one third the levels in CSF. Qualitative differences between the compartments indicate the existence of barriers between plasma, CSF and ISF [115]. The amino acid profile in ISF differed from that of whole tissue. Three main groups of values may be defined: *amino acids with non-postulated transmitter role; ‡amino acids with known neurotransmitter roles; and °amino acids with intermediate ratio acting as neuromodulators [115]. Experiments were performed on adult Sprague-Dawley rats [115] and normal human individuals after overnight fast [120]. Tissue / ISF ratios were calculated taking the tissue density value as 1.0 [115]. ISF was cited in the literature as ECF.

The CSF is characterized by a low content of amino acids, presumably a condition necessary for neuronal sensitivity in neurotransmission. The concentrations of all naturally occurring amino acids in the CSF, with the exception of glutamine, are ~10% or less than the plasma concentrations [1] (see Figure 8). The mean total concentration of free amino acids in the CSF was found to be 826 µmol/L (± 102), glutamine being the major amino acid component (67.4%). The mean total concentration of free amino acids in plasma was found to be 3556 µmol/l (± 904). [120] Plasma is a major determinant of the CSF concentration. A low CSF / plasma concentration ratio is constant for each amino acid [120] (see Table 2 and Table 3). The CSF concentration of threonine, serine, glutamate, glutamine, glycine, methionine, leucine, tyrosine, phenylalanine, lysine, histidine, and arginine has been shown to be directly related to the plasma concentration. However, asparagine, valine, and isoleucine did not show such a relationship. [120] This indicates that the plasma amino acid concentration is not the only determinant of the CSF concentration. The differences in the concentrations of the cerebral amino acids can not be explained by the consumption of amino acids by brain [1] or the energy requirements of the various transporters [121]. As possible explanation it has been suggested that amino acids leave the brain against a concentration gradient [1]. Concerning the amino acid concentrations in plasma it has to be considered that there are differences in the profile between arterial and venous blood and that the arterial concentrations are more

representative of amino acid homeostasis [122]. Furthermore, the plasma levels differ from those of whole blood [122]. There are also gender and age differences measured, with higher concentrations of phenylalanine, proline, and ornithine in males than in females, and lower concentration of BCAAs in old than in young adults [122].

Figure 8: Comparison of CSF and plasma amino acid concentrations.

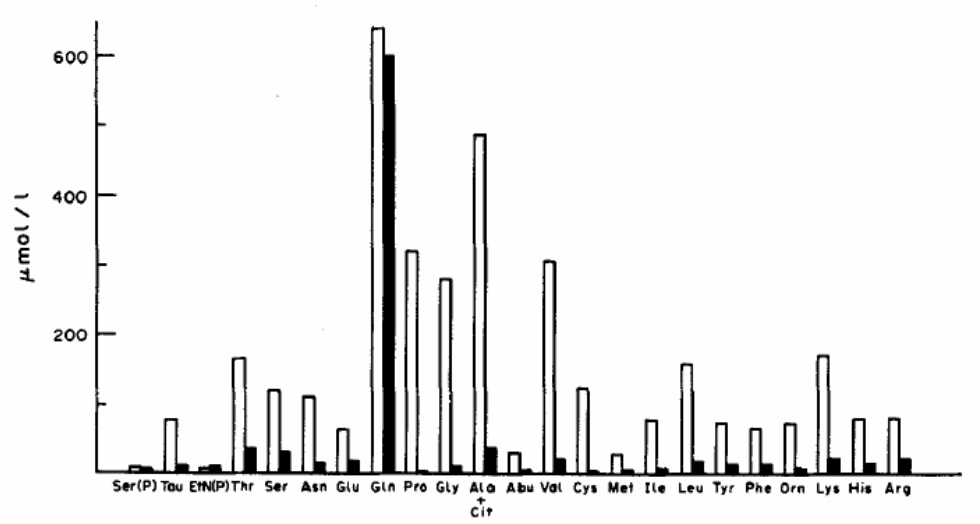

Comparison of mean normal CSF (shaded bars) and plasma (open bars) amino acid concentrations in 37 normal human individuals of both genders. Individuals were on a normal diet and lumbar CSF and blood were collected simultaneously after 16 h overnight fast. With the exception of phosphoserine, phosphoethanolamine and glutamine, mean concentrations are much higher in plasma than in CSF. Ser (P), phosphoserine; EtN (P), phosphoethanolamine; Tau, taurine; Cit, citrulline; Abu, 2-aminobutyric acid; Orn, ornithine. Source: Figure 1 from McGale *et al.* [120].

3.5.5 Diseases related to amino acid misbalance.

An optimal balance among amino acids in the diet is crucial for whole body homeostasis. Elevated amino acid levels are pathogenic factors for neurological disorders [95]. Imbalance in brain amino acid concentrations are known to occur in a number of conditions, including liver disease, diabetes, uremia and the aminoacidurias [93].

Phenylketonuria (PKU). PKU is an inborn error of amino acid metabolism that results in severe mental retardation and seizures if not treated early [110]. Classical PKU results from impaired activity of the liver enzyme phenylalanine hydroxylase (PAH) [123]. The result is a raised blood phenylalanine level and a reduction in the level of tyrosine [123]. Although PAH deficiency occurs at the hepatic level, the clinical effects of hyperphenylalaninaemia are on brain development and function [110]. Untreated patients show a progressive and irreversible neurological impairment, with low IQ levels, hyperactivity, stereotypy, aggressiveness,

anxiety, social withdrawal, a mousy odour, reduced pigmentation, reduced growth and microcephaly [110]. Since the brain phenylalanine concentration results mainly from its transport across the BBB (see section 3.6.1), the primary consequence of increased blood phenylalanine is increased brain phenylalanine [110]. The neurotoxicity of phenylalanine is enhanced by the fact that LNAA transport across the BBB by LAT1 is subject to transport competition [102, 110] (see section 3.6.1). This means that blood ratios of LNAAs and the individual affinity of LAT1 for each of them, with highest affinity for phenylalanine, determines their net uptake from blood into the brain [110]. Therefore, high plasma phenylalanine concentrations impairs uptake of the other LNAAs (tyrosine and tryptophan) into the brain [110]. Less tryptophan results in reduction of brain serotonin synthesis, less tyrosine in reduced dopamine, noradrenaline and adrenaline biosynthesis [110] (see Table 3). High brain phenylalanine concentrations have also been shown to cause a reduction in brain weight, increased myelin turnover and decreased myelin production [110]. The treatment of PKU includes a phenylalanine restricted diet [113, 123] supplemented with tyrosine [123]. PKU patients eating a normal protein diet show up to 20-times elevated plasma phenylalanine levels [113].

Maple syrup urine disease (MSUD). MSUD is a rare inherited metabolic disorder that occurs with a frequency of 1:200,000 births. Patients with MSUD exhibit a diminished BCAA metabolism due to defects in the enzyme branched-chain α-keto acid dehydrogenase. [113] As a consequence, plasma and tissue levels of the BCAAs (particularly leucine) [113] and α-ketoisocaproate [124] are greatly elevated. This causes neurotoxicity [113] and neurological dysfunctions, such as seizures, coma, psychomotor delay, and mental retardation [124]. Patients with MSUD show, besides elevated leucine levels, a depletion of glutamate and consequent reduction in the concentration of brain glutamine, aspartate, alanine, and other amino acids [105]. The result is a failure of the malate-aspartate shuttle (see section 3.5.2), a diminished metabolism and rate of protein synthesis [105]. Tetsuka *et al.* [124] suggested that aspartate efflux may be inhibited by the increased concentration of leucine in MSUD.

Nonketotic hyperglycinemia (NKH). Patients with NKH show seizures, coma and apnea, causing death in the neonatal period. In NKH an increase in the CSF / plasma glycine ratio can be observed. Lowering the plasma glycine level by using sodium benzoate leads to improved seizure control. [123]

Table 3: Overview of amino acids, their function, concentration in CSF and plasma, and their transporters from different SLC families.

Amino acids		Nutritional status in brain [4]	products	Non-protein functions [95]	CSF [µM] [4]	Plasma / CSF [4]	transported by [124]
Alanine	A	NE	directly	gluconeogenesis; transamination; glucose-A cycle	20	12	ASCT1; ASCT2; $ATB^{0,+}$ [125]; NTT4 [126]; B^0AT3/Coll [127]; B^0AT1/Coll [128]; y^+LAT2/4F2hc [129]; LAT2/4F2hc [130]; $b^{0,+}AT$/rBAT [130]; Asc1/4F2hc [129]; PAT1; PAT2; SNAT1; SNAT2; SNAT3; SNAT4
Arginine	R	E	directly	mTOR signaling; antioxidant; NH_4^+ detoxification; immunity; N reservoir; methylation and deimination of proteins	10	5	$ATB^{0,+}$ [125]; CAT-1 [129]; CAT-2 [125]; CAT-3 [125]; y^+LAT2/4F2hc [129]; y^+LAT1/4F2hc [129]; $b^{0,+}AT$/rBAT [130]; ORC2; ORC1
			NO	signaling molecule; regulator of nutrient metabolism, vascular tone, angiogenesis, immunity, neurotransmission			
			Ornithine	NH_4^+ detoxification; synthesis of P, E, and polyamines	2	22	CAT-1 [129]; $b^{0,+}AT$/rBAT [129]; ORC2; ORC1
			Methylarginine	competitive inhibition of NOS			
			Creatine (R, M, and G)	antioxidant; antiviral; energy metabolism in muscle and brain; neurological and muscular development and function			CT1; CT2
Asparagine	N	NE	directly	cell metabolism and physiology; immunity; NH_4^+ detoxification; CNS function	8	7	$ATB^{0,+}$ [125]; B^0AT1/Coll [128]; LAT2/4F2hc [130]; SNAT1; SNAT2; SNAT3; SNAT4; SNAT5
Aspartate	D	NE	directly	purine, pyrimidine, N, and R synthesis; transamination; urea cycle; activation of NMDA receptors	0.2	20	EAAT3; EAAT2; EAAT1; EAAT4; EAAT5; AGT-1; AGC1
Cysteine	C	E	directly	disulfide linkage; transport of sulphur; immunity; cellular metabolism and nutrition	3	21	ASCT1; ASCT2; $ATB^{0,+}$ [125]; B^0AT1/Coll [128]; y^+LAT2/4F2hc [129]; LAT2/4F2hc [130]; Asc1/4F2hc [129]; SNAT1; SNAT2; SNAT4
			Taurine	antioxidant			TAUT; PAT1

		Glutathione (C, E, and G)	antioxidant; formation of leukotrienes; apoptosis; immunity			
Amino acids	Nutritional status in brain [4]	products	Non-protein functions [95]	CSF [μM] [4]	Plasma / CSF [4]	transported by [124]
Glutamate E	NE	directly	Q, citrulline, and R synthesis; bridging urea cycle with TCA cycle; transamination; NH_4^+ assimilation; activation of NMDA receptors	3	30	EAAT3; EAAT2; EAAT1; EAAT4; EAAT5; xCT/4F2hc; AGT-1; vglut2; vglut1; vglut3; AGC1; GC2; GC1
		GABA	excitatory neurotransmitter; inhibition of T-cell response and inflammation			GAT1; GAT3; BGT1; GAT2; VGAT; PAT1
		Citrulline	antioxidant; R synthesis; osmoregulation; NH_4^+ detoxification; N reservoir			ORC2; ORC1
Glutamine Q	NE	directly	mTOR signaling; immunity; major fuel for rapidly proliferating cells; inhibition of apoptosis; syntheses of purine, pyrimidine, ornithine, citrulline, R, N, and P; N reservoir; synthesis of NAD(P)	547	1	ASCT2; $ATB^{0,+}$ [125]; B^0AT1/Coll [128]; (LAT1/4F2hc [130]); y^+LAT2/4F2hc [129]; y^+LAT1/4F2hc [129]; LAT2/4F2hc [130]; SNAT1; SNAT2; SNAT3; SNAT5
		E and D	excitatory neurotransmitters; components of the malate shuttle; cell metabolism; NH_4^+ detoxification			
		Glucosamine-6-P	synthesis of aminosugars and glycoproteins; inhibition of NO synthesis			
		Ammonia (NH_4^+)	renal regulation of acid-base balance; synthesis of E			NHE1; NHE2; NHE3; RhAG; RhBG; RhCG
Glycine G	NE	directly	Ca^{2+} influx (G-gated channel); purine and S synthesis; antioxidant; one-carbon unit metabolism; inhibitory neurotransmitter in CNS; co-agonist with E for NMDA receptors	6	23	GlyT2; GlyT1; NTT4 [126]; B^0AT3/Coll [127]; B^0AT1/Coll [128]; (LAT2/4F2hc [130]); Asc1/4F2hc [129]; VGAT; PAT1; PAT2; SNAT2; SNAT4
		Heme	Hemoproteins; production of CO			

Amino acids		Nutritional status in brain [4]	products	Non-protein functions [95]	CSF [µM] [4]	Plasma / CSF [4]	transported by [124]
Histidine	H	NE	directly	protein methylation; antioxidative dipeptides; one-carbon unit metabolism	4	10	$ATB^{0,+}$ [125]; B^0AT1/Coll [128]; CAT-1 [129]; CAT-2 [125]; LAT1/4F2hc [130]; y^+LAT2/4F2hc [129]; y^+LAT1/4F2hc [129]; LAT2/4F2hc [130]; PHT2; PHT1; ORC2; SNAT1; SNAT2; SNAT3; SNAT5
			Histamine	allergic reaction; vasodilator; central acetylcholine secretion; regulation of gut function			VMAT1; VMAT2
Isoleucine	I	E	directly	synthesis of Q and A; balance among BCAA	3	15	$ATB^{0,+}$ [125]; B^0AT2 [129]; B^0AT3/Coll [127]; B^0AT1/Coll [128]; LAT1/4F2hc [130]; LAT2/4F2hc [130]; LAT3 [131]; LAT4 [132]
Leucine	L	E	directly	immunity; inhibits NO production by endothelium; mTOR signaling; activator of glutamate dehydrogenase; BCAA balance	6	12	$ATB^{0,+}$ [125]; B^0AT2 [129]; NTT4 [126]; B^0AT3/Coll [127]; B^0AT1/Coll [128]; LAT1/4F2hc [130]; y^+LAT2/4F2hc [129]; y^+LAT1/4F2hc [129]; LAT2/4F2hc [130]; $b^{0,+}$AT/rBAT [130]; LAT3 [131]; LAT4 [132]
			Q and A	interorgan metabolism of nitrogen and carbon			
Lysine	K	E	directly	regulation of NO synthesis; protein methylation, acetylation, ubiquitination, *O*-linked glycosylation	9	16	$ATB^{0,+}$ [125]; CAT-1 [129]; CAT-2 [125]; CAT-3 [125]; y^+LAT2/4F2hc [129]; y^+LAT1/4F2hc [129]; $b^{0,+}$AT/rBAT [130]; ORC2; ORC1
			OH-lysine	structure and function of collagen			
Methionine	M	E	directly	C, carnitine synthesis; SAM as methyl donor; immunity; one-carbon unit metabolism	1	20	$ATB^{0,+}$ [125]; B^0AT2 [129]; B^0AT3/Coll [127]; B^0AT1/Coll [128]; (LAT1/4F2hc [130]); y^+LAT2/4F2hc [129]; y^+LAT1/4F2hc [129]; LAT2/4F2hc [130]; SNAT2; LAT3 [131]; LAT4 [132]
			Homocysteine	oxidant; inhibition of NO synthesis			
			DCSAM	methylation of proteins and DNA; polyamine synthesis			

		Taurine	antioxidant; osmoregulation; organ development; vascular functions; anti-inflammation			
Amino acids	Nutritional status in brain [4]	products	Non-protein functions [95]	CSF [μM] [4]	Plasma / CSF [4]	transported by [124]
Phenylalanine F	E	directly	synthesis of Y; neurological development and function	5	9	$ATB^{0,+}$ [125]; B^0AT1/Coll [128]; LAT1/4F2hc [130]; LAT2/4F2hc [130]; TAT1 [133]; LAT3 [131]; LAT4 [132]
Proline P	NE	directly	collagen structure and function; neurological function; osmoprotectant	5	28	PROT; B^0AT2 [129]; NTT4 [126]; B^0AT1/Coll [128]; SIT1/Coll; PAT1; PAT2; SNAT2
		H_2O_2	killing pathogens; intestinal integrity; a signaling molecule; immunity			
		OH-proline	structure and function of collagen			
Serine S	NE	directly	one-carbon unit metabolism; syntheses of C, G, purine, pyrimidine, ceramide and phosphatidylserine; gluconeogenesis; protein phosphorylation	15	6	ASCT1; ASCT2; $ATB^{0,+}$ [125]; B^0AT3/Coll [127]; B^0AT1/Coll [128]; LAT2/4F2hc [130]; Asc1/4F2hc [129]; SNAT1; SNAT2; SNAT4; SNAT5
		D-Serine	activation of NMDA receptors			
Threonine T	E	directly	synthesis of the intestinal mucin protein; immunity; protein phosphorylation and *O*-linked glycosylation; G synthesis	13	6	ASCT2; $ATB^{0,+}$ [125]; B^0AT1/Coll [128]; LAT2/4F2hc [130]; Asc1/4F2hc [129]; SNAT4
Tryptophan W	E	directly		1	30	$ATB^{0,+}$ [125]; B^0AT1/Coll [128]; LAT1/4F2hc [130]; LAT2/4F2hc [130]; TAT1 [133]
		Serotonin	neurotransmitter; inhibiting production of inflammatory cytokines and superoxide			SERT
		Melatonin	antioxidant; inhibition of the production of inflammatory cytokines and superoxide			
		Niacin	component of NAD(P)			

Amino acids		Nutritional status in brain [4]	products	Non-protein functions [95]	CSF [µM] [4]	Plasma / CSF [4]	transported by [124]
Tyrosine	Y	E	directly	protein phosphorylation, nitrosation, and sulfation; thyroid hormones	7	9	$ATB^{0,+}$ [125]; B^0AT1/Coll [128]; LAT1/4F2hc [130]; LAT2/4F2hc [130]; $b^{0,+}AT$/rBAT [130]; TAT1 [133]
			Dopamine	neurotransmitter; regulation of immunity			NET; DAT; VMAT1; VMAT2
			Epinephrine and Norepinephrine*	neurotransmitters; cell metabolism			NET*
Valine	V	E	directly	synthesis of Q and A; balance among BCAA	12	15	$ATB^{0,+}$ [125]; B^0AT2 [129]; B^0AT3/Coll [127]; B^0AT1/Coll [128]; LAT1/4F2hc [130]; LAT2/4F2hc [130]; LAT3 [131]; LAT4 [132]

Major metabolites and functions of amino acids in addition to functions in protein synthesis, as osmolytes, in regulation of hormone secretion, gene expression and cell signaling are given (adapted from [95]). The nutritional status in brain (after [4]), the amino acid concentrations in CSF (in µM) and respective plasma / CSF ratio (after [4]) is given for each amino acid separately. The possible transporters of different SLC families (see also Table 4) are listed according to their reported substrates (adapted from [125] where not otherwise stated).

Essential amino acids cannot be synthesized by brain at adequate rates to meet the needs for brain metabolism and protein synthesis and must therefore be supplied from the diet [93]. Conditionally essential amino acids are those that normally can be synthesized in adequate amounts by the organism, but which must be provided from the diet to meet optimal needs under conditions where rates of utilization are greater than rates of synthesis. Nonessential amino acids are those amino acids which can be synthesized *de novo* in adequate amounts by the body to meet optimal requirements. [95]

AA, amino acid; BCAA, branched-chain AA; CNS, central nervous system; DCSM, decarboxylated S-adenosylmethionine; E, essential AA; GABA, γ-aminobutyrate; mTOR, mammalian target of rapamycin; NE, non-essential AA; NMDA, N-methyl-D-aspartic acid; NOS, nitric oxide synthase; SLC, solute carrier; TCA, tricarboxylic acid cycle.

3.6 Transport processes across the blood-brain barrier.

The BBB protects the brain from fluctuations in blood, provides an optimal chemical environment for cerebral function, and guarantees the nutrition of the brain by uptake of substrates from blood via transporters expressed at the BBB [1] (see section 3.3.1.1).
For a solute to enter the brain from blood it has to pass the blood-brain barrier (BBB) or the blood-cerebrospinal fluid barrier (BCSFB) (see section 3.3). But since the brain microvessels comprising the BBB have a surface area of up to 5,000 times that of the choroid plexus [52], the extent to which a solute enters the brain is determined almost exclusively by the permeability characteristics of the BBB [4], implicating the major role of the BBB in brain (amino acid) homeostasis.
After amino acids have entered the brain they must be transported into brain cells (neurons, glia). Since the surface area of the brain cell membranes is much greater than the surface area of the BBB, transport across the BBB is the rate limiting step in amino acid movement from blood to brain intracellular spaces [83].

There is more than one barrier between blood and brain. In addition to the endothelial cells that are in direct contact with the blood and its constituents, all the layers of the neurovascular unit (see section 3.3.1) can potentially restrict the movement of solutes into the brain [1, 7] and influence their distribution into various brain regions [135]. This is also true for the negatively charged basement membrane (see section 3.3.1.2), which is almost as thick as the endothelial cytoplasm (in human 200 nm [42]) and which may influence movement of charged solutes between blood and brain ISF [52]. The endothelial cells themselves possess several lines of defense, first the negatively charged endothelial glycocalyx [136], then the metabolically active endothelial cytoplasm [136], and the luminal and abluminal membranes, the combined characteristics determine which molecules cross the barrier and how fast [1, 7].

Transport across the BBB can occur via different routes, depending on the characteristics of the molecule to be transported (see Figure 9). The BBB can not simply be seen as a passive barrier, the cells actively participate in regulating the composition of the brain ISF.

Paracellular diffusion. The tight junctions connecting the endothelial cells of the BBB inhibit paracellular diffusion (see section 3.3.1.1.1). The high TEER of the BBB *in vivo* is indicative of a restriction to the movement of even ions [1, 7]. Most hydrophobic molecules can still

passively diffuse across the BBB, also the blood gases oxygen and carbon dioxide, but entry of hydrophilic solutes from blood to brain has to be guaranteed and regulated via different transport systems. There is a correlation between the rate a solute enters the brain and its lipid solubility [26].

Transport proteins. It is generally assumed that at least 5% (>2,000) of all human genes are transporter-related [137] and it is estimated that about 15% of all genes selectively expressed at the BBB encode for transporter proteins [33].

Transporters can be divided into active and passive transporters. Passive (facilitative) transporters transport solutes across membranes down their electrochemical gradients. Active transporters are classified as primary- or secondary-active transporters and build up ion or solute gradients across membranes. Primary-active transporters are directly ATP dependent, e.g. ATPases and members of the ATP-binding cassette (ABC) transporter family. Secondary-active transporters, like SNAT1 (Slc38a1), use the electrochemical gradient build up by primary-active transporters, like Na^+/K^+-ATPase, to drive solute transport against a concentration gradient. [137] Even if not directly coupled to the sodium gradient, transporters can be dependent on the substrate gradient generated by secondary active transporters and are therefore named tertiary active transporters (e.g., LAT1-4F2hc) [138]. The polarized BBB endothelial cells selectively localize specialized transport systems to the luminal and / or abluminal membrane. This polarized distribution is assumed to be the prerequisite for directional transcellular transport from blood to brain or from brain to blood (see section 3.6.1.2 and 6).

Solute carriers. The solute carrier (SLC) gene series currently includes 48 families and 368 transporters genes [125]. SLC members encode for passive transporters, ion-coupled transporters and exchangers of various substrates. Members of a SLC family have at least 20-25% amino acid sequence identity [137]. Names are given using the root symbol SLC, followed by a numeral indicating the family, the letter A (which acts as a divider between the numerals) and the number of the individual transporter [137].

The best examined SLC member at the BBB, in regards to its expression, localization, and regulation, is GLUT1 (Slc2a1). GLUT1 is a sodium-independent, facilitative diffusion protein transporting glucose, galactose, mannose, and glucosamine. It is highly expressed in blood-tissue barriers, in particular in the BBB endothelial cells [139], where it is even considered as a marker molecule. GLUT1 is reported to be asymmetrically distributed, with about 11% located in the luminal membrane, 44 % in the abluminal membrane, and 45% intracellular

[140-141]. Additionally, to explain the observed discrepancy of polarized expression, but equal glucose transport activity in the two membranes, a conformational alteration in the GLUT1 proteins on the luminal membrane has been suggested [140]. Recently, Glut1-mRNA was shown to be expressed at very high levels in primary, non-cultured mouse brain microvascular endothelial cells, and to be linked to BBB transendothelial transport *in vivo* [2].

ABC transporters. ABC transporters in the human are a superfamily with 48 members grouped into seven sub-families based on structural homology [26] and function as active efflux pumps, carrying a neuroprotective and detoxifying function. They posses a polarized expression like the SLCs, with luminal expression of e.g. P-gp (P-glycoprotein, ABCB1) and BCRP (Breast Cancer Resistance Protein, ABCG2), in a position to transport substrate from the BBB endothelial cells to blood [26].

Additional "non-SLC" transporters. Channels, receptors, and aquaporins are also involved in transport processes across membranes [137]. Channels control ion / solute flow via gating mechanisms, not by a fixed stoichiometry like transporters.

Transport of macromolecules via transcytosis. Endocytotic mechanisms provide the main route by which large molecular weight solutes such as proteins and peptides can enter the CNS intact [26]. In general, the rate of transcytosis across the BBB is reduced, since the endothelial cells are characterized by reduced numbers of endocytotic vesicles in the cytoplasm (see section 3.3.1.1), e.g., only 16-20% of that seen in muscle capillary endothelia [1, 26]. Smaller peptides can also be transported by either non-specific fluid-phase endocytosis or peptide-specific transport proteins [26]. Transcellular permeability is caveolae-mediated [22].

Receptor-mediated transcytosis (RMT). Binding of ligands, e.g. insulin, to specific receptors on the cell surface trigger endocytosis, followed by exocytosis at the opposite pole of the cell [26].

Adsorptive-mediated transcytosis (AMT). Cationic molecules, e.g. lectins, interact with cell surface binding sites, which induce endocytosis and subsequent transcytosis [26].

Movement of cells. In the normal BBB, mononuclear cells penetrate via diapedesis directly through the cytoplasm of the endothelial cells. In inflammatory pathological states, mononuclear cells can enter by both transcellular and paracellular routes [26].

Figure 9: Possible transport processes across the blood-brain barrier endothelium.

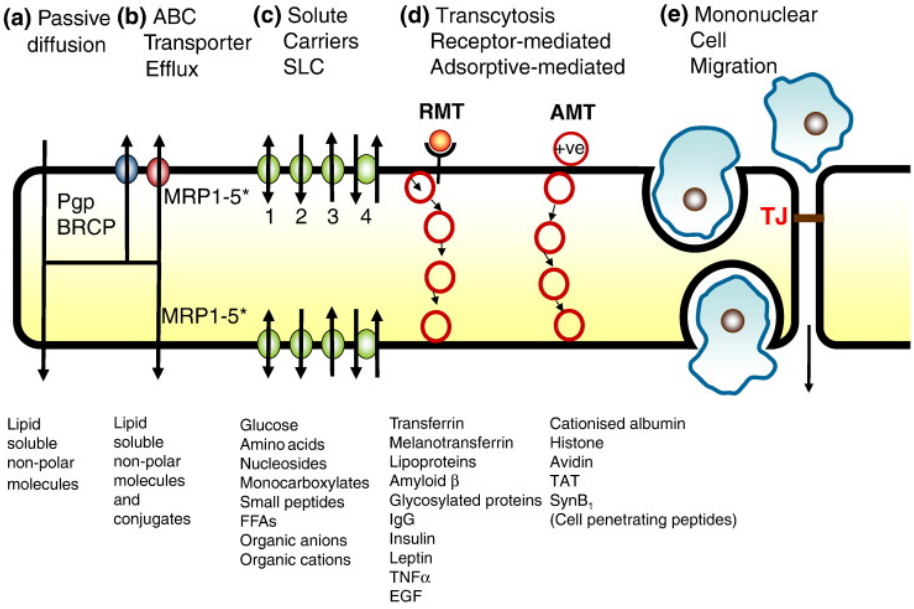

Routes of transport across the BBB. **(a)** Solutes may passively diffuse through the cell membrane and cross the endothelium; **(b)** Active efflux carriers (ABC transporters) may intercept some of these passively penetrating solutes and pump them out of the endothelial cell either as they diffuse through the cell membrane or from the cytoplasm; **(c)** Carrier-mediated influx via solute carriers (SLCs) may be passive or primarily or secondarily active and can transport many essential polar solutes into the CNS. The SLCs may be bi-directional, the direction of net transport being determined by the substrate concentration gradient (1), unidirectional either into or out of the cell (2/3), or involve an exchange of one substrate for another or be driven by an ion gradient (4). In this last case the direction of transport is also reversible depending on electrochemical gradients; **(d)** RMT requires receptor binding of ligand and can transport a variety of macromolecules such as peptides and proteins across the cerebral endothelium (transcytosis). AMT appears to be induced in a non-specific manner by positively charged macromolecules and can also transport across the endothelium. Both RMT and AMT appear to be vesicular-based systems; **(e)** Leukocytes cross the BBB either by a process of diapedesis through the endothelial cells, or via modified tight junctions. Source: Figure 4 from Abbott *et al.* (2010) [26].

3.6.1 Amino acid transport.

Amino acid transporters are members of different solute carrier (SLC) families, with different substrate specificities, transport mechanisms, and ion dependencies [137]. Amino acid transporters are grouped according to their structure (SLC families), their transport mechanisms, and their substrate specificities (transport systems, see Table 4). In respect to structure, only SLC7 family members are heterodimeric proteins, constituted by a heavy (SLC3 member) and a light chain (SLC7 member). The light chain determines the functional properties of the transporter, the main function of the heavy chain is the trafficking of the complex to the plasma membrane. [142]

Prior to the molecular identification of amino acid transporters, transport was described in terms of transport systems. Conventions for the naming of amino acid transport systems include: “(1) upper case to indicate sodium-dependence, lower case for sodium-independence

(exception: system L); (2) designations y^+ and x^- for transporters of cationic and anionic amino acids, respectively; (3) the superscript 0, indicating transport of zwitterionic amino acids, used single or in combination with + or – for transporter of amino acids with differing net charge" [143]. Furthermore, systems indicate substrate preferences, e.g. members of the sodium-independent system L prefer amino acids like leucine (hence "L") [143]. System A members transport substrates like alanine in a sodium-dependent way (hence "A"), and system ASC transports substrates like alanine, serine, and cysteine also in a sodium-dependent way [143] (see Table 3 and Table 4).

In respect to physiological functions, transporters can be grouped into highly accumulating transporters (e.g., EAATs), weakly accumulating transporters (e.g., SLC38 members), antiporters or exchangers, and uniporters [142] (see Table 4). Antiporters represent the majority of amino acid transporters in mammalian tissues and mediate preferentially an exchange of essential amino acids against nonessential amino acids without causing a net loss or increase of the total amount of amino acids. Antiporters can also display an asymmetry, particularly when they are involved in vectorial transport. One example for asymmetry is LAT1-4F2hc, which shows a higher substrate binding affinity extra- than intracellular [144]. [142] Furthermore, the driving force of a transporter can be fine-tuned by co-transporting ions like protons, potassium or chloride which are close to electrochemical equilibrium (see section 3.6.1.3.2). Therefore, "one cannot judge the net direction of a transport solely by the direction in which its gradient is oriented" [145]. The number of true uniport systems is low, maybe because this mechanism does not protect the cell from fluctuations in the plasma. An exception is the transport of cationic amino acids (see Table 4), therefore it has been suggested that the intracellular arginine concentration reflects the nutritional status and could present a metabolic signal. In this regard it is interesting that LAT1 (Slc7a5) is regulated by arginine availability, although arginine is not a substrate of the transporter. [142]

Amino acid transport across the BBB. Amino acid uptake into brain depends on the type of amino acid. Nonessential amino acids show minimal uptake from blood since they are derived from intracerebral synthesis. Essential amino acids, in contrast, are derived almost exclusively from the blood. [93] By increasing plasma levels of glycine, tryptophan, aspartate, arginine, serine, threonine, isoleucine, and methionine above brain levels in the mouse, it could be observed that the relative uptake of the amino acids normally high in the brain was smaller than that of amino acids at lower levels in brain (e.g., isoleucine, methionine) [135]. Although brain levels increased, for example, about four-fold in the case of isoleucine, none of the

amino acids reached levels in brain equal to those in plasma (see Table 3) [135]. The excitatory neurotransmitter amino acids aspartate and glutamate were not taken up by brain [135]. The rate of synthesis and the brain concentration of neurotransmitters has been shown to be influenced by brain levels of the respective precursor amino acids, since the key rate-limiting enzymes are not saturated at normal brain concentrations [93]. Furthermore, in pathological conditions like the hyperaminoacidemias (see section 3.5.5), protein synthesis becomes substrate limited and rate affected by amino acid transport across the BBB [119].

Functional experiments *in vivo* and *in vitro* have been performed to characterize the transendothelial transport of specific amino acids. Studies on isolated membrane vesicles have been used to determine the distinct role of the luminal and abluminal membranes of the microvascular endothelial cells in this process, and the identity and functionality of the transporters involved [5-6, 79, 82]. In this way, it was proposed that system ASC, A, N, EAAT, and LNAA members are expressed exclusively abluminal, system n, and X_G^- exclusively on the luminal membrane, and system L1 and y^+ members on both membranes [1] (see Table 4, Figure 10, and section 3.6.1.1/2).

In general, transporters expressed in CNS and the same transporters expressed in peripheral tissues are not necessarily controlled the same way, as shown e.g. for SNAT1 (Slc38a1) and SNAT2 (Slc38a2) [106]. This could in some cases be explained by the special microenvironment of the BBB endothelial cells and the special role the single amino acids play in the CNS. For example, a greater activity of system y^+ on the endothelial abluminal membrane was observed and suggested to be due to the proximity to the astrocytic arginine stores [6]. Arginine is an essential amino acid and precursor of the vasodilator nitric oxide (NO) [6]. ASCT2 (Slc1a5) is known to be involved in stereoselective L-aspartate efflux across the abluminal membrane [146]. This is consistent with the function of the different isomers (see also section 3.5.2). The accumulation of L-aspartate would lead to excitatory neurotoxicity. Contrary, D-aspartate influences the secretion of hormones like testosterone, melatonin and oxytocin, and needs therefore to be stored [146].

The first described and best characterized amino acid transporter of the BBB, the sodium-independent exchanger of the system-L family, LAT1 (Slc7a5), is composed of two subunits that are both required for functional cell-surface expression (see Table 3 and Table 4). The catalytic subunit of this heterodimeric transporter is LAT1, which was first cloned 1998 [147-148]; the second subunit is a type-II glycoprotein called 4F2hc or CD98 (Slc3a2). The two subunits of the LAT1-4F2hc heterodimer are linked by a disulfide bridge and together mediate transport of LNAAs, T3, T4, and L-DOPA into growing cells and across secretory or

bidirectionally transporting endothelial / epithelial barriers [138]. Along with its role in amino acid transport, 4F2hc is also involved in cell survival, cell fusion, and integrin activation, and LAT1 contributes to neuronal cell proliferation [149]. In functional studies it was found that the affinity of BBB neutral amino acid transport is higher than in peripheral organs, also compared to plasma amino acid concentrations, leading to renaming it system L1 [86]. System L1 is localized to both the luminal and abluminal membrane of the BBB [3, 150], with equal expression but different activity [5]. The clearance by the luminal membrane is with 32 $\mu l \bullet min^{-1} \bullet mg^{-1}$ higher than the one by the abluminal membrane (14 $\mu l \bullet min^{-1} \bullet mg^{-1}$) [5]. Transport via LAT1-4F2hc is competitive (see section 3.5.4.3 and 3.6.1.1) and almost fully saturated at normal plasma LNAA concentrations. Therefore, the uptake of each LNAA into brain is dependent on its own plasma concentration but also on that of each of its competitors [113]. It also has been shown that entry into the brain of excluded amino acids can be increased by raising their concentration in the blood [101]. 4F2hc shows a broader expression pattern in brain than LAT1 since it is needed for the proper membrane insertion also of other SLC7 family members highly expressed in whole brain, e.g. y^+LAT2 (Slc7a6) and xCT (Slc7a11) [151]. The localization of LAT1-4F2hc on both membranes and its role as tertiary active transporter (see section 3.6) puts it in a position to participate in transendothelial transport and in modulation of intracellular amino acid concentrations. This view was supported by our recent study comparing the mRNA expression of Lat1-4F2hc in the mouse BBB *in vivo* and *in vitro* [2].

Table 4: Overview of amino acid transport systems.

Transport system	Transporter	Transport mechanism
A	SNAT1 (Slc38a1); SNAT2 (Slc38a2); SNAT4 (Slc38a4)	1 Na^+ / AA (symport)
ASC	ASCT1 (Slc1a4); ASCT2 (Slc1a5)	1 Na^+ / AA (symport); AA (antiport)
asc	Asc1/4F2hc (Slc7a10/Slc3a2)	AA (antiporter)
B^0	B^0AT2 (Slc6a15); $B^{0,+}$AT3/Coll (Slc6a18); B^0AT1/Coll (Slc6a19)	1 Na^+ / AA (symport)
$B^{0,+}$	$ATB^{0,+}$ (Slc6a14)	2 Na^+ / 1 Cl^- / AA (symport)
$b^{0,+}$	$b^{0,+}$AT/rBAT (Slc7a9/Slc3a1)	AA (antiport)
β	GAT1 (Slc6a1); TAUT (Slc6a6); GAT3 (Slc6a11); BGT1 (Slc6a12); GAT2 (Slc6a13)	2-3 Na^+ / 1 Cl^- / AA (symport)
Gly	GlyT2 (Slc6a5); GlyT1 (Slc6a9)	2-3 Na^+ / 1 Cl^- / AA (symport)
IMINO	SIT1/Coll (Slc6a20)	2 Na^+ / 1 Cl^- / AA (symport)
L	LAT1/4F2hc (Slc7a5/Slc3a2); LAT2/4F2hc (Slc7a8/Slc3a2); LAT3 (Slc43a1); LAT4 (Slc43a2)	AA (antiport) AA (uniport)
N	SNAT3 (Slc38s3); SNAT5 (Slc38a5)	1 Na^+ / AA (symport) / 1 H^+ (antiport)
PAT	PAT1 (Slc36a1); PAT2 (Slc36a2)	1 H^+ / AA (symport)
T	TAT1 (Slc16a10)	AA (uniport)
X^-_{AG}	EAAT3 (Slc1a1); EAAT2 (Slc1a2); EAAT1 (Slc1a3); EAAT4 (Slc1a6); EAAT5 (Slc1a7)	3 Na^+ / 1 H^+ / AA (symport) / 1 K^+ (antiport)
x^-_c	xCT/4F2hc (Slc7a11/Slc3a2)	AA (antiport)
y^+	CAT-1 (Slc7a1); CAT-2A/B (Slc7a2); CAT-3 (Slc7a3)	AA (uniport)
y^+L	y^+LAT2/4F2hc (Slc7a6/Slc3a2); y^+LAT1/4F2hc (Slc7a7/Slc3a2)	1 Na^+ / AA (symport); AA / AA^+ (antiport)

Overview of amino acid transport systems, corresponding proteins and genes (in brackets). Corresponding substrates are listed in Table 3. Accessory proteins are given where known: 4F2hc, rBAT, and Coll (Collectrin). Slc, solute carrier; AA, amino acid. Adapted from Bröer (2008) [130], Bröer (2002) [142], and Hyde *et al.* (2003) [126]. Systems used in Hawkins *et al.* (2006) [1] correspond, based on substrate profiles, most properly to system X^-_{AG} ("EAAT"), system N ("n", but sodium-dependent), and system "Na^+-LNAA" shows overlapping profiles with B^0AT1 (system B^0) and LAT2 (system L).

3.6.1.1 Short literature review on BBB amino acid transport.

The following section includes a selective chronological review of the research progress concerning amino acid transport across the BBB. It has to be mentioned that the interpretation of the data given by the authors and reported here was limited by the absence of kinetic information of the involved transporters that were identified only very recently after their cloning during the last 20 years. In particular, many of the given interpretations do not account for the fact that LAT1-4F2hc (corresponding to system L1) functions as an obligatory exchanger (antiport) and not as a facilitated diffusion pathway (uniport). To underline this crucial interpretation problem, evident questionable interpretations are labeled in the following review (and in section 3.6.1.2) with a "(!)". Nonetheless, the interpretations of the authors are given here without pointing each time to their limitations.

In 1978 *Betz and Goldstein* demonstrated that αMeAIB‡ was not transported from blood to brain *in vivo* and concluded that **system A** transport does not exist at the BBB [3]. On the other hand, some system A substrates were found to be transported from brain to blood against a concentration gradient [3]. They finally concluded that system A transport occurs at the abluminal, but not on the luminal membrane [3]. They also already pointed out the impact of this polarity in actively regulating the composition of brain ISF against a concentration gradient [3]. Furthermore, they saw a link between the operation of abluminal sodium-dependent transporters and the high mitochondrial density in BBB endothelial cells, and pointed out the difficulty to interpret *in vivo* data due to the presence of amino acid transporters in choroid plexus and brain cells [3].

Also *James and Fischer* (1981) [152] examined the transport of neutral amino acids at the BBB. They discussed the existence of exclusively system L at the luminal membrane. However, they also pointed out that transendothelial transport is the sum of influx and efflux and that it is not known if efflux is mediated via the same transport systems than influx, different from or supplementary to it. This lack of knowledge regarding efflux, together with the possible impact of metabolism and cooperation with astrocytes in transport processes led the authors to conclude that one can not judge the impact of transport in the regulation of brain neutral amino acid concentrations.
It was previously proposed that transport of neutral amino acids into cells is mediated by **systems L, A, ASC, and Gly**. The participation of system ASC in blood to brain transport

‡ 2-(methylamino)isobutyric acid

could neither be confirmed nor disproven, whereas that of system Gly could be disproven. The properties of neutral amino acid transport into brain are consistent with the existence of an active L system and an absent or negligible A system. Influx of neutral amino acids showed substrate specificity, with most active uptake into brain for phenylalanine, leucine and tyrosine. In addition to saturable transport, a not characterized nonsaturable blood to brain transport of amino acids has been repeatedly demonstrated.
The authors [152] also mentioned that BCAAs are metabolized to a higher extend than aromatic amino acids, and that the brain therefore must synthesize nonessential system-L substrates to guarantee equal exchange with essential amino acids**.** They suggested that system A on the abluminal membrane could act to concentrate nonessential amino acids such as alanine or glutamine, with a low affinity for system L, to high levels in the intraendothelial compartment, to then be exchanged with other neutral amino acids from blood. Glutamine would be a good candidate for exchange via system L due to its high CSF concentrations and since it could be shown that increased brain glutamine stimulates brain neutral amino acid uptake. They pointed out that an active uptake of amino acids on the abluminal side could also explain the low CSF / plasma ratios of most neutral amino acids. Another aspect the authors mentioned was competition for uptake among amino acids on the blood side. In this way the uptake of one neutral amino acid relative to that of another can be regulated. However, they point out that the factors regulating the uptake of all neutral amino acids, as a group, are not known.

Cangiano et al. [153] showed two years later that in isolated brain microvessels an intracellular accumulation of glutamine via **system A** trans-stimulated the uptake of neutral amino acids via **system L**. Therefore the authors suggested cooperation between the two differentially localized transport systems to regulate the rate of neutral amino acid uptake into brain over the BBB.

Five years later, *Hargreaves and Pardridge* (1988) [86] examined neutral amino acid transport at the human BBB, showing that phenylalanine is transported exclusively by system L, whereas leucine is transported equally by **system L and ASC**. They located system L activity to both the luminal and abluminal membrane, whereas system ASC seemed to be restricted to the abluminal membrane. They mentioned also an *in vivo* study in rats after which system ASC may also function at the luminal membrane. The affinity of human BBB neutral amino acid transport was shown to be very high, with an about 100-fold lower K_m

value than in peripheral tissues. They also mention species differences, with 8-40-fold lower K_m values in human BBB than in the rat BBB *in vivo*. In addition, the authors tested the inhibitory effect of other neutral amino acids on the transport of leucine into human brain capillaries and found inhibition by BCAAs and ArAAs, but none by glutamate, arginine or proline. Leucine, tyrosine, and tryptophan trans-stimulated phenylalanine transport, indicating transport via the same transport system. Contrary to previous studies, also glycine and alanine had an inhibitory effect on leucine transport. Therefore the authors suggested that more than one transport system for neutral amino acids exists. The transport of neutral amino acids into isolated human brain capillaries was found to be mediated, in most cases, by both a high affinity (up to 97% of amino acid transport) and a low affinity system.

Four years later in a 1992 study *Sánchez del Pino et al*. [82] used membrane vesicles for the first time to investigate neutral amino acid transport at the BBB. They demonstrated the sodium- and proton-independence of L-phenylalanine transport and its almost complete inhibition by other LNAAs, BCH§, and D-phenylalanine. The authors mentioned a second, non-saturable, transport component that could be a low affinity, high capacity transport system, or a non-facilitated diffusion process. Furthermore, the authors pointed out the discrepancy between missing "obvious" morphological, but well established biochemical polarity of brain endothelial cells. For instance the abluminal, but not the luminal membrane, contains Na^+/K^+-ATPase activity, whereas γ-glutamyl transpeptidase and alkaline phosphatase are located luminal. The authors proposed that this enzymatic polarity also exists for transport of glucose and amino acids. In contrast to Hargreaves and Pardridge [86], Sánchez del Pino *et al*. debated the localization of **system ASC**. However, they agreed that there is no *in vivo* evidence for luminally expressed **system A**, and that sodium-dependent transport systems are restricted to the abluminal membrane. In addition Sánchez del Pino *et al*. pointed out that the methods on which the concept of **system L** localization on both BBB membranes rely on are relatively insensitive.

In 1995 *Sánchez del Pino et al.* [79] characterized phenylalanine transport by the high affinity **system L1** (K_m = 10 ± 2 μM) using isolated luminal and abluminal BBB membranes. They described that both membranes contain the same sodium-independent transporter which is symmetrically distributed, and that system L1 has in both membranes the same substrate specificities. They found 65% of alanine uptake to be sensitive to MeAIB (**system A**), 24% to

§ BCH, 2-aminobicyclo-(2,2,1)-heptane-2-carboxylic acid

BCH (**system $B^{0,+}$**), and 11% of the uptake due to a non-saturable and sodium-independent mechanism. The remaining sodium-dependent alanine uptake was ascribed to **system ASC**. System A and $B^{0,+}$ are both reported to be exclusively located at the abluminal membrane. Based on their experiments the authors [79] describe the transport polarity at the BBB such that sodium-dependent transport activities are enriched in the abluminal-rich membrane fraction, whereas the luminal-rich membrane fraction contains a greater extent of sodium-independent transport activity. The observed sodium stimulated uptake by the luminal-rich membrane fractions was discussed to be completely due to abluminal vesicle contamination. They also mention **system T**, which they propose, if present, to be a minor transport component, and again pointed out the discrepancy regarding expression of **system ASC** at the BBB.

In the same year, *Sánchez del Pino et al.* [154] examined the polarized expression of enzymes and transporters at the BBB to identify marker molecules. Isolated bovine brain endothelial cell membrane vesicles showed expression of γ-glutamyl transpeptidase restricted to the luminal and **system A** to the abluminal membrane. 5´-nucleotidase and alkaline phospatase were found to be symmetrically distributed on both membranes. Na^+/K^+-ATPase activity was mainly located to the abluminal membrane, but about 25% of the activity was found luminal, with a different ouabain sensitivity than the one expressed abluminal. Therefore the authors suggested that different Na^+/K^+-ATPase isoforms are expressed at the different membranes and that this distribution could favour a net blood to brain transport of sodium.

Tamai et al. [155] examined transport of **taurine** at the BBB *in vitro* in bovine and *in vivo* in rats. Taurine was found to be taken up in a sodium-and chloride-dependent manner on both the luminal and abluminal membranes. The uptake of taurine, for which no metabolism in cells has been observed, was carrier mediated and transport was from blood to brain. Transport efficiency was similar on both membranes, but inhibition of taurine uptake by cysteine, methionine, and phenylalanine was found to be different. Furthermore, the luminal and abluminal transporter showed different substrate specificities, with glutamate stimulating taurine uptake at the luminal membrane, but inhibiting abluminal taurine uptake.

Boado et al. 1999 [83] showed the selective expression of the system L1 transporter **LAT1** at the BBB. LAT1 mRNA was not detected in rat liver, heart, lung, or kidney. In rat brain and rat C6 glioma cells LAT1 mRNA was present, but the level in isolated bovine brain

capillaries was 100-fold higher. Furthermore, LAT1 was found to be the most abundant transcript at the BBB, higher than 4F2hc, actin, or GLUT1. The level of **4F2hc** mRNA in the BBB was <10% of than in either total brain or C6 glioma cells. The ratio of 4F2hc mRNA to LAT1 mRNA was shown to be <1 at the BBB. The authors suggest that this indicates that the availability of 4F2hc is rate limiting in the formation and membrane expression of LAT1-4F2hc. They discussed the possibility that even if LAT1 mRNA is expressed at higher levels than GLUT1 mRNA, the reverse may be true on the protein level, since V_{max} for D-glucose transport at the BBB is much higher than for LNAA transport. As another explanation they discussed the possibility that the LAT1 transcript has a high turnover rate. In addition, the 5`-UTR and 3`-UTR of the BBB LAT1 transcript contain cis-regulatory sequences suggesting that LAT1 gene expression may be posttranscriptionally regulated. Further, bovine LAT1-4F2hc injected into frog oocytes increased tryptophan transport 10-fold. This transport was characterized by a K_m of 31.5 ± 5.5 μM, by sodium-independence and by transport inhibition by other LNAAs and BCH, but not by alanine, glutamate or arginine. They also suggested that LAT1 seems to be the major system L transporter at the BBB, since **LAT2** represents a high-K_m system and is not selective for LNAAs. The authors mention that this selective expression of LAT1, normally saturated by the plasma concentrations of LNAAs, is believed to be the reason why the brain is selectively sensitive to hyperaminoacidemias (see section 3.5.5) but not to hypoaminoacidemias.

In the same year, *O'Kane et al.* [156] described the expression of the sodium-dependent glutamate transporters **EAAT1**, **EAAT2**, and **EAAT3** in bovine cerebral capillaries and showed that their protein expression is restricted to the abluminal membrane of BBB endothelial cells. By examining the three transporters as aggregate, voltage dependence, potassium dependence, an apparent K_m of 14 μM (at -61 mV), a V_{max} of 151 ± 20 pmol•mg^{-1}•min^{-1}, and inhibition of glutamate transport by kainic acid (EAAT2) and cysteine (EAAT3) could be shown. The relative activity of the transporters was measured as 1:3:6 (EAAT1:EAAT2:EAAT3). Furthermore, glutamate transport in the absence of sodium was 50-70% reduced and intravesicular potassium increased uptake by 56.5%. The authors assumed that other glutamate transporters do not play a significant role, since the activity of EAAT1-3 accounted for all the transport activity measured by the method.

A 2000 review by *Smith* [17] summarized the expression and localization of different amino acid transport systems as followed: **system L** (high affinity), **system y^+** (moderate affinity),

system T (high affinity), and **system x^-** (high affinity), with systems L and y^+ localized to both membranes. In contrast, **systems A**, **$B^{0,+}$**, **ASC**, and **X^-** were found to be primarily expressed at the abluminal membrane. Transport of β-alanine and taurine was shown to be mediated by **system β**. **System N** mediates glutamine uptake into brain and was found on either luminal or abluminal membrane by different studies. The author also pointed out that in 1993 system y^+ (**CAT-1**) was the first molecular characterization of a BBB amino acid transporter.

Also in 2000, *Matsuo et al.* [150] showed for the first time immunohistochemical evidence for the assumption, based on functional data, that **LAT1** and **4F2hc** are symmetrically expressed on both membranes of the endothelial BBB. Both LAT1 and 4F2hc were found in a "double line appearance" surrounding endothelial cell nuclei. The authors proposed due to the co-expression of the heterodimer LAT1-4F2hc, that LAT1 is functional in the plasma membrane. The authors also speculate that LAT1 function is highly regulated at the BBB, e.g. via protein kinase-dependent phosphorylation. They also mention that even if GLUT1, MCT1 and MDR1 have been identified previously at the BBB, LAT1-4F2hc is the first amino acid transporter. They pointed out that the molecular identity of other proposed BBB amino acid transport systems, such as N, A, and y^+, remained to be determined.

A second study examining **LAT1** CNS localization using immunohistochemistry was published in the same year by *Kageyama et al.* [149]. They found LAT1 expressed in microvessels in the brain parenchyma and in the ependymal cells, but neither in the choroid plexus nor in neuronal and glial cells in the cerebral cortex, caudate putamen, cerebellum and brain stem. LAT1 showed a high expression in the subfornical organ (see section 3.3), therefore the authors suggested that this organ may play a role in amino acid homeostasis by monitoring peripheral amino acid contents. It had been previously demonstrated that the uptake of neutral amino acids from the blood into the choroid plexus is mediated by system L, which stands in contrast to the present study. In contrast the authors found **4F2hc** to be expressed and therefore they suggested that in the choroid plexus of mice other system L isoforms are expressed. They pointed out that LAT1 mRNA expression was generally found to be correlated with proliferating cells rather than differentiated cells of the same origin, and that there is the possibility that LAT1-4F2hc might regulate the migration of neuronal progenitor cells.

Takanaga et al. [157] showed for the first time brain to blood transport of glycine and L-proline and the involvement of **system A** transport in this process. The primary system A transporter at the BBB, **ATA2** (SNAT2; see section 3.6.1.3), was found to be upregulated by 373% under hypertonic conditions. Therefore the authors suggested that ATA2 may play a role in maintaining cerebral osmotic pressure and in maintaining barrier properties of the BBB due to endothelial cell volume regulation. The system A specific substrate MeAIB was not found to be transported into the blood, in contrast to L-proline and glycine, suggesting that system A expression is restricted to the abluminal membrane and that there may be another transport system responsible for transport of the amino acids across the luminal membrane.

In 2003 *Tetsuka et al.* [124] demonstrated **ASCT2** expression at the abluminal membrane of BBB endothelial cells, with mRNA expression of ASCT2 being 6.67-fold greater than of **ASCT1**. They also showed for the first time that these transporters mediate stereoselective brain to blood transport of L-aspartate across the mouse BBB (see section 3.6.1), mainly via ASCT2 in a pH-dependent manner with low affinity. L-aspartate uptake was found to be both sodium-dependent and -independent, while D-aspartate uptake was mainly sodium-independent. Sodium-independent L-aspartate uptake could be inhibited by L-glutamate (85.7%) and D-aspartate (41.5%), and could be increased by L-serine to 146%. **ATB^{0+}** mRNA expression was found to be absent in BBB cells, and therefore it was concluded that **system $B^{0,+}$** is not involved in L-aspartate uptake. The authors mentioned the discrepancy between transport affinity of BCH and L-leucine for **system ASC** and the lack of inhibition by these two substrates for sodium-dependent L-aspartate uptake. They also concluded that further studies are needed to identify efflux systems for L-aspartate on the luminal membrane, to identify the possible additional contribution of sodium-independent L-aspartate transport, and the contribution of other amino acid transporters.

O'Kane et al. (2003) [4] used isolated cow brain microvascular abluminal-enriched membrane fractions to study sodium-dependent transport of LNAAs. The yet unknown transport system was characterized by voltage sensitivity, inhibition by BCH, high affinity for leucine (K_m 21 ± 7 μM) and inhibition by other neutral amino acids. The spectrum of inhibitors was similar to the ones of **LAT1**. The authors excluded a role of **system ASC / B^0** in the observed transport process since alanine transport could not be inhibited by phenylalanine, tryptophan or tyrosine.

They also described the results of previous studies showing sodium-dependent **systems A**, **ASC**, **$B^{0,+}$**, **N** and **EAAC** are expressed at the abluminal membrane, and showing that blood to brain transport of essential neutral amino acids is greater than of nonessential amino acids. The observed sodium-dependent brain to blood transport of essential amino acids further highlights the complex mechanisms controlling brain amino acid concentrations.

One year later, *O´Kane et al.* [5] functionally described the four known sodium-dependent systems present at the abluminal membrane of the BBB transporting neutral amino acids, namely **system A**, **ASC**, **N**, and **Na^+-LNAA**. The different systems are described by overlapping substrate specificities, and system A was shown to be voltage dependent, in contrast to system ASC and N. System A and N transport only nonessential amino acids, whereas system ASC and Na^+-LNAA transport in addition essential amino acids. The authors point out that the primary focus in the past has been on facilitative transport via **system L1** (!), expressed on both membranes, which is believed to guarantee transport of (essential) neutral amino acids from blood to brain. The presence of sodium-dependent transporters on the abluminal membrane is believed to enable maintaining neutral amino acid concentrations in the brain ISF at ~10% those of the plasma. This situation was also accounted for by the presence of active amino acid uptake by brain cells, and metabolism, once they entered brain ISF. Since arteriovenous differences could never be measured, the authors favoured the explanation that brain influx and efflux of neutral amino acids occurs at the same rate, due to sodium-dependent transporters being exclusively located to the abluminal membrane. They pointed out that nonessential neutral amino acids have not been found to be transported from blood to brain, but that there is possibly a transport of small nonessential amino acids by a yet unknown system.

Two years later, in 2006, *O´Kane et al*. [6] found transport of cationic amino acids across the BBB to be exclusively mediated by **system y^+**. The authors hypothesized this may be important to provide arginine for NO synthesis, a statement supported by the fact that all three NO synthases are present in BBB endothelial cells. System y^+ was shown to be voltage dependent, with highest affinity for arginine, followed by lysine and ornithine. **System $B^{0,+}$**, **$b^{0,+}$**, and **y^+L** were not found to be active at the BBB in the past. Therefore, cationic amino acid transport at the BBB is unique since it is mediated exclusively by facilitative transport. The authors suggested that the majority of lysine transport is via system y^+, and they showed that it is about 40-times higher expressed in microvessels than in whole brain. Previously it

was proposed that system y^+ exists on both membranes, but this was not measured directly. The authors found cationic amino acid transport activity predominantly abluminal, with some activity on the luminal membrane (about 4:1 for lysine transport).

A 2006 review by *Hawkins et al.* [1] summarized the current knowledge about polarized expression of amino acid transporters at the BBB. The authors described facilitated amino acid transporters as being expressed at the luminal membrane, and as being saturable and stereoselective (**system L1**, **y^+**, **x_G^-**, **n**). System L1 and y^+ were both shown to be expressed in the luminal and abluminal membranes, but with different luminal:abluminal stoichiometry (L1 2:1; y^+ predominantly abluminal). Systems x_G^- and n were described to be restricted to the luminal membrane. The transport of glutamine was found to be not completely inhibited by the system L1 inhibitor BCH, therefore it was proposed that glutamine transport occurs also via system n. System y^+ has been characterized by a weak sodium-dependent interaction with neutral amino acids, and an about 10-fold greater affinity compared to system L1.
Sodium-dependent transport **systems** (**A**, **ASC**, **N**, **EAAT**, **Na^+-LNAA**) are described to be exclusively expressed at the abluminal membrane and to show a higher or at least similar transport capacity than the facilitative (!) transporters. Glutamine transport was found to be to 80% mediated by system N, and to 20% by system A, the latter being the first system characterized. Sodium-dependent transport of LNAAs was first thought to be mediated by **system $B^{0,+}$**; and EAAT1-3 have been shown to be together the most effective clearance system at low amino acid concentrations.

In 2008 *Czeredys et al.* [158] examined the localization of **$ATB^{0,+}$**, a sodium-chloride-dependent transporter of both neutral and cationic amino acids. $ATB^{0,+}$ was shown to be expressed in brain capillary endothelial cells with mostly luminal localization, a small fraction being also localized to the abluminal membrane. Experiments showed $ATB^{0,+}$ can mediate transport of D-serine, contributes by more than $^1/_3$ to leucine accumulation in endothelial cells, and, in contrast to LAT1, can be activated by an increase in plasma amino acid concentrations. The authors also reviewed the localization of **ASCT2**, **ATA2**, **EAAC**, **LNAA**, **OCTN2** and **noradrenaline transporter** at the abluminal membrane. **Taurine**, **creatine** and **serotonine transporters** were previously described to be localized to both membranes, and **GAT2/BGT1** to colocalize with P-gp on the luminal membrane.

Taken together, these studies represent a sum of important observations on transendothelial BBB amino acid transport. However, they also point to the lack of sufficient knowledge of the involved transporters, of their kinetics and their cooperation, which was the motivation for the present work.

3.6.1.2 Asymmetrical distribution of sodium-dependent transporters at the BBB.

The two membranes of the brain endothelial cells face chemically different compartments. The luminal membrane is in direct contact with the blood and its constituents, the abluminal membrane faces the brain ISF. The amino acid concentration in the ISF is considered to be about 10% those of plasma, with exception of glutamine, a condition necessary for brain function [1, 5, 7-8] (see section 3.5.4 and Figure 8). Due to this gradient over the endothelial cells, it has been proposed that the two membranes work in a complementary fashion [7], with facilitated diffusion processes primarily at the luminal membrane (!), allowing amino acids to enter and exit the endothelial cells along their concentration gradient [6-7]. The abluminal membrane of the BBB was shown to express mostly sodium-dependent transport systems [7], i.e. systems A, ASC, N, Na^+-LNAA, and EAAT [6] (see also section 3.6.1.1). In addition, facilitative transport occurs at the abluminal membrane (!) [5]. One example for coordinated transport between the two membranes is system N transport of glutamine and system EAAT transport of glutamate, which is directed from the brain ISF into the endothelial cell [5]. The luminal facilitative carriers for both glutamate and glutamine can then transport them to the plasma [5]. The asymmetrical distribution of transporters allows brain-derived amino acids, as well as amino acids previously transported from blood to brain, to be actively and selectively transported from brain to blood against their concentration gradient [1, 5, 7-8]. It even has been suggested that secondary active transporters expressed at the abluminal membrane are responsible for the existing amino acid gradient between plasma and brain ISF [120]. The existence of a sodium-gradient flowing from the brain ISF into the endothelial cytoplasm, which is maintained by the (abluminal) Na^+/K^+-ATPase, is consistent with this proposed mechanism [1, 8]. Together with the fact that transport systems show overlapping substrate specificities, this organization can also restrict the availability of amino acids to the brain [8] and can guarantee the access to essential amino acids (via the facilitative systems (!)) [5].

Figure 10: Proposed distribution of transporter and systems based on literature.

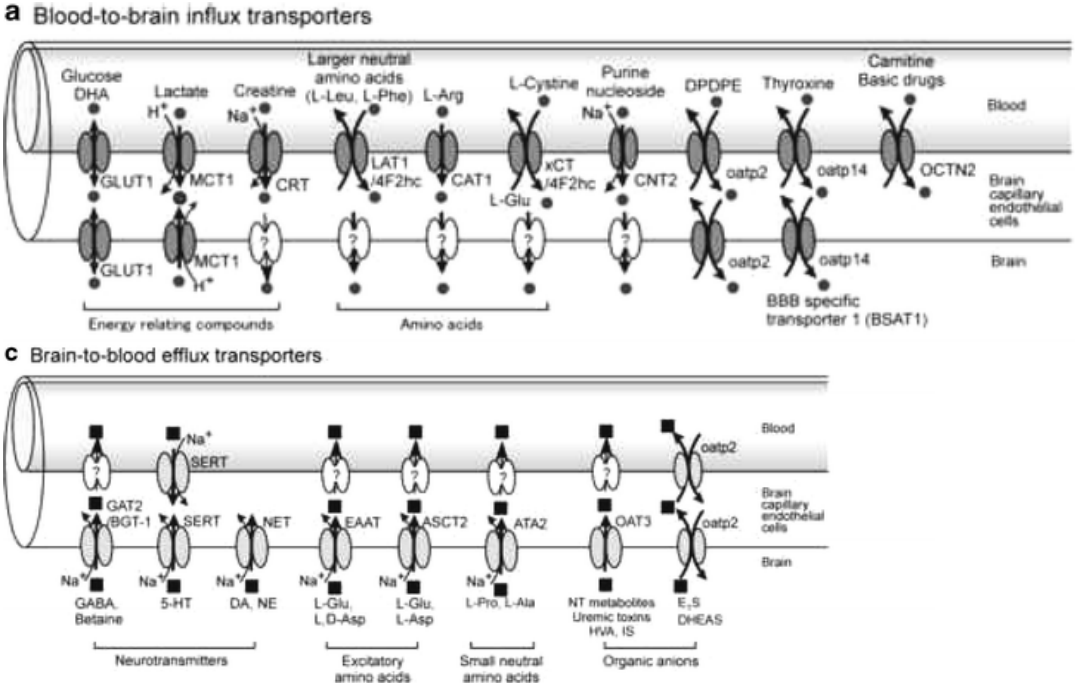

Transporters at the BBB. **a)** Transporters mediating the blood-to-brain influx transport. **c)** Transporters mediating the brain-to-blood efflux transport. Source: Figure 2 a, c from Ohtsuki and Terasaki (2007) [159].

3.6.1.3 The SLC38 gene family.

The SLC38 gene family is a family of sodium-coupled neutral amino acid transporters (SNATs) with system A and system N transport activities [106] (see Table 4). With the exception of SNAT4, glutamine is the favoured substrate throughout the family [106]. SLC38 transporters play an important role in the glutamate/GABA-glutamine cycle in brain (see section 3.5.3.2 and Figure 7).

System A subtypes SNAT1 (Slc38a1), SNAT2 (Slc38a2), and SNAT4 (Slc38a4), transport small, aliphatic amino acids (alanine, asparagine, cysteine, glutamine, glycine, methionine, and serine) and MeAIB** [106]. It has been suggested that SNAT2 is the responsible transporter for system A efflux transport at the BBB [146]. A unique characteristic of system A transport is that cytoplasmic amino acids can inhibit the uptake of extracellular amino acids via the transporter, a phenomenon called trans-inhibition [126]. Furthermore, most of SNAT1 and SNAT2 proteins are localized to intracellular organelles including endosomes [106]. System A is also known to be regulated by osmolarity, amino acid availability and hormonal stimuli [142].

** transport of MeAIB, 2-(methylamino)isobutyric acid, is a characteristic of system A transport

System N subtypes SNAT3 (Slc38a3) and SNAT5 (Slc38a5) transport small, zwitterionic amino acids with a narrower substrate profile than system A subtypes (glutamine, histidine, and asparagine) and with low affinity [106].

It is known that system A transporters can accumulate and maintain high intracellular concentrations of nonessential amino acids, like glutamine and alanine, which can then be used to accumulate essential amino acids via exchangers like ASCT2 [142], LAT1 and LAT2 [138] (tertiary active amino acid uptake system) (see section 3.6). System A can accumulate substrates to a much higher degree than the electroneutral transport of system N is able to. "Thus, glutamine transport via system N is readily reversible, whereas system A transport reverses only when the membrane is depolarized or when the intracellular sodium concentration is elevated" [142]. The presence of system N in addition to system A is probably important for the decision if a cell releases glutamine or accumulates it [142]. In general, expression of system N seems to indicate a glutamine releasing site [142].

3.6.1.3.1 The system A transporter SNAT1.

SNAT1 (Slc38a1; previously referred to as ATA1, GlnT, SA2, SAT1, or mouse NAT2), a sodium-dependent, pH-sensitive, neutral amino acid transporter of the system A subfamily. SNAT1 transports small aliphatic amino acids, preferentially alanine, asparagine, cysteine, glutamine, glycine, methionine, histidine, and serine, in an unidirectional, concentrative manner with 1:1 stoichiometry [106]. The primary effect of protons is to reduce the apparent affinity for sodium [106]. SNAT1 is predicted to have eleven transmembrane domains (TMD), with a large glycosylated loop between TMD V and VI, a short extracellular C-terminus, and a cytoplasmic N-terminus [106]. SNAT1 is predominantly expressed in brain, spinal cord, retina, placenta, and heart, but also in lung, skeletal muscle, spleen and intestine [106]. It is expressed in central glutamatergic and GABAergic neurons, in dopaminergic neurons of the substantia nigra, cholinergic motoneurons, and in retinal ganglion cells, but not in astrocytes [106]. On the other hand, Melone *et al.* [160] found that >95% of SNAT1 expressing cells are neurons, but that SNAT1 is also expressed in non-neuronal cells in leptomeninges, in luminal membranes of the ependyma [106], in the choroid plexus, and in astrocyte foot processes facing the abluminal membrane of the BBB. Functional studies by Sánchez del Pino *et al.* [79] demonstrated system A activity at the BBB. It was shown that system A activity is linked to the cell cycle and cell growth rate [106, 161], is inhibited by high concentrations of intracellular amino acids [161], and is up-regulated in mammalian cells

in response to amino acid deprivation [161]. SNAT1 may also play a role in driving metabolism and in providing the precursors for glutathione synthesis [106] (see Table 3). Recently we showed Snat1-mRNA to be expressed at very low levels in primary, non-cultured mouse brain microvascular endothelial cells, and to be linked to intraendothelial metabolism and cell proliferation [2].

3.6.1.3.2 The system N transporter SNAT3.

SNAT3 (Slc38a3; also referred to as SN1, NAT, or g17) is a system N, sodium-dependent cotransporter for small, zwitterionic amino acids like glutamine, asparagine, alanine, and histidine across membranes with 1:1 stoichiometry [106]. System N transport is proposed to be electroneutral, and not unidirectional [106].

SNAT3 transport is inhibited at low extracellular pH due to the proton-coupled countertransport, which may explain the reversibility of amino acid transport [106]. It is known that sodium binding to SNAT3 promotes amino acid uptake, a process which can be competitively inhibited by protons, and that proton binding promotes amino acid efflux [107]. At pH 6.0 SNAT3 releases glutamine, while at pH 8.0 glutamine is accumulated [142]. It was also shown that at high glutamine levels (~0.5 mM) SNAT3 mediates substrate uptake, while at low glutamine concentrations SNAT3 mediates efflux [107]. Therefore, SNAT3 can just generate a shallow amino acid concentration gradient between blood and brain, suggesting that glutamine uptake into cells is mainly mediated by system A transporters [107].

SNAT3 is reported to be expressed abundantly in liver, kidney, heart, skeletal muscle, and adipose tissue [106]. It was also shown that SNAT3 plays a role in hepatic ammonia detoxification and is involved in the renal response to acidosis [106]. In brain, SNAT3 is abundant in astrocytes, expressed in the choroid plexus and ependyma, but absent from neurons and oligodendrocytes. In the adult, SNAT3 was suggested not to be expressed in the vascular endothelium [162] (however, see section 5 for details). SNAT3 expression peaks at P14 with twice the adult level, showing also strong expression in the vascular endothelium, which disappears before P21 [163]. The peak in the expression of SNAT3 protein in the developing rat brain (twice the level seen in adult) coincides with increasing CNS levels of glutamate and GABA and a critical period in synaptogenesis [106]. Functional studies by Lee *et al.* [9] demonstrated system N activity at the BBB. Recently, Snat3-mRNA was shown to be expressed at very high levels in primary, non-cultured mouse brain microvascular endothelial cells, and to be linked to BBB transendothelial transport *in vivo* [2].

Generation of Snat3 knock-out ($^{-/-}$) animals was done by treating male C57BL/6J mice with the potent mutagen, N-ethyl-N-nitrosourea (ENU), resulting in offspring carrying a single nucleotide polymorphism. This mutation was a "C" to "T" mutation, known as "SLC38a3-Q263X", causing a premature stop codon deleting the second half of the protein [164]. Snat3$^{-/-}$ mice die within the first 3 weeks after birth [164]. They show growth retardation, display mild forms of ataxia with an uncoordinated gait, and neurological disturbances. After postnatal day 15-18, knock-out mice weigh significantly less than their wildtype or heterozygote littermates, with a larger mean relative brain weight in knock-out animals. [164] (see also section 5)

3.6.1.4 γ-Glutamyl cycle as possible link between luminal and abluminal transport.

In general, transporters in the plasma membrane are in a position to monitor extra- as well as intracellular amino acid concentrations and to integrate and coordinate intracellular events [126].

Transporters expressed at the luminal respective abluminal membrane could integrate the signals from both compartments, plasma and brain ISF, to respond to environmental changes and to keep the gradient over the BBB. One possible link between transport processes located to the luminal and abluminal membrane is the γ-glutamyl cycle (see Figure 11).

The activity of γ-glutamyl transpeptidase (GGT) is high in tissues that actively transport amino acids, such as the apical portion of the intestinal epithelium [8, 165]. In contrast, brain capillaries have a high GGT activity without being associated with active amino acid uptake from plasma [8]. Expression of GGT has been identified as indicator of the barrier phenotype in endothelial cells. Levels of GGT have been found to be decreased when endothelial cells are placed in culture, whereas treatment of endothelial cells with TGF-β increased GGT activity [166], indicating an expression correlating with differentiation [163].

The first reaction of the γ-glutamyl cycle (GGC) occurs extracellularly and is catalysed by GGT, an integral protein of the luminal membrane of brain endothelial cells [154, 167]. Subsequently, pyroglutamate (also known as oxoproline, the cyclized amide of glutamate) is produced intracellularly (see Figure 11) [8]. The GGC was proposed to be directly involved in amino acid transport, but this suggestion has been controversial (e.g., support [168], criticism [169]) [8, 165]. An alternative theory, proposed by Viña *et al.* [170-171] is that pyroglutamate acts indirectly by stimulating sodium-dependent amino acid transport and thereby the uptake of amino acids [7, 165]. The role of pyroglutamate as a regulator of sodium-dependent amino acid transport by the BBB was further supported by Lee *et al.* [8] who found that intracellular

pyroglutamate stimulates systems A and $B^{0,+}$ at the abluminal membrane by 70 and 20%, respectively. Hawkins *et al.* [165] found that pyroglutamate stimulates sodium-dependent transport of glutamate by 46%, and that it inhibits facilitative glutamate uptake in luminal membranes. Furthermore, the effect of pyroglutamate was found to be specific and not limited to glutamate, it stimulates system A [8] and ASC [165], but not system N [165]. System N transports glutamine, the only amino acid in brain ISF that has a similar concentration to that of plasma. Thus, glutamine appears to be treated differently [165]. It has been suggested that the GGC and luminal GGT serve to monitor the availability of amino acids to the brain, being at least part of a short-term regulatory mechanism that influences the accessibility and content of brain amino acids [8, 165].

In conclusion, pyroglutamate was shown to stimulate the sodium-dependent removal of glutamate from the brain ISF while simultaneously decreasing its plasma uptake [165], leading to an increased glutamate clearing efficiency from the CNS when the availability is excessive [8, 165].

Figure 11: γ-Glutamyl cyle – a possible (intracellular) link between luminal and abluminal transport processes.

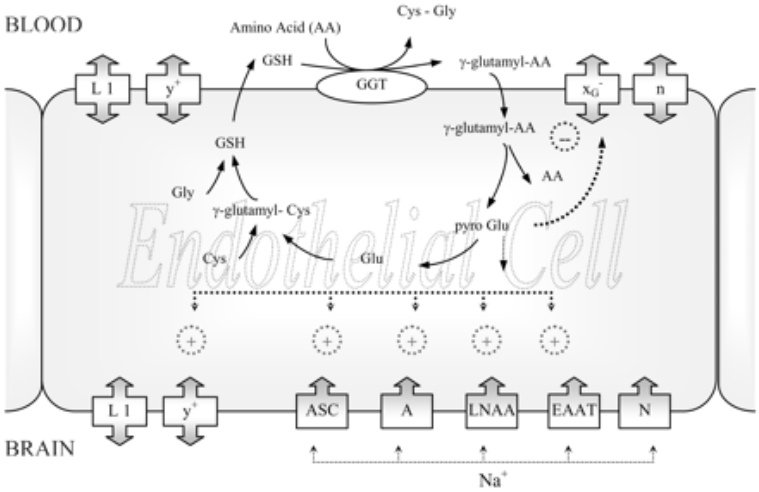

Scheme of the influence of pyroglutamate on amino acid transport across the BBB. γ-Glutamyl amino acids are formed at the outer surface of luminal membranes by transfer of the γ-glutamyl moiety of glutathione to extracellular amino acids, a reaction catalysed by GGT. The γ-glutamyl amino acids that result enter the endothelial cells by a transport system that is not shared by free amino acids. Intracellularly, γ-glutamyl amino acids are substrates of γ-glutamyl cyclotransferase, which converts the γ-glutamyl amino acids into pyroglutamate and the corresponding free amino acids. The subsequent conversion of pyroglutamate to glutamate by oxoprolinase is the rate-limiting step of the GGC [172]. The sodium-dependent transport systems $B^{0,+}$ [8], A [1, 8], ASC, Na^+-LNAA, EAAT, and y^+ [1], all located on the abluminal side, are activated by pyroglutamate, thereby reducing the net influx of amino acids to the brain [1]. N was the only system not stimulated [1]. The transport system L1 is distributed symmetrically between luminal and abluminal membrane and is not affected by pyroglutamate [1, 8]. Source: Figure 6 from Hawkins *et al.* (2006) [1].

3.6.2 Gene and protein expression of BBB transporters - a short review.

To keep brain homeostasis, the concentration of each amino acid has to be tightly regulated to vary within fixed limits [122]. Different biochemical agents, protein-protein interactions and signalling pathways are reported in the literature to regulate transporter expression, localization, and function at various levels in response to certain triggers, like substrate deprivation.

The knowledge on protein expression and localization of SLC members (see Figure 12 for overview), as well as their regulation, is less pronounced. One recent proteomics study identified and quantified the protein expression of several transport proteins and found Glut1 to be highest expressed in mouse brain capillaries, followed by 4F2hc, Taut, Lat1, and Asct2 [173]. Most effort so far was made to unravel gene expression pattern specific for BBB, recently also in different physiological situations. The anatomical gene expression of SLC members in the adult mouse brain is mapped in the Allen Brain Atlas [174], but their expression and distribution in the different brain cell types is still largely unknown. Dahlin *et al.* [175] discovered 36 SLC genes specifically enriched at the BBB, with ~70% being nutrient transporters and ~22% being amino acid transporters (Slc1a2, Slc3a1, Slc6a6, Slc6a20, Slc7a5, Slc7a11, Slc38a3, Slc38a5). Also in other studies, the expression of SLC members has been investigated by different approaches, broadening the knowledge of the single players of the BBB transportome [2, 173, 176-179]. Furthermore, the results of Lyck *et al*. [2] imply specific roles of the single transporters in the differentiated BBB, e.g. for transendothelial amino acid transport *in vivo* (Slc1a1, Slc3a2, Slc6a6, Slc7a1, Slc7a5, Slc38a2, Slc38a3, Slc38a5), and for providing amino acids for endothelial-cell metabolism (Slc7a6, Slc7a11, Slc38a1, Slc43a1-3).

Figure 12: Localization data available for amino acid transporters at the brain vasculature.

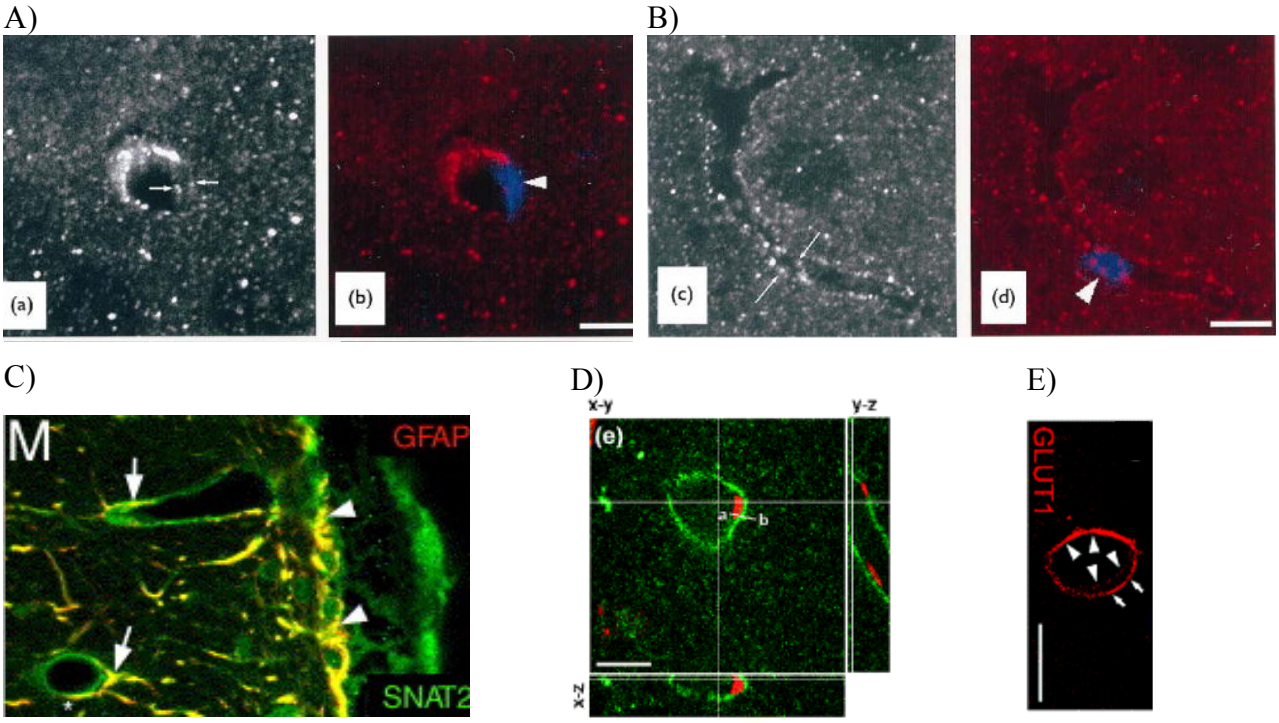

Studies to examine the localization of amino acid transporters at the BBB using immunohistochemistry are rare. **A)** Double line appearance of immunoreactivity for LAT1 (a) is indicated by arrows. (b) LAT1 (red) and nucleus (blue). Scale bar: 10 µm. Source: Figure 4 a, b from Matsuo *et al.* [150]; **B)** Double line appearance of immunoreactivity for 4F2hc (c) is indicated by arrows. (d) 4F2hc (red) and nucleus (blue). Scale bar: 10 µm. Source: Figure 4 c, d from Matsuo *et al.* [150]; **C)** SNAT2 (green) and GFAP (red) co-localize (yellow) in glia limitans (arrowheads) and in astrocytes (arrows) surrounding blood vessels (asterisks). Scale bar: 33 µm. Source: Figure 5 M from González-González *et al.* [180]; **D)** Immunohistochemical analysis of mASCT2 (green) in mouse brain. 3D-reconstructed image, nucleus in red. Scale bar: 10 µm; Source: Figure 6 e from Tetsuka *et al.* [124]; **E)** Immunostaining of GLUT1 (red) in the cerebral cortex of rat brain. Scale bar: 10 µm. Source: Figure 5 e from Hori *et al.* [181].

4. Original research article: Culture-induced changes in blood-brain barrier transcriptome: implications for amino-acid transporters *in vivo*.

This section contains an original research article that was accepted for publication in the Journal of Cerebral Blood Flow & Metabolism and published online on June 3rd 2009 [2].

My contribution to this paper concerns the data analysis of microarray experiments, qPCR analyses, and data presentation.
The cells were isolated, cultured, and the RNA extracted by Dr. Ruth Lyck with whom first authorship is shared.

Journal of Cerebral Blood Flow & Metabolism (2009) 29, 1491–1502

www.jcbfm.com

Culture-induced changes in blood–brain barrier transcriptome: implications for amino-acid transporters *in vivo*

Ruth Lyck[1,4], Nadine Ruderisch[2,4], Anton G Moll[2], Oliver Steiner[1], Clemens D Cohen[2,3], Britta Engelhardt[1], Victoria Makrides[2,5] and Francois Verrey[2,5]

[1]*Theodor Kocher Institute, University of Bern, Bern, Switzerland;* [2]*Institute of Physiology, University of Zurich, Zurich, Switzerland;* [3]*Clinic for Nephrology, University Hospital, Zurich, Switzerland*

Tight homeostatic control of brain amino acids (AA) depends on transport by solute carrier family proteins expressed by the blood–brain barrier (BBB) microvascular endothelial cells (BMEC). To characterize the mouse BMEC transcriptome and probe culture-induced changes, microarray analyses of platelet endothelial cell adhesion molecule-1-positive (PECAM1$^+$) endothelial cells (ppMBMECs) were compared with primary MBMECs (pMBMEC) cultured in the presence or absence of glial cells and with b.End5 endothelioma cell line. Selected cell marker and AA transporter mRNA levels were further verified by reverse transcription real-time PCR. Regardless of glial coculture, expression of a large subset of genes was strongly altered by a brief culture step. This is consistent with the known dependence of BMECs on *in vivo* interactions to maintain physiologic functions, for example, tight barrier formation, and their consequent dedifferentiation in culture. Seven (*4F2hc*, *Lat1*, *Taut*, *Snat3*, *Snat5*, *Xpct*, and *Cat1*) of nine AA transporter mRNAs highly expressed in freshly isolated ppMBMECs were strongly downregulated for all cultures and two (*Snat2* and *Eaat3*) were variably regulated. In contrast, five AA transporter mRNAs with low expression in ppMBMECs, including *y$^+$Lat2*, *xCT*, and *Snat1*, were upregulated by culture. We hypothesized that the AA transporters highly expressed in ppMBMECs and downregulated in culture have a major *in vivo* function for BBB transendothelial transport.
Journal of Cerebral Blood Flow & Metabolism (2009) **29,** 1491–1502; doi:10.1038/jcbfm.2009.72; published online 3 June 2009

Keywords: amino-acid transport; blood–brain barrier; brain microvascular endothelium; gene expression; solute carrier family SLC; tight junction

Introduction

In most regions of the brain, unlike in the peripheral vasculature, specialized capillaries form a selective blood–brain barrier (BBB) between the plasma and the surrounding brain parenchyma. The BBB microvascular endothelial cells (BMECs) are associated with pericytes (embedded within the endothelial cell basement membrane), perivascular antigen-presenting cells, astrocytic endfeet (with an associated parenchymal basement membrane), and neurons. Together this intricate cellular matrix comprises the neurovascular unit. Uniquely among endothelium, BMECs express contiguous tight junctions (TJ) sealing the paracellular diffusion pathway to most solutes. Likewise, the lack of fenestrae and extremely low pinocytotic activity inhibits the BMEC transcellular passage of molecules. In addition, to supply the high central nervous system (CNS) metabolic needs, BMEC express specific plasma membrane transporters for nutrients into and toxic metabolites out of the CNS. Although, through expression of TJs, numerous transport, and other specialized proteins, BMECs form the barrier proper; they alone do not account for all of the unique CNS microvascular cell properties. Rather, interactions with the complex cellular and extracellular matrix influence BMEC morphology, biochemistry, and function resulting in an endothelium

Correspondence: Dr F Verrey or Dr V Makrides, Institute of Physiology, University of Zurich, Winterthurerstrasse 190, CH-8057 Zurich, Switzerland. E-mail: verrey@access.uzh.ch or makrides@access.uzh.ch
[4]These co-authors contributed equally to this work.
[5]These co-authors contributed equally to this work.
This research was supported by Grant 31-108021/1 of the Swiss NF to FV and by the Functional Genomics Center Zurich.
Research performed at the TKI has been partially funded by the European Union's Seventh Framework Program (FP7/2007-2013) under grant agreements No. 201024 and No. 202213 (European Stroke Network).
Received 23 December 2008; revised 27 March 2009; accepted 11 May 2009; published online 3 June 2009

distinguishable from any other in the body (Engelhardt, 2003; Pardridge, 2005*b*).

Homeostatic brain interstitial fluid solute concentrations, which as for amino acids (AA) may differ significantly from plasma, are maintained in part by BMEC-regulated transendothelial transport. For AAs, tight control of brain availability is crucial because of involvement in a number of sensitive CNS pathways including neurotransmission and energy metabolism (Pardridge and Oldendorf, 1977). For example, the cerebrospinal fluid AA concentrations (with the exception of glutamine) are approximately 10-fold lower than in blood plasma (O'Kane and Hawkins, 2003). In general, AA movement across membranes is mediated by specialized transporter proteins belonging to several families of the solute carrier gene series (Slc). Throughout the body, Slc family transporters provide essential gatekeeping functions controlling uptake and efflux of physiologically crucial compounds (Hediger *et al*, 2004). Analogously to functions in kidney and gut epithelium, BBB transporters not only supply endogenous BMEC needs but are also key regulators of transendothelial fluxes participating in brain interstitial fluid homeostasis. Further, radiolabeled AAs are preferred tracers for intracranial tumor imaging by positron emission tomography (Lahoutte *et al*, 2004; Makrides *et al*, 2007). In addition, exploitation of carrier-mediated transporters such as AA transporters has been proposed as one promising avenue for therapeutics to reach CNS targets (Jones and Shusta, 2007; Ohtsuki and Terasaki, 2007; Pardridge, 2007). Therefore, identifying the BBB Slc transcriptome supports both understanding regulatory mechanisms as well as furthers key translational research (Neuwelt *et al*, 2008). Despite the molecular identification of a few BBB AA transporters, it is likely that several proteins potentially having an important *in vivo* function in BBB transendothelial AA transport have yet to be identified. However, the contributions of specific transporters to cellular housekeeping metabolism must be teased apart from functions in transendothelial transport.

One experimental approach for the study of normal and pathologic BBB physiology is the use of *in vitro* cell models. Models derived from mouse BMECs have the added advantages of being suitable for complementary *in vivo*/*in vitro* strategies and of the availability of specialized experimental techniques and tools, such as antibodies, microarrays, transgenic animal models. Indeed, *in vitro* mouse BBB models, for example, the primary mouse brain microvascular endothelial culture (pMBMEC) developed by Coisne *et al* (2005) or the immortalized mouse brain b.End5 endothelioma cell line (Rohnelt *et al*, 1997) have been applied to functional and other studies (Coisne *et al*, 2006; Lyck *et al*, 2003; Nottebaum *et al*, 2008). However, when removed from an *in vivo* context cultured BMECs rapidly dedifferentiate as indicated, for example, by loss of the characteristic *in vivo* BBB tight barrier (Couraud *et al*, 2003). Immortalization introduces further alterations in BBB phenotype. Conversely, identification of *in vitro*-specific changes in the BMEC transcriptome potentially reveals gene products with functions specific to the *in vivo* environment. Therefore, culture-induced decreases in AA transporter gene expression may reflect the diminished importance of transendothelial transport *in vitro* thereby highlighting possible transporter *in vivo* contributions in this capacity.

The aim of our study was to (1) determine the *in vivo* BMEC transcriptome, in particular for AA transporters, but also including several classes of genes whose products are important for differentiated BBB functions, that is, the TJ, ATP-binding cassette (ABC), and Slc family genes; and (2) catalogue culture-induced changes in gene expression. Therefore, we analyzed rapidly isolated and highly pure platelet endothelial cell adhesion molecule-1-positive (PECAM1$^+$) mouse brain microvascular endothelial cells (ppMBMEC) by cDNA microarray. Furthermore, we described differences in gene expression induced by primary culture and in the immortalized b.End5 endothelioma. Finally, the differential mRNA expression for a selected set of genes focusing on AA transporters was assessed by reverse transcription quantitative real-time PCR (RT-qPCR).

Materials and methods

All animal procedures were performed in accordance with Swiss legislation on the protection of animals and approved by the appropriate governmental authorities (permission numbers 55/04, 104/04, and 4/05).

Preparation of Mouse Brain Microvascular Cells

Microvascular brain capillaries were isolated by the method of Coisne *et al* (2005) as follows: for each preparation cortices from ten 4-week-old female C57BL/6 mice (Charles River, L'Arbresle, France) were isolated and outer vessels and meninges were removed. Preparations were pooled and homogenized in Hank's balanced salt solution containing 10 mmol/L 4-(2-hydroxyethyl)-1-piperazineethanesulfonic acid, and 0.1% bovine serum albumin. The homogenate was mixed with 30% dextran and centrifuged at 3000*g* for 25 mins at 4°C. The pellet containing the vascular fraction was resuspended and filtered through a 60 μm nylon mesh. The capillary-enriched filtrate was digested in DNase I (10 mg/mL), TLCK (0.147 mg/mL), and collagenase/dispase (2 mg/mL) for 30 mins at 37°C. The digestion was stopped by an excess of wash buffer and filtered through a 20 μm nylon mesh. The crude cell preparation of freshly isolated mouse brain endothelial cells (crude EC fraction) was either further purified by anti-PECAM1 magnetic bead sorting (noncultured ppMBMEC) or plated on Transwell filters for culture alone (single-cultured pMBMEC) or coculture with primary glial cells (cocultured pMBMEC).

Culture of Isolated Brain Capillaries

After washing and centrifugation, the crude EC fraction was resuspended in 3 mL of media (Dulbecco's modified Eagle's medium, 20% fetal bovine serum, 2% sodium pyruvate, 2% essential AA, 50 μg/mL gentamycin, and 1 ng/mL basic fibroblast growth factor). For culture, 100 μL of the cell suspension was seeded per Transwell filter insert (pore size 0.4 μm; Corning Costar Corporation, Cambridge, MA, USA). After 24 h, red blood cells, cell debris, and nonadherent cells were removed by two washing steps. Cells that were further cultured for a total of 5 days without passaging and in the absence of glial cells constituted the single-cultured pMBMEC condition. For cocultured pMBMECs, 24 h after isolation filters seeded with pMBMEC were washed (as described above) and placed into dishes containing lower chamber wells that had been previously seeded with mouse brain primary glial cells (see 'Preparation of primary glial cell cocultures' below) and grown for an additional 4 days as described for single-cultured pMBMECs.

Preparation of Primary Glial Cell Cocultures

Glial cells were isolated from 2- to 3-day-old mice as previously described (Coisne *et al*, 2005) and cultured in the lower wells of Costar two-chamber Transwell system (Corning Costar Corporation) for 3 weeks. At 3 weeks, glial cell cultures consisted of approximately 85% astrocytes (Coisne *et al*, 2005) and were then used for coculturing with pMBMECs.

Preparation of PECAM1$^+$-Purified Noncultured ppMBMECs

Freshly isolated MBMEC were immediately incubated with anti-PECAM1 antibody (Mec13.3)-coated sheep anti-rat IgG Dynabeads (Invitrogen Dynal AS; Invitrogen, LuBioScience GmbH, Lucerne, Switzerland) for 20 mins with mixing at 4°C in wash buffer (Hank's balanced salt solution, 10 mmol/L 4-(2-hydroxyethyl)-1-piperazineethanesulfonic acid, and 0.1% bovine serum albumin). Subsequently, beads were washed four times with wash buffer. For RNA isolation cells bound to beads were lysed by repeated trituration in 400 μL of RNAready kit lysis buffer (BioDiagnostik, University Bern, Bern, Switzerland) and lysates were collected separately from beads. To minimize RNA degradation and *de novo* RNA synthesis, from decapitation until RNA isolation (total time 5 to 6 h), cell preparations were maintained at 4°C to 10°C (with the exception of the 30 mins 37°C collagenase digestion).

RNA Extractions

For microarray analyses endothelial RNA was isolated from three individual preparations from four MBMEC sources: (1) noncultured PECAM1-purified ppMBMEC; (2) single-cultured pMBMEC; (3) cocultured pMBMEC; and (4) b.End5 endothelioma cell line (Rohnelt *et al*, 1997). RNA extractions were performed using RNAready kit (BioDiagnostik) according to the manufacturer's protocol including an on-column DNase digestion. In addition, for quantitative real-time PCR (qPCR), RNA was prepared from total mouse brain homogenates and mouse brain glial cell cultures using the RNAeasy kit (Qiagen AG, Hombrechtikon, Switzerland). Quality and quantity of all isolated RNAs were determined with a NanoDrop ND 1000 (NanoDrop Technologies, Wilmington, DE, USA) and a Bioanalyzer 2100 (Agilent, Waldbronn, Germany). The RNA integrity numbers in all cases were from 8.7 to 9.7 indicating minimal RNA degradation (Schroeder *et al*, 2006).

Microarray Analysis

The Mouse Genome 430 2.0 Arrays (Affymetrix UK, High Wycombe, UK) were used to compare gene expression for triplicate samples of RNAs isolated from MBMEC preparations. The cDNA preparation and labeling and microarray hybridizations were performed by the Functional Genomics Center Zurich. Briefly, cDNAs were prepared by RT (WT-Ovation Pico System; NuGEN, San Carlos, CA, USA) according to the manufacturer's protocol from total isolated RNAs. Single-stranded cDNA quality and quantity was determined using NanoDrop ND 1000 and Bioanalyzer 2100. Fragmented and biotin-labeled single-stranded cDNA targets were generated with the FL-Ovation cDNA Biotin Module V2 (4200-12; NuGEN) according to the manufacturer's protocol.

Three GeneChip Mouse Genome 430 2.0 were used for microarray hybridization of each sample condition (i.e., noncultured, single-cultured, cocultured, cell-line). The biotin-labeled cDNA targets were mixed in 220 μL of Hybridization Mix (Affymetrix Inc.; P/N 9007200) containing Hybridization controls and Control Oligonucleotide B2 (Affymetrix Inc.; P/N 900454). Samples were hybridized to GeneChip arrays for 18 h at 45°C. Arrays were washed using Affymetrix Fluidics Station 450 FS450_0004 protocol. An Affymetrix GeneChip Scanner 3000 (Affymetrix Inc.) was used to measure fluorescent intensities emitted by labeled targets and signals were saved to a CEL file format. Microarray data (CEL, CHP, and RMA files) are available at GEO with the accession number GSE14375.

Microarray Data Processing

Quality control measures were performed before performing statistical analysis. Quality control included visual inspection, adequate scaling factors (between 1 and 3 for all samples), and appropriate numbers of present calls calculated by application of a signed-rank call algorithm. CEL file date were normalized using RMAExpress 0.5 (Robust Multichip Average) (Bolstad *et al*, 2003) and Custom CDF version 10 (Mm430_Mm_REFSEQ.cdf) (Dai *et al*, 2005). The RMAExpress options background-adjustment and quantile normalization were enabled. To exclude probe sets in the lower end of the signal range, which have large signal variation, a cutoff value was defined as the maximal signal value obtained from non-murine Affymetrix-control probe sets multiplied by a factor

of 1.2. In this data set, the cutoff value was $\log_2 5.78$. Probe sets with a signal below cutoff in every array of the corresponding comparison, as well as Affymetrix control probe sets (prefix of 'AFFX'), were excluded from further analysis. To examine gene changes, we performed pairwise significance analysis between each of the cultured MBMEC conditions (single-cultured, cocultured and cell-line) and the noncultured ppMBMECs, that is, three comparisons with three versus three arrays each. The Excel-plugin of SAM, version 2.23A was used with the parameters *t*-test and 100 random permutations (Tusher *et al*, 2001). In each comparison, between 8,000 and 10,000 probe sets had a *q*-value below 5%. For all genes scored, the fold change (FC) was calculated by dividing the values from the cultured (single-cultured, cocultured, cell-line) conditions by the value from the noncultured condition. In addition, the sets of genes with mean expression ≥ 2 FC increased or decreased for each of the cultured samples relative to noncultured MBMECs were identified.

Quantitative Real-Time PCR Analyses

Selected sets of genes were tested either using SYBR Green or TaqMan real-time RT-qPCR as indicated in the text. With the exception of 18S rRNA primers (Applied Biosystems, Life Technologies, Carlsbad, CA, USA) primer sequences are listed in Supplementary Table 1. For each gene, the negative control cDNAs produced without RT enzyme were assayed in parallel and a reference (s16 ribosomal protein mRNA for SYBR Green and 18S rRNA for TaqMan qPCR reactions) was included. For validation of the PECAM$^+$1 MBMEC purification protocol, RNAs were analyzed by SYBR Green qPCR. For SYBR Green qPCR, RT was performed with SuperScript III First-Strand Synthesis System (Invitrogen) using random hexamers and qPCR was performed using the MESA GREEN qPCR MasterMix Plus (Eurogentec, Seraing, Belgium) according to the manufacturer's protocol. For confirmatory TaqMan qPCR analyses of the microarray experiments, pools were made by sample type from aliquots of the same noncultured, single-cultured, cocultured, and cell-line RNAs used for microarray. Reverse transcription of pooled RNA and RNA isolated from whole mouse brain and cultured mouse glial cells was performed with the TaqMan RT kit using random hexamers (Applied Biosystems). The cDNA was prepared from either 250 ng of total RNA (single-cultured, cell-line), 500 ng (total brain, glial cells), or 200 ng (cocultured, noncultured) of each pooled sample type. Quantitative real-time PCR (1 ng cDNA per reaction in triplicate) was performed according to the manufacturer's protocol using MicroAmp Fast Optical 96-Well Reaction Plates (Applied Biosystems). All qPCR reactions were performed using the Fast Real-Time PCR System 7500 (Applied Biosystems). Relative expression values were calculated according to the comparative ΔC_T method (relative expression $= 2^{-\Delta C_T}$, ΔC_T value = average C_T value of target − average C_T value of endogenous reference). After determination that the efficiency of a representative set of 15 primer pairs (including 18S rRNA) was in the range of 1.7 to 2.1, the idealized primer efficiency value of 2 was used for all relative expression calculations. The standard deviation of the ΔC_T value was calculated from the standard deviations (s) of the individual C_T values (s_1, s_2) using the following formula: $s = \sqrt{(s_1^2 + s_2^2)}$. Each SYBR Green value is from three independently prepared samples assayed in triplicate per run. TaqMan values are nonexperimental triplicate reactions performed on pools (by condition type) from the same RNA samples previously tested by microarray.

Statistical Analyses of Real-Time PCR (qPCR) Data

Statistical analyses of data from TaqMan qPCR reactions were calculated using one-way nonparametric analysis of variance followed by Dunnett multiple comparison tests, with the statistical significance set at $P < 0.05$.

Results

Freshly Isolated Mouse Brain Microvascular Endothelial Cells

To profile *in vivo BBB* gene expression, we rapidly isolated fresh PECAM1$^+$ MBMECs (ppMBMEC) from a crude EC fraction consisting of short capillary fragments, single ECs, erythrocytes, and glial cells (Supplementary Figure 1A and 1B). The nature of the purified ppMBMECs was confirmed by immunostaining of the TJ protein, Claudin5 (CLDN5), and nuclear staining. The images shown indicate erythrocytes were depleted and at least 95% of nucleated cells were ECs (Supplementary Figure 1B–1D). In addition, RNA samples were tested by qPCR (SYBR Green, s16 ribosomal protein mRNA endogenous reference) for the presence of specific cell-type markers (Table 1). The erythrocyte-specific hemoglobin β-chain (*Hbb-β1*) mRNA was reduced 98%, whereas the EC marker vascular endothelial cadherin (*Ve cadherin*) (CD144) remained essentially unchanged in all MBMECs. Furthermore, in ppMBMECs, glial fibrillar acidic protein (*Gfap*), an astrocyte-specific marker, was below the limit of detection. And, the pericyte marker platelet-derived growth factor β-receptor (*Pdgfr-β*) was reduced 90%. This is a respectable decrease considering pericytes share a common basal membrane with ECs. The neuron-specific synaptophysin (*Syp*) expression already very low in the crude EC fraction was below the detection limit in both purified and cultured MBMECs. Finally, 99% of the choroid plexus epithelial cell marker transthyretin mRNAs were removed from ppMBMECs. Thus qPCR data confirmed the high degree of endothelial ppMBMECs purity observed by microscopy.

MBMEC Gene Expression Changes in Culture

As diagrammed in Figure 1, gene expression was surveyed by Affymetrix cDNA microarray hybridizations (mouse array 430.2) from four sources of

Table 1 Assessment of PECAM1$^+$ ppMBMEC by qPCR

mRNA *Cell specificity*	*ppMBMECs* *Pecam1-purified*	*ppMBMECs* *Pecam1-purified*	*Crude EC fraction* *Freshly isolated*	*pMBMECs* *Single-cultured*	*Glial cells* *3-week cultures*
	C_T *target* C_T *reference*	*Expression relative to* s16 ribosomal protein			
VE-cadherin Endothelium	26.97 ± 0.05 28.11 ± 0.02	2.21 ± 0.078	3.42 ± 0.03	3.76 ± 0.02	0.060 ± 0.004
Hbb-β1 Erythrocytes	26.46 ± 0.06 27.65 ± 0.12	2.27 ± 0.21	144 ± 13.2	ND	ND
Gfap Astrocytes	ND	ND	0.017 ± 0.009	$9.5 \times 10^{-4} \pm 3.9 \times 10^{-4}$	18.2 ± 0.72
Pdgfr-β Pericytes	32.14 ± 0.08 27.65 ± 0.12	0.045 ± 0.005	0.44 ± 0.04	0.046 ± 0.003	0.232 ± 0.01
Syp Neurons	ND	ND	0.024 ± 0.005	ND	0.005 ± 0.001
Ttr Choroid plexus	32.01 ± 0.21 27.65 ± 0.12	0.049 ± 0.008	3.31 ± 0.03	0.014 ± 0.001	ND

MBMEC, mouse brain microvascular endothelial cell; ND, not detected (indicates C_T values below limit of detection).
Values are the mean ± s.d. of triplicate samples for gene expression relative to s16 ribosomal protein mRNA as determined by SYBR Green qPCR. For comparison, raw C_T values for Pecam1-purified ppMBMEC and reference gene samples are given. For ΔC_T values refer to Supplementary Table 3.

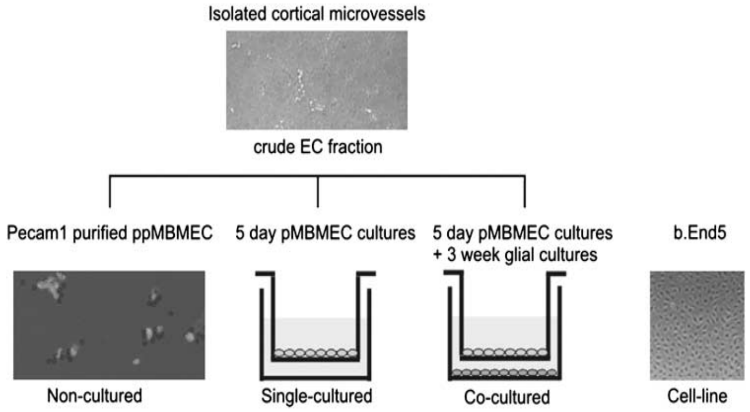

Figure 1 Mouse brain microvascular endothelial cell (MBMEC) RNAs tested by microarray and qPCR. A simple scheme outlining the source of each of the MBMEC RNA samples (i.e., noncultured, single-cultured, cocultured and cell-line) tested by Affymetrix microarray and by TaqMan qPCR.

MBMECs: (1) PECAM1$^+$-purified ppMBMECs (noncultured); (2) primary *in vitro* mouse BBB model, pMBMECs, (Coisne *et al*, 2005) cultured without passage either in the absence (single-cultured); or (3) noncontact presence of primary mouse brain glial cultures (cocultured); and (4) an *in vitro* BBB cell model, the immortalized mouse brain endothelioma b.End5 (cell-line) (Rohnelt *et al*, 1997). Selected gene expressions were verified by qPCR (TaqMan, 18S rRNA reference). Although, microarray values of the EC marker von Willebrand factor were 97% lower for the b.End5 cell-line compared with other MBMECs, *Ve cadherin*, *Pecam1*, and intercellular adhesion molecule-2 were well above cutoff for all MBMECs (data not shown). Furthermore, qPCR confirmed enrichment of *Ve cadherin*, *Pecam1*, and of the main BBB glucose transporter *Glut1* mRNAs for all MBMECs relative to glial cultures and total brain. It also confirmed the negligible contamination of ppMBMECs by pericytes, astrocytes, and neurons (Table 2). Finally, individual gene expression values obtained by microarray hybridization correlated well with qPCR data ($r^2 = \sim 0.7$; Supplementary Figure 2).

A total of 15,100 out of 21,625 annotated genes surveyed by microarray met the criteria to be considered expressed (i.e., mean hybridization signal above cutoff) for at least one MBMEC condition. Pairwise comparisons between the noncultured versus

Table 2 Expression of selected cell marker, TJ and ABC transporter mRNAs in MBMECs by qPCR

	Noncultured	*Noncultured*	*Single-cultured*	*Cocultured*	*Cell-line*	*Brain*[a]	*Glial*[b]
mRNA	C_T *values*	*Expression relative to 18S rRNA* ($\times 10^{-6}$)					
Cellular markers							
Pecam1	27.3 ± 0.08	234 ± 12.5	1216 ± 97.9	387 ± 11.7	490 ± 26.7	0.59 ± 0.18	ND
VE-cadherin	28.6 ± 0.33	90.5 ± 20.1	602 ± 43.8	197 ± 5.17	163 ± 8.84	0.23 ± 0.07	2.13 ± 0.34
Glut1 (Slc2a1)	25.3 ± 0.04	1066 ± 26	440 ± 206	306 ± 19.9	24.4 ± 1.95	5.69 ± 1.15	20.51 ± 2.4
Pdgfr-β	32.5 ± 0.12	5.60 ± 0.44	16.9 ± 1.03	12.1 ± 0.64	ND	1.39 ± 0.02	20.2 ± 0.50
Gfap	36.8 ± 0.33	0.41 ± 0.09	0.67 ± 0.22	0.30 ± 0.32	1.18 ± 0.04	29.0 ± 1.47	3068 ± 77
Syp	36.6 ± 0.24	0.32 ± 0.05	0.04 ± 0.02	ND	ND	90.6 ± 8.02	0.91 ± 0.11
18S rRNA	15.2 ± 0.32						
Tight junctions							
Zo1	28.1 ± 0.05	181 ± 6.44	201 ± 4.46	79.8 ± 6.98	90.4 ± 4.46	7.75 ± 0.95	31.0 ± 3.90
Cldn5	28.6 ± 0.17	130 ± 15.8	35.3 ± 7.33	19.2 ± 6.21	90.7 ± 7.99	0.24 ± 0.16	ND
Ocldn	29.4 ± 0.09	76.1 ± 4.59	62.5 ± 4.50	21.8 ± 1.56	1.34 ± 0.10	0.41 ± 0.09	0.09 ± 0.07
ABC transporters							
Mdr1a	28.5 ± 0.05	128.8 ± 4.71	27.4 ± 7.66	10.0 ± 0.15	1.08 ± 0.29	0.27 ± 0..67	0.09 ± 0.01
Mrp1	34.0 ± 0.13	3.00 ± 0.27	61.7 ± 9.62	27.9 ± 1.77	21.0 ± 1.60	2.77 ± 0.83	32.0 ± 2.27

MBMECs, mouse brain microvascular endothelial cells; ND, not detected (indicates C_T values below limit of detection).
Values are the mean ± s.d. of technical triplicates for gene expression relative to 18S ribosomal rRNA as determined by TaqMan qPCR. For comparison, raw C_T values for noncultured and reference rRNA samples are given. For ΔC_T values refer to Supplementary Table 3.
[a]Brain, total brain homogenates.
[b]Glial, 3-week mouse brain glial cultures.

cultured (single-cultured, cocultured, cell-line) conditions revealed a large proportion of mRNAs that were significantly differentially expressed ($q \leq 0.05$) (84% of expressed mRNAs in at least one, and 35% under all culture conditions) (Figure 2A). Further, approximately a third of all transcripts were ≥2 FC) for at least one cultured condition, with almost two-thirds of these likewise altered in a second condition (Figure 2B). Overall, nearly equal proportions of genes were up- and downregulated for each individual culture condition versus noncultured ppMBMECs. Moreover more than half of these genes were regulated in the same direction for a second culture condition (data not shown). Coculture with glial cells has been reported to partially restore the differentiated phenotype of primary brain ECs (Coisne *et al*, 2005). However, only 5% (724) of all genes (or 2% of genes with ≥2 FC) were expressed differently between the two primary culture conditions (data not shown). Thus even a brief culture step strongly impacted the expression of a large subset of MBMEC genes in a similar manner whereas noncontact coculture for 4 days with glial cells did not generally restore the *in vivo* BBB transcriptome phenotype.

MBMEC Gene Expression for TJ and ABC Transporters

We then sought to understand the impact of culture on two important classes of genes expressed *in vivo* by differentiated BMECs, the TJ protein and ABC transporters. The microarray gene expression data showed significant expression for 10 of the 26 investigated TJ-associated protein genes (Supplementary Table 2). For noncultured ppMBMECs, the mean hybridization signals for the zona occludens (*Zo1*, *Zo2*), occludin (*Ocldn*), claudins (*Cldn5*, *Cldn6*, *Cldn12*), endothelial-cell-selective adhesion molecule (*Esam*), and junctional adhesion molecules (*JamA*, *JamB*, *JamC*) were above cutoff. *Cldn5*, *Ocldn*, and *Zo1* were further assessed by qPCR with mRNA expression of *Zo1* > *Cldn5* > *Ocldn* (Table 2). In cocultured and cell-line but not in single-cultured samples *Zo1* mRNA decreased ~50%. Whereas, *Cldn5* levels were approximately 70% to 80% lower in single- and cocultured but not cell-line samples. Although *Ocldn* levels, which fell moderately in cocultured but not single-cultured, were strongly reduced in cell-line samples. Overall, b.End5 cell-line samples exhibited the greatest number and extent of downregulated TJ mRNAs (Supplementary Table 2).

Noncultured ppMBMEC expressed 26 ABC transporter genes above cutoff (Supplementary Table 2). The six with the highest mean signals were *Abc1a1* (ABC), *Abcb1a* (MDR1a/Pgp), *Abcc4* (MRP4), *Abcd3* (PMP68), *Abcg1* (WHITE), and *Abcg2* (ABCP). Approximately one-third were changed in cultured conditions. Notably, by qPCR as well as by microarray, *Mdr1a/Pgp* mRNA was found strongly downregulated for all cultured conditions (Table 2; Supplementary Table 2). Meanwhile, we found ≥2-fold increases of several genes that were expressed in noncultured ppMBMECs at levels near cutoff (*Abcb1b*/MDR1b, *Abcc1*/MRP1), or below (*Abcc3*/MRP3). In particular, as opposed to *Mdr1a*, after culture *Mrp1* mRNA increased to very high levels (Table 2; Supplementary Table 3).

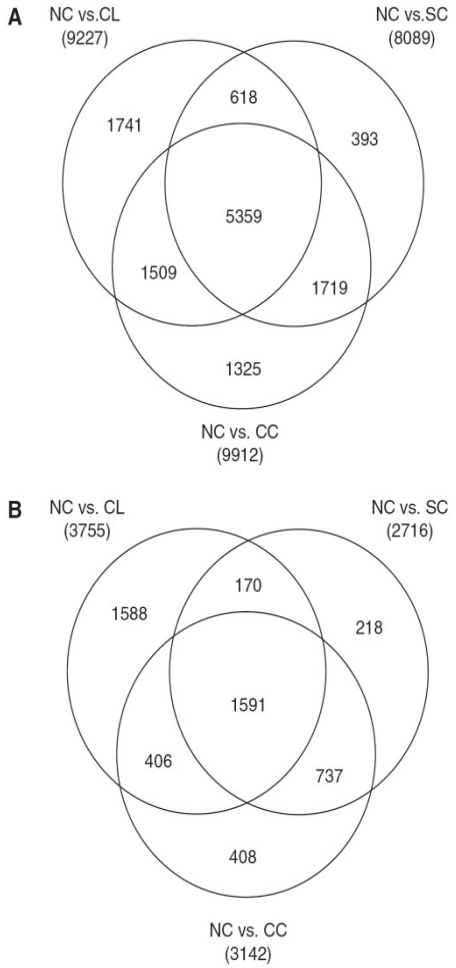

Figure 2 Changes in gene expression patterns for cultured relative to noncultured MBMECs. Venn diagrams of the pair-wise comparisons of mean gene expression as determined by microarray of noncultured (NC) ppMBMECs versus each cultured condition were constructed for single-cultured (SC), cocultured (CC), and cell-line (CL) MBMECs. Shown are overlapping sets of SC, CC, and CL, respectively versus NC for: (**A**) all significantly ($q < 0.05$) regulated genes and (**B**) genes with greater than or equal to twofold changes (≥ 2 FC) in expression. For both panels the total number of similarly regulated genes is identified within the circled subset for each pair-wise comparison. Abbreviations: MBMEC, mouse brain microvascular endothelial cell; ppMBMEC, PECAM1$^+$ MBMEC.

AA Transporter Gene Expression Profiles in MBMECs

Including AA transporters, 167 genes belonging to Slc families were expressed above cutoff in one or more MBMEC samples (Table 3; Supplementary Table 2). Consistent with previous reports, *Glut1* (*Slc2a1*), *Mct1* (*Slc16a1*), *Mct8/Xpct* (*Slc16a2*), *Oatp1a4* (*Slco1a4*), and *Oatp1c1* (*Slco1c1*) genes were found highly expressed in noncultured ppMBMECs (Enerson and Drewes, 2006; Kamiie *et al*, 2008; Pardridge, 2005*b*; Roberts *et al*, 2008; Shusta *et al*, 2002). Of these, four (*Mct1*, *Mct8*, *Oatp1a4*, and *Oatp1c1*) were reduced for all cultured MBMECs. Strikingly, qPCR confirmed that b.End5 *Glut1* expression was only ~2% of noncultured ppMBMEC mRNA levels (Table 2; Supplementary Table 3).

Almost half (31 out of 76) of annotated genes for known or putative AA transporters were expressed in one or more MBMEC condition (Table 3). Twenty AA transporters were selected for further testing by qPCR. In noncultured ppMBMECs, *4F2hc* was the most prominently expressed mRNA at levels 5- to 10-fold higher than *Lat1*, *Taut*, *Snat2*, *Snat5*, *Eaat3*, and *Cat1*. Next 10- to 20-fold lower were *Pat1*, *Lat4*, *y*$^+$*Lat2*, and *Cat3*. Some AA transporter mRNAs (*Eaat1*, *Eaat 2*, *Eaat 4*, *y*$^+$*Lat2*, *xCT*, *Snat1*, *Snat3*, *Lat3*, and *Eeg1*) were more highly expressed (~2- to 400-fold) in glial cultures than in ppMBMECs (Figure 3; Supplementary Table 3). With a few exceptions, for all cultured MBMECs, *4F2hc*, *Lat1*, *Taut*, *Snat5*, *Cat1*, *Cat3*, *Pat1*, *Eaat1* (except versus cocultured), and *Eaat2* (except versus single-cultured) were significantly ($P \leq 0.05$) downregulated compared with the noncultured ppMBMECs (Figures 3 and 4; Supplementary Table 3). Single- and coculture of MBMECs resulted in similar patterns of AA transporter expression; for both, *Snat5* showed the greatest down- and *Snat1* the highest upregulation. As for TJs and ABC transporters, b.End5 cell-line had a distinct AA transporter mRNA expression pattern. Notably, mRNAs for *Eaat1*, *Eaat2*, *Eaat3*, *Eaat4*, and *Snat5* were below the limit of detection. *Snat3* and *Lat1* mRNA levels, already strongly decreased in primary cultures, were from 3- to 20-fold lower in b.End5 cell-line samples. Although unlike in primary cultures, *Snat1* and *y*$^+$*Lat2* b.End5 expression did not increase above noncultured ppMBMEC levels (Figures 3 and 4; Supplementary Table 3). Taken together the data show that although the cell-line b.End5 gene expression deviated most from that of noncultured ppBMEC transcriptome patterns, even a brief culture step induced significant changes in the expression of many TJ, ABC, AA transporter and other Slc genes.

Discussion

Characterizing *in vivo* BMEC gene expression is one of the first steps in understanding the mechanisms regulating BBB transendothelial transport (Neuwelt *et al*, 2008). To address this aim, we freshly isolated noncultured PECAM1$^+$ ppMBMECs. Microscopy and qPCR data showed that we effectively prepared nearly pure ppMBMECs yielding high-quality RNA for microarray and qPCR analyses. In addition, we surveyed the impact of culture on the MBMEC transcriptome, finding a large proportion of the total transcriptome to be altered in a similar manner in all culture conditions. Although a main focus of this study was on defining AA transporter mRNA expression, we also investigated several classes of genes whose products serve essential physiologic

Table 3 Relative expression of Slc family AA transporter genes in MBMECs as determined by microarray

Gene	*Protein*	*Accession no.*	*Noncultured*	*Single-cultured*		*Cocultured*		*Cell-line*	
			Mean expression	*Fold changes relative to noncultured MBMEC*					
High-affinity glutamate and neutral AA transporter family									
Slc1a1	EAAT3	NM_009199	+++	NS	+++	NS	+++	−153.79	bc
Slc1a2	EAAT2	NM_001077514	+	−2.92	bc	−3.05	bc	−2.59	bc
Slc1a3	EAAT1	NM_148938	+	−2.46	bc	−2.92	bc	−4.57	bc
Slc1a4	ASCT1	NM_018861	+	2.44	++	NS	+	NS[a]	+
Slc1a5	ASCT2	NM_009201	+	NS[a]	+	2.29	+	NS[a]	+
Slc1a6	EAAT4	NM_009200	bc	3.26	+	4.39	+	NS[a]	bc
Heavy subunits of heteromeric AA transporters									
Slc3a1	rBAT	NM_009205	+	NS[a]	+	NS[a]	+	NS[a]	+
Slc3a2	4F2hc	NM_008577	+++	−3.56	+++	−3.63	+++	−4.64	+++
Sodium- and chloride-dependent neurotransmitter transporter family									
Slc6a6	TAUT	NM_009320	+++	−4.44	+++	−12.35	++	−18.70	++
Slc6a9	GLYT1	NM_008135	+	NS[a]	+	NS[a]	+	NS[a]	+
Slc6a17	NTT4	NM_172271	+	NS	+	NS	bc	NS	bc
Cationic amino-acid transporter/glycoprotein-associated family									
Slc7a1	CAT1	NM_007513	+++	−8.43	++	−8.56	++	−14.42	++
Slc7a3	CAT3	NM_007515	++	−12.43	bc	−13.58	bc	−4.67	+
Slc7a5	LAT1	NM_011404	+++	−5.88	+++	−5.10	+++	−16.68	++
Slc7a6	y$^+$LAT2	NM_178798	+	2.50	++	2.68	++	NS	+
Slc7a7	y$^+$LAT1	NM_011405	+	NS	+	NS	+	5.90	++
Slc7a8	LAT2	NM_016972	+	−2.15	bc	NS	bc	−3.57	bc
Slc7a11	xCT	NM_011990	bc	4.55	+	2.20	bc	NS[a]	bc
Mitochondrial carrier family									
Slc25a12	AGC1	NM_172436	+	NS[a]	+	NS	++	NS	++
Slc25a13	AGC2	NM_015829	bc	2.11	+	5.32	+	2.86	+
Slc25a15	ORC1	NM_011017	+	NS	+	NS	+	NS	+
Slc25a22	GC1	NM_026646	+	NS	+	NS	+	NS[a]	+
Slc25a26	SAMC	NM_026255	+	NS[a]	+	NS[a]	+	NS[a]	+
Proton-coupled AA transporter family									
Slc36a1	PAT1	NM_153139	++	NS	+	−2.41	+	NS	++
System A and N, sodium-coupled neutral AA transporter family									
Slc38a1	SNAT1	NM_134086	bc	3.45	+	4.07	+	NS	+
Slc38a2	SNAT2	NM_175121	+++	NS	+++	NS	+++	NS	+++
Slc38a3	SNAT3	NM_023805	+++	−18.68	+	−9.34	+	−28.34	+
Slc38a4	SNAT4	NM_027052	bc	NS	bc	8.30	+	NS[a]	bc
Slc38a5	SNAT5	NM_172479	+++	−18.36	+	−28.65	+	−358.28	bc
Sodium-independent, system L-like AA transporter family									
Slc43a2	LAT4	NM_173388	+	NS	+	NS[a]	+	−2.54	+

MBMEC, mouse brain microvascular endothelial cell; bc, below cutoff (probe set expression values ≤5.78); NS, not significant; +, probe set expression values >5.78–8; ++, probe set expression values >8–10; +++, probe set expression values >10; –, downregulation.
Probe sets of genes either showing expression below cutoff (bc) for all conditions or showing expression bc and $q > 0.05$ and/or fold change <2: *Slc1a7* (NM_146255); *Slc6a7* (NM_201353); *Slc6a14* (NM_020049); *Slc6a15* (NM_175328); *Slc6a16* (XM_355900; XM_914689); *Slc6a19* (NM_028878); *Slc6a20* (NM_011731); *Slc7a2* (NM_001044740; NM_007514); *Slc7a9* (NM_021291); *Slc7a10* (NM_017394); *Slc7a13* (NM_028746); *Slc16a10* (NM_028247); *Slc17a6* (NM_080853); *Slc17a7* (NM_182993); *Slc25a2* (XM_909128; XM_111757); *Slc25a18* (NM_001081048); *Slc32a1* (NM_009508); *Slc36a2* (NM_153170); *Slc43a1* (NM_024497; NM_001081349; NM_001083809).
[a]$q > 0.05$.

BMEC functions, namely TJ, ABC, and total Slc family members.

In Vivo Versus *In Vitro* Expression of TJ and ABC Protein Genes

The *in vivo* control of transendothelial transport depends critically on BMEC expression of contiguous TJs to prevent the paracellular passage of most solutes. Furthermore, the physiologically tight barrier is rapidly compromised when BMECs from most species are cultured *in vitro*. Indeed, *in vitro* cultured BMECs generally show reduced tightness and require specific culture conditions to develop barrier properties. To examine the effect of culture, we surveyed expression of a subset of TJ-associated protein genes. Our microarray results

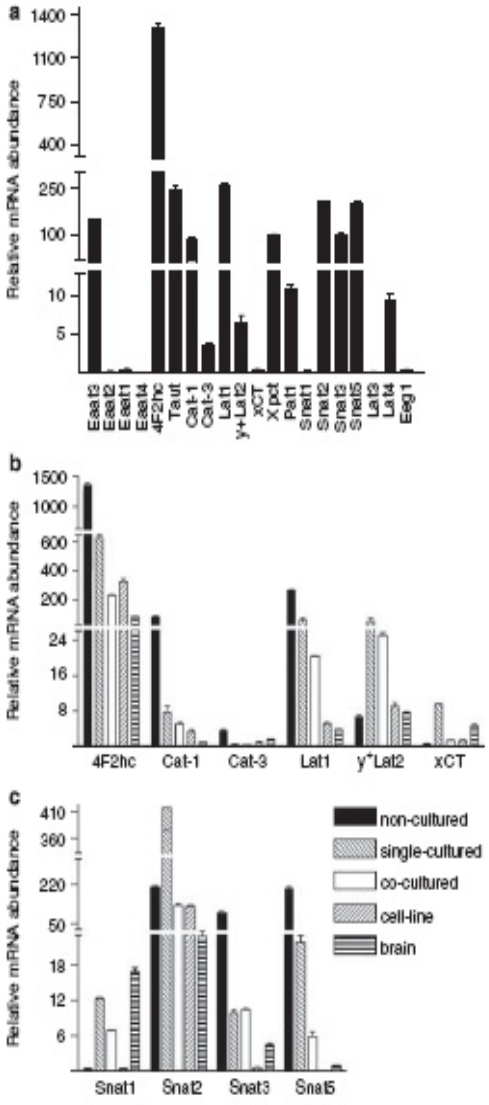

Figure 3 Assessment of AA transporter mRNA expression by qPCR. (**A**) Gene expression in noncultured ppMBMECs for all AA transporter mRNAs tested by qPCR. (**B**) Data for the *Slc3a* and *Slc7a*, and (**C**) *Slc38a* family AA transporter genes tested. For both **B** and **C**, in addition to the noncultured ppMBMECs, the expression of single-cultured, cocultured and cell-line MBMECs and for RNA isolated from total brain homogenates is shown. AA transporter gene mRNA values are the mean ± s.d. of technical triplicates relative to the endogenous reference, 18S rRNA (relative expression per 10^6), as determined by TaqMan qPCR. Supplementary Table 3 reports ΔC_T for all tested mRNAs. Statistical analyses of data were performed using one-way nonparametric analysis of variance followed by Dunnett multiple comparison tests. All pair-wise comparisons with noncultured ppMBMECs indicated statistically significant ($P \leq 0.05$) differences in AA transporter mRNA expression except: (1) *y+Lat2* in cell line and brain, and (2) *Snat1* in cell line. Abbreviations: MBMEC, mouse brain endothelial cell; ppMBMEC, PECAM1$^+$ MBMEC.

showing high expression of *Esam*, *Ocldn*, and *Cldn5* and low *Cldn1* and *Cldn3* levels (Table 2; Supplementary Table 2) in freshly isolated ppMBMECs are in agreement with a recent qPCR study reporting TJ mRNA expression in PECAM1$^+$-isolated MBMEC (Ohtsuki *et al*, 2008). However, unlike Ohtsuki and co-workers, we detected *Cldn12*, which is hypothesized to account for the presence of morphologically normal TJs in CLDN5 knockout mice (Nitta *et al*, 2003), expressed well above cutoff in all MBMECs (Supplementary Table 2).

Overall, single- and cocultured pMBMECs TJ transcript levels were comparable possibly because the coculture was only for a short period and in noncontact mode. In addition, *in vitro* brain microvascular cultures have also been shown to respond to glial coculture with enhanced tight barrier function without increased TJ protein expression (Hamm *et al*, 2004). Further, TJs were altered to a greater extent for b.End5 cell-line than for either primary cultured pMBMECs. For example, *Ocldn* mRNA plummeted ~60-fold to very low levels in b.End5 but was less strongly impacted by primary culture. The function of OCLDN in tight barrier formation is unclear. For example, OCLDN knockout mice have normal TJs (Saitou *et al*, 2000) whereas in humans decreased OCLDN and CLDN3 levels have been implicated in glioma-induced BBB disruption (Wolburg *et al*, 2003; Ishihara *et al*, 2008). In summary, many investigated TJ-associated protein genes were downregulated in culture, consistent with the known reduction of tight BMEC cell–cell contacts *in vitro*, and possibly, as a consequence of a switch from differentiative to proliferative cellular conditions.

The energy-dependent efflux of many metabolites and drugs by ABC transporters is an essential BMEC physiologic function, which also contributes to the 'BBB bottleneck' in CNS drug delivery (Loscher and Potschka, 2005; Pardridge, 2005*a*). In the current study, 30 genes from the 7 ABC subfamilies were identified by microarray as present above cutoff in one or more MBMEC samples (Supplementary Table 2). The noncultured cohort included 16 out of the 17 genes identified as expressed in rat brain microvessels by serial analysis of gene expression (Enerson and Drewes, 2006). For example, noncultured ppMBMEC expressed *Mrp1* mRNA consistent with the reported localization of MRP1 protein to luminal BMEC membranes (Soontornmalai *et al*, 2006). However, the sterol transporter *Abc1*, whose product is implicated in BBB regulation of β-amyloid, was among genes expressed above cutoff in noncultured ppMBMECs that was not found by serial analysis of gene expression (Akanuma *et al*, 2008). As for TJs, the cultured MBMEC (especially b.End5) ABC transporter gene expression profiles deviated from the *in vivo* transcriptome, particularly for some of the best-characterized members. For example, in b.End5 *Pgp/Mdr1a* and *Mrp4* were reduced whereas *Mdr1b* and *Mrp1* mRNAs were upregulated (Table 2; Supplementary Table 2). Taken together, the data

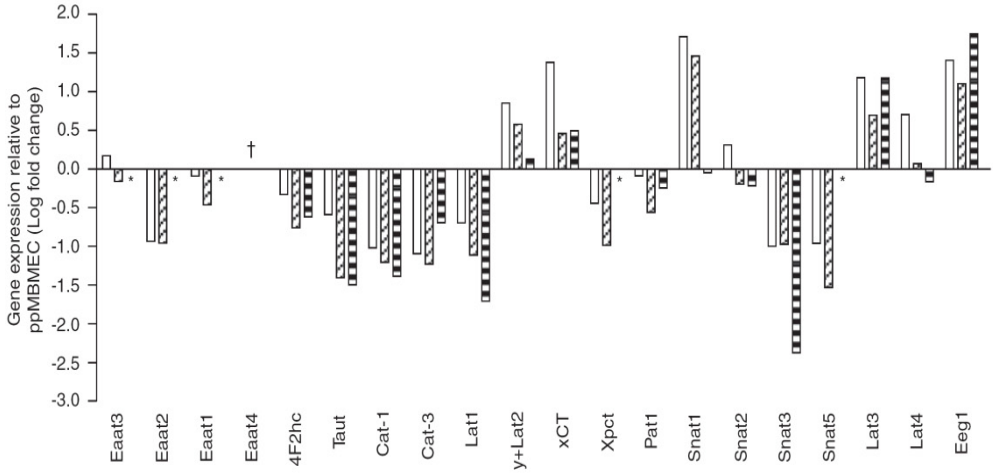

Figure 4 Fold changes in AA transporter genes expression by MBMEC cultures relative to noncultured ppMBMECs. Culture of MBMEC resulted in the downregulation of gene expression for the majority of the AA transporter genes tested. For each AA transporter gene, mRNA levels were measured by TaqMan qPCR relative to 18S rRNA. The fold change in gene expression relative to ppMBMEC by single-cultured (open), cocultured (diagonal hatched lines), and cell-line (horizontal hatched lines) samples was plotted as $\log_{10}$ fold change. For ΔC_T values refer to Supplementary Table 3. All pair-wise comparisons with ppMBMECs indicated statistically significant (one-way nonparametric analysis of variance followed by Dunnett multiple comparison tests, $P \leq 0.05$) differences in AA transporter mRNA expression except: (1) *Eaat2*, *Lat3* in single-cultured; (2) *Lat3*, *Lat4* in cocultured; and (3) *Snat1*, y^+*Lat2* in cell-line. Key: *, not detected in cell-line (b.End5) samples; †, not detected in ppMBMECs. Abbreviations: MBMEC, mouse brain microvascular endothelial cell; ppMBMEC, PECAM1$^+$ MBMEC.

suggest *in vitro* cell models may not necessarily faithfully replicate BBB *in vivo* ABC transporter substrate specificity and kinetics.

AA Transporter Expression: Implications for Transcellular Transport Functions

Microarray screening identified 25 AA transporters expressed in noncultured ppMBMECs. However, as AA transporters have various functions for the cells, their involvement in transendothelial transport must be distinguished from, for instance, their functions mainly supporting housekeeping cellular metabolism. Given that *in vitro* the proliferative cellular functions likely take precedence over differentiative ones (e.g., transendothelial transport), examining culture-induced changes may provide clues as to which transporters are central for each function. In this regard, Calabria and Shusta (2008) hypothesized a general decrease in critical BBB transendothelial vesicular transporter expression as a result of culture. We, too, identified decreasing expressions for particular Slc family members in cultured MBMECs (Figures 3 and 4; Supplementary Tables 2 and 3). For example, *Slc22a8*/*Oct1* and many of the Slc21/*Slco* family members, a number of which also transport drugs, were found highly expressed in noncultured ppMBMECs and strongly depressed *in vitro*. In contrast, cultured MBMECs continued to express high mRNA levels for most transporters of essential cellular substrates such as nucleoside sugars (*Slc35* family) and zinc (*Slc30* family) (Supplementary Table 2).

Consistent with the known function of LAT1-4F2hc in BBB transendothelial transport, for example of radiolabeled AA positron emission tomography tracers (Lahoutte *et al*, 2004; Makrides *et al*, 2007), its gene expression was high in noncultured cells and strongly downregulated under all culture conditions. Further, using this logic, we hypothesize other transporters with high mRNA levels in noncultured ppMBMECs and strongly reduced ones *in vitro* (CAT1, SNAT2, SNAT3, SNAT5, EAAT3, and TAUT) to mediate together with LAT1-4F2hc the bulk of transendothelial AA transport *in vivo* (Figures 3 and 4; Supplementary Table 3). Conversely, transporter mRNA upregulation *in vitro* (y^+*Lat2*, *Snat1*, *Snat2*, *xCT*, *Lat4*, *Lat3*, and *Eeg1*) is postulated to be in response to increased cellular AA demands for growth. One caveat is the likelihood some transporters have dual functions in both transendothelial AA transport and in providing AAs for cellular metabolism. Therefore, transporters such as 4F2hc, LAT1, EAAT3, SNAT2, SNAT5 whose mRNAs remain at high levels as well as those with variably regulated gene expression in culture (EAAT3 and SNAT2) likely contribute to both processes.

A next step required for understanding mechanisms underlying AA transendothelial transport is the localization of transporters to luminal and/or abluminal BMEC membranes. One hypothesis is that the low brain interstitial fluid to plasma AA concentrations

are maintained by active AA efflux driven by Na^+-dependent transporters whose expression is restricted to abluminal BMEC membranes (O'Kane and Hawkins, 2003). With a more comprehensive picture of the full *in vivo* AA transporter transcriptome in place this hypothesis can be directly assessed. In this regard, preliminary data indicate the possible localization to luminal BMEC membranes for at least one of the Na^+ symporters (data not shown).

Comparison of mRNA profiles of freshly isolated ppMBMECs with that of *in vitro* cultured ones identified >5,000 genes changed for all cultured conditions highlighting the large-scale changes in transcription induced by even a short period in culture. Taken together, we propose that culturing BMECs outside their *in vivo* context results in (1) the development of expression profiles reflecting the new metabolic demands imposed by *in vitro* culture; and (2) the loss of differentiative cues, which further leads to a rapid downregulation in the cellular expression of gene products involved in many BBB-specific functions. By these criteria, we hypothesize that 4F2hc, LAT1, CAT1, SNAT2, SNAT3, SNAT5, EAAT3, and TAUT may represent main components of the BBB transendothelial AA transport machinery.

Acknowledgements

We thank Marzanna Kuenzli-Gontarczyk, Hubert Rehrauer, Andrea Patrignani, Ulrich Wagner, and Ralph Schlapbach (Functional Genomics Center Zurich) for their support of this project.

Disclosure/Conflict of interest

The authors declare no conflict of interest.

References

Akanuma S, Ohtsuki S, Doi Y, Tachikawa M, Ito S, Hori S, Asashima T, Hashimoto T, Yamada K, Ueda K, Iwatsubo T, Terasaki T (2008) ATP-binding cassette transporter A1 (ABCA1) deficiency does not attenuate the brain-to-blood efflux transport of human amyloid-beta peptide (1–40) at the blood–brain barrier. *Neurochem Int* 52:956–61

Bolstad BM, Irizarry RA, Astrand M, Speed TP (2003) A comparison of normalization methods for high density oligonucleotide array data based on variance and bias. *Bioinformatics* 19:185–93

Calabria AR, Shusta EV (2008) A genomic comparison of *in vivo* and *in vitro* brain microvascular endothelial cells. *J Cereb Blood Flow Metab* 28:135–48

Coisne C, Dehouck L, Faveeuw C, Delplace Y, Miller F, Landry C, Morissette C, Fenart L, Cecchelli R, Tremblay P, Dehouck B (2005) Mouse syngenic *in vitro* blood–brain barrier model: a new tool to examine inflammatory events in cerebral endothelium. *Lab Invest* 85:734–46

Coisne C, Faveeuw C, Delplace Y, Dehouck L, Miller F, Cecchelli R, Dehouck B (2006) Differential expression of selectins by mouse brain capillary endothelial cells *in vitro* in response to distinct inflammatory stimuli. *Neurosci Lett* 392:216–20

Couraud PO, Greenwood J, Roux F, Adamson P (2003) Development and characterization of immortalized cerebral endothelial cell lines. *Methods Mol Med* 89:349–64

Dai M, Wang P, Boyd AD, Kostov G, Athey B, Jones EG, Bunney WE, Myers RM, Speed TP, Akil H, Watson SJ, Meng F (2005) Evolving gene/transcript definitions significantly alter the interpretation of GeneChip data. *Nucleic Acids Res* 33:e175

Enerson BE, Drewes LR (2006) The rat blood–brain barrier transcriptome. *J Cereb Blood Flow Metab* 26:959–73

Engelhardt B (2003) Development of the blood–brain barrier. *Cell Tissue Res* 314:119–29

Hamm S, Dehouck B, Kraus J, Wolburg-Buchholz K, Wolburg H, Risau W, Cecchelli R, Engelhardt B, Dehouck MP (2004) Astrocyte mediated modulation of blood–brain barrier permeability does not correlate with a loss of tight junction proteins from the cellular contacts. *Cell Tissue Res* 315:157–66

Hediger MA, Romero MF, Peng JB, Rolfs A, Takanaga H, Bruford EA (2004) The ABCs of solute carriers: physiological, pathological and therapeutic implications of human membrane transport proteins: introduction. *Pflugers Arch* 447:465–8

Ishihara H, Kubota H, Lindberg RL, Leppert D, Gloor SM, Errede M, Virgintino D, Fontana A, Yonekawa Y, Frei K (2008) Endothelial cell barrier impairment induced by glioblastomas and transforming growth factor beta2 involves matrix metalloproteinases and tight junction proteins. *J Neuropathol Exp Neurol* 67:435–48

Jones AR, Shusta EV (2007) Blood–brain barrier transport of therapeutics via receptor-mediation. *Pharm Res* 24:1759–71

Kamiie J, Ohtsuki S, Iwase R, Ohmine K, Katsukura Y, Yanai K, Sekine Y, Uchida Y, Ito S, Terasaki T (2008) Quantitative atlas of membrane transporter proteins: development and application of a highly sensitive simultaneous LC/MS/MS method combined with novel in-silico peptide selection criteria. *Pharm Res* 25:1469–83

Lahoutte T, Caveliers V, Camargo SM, Franca R, Ramadan T, Veljkovic E, Mertens J, Bossuyt A, Verrey F (2004) SPECT and PET amino acid tracer influx via system L (h4F2hc-hLAT1) and its transstimulation. *J Nucl Med* 45:1591–6

Loscher W, Potschka H (2005) Role of drug efflux transporters in the brain for drug disposition and treatment of brain diseases. *Prog Neurobiol* 76:22–76

Lyck R, Reiss Y, Gerwin N, Greenwood J, Adamson P, Engelhardt B (2003) T-cell interaction with ICAM-1/ICAM-2 double-deficient brain endothelium *in vitro*: the cytoplasmic tail of endothelial ICAM-1 is necessary for transendothelial migration of T cells. *Blood* 102:3675–83

Makrides V, Bauer R, Weber W, Wester HJ, Fischer S, Hinz R, Huggel K, Opfermann T, Herzau M, Ganapathy V, Verrey F, Brust P (2007) Preferred transport of *O*-(2-[18F]fluoroethyl)-D-tyrosine (D-FET) into the porcine brain. *Brain Res* 1147:25–33

Neuwelt E, Abbott NJ, Abrey L, Banks WA, Blakley B, Davis T, Engelhardt B, Grammas P, Nedergaard M, Nutt J, Pardridge W, Rosenberg GA, Smith Q, Drewes LR (2008)

Strategies to advance translational research into brain barriers. *Lancet Neurol* 7:84–96

Nitta T, Hata M, Gotoh S, Seo Y, Sasaki H, Hashimoto N, Furuse M, Tsukita S (2003) Size-selective loosening of the blood–brain barrier in claudin-5-deficient mice. *J Cell Biol* 161:653–60

Nottebaum AF, Cagna G, Winderlich M, Gamp AC, Linnepe R, Polaschegg C, Filippova K, Lyck R, Engelhardt B, Kamenyeva O, Bixel MG, Butz S, Vestweber D (2008) VE-PTP maintains the endothelial barrier via plakoglobin and becomes dissociated from VE-cadherin by leukocytes and by VEGF. *J Exp Med* 205:2929–45

O'Kane RL, Hawkins RA (2003) Na+-dependent transport of large neutral amino acids occurs at the abluminal membrane of the blood–brain barrier. *Am J Physiol Endocrinol Metab* 285:E1167–73

Ohtsuki S, Terasaki T (2007) Contribution of carrier-mediated transport systems to the blood–brain barrier as a supporting and protecting interface for the brain; importance for CNS drug discovery and development. *Pharm Res* 24:1745–58

Ohtsuki S, Yamaguchi H, Katsukura Y, Asashima T, Terasaki T (2008) mRNA expression levels of tight junction protein genes in mouse brain capillary endothelial cells highly purified by magnetic cell sorting. *J Neurochem* 104:147–54

Pardridge WM (2005*a*) The blood–brain barrier: bottleneck in brain drug development. *NeuroRx* 2:3–14

Pardridge WM (2005*b*) Molecular biology of the blood–brain barrier. *Mol Biotechnol* 30:57–70

Pardridge WM (2007) Drug targeting to the brain. *Pharm Res* 24:1733–44

Pardridge WM, Oldendorf WH (1977) Transport of metabolic substrates through the blood–brain barrier. *J Neurochem* 28:5–12

Roberts LM, Woodford K, Zhou M, Black DS, Haggerty JE, Tate EH, Grindstaff KK, Mengesha W, Raman C, Zerangue N (2008) Expression of the thyroid hormone transporters monocarboxylate transporter-8 (SLC16A2) and organic ion transporter-14 (SLCO1C1) at the blood–brain barrier. *Endocrinology* 149:6251–61

Rohnelt RK, Hoch G, Reiss Y, Engelhardt B (1997) Immunosurveillance modelled *in vitro*: naive and memory T cells spontaneously migrate across unstimulated microvascular endothelium. *Int Immunol* 9:435–50

Saitou M, Furuse M, Sasaki H, Schulzke JD, Fromm M, Takano H, Noda T, Tsukita S (2000) Complex phenotype of mice lacking occludin, a component of tight junction strands. *Mol Biol Cell* 11:4131–42

Schroeder A, Mueller O, Stocker S, Salowsky R, Leiber M, Gassmann M, Lightfoot S, Menzel W, Granzow M, Ragg T (2006) The RIN: an RNA integrity number for assigning integrity values to RNA measurements. *BMC Mol Biol* 7:3

Shusta EV, Boado RJ, Mathern GW, Pardridge WM (2002) Vascular genomics of the human brain. *J Cereb Blood Flow Metab* 22:245–52

Soontornmalai A, Vlaming ML, Fritschy JM (2006) Differential, strain-specific cellular and subcellular distribution of multidrug transporters in murine choroid plexus and blood–brain barrier. *Neuroscience* 138:159–69

Tusher VG, Tibshirani R, Chu G (2001) Significance analysis of microarrays applied to the ionizing radiation response. *Proc Natl Acad Sci USA* 98:5116–21

Wolburg H, Wolburg-Buchholz K, Kraus J, Rascher-Eggstein G, Liebner S, Hamm S, Duffner F, Grote EH, Risau W, Engelhardt B (2003) Localization of claudin-3 in tight junctions of the blood–brain barrier is selectively lost during experimental autoimmune encephalomyelitis and human glioblastoma multiforme. *Acta Neuropathol* 105:586–92

Supplementary Information accompanies the paper on the Journal of Cerebral Blood Flow & Metabolism website (http://www.nature.com/jcbfm)

Supplemental Information.

Read me – instructions for supplemental information viewing.

Supplemental information with: 1) Materials and methods for supplemental Figure 1, 2) Titles and legends to supplemental figures, and 3) 3 tables (microarray, qPCR data) is provided in a word file in compatibility mode.

Supplemental Figure 1) images showing purification quality, and Supplemental Figure 2) graph of microarray mean hybridization signals v.s. qPCR data are provided as JPEG files.

Supplemental Information.

Supplemental information (.doc) with: 1) Materials and methods for supplemental figure 1, 2) Titles and legends to supplemental figures, and 3) 3 tables (microarray, qPCR data). Two jpg files show: Supplemental Figure 1) images showing purification quality, and Supplemental Figure 2) graph of microarray mean hybridization signals v.s. qPCR data.

Supplemental Materials and Methods.

Immunofluorescent staining of PECAM-1 purified MBMECs.

For immunofluorescent staining of PECAM-1 purified ppMBMECs, 30 □L of washed cell suspensions were allowed to adhere for 20 min to poly-d-lysine coated glass slides (SIGMA, Buchs, Switzerland), before fixation in ice cold methanol followed by permeabilization for 15 min in 0.1% TX-100 in blocking solution (10% normal goat serum (NGS), PBS). Primary rabbit anti-Claudin5 antibody (10 μg/ml final concentration in blocking solution) was applied for 30 min, RT (Invitrogen, Basel, Switzerland). After washing, slides were incubated for 30 min, RT with Alexa Fluor 488 conjugated goat anti-rabbit IgG secondary antibody in blocking solution (Invitrogen, Basel, Switzerland). During the final wash, nuclei were counterstained with 1 μg/ml DAPI in PBS (SIGMA, Basel, Switzerland). Preparations were mounted in Mowiol (Calbiochem, VWR International, Dietikon, Switzerland) and imaged with either an inverted fluorescence microscope ((200x magnification; Axiovert 35, Carl Zeiss, Germany) or Z-sections captured (60 slices, 0.2 μm) by confocal microscopy (LSM 510 Meta, Carl Zeiss, Germany). Confocal image processing was carried out using the IMARIS software (Bitplane, Zurich, Switzerland).

Titles and Legends to Supplemental Figures.

Supplemental Figure 1: Characterization of purified endothelial cells from freshly isolated mouse brain microvessels. Representative 200X phase contrast image of endothelial cells is shown before (**A**) and after (**B**) anti-PECAM-1 magnetic bead sorting. In panel **B** the phase contrast image is overlaid with DAPI (blue) staining of nuclei. Beads can be seen as dark spheres. In panels **C** and **D**, DAPI (blue) staining is coupled with anti-Claudin5 (green) immunofluorescence of endothelial preparations following purification (ppMBMEC). Panel **D** shows a high magnification image of a single isolated microvessel. Scale bars are 50 □m for **B** and **C**, and 8 □m for panel **D**.

Supplemental Figure 2: Correlation of gene expression as determined by microarray vs. by qPCR. For each gene tested by both qPCR and microarray, mean C_T values (qPCR) were plotted against mean normalized hybridization signals (microarray) for each of the MBMEC samples: **A**) non-cultured (r^2=0.863 for genes with microarray mean hybridization signal above cutoff), **B**) single-cultured (r^2=0.674), **C**) co-cultured (r^2=0.591), and **D**) cell-line (r^2=0.676). The vertical line indicates the microarray cutoff level.

Supplemental Table 1: Real-Time RT-PCR primers and probes.

SYBR Green® primers and probes used for data shown in Table 1.

Target mRNA	*Accession number*	*Sequence*	
Hbb-β1	NM_008220	sense:	TGCATGTGGATCCTGAGAAC
		antisense:	GTGAAATCCTTGCCCAGGT
Pdgfrβ	NM_008809	sense:	TGCAGAGACCTCAAAAGGTG
		antisense:	CCTGATCTTCCTCCCAGAAA
Gfap	NM_010277	sense:	ACAGACTTTCTCCAACCTCCAG
		antisense:	CCTTCTGACACGGATTTGGT
Syp	NM_009305	sense:	AACAACAAAGGGCCAATGAT
		antisense:	TAGCCACATGAAAGCGAACA
Transthyretin (Ttr)	NM_013697	sense:	CATGAATTCGCGGATGTG
		antisense:	GATGGTGTAGTGGCGATGG
VE-Cadherin	NM_009868	sense:	GTTCAAGTTTGCCCTGAAGAA
		antisense:	GTGATGTTGGCGGTGTTGT
ribosomal protein S1(	NM_013647	sense:	GATATTCGGGTCCGTGTGA
(Rps16)		antisense:	TTGAGATGGACTGTCGGATG

TaqMan® primers and probes used for data shown in Figures 3 and 4, Table 3, Supplemental Table 3.

Target (mRNA)	*Accession number*	*Sequence*	
Claudin5	NM_013805	sense:	GCTCAGAACAGACTACAGGCACTTT
		antisense:	GTGGCCAACTGCGCATAGA
		probe:	AACTTGACCGACCTTTT
Zo1	NM_009386	sense:	ACGAGGCATCATCCCTAATAAGAA
		antisense:	ACCCGCTGTCTTTGGAAGTG
		probe:	AACAGTTAGCCAGTGTACAGTA
Occludin	NM_008756	sense:	TGACTATGCGGAAAGAGTTGACA
		antisense:	GGCACCAGAGGTGTTGACTTATAGA
		probe:	CAAAGTGAATGGCAAGCGATCATACCCA
Pecam1 (CD31)	NM_008816	sense:	TCCCCGAAGCAGCACTCT
	NM_001032378	antisense:	CCGCAATGAGCCCTTTCTT
		probe:	TCAGAGTCTTCCTTGCCCCA
VE-Cadherin	NM_009868	sense:	AGCGCAGCATCGGGTACT
(CD144)		antisense:	TCGGAAGAATTGGCCTCTGT
		probe:	CATCCGCAAGACCAGT
Pdgfrβ	NM_008809	sense:	CCAACGGCATGGACTTCTTAG
		antisense:	CCCTCGCAGATGAGCACATT

		probe:	TAAGAACTGTGTTCACCGAGAC
Hbb-β1	NM_008220	sense:	GACAAGCTGCATGTGGATCCT
		antisense:	CCCAGCACAATCACGATCATA
		probe:	AGAACTTCAGGCTCCTG
Synaptophysin	NM_009305	sense:	GGGCCAATGATGGACTTCCT
(Syp)		antisense:	GGATGAGCTAACTAGCCACATGAA
		probe:	CACAGCAGTGTTCGC
Gfap	NM_010277	sense:	CACAGCGGCCCTGAGAGA
		antisense:	GTCTGCAAACTTAGACCGATACCA
		probe:	ACTCAATACGAGGCAGTGGCCACCAGTAA
Slc2a1 (Glut1)	NM_011400	sense:	TCGTCGTTGGCATCCTTATTG
		antisense:	TGCATTGCCCATGATGGA
		probe:	CCAGGTGTTTGGCTTAG
Abcb1a (Mdr1a)	NM_011076	sense:	GCATTCTGGTATGGGACTTCCT
		antisense:	CCAATTAACACGGAAAAGAAGACA
		probe:	AATACTCTATTGGACAAGTGC
Abcc1 (Mrp1)	NM_008576	sense:	CAGTGGCATGCGCATCAA
		antisense:	TTTCTAGCTGCATTGGTGATCAA
		probe:	CTGTGGTGGGCGCTGTCTATCGTAAGGC
Slc1a1 (Eaat3)	NM_009199	sense:	TGTTGACTGGCTCCTGGACC
		antisense:	GCTCCAGCTCCTTCTTCGAGA
		probe:	ATGCGTTTGGGACGGGCATCG
Slc1a2 (Eaat2)	NM_001077514	sense:	TGCTCATCCTCCCTCTTATCATC
		antisense:	GGCCGCTGGCTTTAGCAT
		probe:	AGTTTAATCACAGGGTTGTC
Slc1a3 (Eaat1)	NM_148938	sense:	GAAGCCATCATGCGATTGGT
		antisense:	CCCTGCGATCAAGAAGAGGAT
		probe:	CGGTGATAATGTGGTATGC
Slc1a6 (Eaat4)	NM_009200	sense:	CCCCAGGCAGGACTGGTTA
		antisense:	TTGTACGAAGTCGGTCAAGGAA
		probe:	TGATTGTGCTCACATCCGTCGGC
Slc3a2 (4F2hc)	NM_008577	sense:	GTTTTTGAATGCCACTGGCA
		antisense:	AAAGTCTGCGAGGAGTCCTGC
		probe:	ATGGTGCAGCTGGAGTGTGTCGCA
Slc6a6 (Taut)	NM_009320	sense:	GCAACGTCTGGCGTTTCC
		antisense:	AGGCCGCTCCCAAACAG
		probe:	TGCGTTCCTCATACCGT
Slc7a1 (Cat-1)	NM_007513	sense:	TGAGAAGTCCCACGAGTCTTACAG
		antisense:	TTCCGGCGCAGCATCT
		probe:	ATTCGCTCAGCACAATG
Slc7a3 (Cat-3)	NM_007515	sense:	CACTGACCTCGTGGACCTCAT

		antisense:	TCTTCAACACTCTTCATTTCCTGATC
		probe:	TTGCTCACTCCCTGGTGTCCATTTGTGT
Slc7a5 (Lat1)	NM_011404	sense:	GGAGGATGGAACTATCTGAATTTTG
		antisense:	GGTTGGTAGAGAGGGTAGTGAAATAGG
		probe:	CTACAGGAACCTGCCCCTGGCCA
Slc7a6 (y^+Lat2)	NM_178798	sense:	TACATCCTGACCAACGTGGC
		antisense:	ATGCCGAATGTCTGGTCAGC
		probe:	TCCATAAGAGTGACGCTGTGCCTGTGA
Slc7a11 (xCT)	NM_011990	sense:	TGGAACTGCTCGTAATACGCC
		antisense:	GGTTCCAGGATGTAGCGTCC
		probe:	TGGAGCTACTGCTGTGATATCCCTGGCAT
Slc16a2 (Xpct)	NM_009197	sense:	GCCGCTGTTGCTTTCATTG
		antisense:	GCAGCGACAACCAAACAGAAT
		probe:	CTCCTTCACCAGCTCCCTAAGCCTGC
Slc36a1 (Pat1)	NM_153139	sense:	TCTGCTGTGTCTACTTCGTGTTTCT
		antisense:	GTTGGTGGTGGTCCCATTG
		probe:	AACTTTAAGCAGGTGATAGAG
Slc38a1 (Snat1)	NM_134086	sense:	CGCGTGCACACCAAAGTATG
		antisense:	AGATTGGCAGGACGGACG
		probe:	TACCAACCATCGCCTTCGCGTTTG
Slc38a2 (Snat2)	NM_175121	sense:	CCAATGAGATCCGTGCAAAA
		antisense:	TGGACCCAATCCAGCACAAT
		probe:	TCTGTGTTTTCTCCTGAGTGGCATAGTGGTG
Slc38a3 (Snat3)	NM_023805	sense:	CGAATCATGCCCACTGACAA
		antisense:	AACCGCAGCGAAACAAAGG
		probe:	AGCCTGCAAGATCCACCCCTAAAATCCT
Slc38a5 (Snat5)	NM_172479	sense:	CCCTCACTGTGCCTGTTGTG
		antisense:	CTTGCTTGGAAAGAGCAGCTG
		probe:	CCCTATCCGCCGAGCCCTCCA
Slc43a1 (Lat3)	NM_001081349	sense:	CCCTGAATGAGAATGCTTCCTT
		antisense:	ATGGCATTGGTGAGCTTTTGT
		probe:	AGCACCAAGTTCACTAGACCACGCTACCG
Slc43a2 (Lat4)	NM_173388	sense:	GCTGATTGCATATGGAGCAAGTAAC
		antisense:	CGAAGTGAACGTCATGCACAT
		probe:	CTCTCTGTGCTCATCTTTATCGCCTTGGC
Slc43a3 (Eeg1)	NM_021398	sense:	GCTACATCTTTGACCGCTTCAA
		antisense:	CGCAGGTGTAGAAAAATATGGCTAT
		probe:	ACTACTGTGGCCCGCC

Supplemental Table 2. Mean expression and fold changes of [a]TJ, [b]ABC and [c]non-AA transporter [d]Slc family genes in [e]MBMECs determined by microarray.

Gene / alias	**Accs. no.**	**Non-cultured**	**Single-cultured**		**Co-cultured**		**Cell-line**	
		Mean expression (log_2)	*[a]FC*	*[b]ME*	*FC*	*ME*	*FC*	*ME*
			Tight junction protein genes					
Zo1	NM_009386	+++	n.s.	+++	n.s.	+++	n.s.	+++
Zo2	NM_011597	+++	n.s.[1]	+++	n.s.[1]	+++	-3.09	++
Occludin	NM_008756	+++	n.s.	+++	-2.50	+++	-61.54	+
Claudin5	NM_013805	+++	n.s.	+++	n.s.	+++	n.s.	+++
Claudin6	NM_018777	+	n.s.	+	n.s.[1]	+	-4.54	bc
Claudin12	NM_022890	+++	n.s.[1]	+++	n.s.	+++	n.s.	+++
JamA	NM_172647	+++	n.s	+++	n.s.	+++	-5.62	++
JamB	NM_023844	+++	-11.46	++	-5.16	++	-5.18	++
JamC	NM_023277	+	n.s.	+	2.10	+	6.67	++
Esam	NM_027102	+++	n.s.	+++	n.s.	+++	n.s.	+++
			ABC transporter genes					
Abca1 / ABC1	NM_013454	+++	n.s[1]	+++	n.s.[1]	+++	-4.98	+
Abca2 / ABC2	NM_007379	+	n.s.[1]	+	n.s.	bc	n.s.[1]	+
Abca3 / ABC3	NM_001039581	++	n.s.[1]	++	n.s.[1]	++	n.s.[1]	++
Abca4 / ABC10	NM_007378	+	4.53	++	5.17	++	n.s.	+
Abca5 / ABC13	NM_147219	++	2.18	++	2.02	++	-18.47	bc
Abca7 / ABC51	NM_013850	+	n.s.[1]	+	n.s.[1]	+	n.s.	+
Abcb1a / Mdr1a; Pgp	NM_011076	+++	-4.75	+++	-5.45	+++	-62.64	+
Abcb1b / Mdr1b	NM_011075	bc	12.13	++	12.91	++	4.59	+
Abcb2 / TAP1	NM_013683	++	n.s.	+	n.s.	+	n.s.[1]	+

Abcb3 / TAP2	NM_011530	++	n.s.	+	n.s.	++	n.s.	++
Abcb6	NM_023732	++	n.s.	++	n.s.	++	n.s.[1]	++
Abcb8	NM_029020	+	n.s.[1]	+	n.s.[1]	+	n.s.	+
Abcb10 / ABCB12	NM_019552	+	n.s.[1]	+	n.s.[1]	+	n.s.	+
Abcc1 / Mrp1	NM_008576	+	5.92	+++	6.11	+++	3.70	++
Abcc3 / Mrp3	NM_029600	bc	8.99	+	13.51	+	18.45	++
Abcc4 / Mrp4	NM_001033336	+++	-2.03	+++	-2.13	+++	-6.24	++
Abcc5 / Mrp5	NM_176839	++	n.s.	++	n.s.[1]	+	n.s.	++
	NM_013790	+	n.s.[1]	+	n.s.	+	n.s.	+
Abcc6 / Mrp6	NM_018795	+	-9.43	bc	-11.03	bc	-16.14	bc
Abcc9 / Sur2	NM_001044720	+	-6.72	bc	n.s.[1]	+	-2.27	bc
Abcd1 / Ald	NM_007435	++	n.s.	+	n.s.	+	-2.04	+
Abcd3 / Pmp68	NM_008991	+++	n.s.[1]	+++	n.s.[1]	+++	n.s.[1]	+++
Abcd4 / P69r	NM_008992	++	n.s.	++	n.s.	++	n.s.[1]	++
Abce1 / Oabp	NM_015751	++	n.s.	+++	n.s.	+++	n.s.	+++
Abcf1 / ABC50	NM_013854	++	n.s.	++	n.s.	++	n.s.[1]	++
Abcf2 / Drr3	NM_013853	++	n.s.[1]	++	n.s.[1]	++	n.s.	++
Abcf3 / AI326318	NM_013852	++	n.s.[1]	++	n.s.[1]	++	n.s.[1]	++
Abcg1 / WHITE	NM_009593	+++	n.s.[1]	++	n.s.	++	n.s.[1]	+++
Abcg2 / ABCP	NM_011920	+++	n.s.	+++	-2.76	+++	n.s.	+++
Abcg3 / ABCP2	NM_030239	+	n.s.[1]	+	n.s.[1]	+	-11.19	bc
		Non-AA Slc transporters						
		Facilitative GLUT transporter family						
Slc2a1 / Glut1	NM_011400	+++	n.s.	+++	n.s.	+++	-3.96	+++
Slc2a8 / Glut8	NM_019488	+	n.s.	+	n.s.	+	n.s.	+

Slc2a9 / Glut9	NM_001102414	++	n.s.[1]	++	n.s.[1]	++	5.78	+++
Slc2a10 / Glut10	NM_130451	+	n.s.	+	n.s.	+	2.11	+
Slc2a12 / Glut12	NM_178934	+	-2.40	bc	-2.64	bc	-2.63	bc
Bicarbonate transporter family								
Slc4a2 / Ae2	NM_009207	++	n.s.[1]	++	n.s.[1]	++	n.s.	++
Slc4a4 / Nbce1	NM_018760	bc	n.s.[1]	+	n.s.[1]	bc	-2.48	bc
Slc4a7 / Nbcn1	NM_001033270	+	n.s.	++	n.s.	++	2.36	++
Sodium glucose cotransporter family								
Slc5a2 / Sglt2	NM_133254	++	n.s.[1]	+	n.s.	+	n.s.	+
Slc5a3 / Smit	NM_017391	++	2.03	++	n.s.[1]	++	n.s.[1]	++
Slc5a6 / Smvt	NM_177870	++	-8.30	+	-9.61	+	-13.19	bc
Sodium- and chloride- dependent neurotransmitter transporter family								
Slc6a8 / Crtr	NM_133987	++	n.s.	++	n.s.	++	n.s.	++
Slc6a13 / Gat2	NM_144512	+	n.s.[1]	++	-2.11	++	n.s.[1]	++
Na^+/H^+ exchanger family								
Slc9a1 / Nhe1	NM_016981	++	n.s.	++	n.s.[1]	++	n.s.	++
Slc9a2 / Nhe2	NM_001033289	++	-5.21	+	-3.57	+	-8.52	bc
Slc9a5 / Nhe5	NM_001081332	+	n.s.[1]	+	n.s.	+	2.50	+
Slc9a6 / Nhe6	NM_172780	+	n.s.[1]	+	n.s.[1]	+	n.s.[1]	+
Slc9a8 / Nhe8	NM_1489291	+	n.s.[1]	+	n.s.[1]	+	n.s.	+
Sodium bile salt cotransport family								
Slc10a1 / Ntcp	NM_011387	+	-3.59	bc	-6.85	bc	-4.88	bc
Slc10a3 / P3	NM_145406	++	n.s.[1]	++	n.s.[1]	+	n.s.[1]	++
Proton coupled metal ion transporter family								
Slc11a1 / Nramp1	NM_013612	+	6.16	++	6.87	++	-2.60	bc
Slc11a2 / Dmt1	NM_008732	++	n.s.[1]	++	n.s.	++	n.s.[1]	++

		Electroneutral cation-Cl cotransporter family						
Slc12a2 / Nkcc1	NM_009194	++	3.04	+++	2.14	+++	n.s.	+++
Slc12a4 / Kcc1	NM_009195	++	n.s.	++	n.s.	++	n.s.[1]	++
Slc12a6 / Kcc3	NM_133648	+++	n.s.	+++	n.s.	+++	n.s.[1]	+++
Slc12a7 / Kcc4	NM_011390	++	2.21	++	n.s.[1]	++	n.s.[1]	++
Slc12a9 / Cip	NM_031406	+	n.s.[1]	+	n.s.	+	n.s.	++
		Proton oligopeptide cotransporter family						
Slc15a3 / Pht2	NM_023044	bc	2.28	+	3.37	+	n.s.	bc
Slc15a4 / Pht1	NM_133895	++	n.s.[1]	++	n.s.[1]	++	n.s.	++
		Monocarboxylate transporter family						
Slc16a1 / Mct1	NM_009196	+++	-10.93	+	-8.07	+	-24.66	+
Slc16a2 / Xpct	NM_009197	+++	-6.08	++	-6.11	++	-114.77	bc
Slc16a3 / Mct4	NM_0010386546	bc	4.93	+	18.02	++	n.s.	+
Slc16a4 / Mct5	NM_146136	+++	-18.52	+	-19.55	+	-39.23	+
Slc16a6 / Mct7	NM_001029842	++	n.s.	++	3.53	++	n.s.[1]	++
	NM_134038	++	n.s.	++	3.53	++	n.s.[1]	++
Slc16a9 / Mct9	NM_025807	++	n.s.[1]	++	-2.02	++	-11.33	+
Slc16a11 / Mct11	NM_153081	++	-2.69	+	-3.55	+	-3.35	+
Slc16a12 / Mct12	NM_172838	+	-2.61	bc	n.s.	+	14.46	+++
Slc16a13 / Mct13	NM_172371	+++	n.s.	++	n.s.	++	n.s.	++
		Vesicular glutamate transporter family						
Slc17a5 / Sialin	NM_172773	+	n.s.[1]	+	n.s.	+	2.06	++
		Vesicular amine transporter family						
Slc18a2 / Vmat2	NM_172523	++	n.s.[1]	++	n.s.[1]	++	3.51	++
		Folate/thiamine transporter family						
Slc19a1 / Rft	NM_031196	+	n.s.	+	n.s.[1]	+	n.s.	+

Slc19a2 / ThTr1	NM_054087	+	n.s.	+	n.s.	++	n.s.	+
Slc19a3 / ThTr2	NM_030556	+++	-57.64	bc	-56.76	bc	-189.08	bc
Type III Na^+-phosphate cotransporter family								
Slc20a1 / PiT-1	NM_015747	++	n.s.	+++	2.70	+++	2.05	+++
Slc20a2 / PiT-2	NM_011394	+	n.s.	+	n.s.	+	n.s.	+
Organic anion transporting family								
Slco1a4 / Oatp1a4	NM_030687	+++	-3.30	+++	-6.18	+++	-1327.17	bc
Slco1a5 / Oatp1a5	NM_130861	+	2.09	++	n.s.[1]	+	-3.53	bc
Slco1c1 / Oatp1c1	NM_021471	+++	-7.26	+++	-11.03	+++	-742.26	bc
Slco2a1 / Oatp2a1	NM_033314	+	n.s.	+	n.s.	+	19.35	+++
Slco2b1 / Oatp2b1	NM_175316	+++	-2.14	+++	n.s.	+++	-171.24	bc
Slco3a1 / Oatp3a1	NM_023908	bc	26.24	+++	20.32	++	43.83	+++
	NM_001038643	+	14.48	++	11.70	++	25.79	+++
Slco4a1 / Oatp4a1	NM_148933	bc	5.48	+	14.54	++	6.61	++
Organic cation/anion/zwitterion transporter family								
Slc22a4 / Octn1	NM_019687	bc	3.01	+	2.76	+	n.s.[1]	bc
Slc22a8 / Oat3	NM_031194	+++	-73.64	+	-82.10	+	-202.74	bc
Slc22a12 / Urat1	NM_009203	+	n.s.[1]	+	n.s.	+	n.s.	+
Slc22a17 / Boit	NM_021551	+	n.s.	bc	n.s.	bc	n.s.[1]	+
Na^+-dependent ascorbic acid transporter family								
Slc23a1 / Svct1	NM_011397	+	n.s.	+	n.s.	+	n.s.[1]	+
Slc23a2 / Svct2	NM_018824	+	n.s.	++	n.s.	++	n.s.[1]	+
$Na^+/(Ca^{2+}$-$K^+)$ exchanger family								
Slc24a1 / Nckx1	NM_144813	bc	n.s.	bc	2.27	bc	17.61	+
Slc24a3 / Nckx3	NM_053195	bc	n.s.[1]	bc	n.s.[1]	bc	20.67	++
Slc24a6 / Nckx6	NM_133221	+	n.s.	+	n.s.[1]	+	2.30	+

				Mitochondrial carrier family				
Slc25a1 / Cic	NM_153150	+	n.s.	+	n.s.	+	n.s.	+
Slc25a3 / Pic	NM_133668	+++	n.s.	+++	n.s.	+++	n.s.	+++
Slc25a4 / Aac1	NM_007450	+++	n.s.	+++	n.s.	+++	n.s.[1]	+++
Slc25a5 / Aac2	NM_007451	+++	n.s.[1]	+++	n.s.[1]	+++	n.s.	+++
Slc25a8 / Ucp2	NM_011671	+++	-4.84	++	-5.12	++	-4.38	++
Slc25a10 / Dic	NM_013770	+	n.s.	+	n.s.	+	2.61	+
Slc25a11 / Ogc	NM_024211	++	n.s.	++	n.s.	++	n.s.[1]	++
Slc25a14 / Ucp5	NM_011398	++	n.s.[1]	++	n.s.	++	n.s.	++
Slc25a16 / Gdc	NM_175194	++	n.s.[1]	++	n.s.	++	n.s.	++
Slc25a17 / Anc1	NM_011399	++	n.s.[1]	++	n.s.[1]	++	n.s.[1]	++
Slc25a19 / Dnc	NM_026071	+	n.s.[1]	+	n.s.[1]	+	n.s.[1]	+
Slc25a20 / Cac	NM_020520	+++	n.s.	+++	n.s.	+++	n.s.	+++
Slc25a23 / Apc2	NM_025877	++	-2.67	+	-3.37	+	-13.20	bc
Slc25a24 / Apc1	NM_172685	++	-2.18	+	n.s.	++	n.s.	++
Slc25a25 / Apc3	NM_146118	++	-2.69	+	-2.43	++	-3.55	+
Slc25a27 / Ucp4	NM_028711	+	n.s.[1]	+	n.s.	+	n.s.[1]	+
Slc25a28 / Mrs3/4	NM_145156	++	n.s.	++	n.s.	++	n.s.	++
Slc25a30 / Kmcp1	NM_026232	+	n.s.	+	n.s.	+	n.s.	+
Slc25a32 / Mftc	NM_172402	+++	n.s.	++	n.s.	++	n.s.	++
Slc25a33	NM_027460	++	n.s.	++	n.s.	++	-6.81	+
Slc25a35 / FLJ40217	NM_028048	+	-2.77	bc	-3.55	bc	-3.10	bc
Slc25a36 / FLJ10618	NM_138756	++	n.s.[1]	++	n.s.	++	n.s.[1]	++
Slc25a37 / HT015	NM_026331	+	n.s.[1]	+	n.s.	+	4.03	++
				Multifunctional anion exchanger family				
Slc26a2 / Dtdst	NM_007885	+	n.s.	+	n.s.	+	n.s.[1]	+

Slc26a6 / Pat-1	NM_134420	+	n.s.[1]	+	n.s.	+	n.s.[1]	+
Slc26a11	NM_178743	+	n.s.[1]	+	n.s.[1]	+	n.s.[1]	+
			Fatty acid transport protein family					
Slc27a1 / Fatp1	NM_011977	++	n.s.	+	-2.47	+	-2.51	+
Slc27a3 / Fatp3	NM_011988	+	-2.06	bc	-2.23	bc	n.s.[1]	+
Slc27a4 / Fatp4	NM_011989	+	n.s.	++	n.s.	++	n.s.[1]	+
			Facilitative nucleoside transporter family					
Slc29a1 / Ent1	NM_022880	+	n.s.[1]	+	n.s.[1]	+	2.90	+
Slc29a3 / Ent3	NM_023596	+	n.s.[1]	+	n.s.	+	n.s.[1]	+
Slc29a4 / Ent4	NM_146257	+	-3.97	bc	-4.16	bc	-6.31	bc
			Zinc efflux family					
Slc30a1 / Znt1	NM_009579	+++	-2.24	+++	-2.42	+++	-3.08	+++
Slc30a4 / Znt4	NM_011774	+++	n.s.	+++	n.s.	+++	n.s.	+++
Slc30a5 / Znt5	NM_022885	+++	n.s.[1]	+++	n.s.	+++	n.s.[1]	+++
Slc30a6 / Znt6	NM_144798	++	n.s.[1]	+++	n.s.[1]	++	n.s.	+++
Slc30a7 / Znt7	NM_023214	++	n.s.	++	n.s.[1]	++	n.s.[1]	++
Slc30a9 / Znt9	NM_178651	++	n.s.	+++	n.s.	+++	n.s.	+++
			Cooper transporter family					
Slc31a1 / Ctr1	NM_175090	+++	n.s.	+++	-2.22	+++	-3.29	++
Slc31a2 / Ctr2	NM_025286	++	n.s.	++	n.s.[1]	++	n.s.[1]	++
			Acetyl-CoA transporter family					
Slc33a1 / Acatn	NM_015728	+	n.s.	++	n.s.	++	2.19	++
			Nucleoside-sugar transporter family					
Slc35a1 / Cst	NM_011895	++	n.s.[1]	++	n.s.[1]	++	n.s.[1]	++
Slc35a2 / Ugt	NM_001083937	+	n.s.[1]	+	n.s.[1]	+	n.s.[1]	+
Slc35a3 / UGTrel2	NM_144902	+++	n.s.[1]	+++	n.s.[1]	++	n.s.[1]	+++

Slc35a4 / UGTrel3	NM_026404	++	n.s.[1]	++	n.s.[1]	++	n.s.[1]	++
Slc35a5 / UGTrel5	NM_028756	+	n.s.	bc	n.s.	+	n.s.[1]	+
Slc35b1 / UGTrel1	NM_016752	+++	n.s.[1]	+++	n.s.[1]	+++	n.s.[1]	+++
Slc35b2 / UGTrel4	NM_028662	+	n.s.	+	n.s.[1]	+	n.s.	+
Slc35b3 / UGTrel6	NM_134060	++	2.50	++	2.21	++	n.s.	++
Slc35b4 / Yea4	NM_021435	+	2.30	++	n.s.	++	n.s.	++
Slc35c1 / Fuct1	NM_211358	+	n.s.	+	n.s..	+	n.s.	+
Slc35c2 / Ovcov1	NM_144893	+	n.s.[1]	++	n.s.[1]	+	n.s.	++
Slc35d2 / UGTrel8	NM_001001321	++	-2.03	++	n.s.	++	n.s.	++
Slc35e1 / FLJ14251	NM_177766	++	n.s.	++	n.s.	++	n.s.[1]	++
Slc35e4	NM_153142	+	n.s.[1]	+	n.s.[1]	+	n.s.[1]	+
Slc35f1	NM_178675	bc	13.14	++	9.10	++	n.s.[1]	bc
Slc35f2	NM_028060	+++	-10.32	++	-10.27	++	-58.16	+
Slc35f5	NM_028787	++	n.s.[1]	++	n.s.	++	n.s.[1]	++
			Sugar-phosphate/phosphate exchanger family					
Slc37a2 / Spx2	NM_020258	bc	2.03	+	n.s.	+	2.77	+
Slc37a3 / Spx3	NM_028123	++	n.s.[1]	++	n.s.[1]	++	n.s.[1]	++
Slc37a4 / Spx4	NM_008063	++	n.s.	+	n.s.	+	n.s.	+
			Metal ion transporter family					
Slc39a1 / Zip1	NM_013901	+++	n.s.	+++	n.s.	+++	n.s.	+++
Slc39a3 / Zip3	NM_134135	++	n.s.	++	n.s.	++	n.s.	++
Slc39a4 / Zip4	NM_028064	bc	9.13	++	6.35	+	n.s.[1]	bc
Slc39a6 / Liv-1	NM_139143	++	2.04	++	2.31	++	n.s.	++
Slc39a7 / Ke4	NM_008202	+++	n.s.	+++	n.s.	+++	n.s.[1]	+++
	NM_001077709	+++	n.s.	+++	n.s.	+++	n.s.[1]	+++
Slc39a8 / BIGM103	NM_026228	+++	-2.73	+++	-3.14	++	-6.78	++

Slc39a10	NM_172653	+++	-6.16	+++	-7.02	++	-5.51	+++
Slc39a11	NM_027216	+	2.21	+	2.10	+	2.47	++
Slc39a13	NM_026721	+	n.s.[1]	+	n.s.	+	n.s.[1]	+
Slc39a14 / Zip14	NM_144808	bc	2.19	+	2.50	+	2.36	+
			Basolateral iron transporter family					
Slc40a1 / Ireg1	NM_016917	+++	-2.35	+++	-5.50	+++	-2.75	+++
			MgtE-like magnesium transporter family					
Slc41a1	NM_173865	+	n.s.	+	n.s.[1]	+	n.s.[1]	+
Slc41a2	NM_177388	+	6.74	++	4.02	+	4.19	+
			Na^+-independent, system L-like amino acid transporter family					
Slc43a3 / Eeg1	NM_021398	+	4.50	++	6.41	+++	12.03	+++
			Choline-like transporter family					
Slc44a1 / Ctl1	NM_133891	++	2.26	+++	n.s.	++	n.s.	++
Slc44a2 / Ctl2	NM_152808	+++	n.s.	+++	n.s.[1]	+++	2.35	+++
			Putative sugar transporter family					
Slc45a4 / KIAA1126	NM_001033219	bc	4.66	+	n.s.	bc	n.s.[1]	bc
			Heme tranporter family					
Slc46a3 / LOC283537	NM_027872	+++	n.s.[1]	+++	n.s.	+++	-6.03	+

[a]FC: Fold-change relative to non-cultured MBMECs. [b]ME: Mean expression (log_2).
Probesets of genes either showing expression below cut-off (bc) in all conditions or showing expression bc and q > 5% and/or fold change < 2:
Tight junction protein genes: ZO-3 (NM_013769); Claudin-1 (NM_016674); Claudin-2 (NM_016675); Claudin-3 (NM_009902); Claudin-4 (NM_009903); Claudin-7 (NM_016887); Claudin-8 (NM_018778); Claudin-9 (NM_020293); Claudin-11 (NM_008770); Claudin-13 (NM_020504); Claudin-14 (NM_019500); Claudin-15 (NM_021719); Claudin-16 (NM_053241); Claudin-18 (NM_019815); Claudin-19 (NM_153105); Claudin-23 (NM_027998); **ABC transporter genes:** Abca6 (NM_147218); Abca8a (NM_153145); Abca8b (NM_013851); Abca13 (NM_178259); Abcb4 (NM_008830); Abcb9 (NM_019875); Abcb11 (NM_021022); Abcc2 (NM_013806); Abcc7 (NM_021050); Abcc8 (NM_011510); Abcc10 (NM_145140; NM_170680); Abcd2 (NM_011994); Abcg4 (NM_138955); Abcg5 (NM_031884); Abcg8 (NM_026180); **Non-AA Slc transporters:** Slc2a2 (NM_031197); Slc2a3 (NM_011401); Slc2a4 (NM_009204); Slc2a5 (NM_019741); Slc2a6 (NM_172659); Slc2a13 (NM_001033633); Slc4a1 (NM_011403); Slc4a3 (NM_009208); Slc4a8 (NM_021530); Slc4a9 (NM_172830); Slc4a10

(NM_033552); Slc4a11 (NM_001081162); Slc5a1 (NM_019810); Slc5a5 (NM_053248); Slc5a7 (NM_022025); Slc5a9 (NM_145551); Slc5a10 (NM_001033227); Slc5a11 (NM_146198); Slc5a12 (NM_001003915); Slc6a1 (NM_178703); Slc6a2 (NM_009209); Slc6a3 (NM_010020); Slc6a4 (NM_010484); Slc6a5 (NM_148931); Slc6a11 (NM_172890); Slc6a12 (NM_133661); Slc6a18 (NM_001040692); Slc7a4 (NM_144852); Slc7a14 (NM_172861); Slc8a1 (NM_011406); Slc8a2 (NM_148946); Slc8a3 (NM_080440); Slc9a9 (NM_177909); Slc10a2 (NM_011388); Slc10a6 (NM_029415); Slc12a1 (NM_183354; NM_001079690); Slc12a3 (NM_019415); Slc12a5 (NM_020333); Slc12a8 (NM_134251; NM_001083902); Slc13a1 (NM_019481); Slc13a2 (NM_022411); Slc13a3 (NM_054055); Slc13a4 (NM_172892); Slc13a5 (NM_001004148); Slc14a1 (NM_028122); Slc14a2 (NM_207651; NM_030683); Slc15a1 (NM_053079); Slc15a2 (NM_021301); Slc16a5 (NM_001080934); Slc16a7 (NM_011391); Slc16a8 (NM_020516); Slc16a14 (NM_027921); Slc17a1 (NM_009198); Slc17a2 (NM_144836); Slc17a3 (NM_134069); Slc18a1 (NM_153054); Slc18a3 (NM_021712); Slco1a6 (NM_023718); Slco1b2 (NM_020495); Slco1b2 (NM_178235); Slco4c1 (NM_172658); Slco5a1 (NM_172841); Slco6b1 (NM_001039475); Slco6c1 (NM_028942); Slco6d1 (XM_129964; XM_910370); Slc22a1 (NM_009202); Slc22a2 (NM_013667); Slc22a3 (NM_011395); Slc22a5 (NM_011396); Slc22a6 (NM_008766); Slc22a7 (NM_144856); Slc22a9 (NM_144785); Slc22a13 (NM_133980); Slc22a14 (NM_001037749); Slc22a16 (NM_027572); Slc22a18 (NM_008767; NM_001042760); Slc23a3 (NM_194333); Slc24a2 (NM_172426); Slc24a4 (NM_172152); Slc25a7(NM_009463); Slc25a9 (NM_009464); Slc25a29 (NM_181328); Slc25a31 (NM_178386); Slc25a34 (NM_001013780); Slc26a1 (NM_174870); Slc26a3 (NM_021353); Slc26a4 (NM_011867); Slc26a5 (NM_030727); Slc26a7 (NM_145947); Slc26a8 (NM_146076); Slc27a2 (NM_011978); Slc27a5 (NM_009512); Slc28a3 (NM_022317); Slc29a2 (NM_007854); Slc30a8 (NM_172816); Slc30a10 (NM_001033286); Slc34a1 (NM_011392); Slc34a2 (NM_011402); Slc34a3 (NM_080854); Slc35a2 (NM_078484); Slc35d3 (NM_029529); Slc35f3 (NM_175434); Slc35f4 (NM_029238); Slc36a3 (NM_172258); Slc37a1 (NM_153062); Slc39a2 (NM_001039676); Slc39a5 (NM_028051; NM_028092); Slc39a12 (NM_001012305); Slc41a3 (NM_027868; NM_001037493); Slc44a3 (NM_145394); Slc44a4 (NM_023557); Slc45a1 (NM_173774); Slc45a2 (NM_053077); Slc45a3 (NM_145977); Slc46a1 (NM_026740); Slc46a2 (NM_021053)

Key: [1]q-value > 5%; not significant (n.s.); below cut-off (bc; probeset expression values ≤ 5.78); +probeset expression values > 5.78-8; ++probeset expression values > 8-10; +++probeset expression values > 10; down-regulation (-). Abbreviations: [a]TJ, tight junction associated protein; [b]ABC transporter, ATP binding cassette transporter; [c]non-AA transporter, non-amino acid transporter; [d]Slc, solute carrier family; [e]MBMEC, mouse brain microvascular endothelial cells.

Supplemental Table 3. Delta C_T values of selected cell marker, TJ, ABC and SLC transporter gene mRNA levels in samples assessed by qPCR.

Part A: *delta C_T values (SYBR Green® qPCR, relative to S16 ribosomal protein mRNA)for genes reported in Table 1.*

mRNA	**ppMBMEC**	**Crude EC fraction**	**pMBMEC**	**Glial[3]**
Cell specificity	*Pecam1 purified*	*Freshly isolated*	*single-cultured*	*3 week cultures*
VE-Cadherin	-1.14±0.05	-1.78±0.12	-1.91±0.06	4.07±0.10
Endothelium				
Hbb-β1	-1.18±0.14	-7.17±0.13	n.d.	n.d.
Erythrocytes				
Gfap	n.d.	5.87±0.77	10.0±0.58	-4.19±0.06
Astrocytes				
Pdgfrβ	4.49±0.15	1.17±0.12	4.43±0.08	2.11±0.07
Pericytes				
Syp	n.d.	5.38±0.28	n.d.	7.58±0.28
Neurons				
Ttr	4.36±0.24	-1.73±0.15	6.20±0.11	n.d.
Choriod plexus				

Part B: *delta C_T values (Taqman® qPCR, relative to 18S rRNA) of* [1]MBMEC *samples previously tested by microarray.*

	Non-cultured	**Single-cultured**	**Co-cultured**	**Cell-line**	**[2]Brain**	**[3]Glial**
Gene (protein)		***Cellular markers***				
Pecam1 (CD31)	12.1±0.08	9.68±0.11	11.3±0.04	11.0±0.08	20.7±0.43	n.d.
VE-Cadherin	13.4±0.33	10.7±0.11	12.3±0.04	12.6±0.08	22.1±0.40	18.8±0.23
Glut1 (Slc2a1)	9.87±0.04	11.2±0.75	11.7±0.10	15.3±0.11	17.4±0.31	15.6±0.17
Pdgfrβ	17.4±0.12	15.9±0.09	16.3±0.08	n.d.	19.5±0.02	15.6±0.04
Gfap	21.2±0.33	20.5±0.45	21.7±1.12	19.7±0.05	15.1±0.07	8.35±0.04

Syp	21.6±0.24	24.5±0.86	n.d.	n.d.	13.4±0.13	20.1±0.18
			Tight junctions			
ZO-1	12.4±0.05	12.3±0.03	13.6±0.12	13.4±0.07	17.0±0.17	15.0±0.18
Cldn5	12.9±0.17	14.8±0.30	15.7±0.43	13.4±0.13	22.0±0.84	n.d.
Ocldn	13.7±0.09	14.0±0.11	15.5±0.10	19.5±0.88	21.2±0.35	23.3±1.04
			ABC transporters			
Mdr1a	12.9±0.05	15.2±0.41	16.6±0.02	19.8±0.41	21.8±0.38	23.3±0.10
Mrp1	18.3±0.13	14.0±0.22	15.1±0.09	15.5±0.11	18.5±0.46	14.9±0.10
			Solute carrier Amino Acid transporters			
	Slc1 – The high affinity glutamate and neutral amino acid transporter family					
Slc1a1 (Eaat3)	12.7±0.02	12.2±0.02	13.3±0.02	n.d.	15.2±0.12	18.8±0.85
Slc1a2 (Eaat2)	22.2±0.39	25.3±0.42	25.3±1.39	n.d.	13.9±0.30	15.8±0.07
Slc1a3 (Eaat1)	20.9±0.05	21.2±0.39	22.5±0.27	n.d.	15.4±0.04	13.3±0.19
Slc1a6 (Eaat4)	n.d.	18.1±0.04	18.9±0.32	n.d.	19.8±0.18	18.7±0.72
	Slc6 – The sodium- and chloride- dependent neurotransmitter transporter family					
Slc6a6 (Taut)	12.0±0.10	14.0±0.52	16.7±0.30	17.0±0.09	18.2±0.10	16.2±0.48
	Slc3 & Slc7 – The cationic amino acid transporter / glycoprotein- associated family					
Slc3a2 (4F2hc)	9.53±0.03	10.6±0.06	12.1±0.03	11.6±0.12	13.6±0.02	10.4±0.04
Slc7a1 (Cat-1)	13.6±0.16	17.0±0.50	17.6±0.27	18.2±0.41	20.2±0.27	19.9±0.18
Slc7a3 (Cat-3)	18.1±0.26	21.8±0.69	22.2±0.16	20.4±0.88	19.3±0.06	23.3±1.34
Slc7a5 (Lat1)	11.9±0.01	14.2±0.05	15.6±0.05	17.6±0.19	18.0±0.04	16.9±0.17
Slc7a6 (y^+Lat2)	17.2±0.32	14.4±0.06	15.3±0.07	16.8±0.29	17.0±0.07	16.2±0.03
Slc7a11 (xCT)	21.3±0.56	16.7±0.04	19.7±0.37	19.6±0.48	17.7±0.08	15.8±0.09
	Slc16 – The monocarboxylate transporter family					
Slc16a2 (Xpct)	13.4±0.06	14.9±0.04	16.7±0.06	n.d.	18.1±0.14	13.9±0.13
	Slc36 – The proton- coupled amino acid transporter family					

Slc36a1 (Pat1)	16.5±0.12	16.8±0.09	18.3±0.13	17.3±0.27	17.8±0.27	18.2±0.20
Slc38 – The system A & N, sodium- coupled neutral amino acid transporter family						
Slc38a1 (Snat1)	22.0±0.65	16.3±0.04	17.1±0.04	22.2±0.04	15.9±0.11	13.4±0.08
Slc38a2 (Snat2)	12.3±0.05	11.2±0.01	12.9±0.06	13.0±0.09	15.4±0.10	12.5±0.06
Slc38a3 (Snat3)	13.3±0.11	16.6±0.16	16.5±0.05	21.2±0.39	17.8±0.18	14.3±0.22
Slc38a5 (Snat5)	12.3±0.09	15.5±0.12	17.4±0.29	n.d.	20.4±0.40	n.d.
Slc43 – The sodium- independent, system-L like amino acid transporter family						
Slc43a1 (Lat3)	23.3±0.10	19.3±0.63	20.9±0.34	19.3±1.87	n.d.	19.8±0.46
Slc43a2 (Lat4)	16.7±0.20	14.3±0.06	16.5±0.05	17.2±0.11	17.8±0.04	16.1±0.10
Slc43a3 (Eeg1)	21.2±0.27	16.5±0.03	17.5±0.06	15.4±0.09	25.0±0.29	18.5±0.23

For samples tested by SYBR Green® qPCR (Part A), values are the mean delta C_T values +/- s.d. relative to the endogenous reference RNA s16 ribosomal protein mRNA for biological triplicates. For samples tested by Taqman® qPCR (Part B), values are the mean delta C_T +/- s.d. relative to 18S ribosomal rRNA of technical triplicates. **Key:** n.d. (not detected) indicates C_T values below limit of detection. [1]MBMECs (mouse brain microvascular endothelial cells) RNA prepared from non-cultured, single-cultured, co-cultured or cell-line samples as defined in the text; [2]Brain to RNA prepared from total brain homogenates; and [3]Glial to RNA from 3 week mouse brain glial cultures.

Supplemental Figure 1

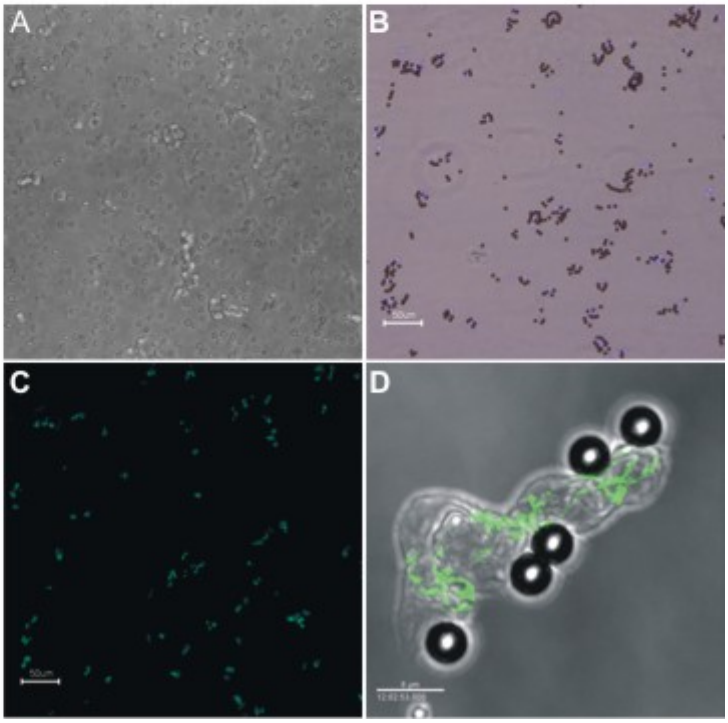

Supplemental Figure 2

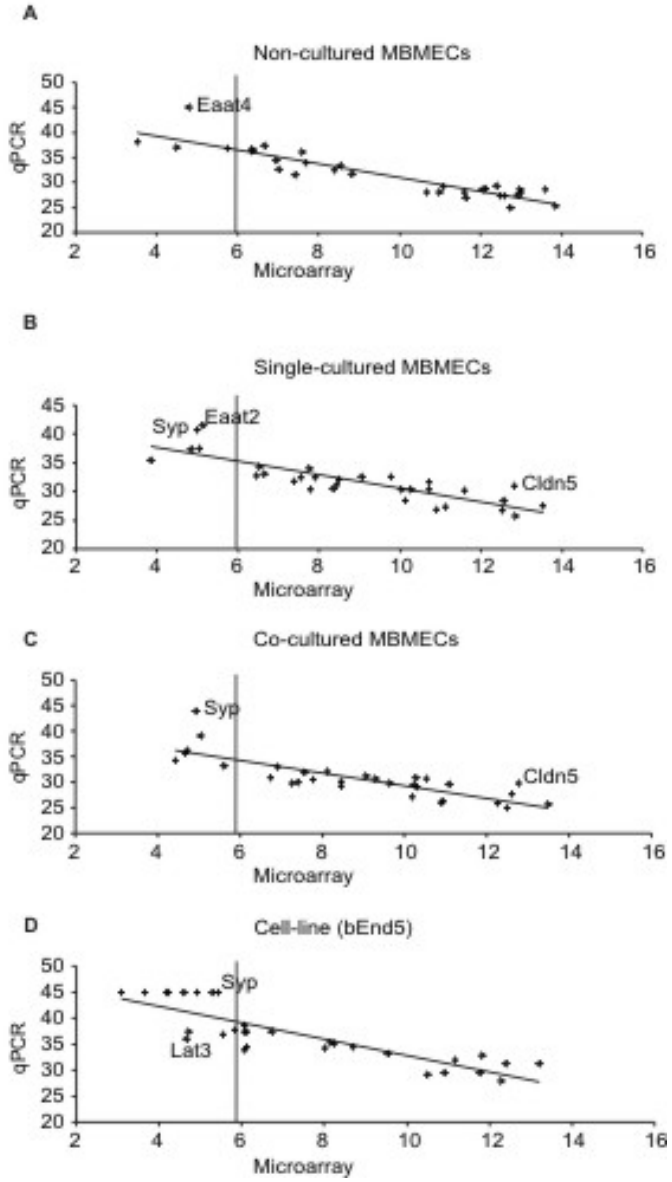

5. Manuscript: Differential axial localization of luminal sodium-dependent glutamine transporters Snat1 and Snat3 along the brain vascular tree.

This section contains the above mentioned manuscript that was submitted October 25th 2010.

My contribution to the manuscript concerns the performance of immunohistochemical as well as *in vivo* biotinylation experiments, data analysis, and data presentation.

Differential axial localization of luminal sodium-dependent glutamine transporters Snat1 and Snat3 along the brain vascular tree

Ruderisch N[a], Virgintino D[b], Makrides V[a*], Verrey F[a*]

[a] Institute of Physiology, University of Zurich, Zurich, CH-8057, Switzerland; [b] Department of Human Anatomy and Histology, University of Bari, Bari, I-70124, Italy.

[*] These authors contributed equally to this work.

Classification: Biological Sciences, Physiology

Keywords: blood-brain barrier, solute carrier family SLC transporter, amino acid transport, brain amino acid homeostasis, system A, system N, glutamine, brain vasculature

Author Contributions:
VM, NR, FV designed research
NR performed research
DV contributed new tools
VM, NR, DV, FV analyzed data
VM, NR, FV wrote paper

Corresponding Author: Francois Verrey, verrey@access.uzh.ch

Abstract

Disturbances in brain amino acid (AA) levels play direct and indirect roles in several neuropathologies e.g. phenylketonuria, stroke and diabetes. Indeed, as indicated by brain interstitial fluid concentrations, which for most AAs are maintained at ~10% plasma levels, regulation of AA homeostasis appears critical for normal CNS function. One mechanism contributing to the establishment and maintenance of the plasma to brain AA gradients involves polarized expression of solute carrier family (SLC) transporters on blood-brain barrier (BBB) endothelial cells. Of particular interest is the localization of sodium-dependent transporters that can actively move substrates against their concentration gradient. In this study, the *in vivo* membrane localization of the sodium-dependent glutamine transporters Snat3 (Slc38a3) and Snat1 (Slc38a1) was investigated in the mouse brain cortical vascular tree using immunofluorescent co-localization with cellular markers. In addition, membrane expression was probed by *in vivo* biotinylation of brain vascular luminal proteins. Both methods detected expression of LAT1 (Slc7a5) as expected. Additionally, a portion of both Snat3 and Snat1 vascular expression was localized on luminal membranes. Importantly, Snat1 expression was restricted to larger cortical microvessels, while Snat3 was additionally expressed on BBB capillary membranes. This differential expression of the system A (Snat1) vs. system N (Snat3) transporters suggests distinct roles for Snat`s in the cerebral vasculature and is consistent with a role for Snat3 in net transendothelial BBB AA transport.

Introduction

The brain is both highly metabolically active and physiologically vulnerable. Amino acids (AA), some of which serve as neurotransmitters, and/or as potentially rate-limiting precursors in protein, energy, and other metabolic pathways, occupy a uniquely sensitive position in the brain milieu. Consequently homeostatic concentrations are highly controlled and, not coincidentally, in interstitial fluid and cerebrospinal fluid most AAs (except glutamine) are maintained at well below plasma levels (1). For example, glutamine, the most abundant circulating AA in the body, is a key constituent of nitric oxide synthesis, energy supply, and nitrogen metabolism pathways. Furthermore, CNS replenishment of the major neuronal excitatory and inhibitory neurotransmitters, glutamate and GABA, involves transfer of glutamine from astrocytes to neurons for conversion to glutamate (the “glutamate-glutamine cycle”). Thus glutamine brain interstitial fluid levels, although approaching those of plasma, are none-the-less regulated (2).

To respond to the brain’s substantial nutrient demands and to provide for the rapid and effective removal of metabolic by-products and toxins a specialized brain capillary vasculature, the blood-brain barrier (BBB), has developed. Anatomically, the BBB is a polarized, selective, diffusion barrier formed by capillary endothelial cells that are uniquely characterized by an increased mitochondrial content, continuous tight junctions, a relative lack of fenestrations and pinocytic vesicles, and the expression of specific transport systems. Additionally, the abluminal endothelium basement membrane is periodically, but irregularly, associated with pericytes (3). Communication between endothelium and the associated cells plays a part in the regulation of various BBB functions including barrier formation and angiogenesis (4-5). This capillary structure is intimately associated with a surrounding cover of astrocyte endfeet that produces a second ~20-40 nm wide astroglial or parenchymal basal lamina. In turn, astrocytes and to some extent capillaries are associated with neurons. The entire structure is known as the “neurovascular unit” (NVU) (3).

The BBB is a dynamic interface between the plasma and the brain parenchyma, which due to the large capillary surface area, forms the primary site of blood-brain exchange. Exchange of solutes requires movement through the two (luminal or blood-facing and abluminal or brain-facing), closely apposed (separated by 200-500 nm) and biochemically distinct BBB endothelial membranes (6). In general, AA movement across membranes is mediated by specialized transporter proteins belonging to several families of the solute carrier (SLC) gene series. Throughout the body SLC family transporters provide essential gate-keeping functions controlling uptake and efflux of physiologically crucial compounds (7).

As for other barrier tissues, brain capillaries exhibit a polarized distribution of luminal and abluminal membrane proteins. For example, the endothelial glucose transporter Glut1 (Slc2a1) is ~4 times higher expressed in mouse brain abluminal cortical BBB membranes (8). Homeostatic brain AA concentrations are thought to be actively maintained to a large extent by polarized BBB transendothelial transport via SLC transporters (3). We and others hypothesize that asymmetric expression of AA transporters with different transport mechanisms and substrate selectivities determine net transendothelial flux. However untilfairly recently, it was only possible to characterize BBB AA transport in terms of transport "systems" described functionally by macroscopic substrate and inhibitor affinities and ion dependencies. From such data a number of hypothetical schemes for the expression of transport systems on luminal and abluminal BBB membranes have been suggested. For example, Hawkins and colleagues propose sodium-dependent AA transport systems to be restricted to abluminal membranes and to operate solely for brain AA efflux (1). Now with the available expression profiling tools it is possible to determine the molecular identity and localization of BBB transporters (6). Therefore, we recently performed a screen of highly pure brain capillary endothelial RNA to determine the first complete *in vivo* BBB transcriptome for AA and other SLC transporters (9). Additionally, culture induced changes in gene expression were assayed. We hypothesized that after isolation endothelial cells rapidly dedifferentiate in culture losing expression of transporters participating in specialized functions, i.e. transendothelial transport. Indeed, we identified a subset of AA transporters with high *in vivo* mRNA levels that were strongly decreased by culture (4F2hc/Slc3a2, Lat1/Slc7a5, Snat3/Slc38a3, Snat5/Slc38a5, and Cat1/Slc7a1). In contrast, culture induced a robust increase in Snat1/Slc38a1, y^+Lat2/Slc7a6 and xCT/Slc7a11 mRNAs indicating their potential involvement in supplying AAs for endogenous cellular metabolism in cell culture conditions (9).

Our current goal is to determine the membrane distribution of selected AA transporters. It is of particular interest to determine the distribution of sodium (Na^+) -dependent transporters, which use the Na^+ electrochemical gradient to actively transport substrates potentially against their concentration gradient. In this study we focus on two Na^+-dependent AA transporters (Snat1 and Snat3) found variably expressed *in vivo* and in culture (9). To investigate BBB membrane localization by direct observation, we examined immunofluorescent labeled mouse brain tissue sections by confocal microscopy focusing on endothelial cell nuclear regions where luminal and abluminal membranes can be distinguished. To independently verify the microscopy findings, an *in vivo* biotinylation approach was used to specifically label proteins expressed at vascular luminal membrane surface (10-11).

Results

Confocal microscopy and *in vivo* biotinylation are complementary strategies for identification of brain microvascular luminal membrane proteins. We first confirmed that the subcellular localization of known membrane proteins could be distinguished on cortical capillaries (~5-10μm) by immunofluorescent co-localization of membrane and cellular markers. Cross-sections where the nucleus (PO-PRO^{TM} nuclear dye) separated the two endothelial membranes were examined. In brain capillaries, Glut1 is unevenly expressed on luminal and abluminal membranes (8) while the transferrin receptor Cd71 is restricted to the lumen (10). As expected, staining for Cd71 (Fig. 1A) co-localized with luminal Glut1 (Fig. 1B, C). Staining for the basement membrane protein laminin was used to approximately demarcate abluminal endothelium from brain parenchyma. Although due to the limit of resolution of light microscopy, some laminin signal overlapped with abluminal Glut1 staining, a portion remained distinct indicating partial discrimination of abluminal Glut1 expression. Importantly, a distinct Glut1 luminal staining was evident confirming the unambiguous visualization of luminal localization in the capillary nuclear region by confocal microscopy (Fig. 1C, D). As a further control, we tested for detection of the previously described BBB expression of the heterodimeric AA transporter Lat1-4F2hc (12). As expected, a relatively even membrane distribution of Lat1 staining co-localizing with Glut1 on luminal and abluminal membranes was observed (Fig. 1E, F).

As a second independent method to probe for membrane localization we used *in vivo* biotinylation to specifically label proteins expressed on the luminal brain vasculature (10-11). Under conditions designed to maintain BBB integrity mice brains were perfussed with PBS/dextran ± sulfo-NHS-LC-biotin. The choroid plexus was removed and the total brain lysate subjected to Neutravidin pull-down. Strepavidin blot detected a strong biotin signal in the Neutravidin-bound protein fraction from biotinylated lysates that was only weakly found or absent in the pull-down fraction from non-biotinylated controls and in total protein lysates and unbound fractions indicating successful exogenous biotinylation of brain proteins (Fig. S1A). Further, the abundant cytoskeletal protein, β-actin, and the basal membrane glycoprotein, laminin, were nearly not detected in the Neutravidin-bound fractions, but strongly present in all other fractions (Fig. 2). Additionally, fluorescent Neutravidin staining of brain tissue confirmed restriction of biotinylation to the vasculature (Fig. S1B, C). These results are consistent with the restriction of the biotin labeling to luminal membrane extracellular protein domains and with negligible non-specific protein pull-down by Neutravidin.

Further, a strong band of the expected MW for Lat1 (~36 kDa) was observed in the Neutravidin-bound fraction from *in vivo* biotinylated lysates but not the corresponding non-biotinylated fraction (Fig. 2). Probing for 4F2hc luminal expression by *in vivo* biotinylation resulted in the previously reported pattern of 3 bands (13) putatively corresponding to ~75 kDa core-glycosylated and ~90 kDa terminally glycosylated 4F2hc, and ~120 kDa 4F2-Lat1 heterodimer in biotinylated but not non-biotinylated Neutravidin pull-downs (Fig. S2A). Results from deglycosylation of the Neutravidin-bound fraction from biotinylated brains were comparable to mouse kidney total membranes with non-glycosylated 4F2hc migrating at ~60 kDa (Fig. S2B). The data confirm that used in concert, confocal microscopy and *in vivo* biotinylation successfully identify known microvascular membrane luminal proteins.

Luminal membrane expression of system N, Na^+-dependent, AA transporter Snat3. This dual strategy was then used to examine the localization of Snat3, which we hypothesize is possibly important for BBB transendothelial AA transport (9). Snat3 has been shown to be expressed in astrocytes but not neurons or oligodendrocytes (14). Labeling of adult mouse brain tissue sections revealed Snat3 co-localization with Glut1 on capillaries (Fig. 3A, B).

Snat3 antibody specificity was tested by comparing immunofluorescence results from Snat3 wild-type ($Snat3^{+/+}$), heterozygous ($Snat3^{+/-}$) and homozygous knockout ($Snat3^{-/-}$) mice. Since $Snat3^{-/-}$ mice generally die before weaning, comparative staining was carried out using tissue from postnatal day 10 mice (Fig. S3). As for adult wild-type mice (Fig. 3A, B), $Snat3^{+/-}$ mice demonstrated robust Snat3 expression in capillaries (Fig. S3B, D, F), and as well, in larger microvessels consisting of multiple endothelial cells and associated pericytes (Fig. S3A, C, E). However, specific Snat3 staining was not observed in the corresponding knockout tissue (Fig. S3H, J) indicating the observed Snat3 labeling is specific.

Following *in vivo* biotinylation, Western blot detected a putative Snat3 band with an apparent MW of ~65 kDa in the Neutravidin-bound but not the corresponding fraction from non-biotinylated mice (Fig. 3C). Consistent with antibody specificity for Snat3, a ~65kDa band was found in blots of total brain and liver lysates from $Snat3^{+/-}$ but not $Snat3^{-/-}$ mice (Fig. S4A). Furthermore, although the banding pattern of glycosylated Snat3 in kidney and liver varies from that of brain, in all cases deglycosylation resulted in a band with the expected apparent MW for non-glycosylated Snat3 of ~43 kDa (Fig. S4A, B). Both the Snat3 knockout and deglycosylation data support the interpretation that the ~65 kDa band in the Neutravidin-bound fraction is glycosylated luminal Snat3. Taken together, the immunofluorescence and *in vivo* biotinylation data demonstrate luminal, and are consistent with abluminal, Snat3 localization in BBB capillaries.

Localization of system A, Na^+-dependent, AA transporter Snat1 on large but not capillary microvessels. Snat1 is known to be expressed by both neurons and to a lesser extent by astrocytic processes (15). Based on our previous RNA study we expected a low expression in the vasculature (9). Figure 4 shows a representative Snat1 staining co-localized with Glut1 in two larger (>15μm) cortical microvessels at a branch point (Fig. 4A, C, S5A). In contrast, a specific Snat1 signal was not evident in capillaries. For example, figure 4B, D shows representative staining of a cross-section in the nuclear region of a capillary (~5μm) endothelial cell and an associated pericyte, both of which are demarcated by Glut1 (16) but where Snat1 staining is not above background (Fig 4B, D, S5B). Western blot after *in vivo* biotinylation resulted in a weak band corresponding to the expected MW of Snat1 (~58 kDa) in the Neutravidin-bound fraction from biotinylated but not non-biotinylated lysates (Fig. 4E). Together the data are consistent with endothelial expression of Snat1 on larger microvessels but not BBB vasculature, and support luminal localization for a portion of the vascular Snat1.

Discussion

A key step in delineating mechanisms of BBB active control of brain AAs is to determine the endothelial membrane (blood/luminal or brain/abluminal) to which plasma AA transporters are localized. In the current study confocal microscopy and *in vivo* biotinylation data for two Na^+-dependent transporters, Snat3 and Snat1, reveal a partially overlapping cortical vascular expression. Snat3 was found expressed in both young and adult mice on larger microvessels as well as BBB capillaries, whereas a specific signal for Snat1 was observed only in the larger microvessels. Methodologically, confocal microscopy is a powerful tool for discerning regional, tissue specific and subcellular localization. However, data interpretation can be confounded by the limit of resolution of light microscopy to at best ~300 nm. This is especially problematic for localization studies of intact brain capillary endothelial membranes that are closely situated and intimately associated with pericytes, astrocytic endfeet and neurons. To address this concern we employed an *in vivo* biotinylation strategy. *In vivo* biotinylation of the brain vessels specifically labels luminal domain proteins thereby

providing an independent assessment of membrane localization. Using this approach we independently confirmed the luminal expression of both Na^+-dependent transporters.

In summary, by both methods we confirmed the protein expression of Slc38a1 and Slc38a3 transporters in the cerebral vasculature. However, importantly, significant levels of Snat3, but not Snat1 protein, are expressed on capillary membranes. Taken together with our previous gene expression study demonstrating differential mRNA expression and regulation, our current localization data underscore the potential differing contributions of Snat3 and Snat1 to BBB transendothelial transport vs. endogenous endothelial cellular metabolism, respectively.

Potential roles of Snat1 and Snat3 in the cerebral vasculature. The differential localization of Snat1 and Snat3 in the vascular tree along with mechanistic differences in each transporter's function may provide clues as to their varying roles. Although subpial, arterioles and venules (10-100 μM) along with capillaries (4-10 μm) are found, only capillaries mediate the full BBB phenotype. Only capillaries are in direct contact with the brain parenchyma without an intervening pial sheath and perivascular space. Moreover, only capillaries express the cohort of transport proteins required for vectorial BBB flux (17). Conversely, cultured endothelial cells from large non-BBB microvessels exhibit relatively rapid proliferation in comparison to cells derived from capillaries (17). Mechanistically, Snat1 is a "system A", Na^+-dependent, pH sensitive transporter for a broad range of small aliphatic AAs (alanine, serine, proline, asparagine, glutamine, histidine), whereas, Snat3 is a system N, Na^+-co- and H^+-anti-porter with a preference for glutamine, histine, and asparagine. An important distinction between the two transporters arises from the 1:1 coupling by Snat1 of AA transport to the Na^+ electrochemical gradient. Consequentially, Snat1 mediates essentially unidirectional AA transport, whereas under appropriate conditions Snat3 flux is reversible (18-19). For example, Chaudhry and co-workers observed that in addition to Na^+, both glutamine and H^+ concentration gradients can influence Snat3 transport direction. They calculated ~400 μM extracellular glutamine as a threshold between uptake (>400 μM) and efflux (<) for their cell model system (20). Glutamine levels in plasma (~0.5-0.9 mM) and cerebrospinal fluid (~0.2-0.5 mM) vary within this range consequently Snat3 may mediate a regulated and reversible transport of glutamine (21). Further, intracellular stores of glutamine, which range from 2-20 mM, are considerably higher than extracellular levels. Therefore, glutamine uptake from either plasma or brain is against the glutamine concentration gradient. Snat1 is potentially capable of aiding endothelial filling of intracellular glutamine by harnessing the Na^+ electrochemical gradient to import glutamine against its concentration gradient. In our earlier gene study we observed a high mRNA expression in BBB, which was unchanged by culture, of a second system A transporter, Snat2 (Slc38a2). Snat2 may therefore operate in capillaries as proposed for Snat1 in larger vessels (9). Additionally, the nearly complete investment of capillaries with astrocyte endfeet has been suggested to likely facilitate transfer of AAs between astrocytes and BBB endothelium (21). This suggests that as for astrocytic Snat3 and neuronal Snat1, which potentially co-operate in transferring glutamine from astrocytes to neurons (18), BBB expressed Snat3 may participate in the endothelial shuttling of glutamine either directly or via astrocytes to and from brain parenchyma.

Snat3 – a luminal Na^+-dependent glutamine BBB transporter? Despite extensive study, the nature and role of luminal cerebral vascular AA transport remains somewhat unclear, this is especially true for Na^+-dependent transport. Both functional transport, as well as, expression of a marker (γ-glutaminyl transferase or GGT) of luminal Na^+-dependent AA transport has been detected. However, based primarily on vesicle studies it has also been proposed that Na^+-dependent transporters are restricted to abluminal BBB membranes (22).

Early *in vivo* studies by Oldendorf and others (23) measured a low but significant brain uptake for glutamine that was attributed to a neutral AA carrier system. Later Ennis and co-workers demonstrated a Na^+-dependent, pH sensitive glutamine luminal transport that was fully inhibited by histidine but not cystine (system A or ASC inhibitors) or BCH (system L inhibitor) and therefore identified as system N (24).

In addition to our present report demonstrating Snat3 protein expression, our previous study found additionally a robust and regulated gene expression of the other system N transporter Snat5 in BBB endothelial cells. Furthermore, a recent report by Agarwal and colleagues found Snat5 to be the most "BBB-selective marker" in a comparison of membrane proteins from liver, kidney, heart and lung vasculatures (25). The other transporters for glutamine reported to be expressed in cerebral vessels are Lat1 (system-L), Asct2 (system ASC) and y^+Lat2 (system y^+) (9, 26), all of which are inhibited by one of the compounds mentioned above (24) and mediate obligatory exchange of AA substrates (27). Therefore, only Snat3 and Snat5 are known molecular candidates for mediating the reported system N luminal BBB glutamine transport. The current *in vivo* demonstration of Snat3 BBB luminal expression lends strong support to the function of Snat3 in mediating at least a portion of the system N, Na^+-dependent luminal glutamine transport observed in BBB.

Materials and Methods

Animals. Female C57BL/6JOlaHsd mice were purchased from Harlan Laboratories B.V. (Venray, Netherlands). Snat3 wild-type and knock-out mice (Q263X Hybrid C3H-C57BL/6J; ENU-mutagenesis) were produced by Ingenium Pharmaceuticals AG (Martinsried, Germany) in the context of the Eugindat Project of the European 6th Framework Programme and kindly provided by C.A. Wagner (University of Zurich, Switzerland). All animal procedures were according to the Swiss Animal Welfare laws and approved by the Kantonales Veterinäramt Zurich (permission number 119/2008).

***In vivo* biotinylation.** The *in vivo* biotinylation protocol was based on the method published by Roesli and others (10-11) with minor modifications. Five-week-old female mice were anesthetized, the abdominal aorta clamped, and the brain perfused through the left cardiac ventricle with prewarmed (38°C) 10% (wt/vol) dextran 40 (Invitrogen, Paisley, UK) in PBS (Sigma-Aldrich, Steinheim, Germany). Drainage was from the right atrium. Perfusion was performed at 100 mm Hg to maintain the integrity of the BBB. For *in vivo* biotinylation, immediately following PBS/dextran, mice were perfused with 5 ml of freshly prepared biotinylation solution, (3 mg/ml EZ-Link® sulfo-NHS-LC-biotin (Thermo Scientific, Rockford, IL, USA) in PBS, 10% dextran 40), followed by 5 min without flow, before quenching with 10% dextran 40, 50 mM Tris, PBS. As a negative control (non- biotinylated) mice were perfused as above without biotin. Immediately after perfusion, brains were excised (cerebellum removed) and snap-frozen in liquid nitrogen. Protein extraction, purification of biotinylated proteins, gel electrophoresis and Western blot ananlysis are described in the Supporting Information.

Immunohistochemistry. Localization of SLC transporters was assessed by confocal microscopy of immunofluorescent co-localization with antibodies for specific cell or tissue type markers (specifications described under "antibodies" in supporting methods). Five-week-old female mice were anesthetized and perfused through the left cardiac ventricle with PBS, pH 7.4, followed by fixative (2% paraformaldehyde (PFA), 0.2% glutaraldehyde in PBS). The brains harvested and postfixed for 2 h, 4°C. After overnight wash in PBS at 4°C, they were stored in 0.02% PFA at 4°C. For staining, 20-µm thick tissue sections were prepared using a

vibrating microtome (Leica VT 1000S; Leica, Heerbrugg, Switzerland). Fluorescence immunolabeling was carried out on free-floating sections at RT. The sections were immersed and gently agitated in 0.5% Triton X-100, PBS for 30 min, followed by 10 min blocking (Protein Block Serum-Free; Dako, Carpinteria, CA, USA), and incubation with primary antibodies (1:200 dilution) overnight, 4°C. Sections were then incubated with secondary antibodies, followed by 10 min in 4% PFA. Nuclear counterstaining was performed by incubation in PO-PRO™-1 iodide (1:400; Invitrogen). The sections were mounted transferred on Polysine™ slides (Kindler, Freiburg, Germany) in Vectashield mounting medium (Vector Laboratories). Specificity of Snat3 antibody was assessed in knockout mice and control littermates (28). Secondary antibodies alone did not produce any significant staining in all tissues tested

Data analysis. Stained tissue sections were viewed with a Leica TCS SP2 confocal laser scanning microscope (Leica) using a 63x objective lens (numerical aperture of 1.4, pinhole set to 1.0 airy unit) with different zoom factors (5-8). A sequential scan procedure was applied during image acquisition and parameters were adjusted to use the full dynamic range of the photomultipliers. Typically, stacks of four to eight images (512 x 512 pixels) were taken and analysed at 122-nm intervals through the z-axis of the section. Representative images from the examined samples were chosen for figure editing. Digital images were processed using the software Imaris (Bitplane, Zurich, Switzerland), Huygens v1.2.3., or Leica Confocal Software LAS-AF (Leica).

Acknowledgements

This work was supported by SNF grant 31-130471 to Francois Verrey, and the Center for Microscopy and Image Analysis, University of Zurich, Switzerland. The authors would like to thank C.A. Wagner for the generous use of the Snat3 knockout mice.

References

1. Hawkins RA, O'Kane RL, Simpson IA, & Vina JR (2006) Structure of the blood-brain barrier and its role in the transport of amino acids. *J Nutr* 136:218S-226S.
2. McKenna MC (2007) The glutamate-glutamine cycle is not stoichiometric: fates of glutamate in brain. *J Neurosci Res* 85:3347-3358.
3. Engelhardt B & Sorokin L (2009) The blood-brain and the blood-cerebrospinal fluid barriers: function and dysfunction. *Semin Immunopathol* 31:497-511.
4. Virgintino D*, et al.* (2004) Immunolocalization of tight junction proteins in the adult and developing human brain. *Histochem Cell Biol* 122:51-59.
5. Virgintino D*, et al.* (2007) An intimate interplay between precocious, migrating pericytes and endothelial cells governs human fetal brain angiogenesis. *Angiogenesis* 10:35-45.
6. Pardridge WM (2005) Molecular biology of the blood-brain barrier. *Mol Biotechnol* 30:57-70.
7. Hediger MA*, et al.* (2004) The ABCs of solute carriers: physiological, pathological and therapeutic implications of human membrane transport proteinsIntroduction. *Pflugers Arch* 447:465-468.
8. Farrell CL & Pardridge WM (1991) Blood-brain barrier glucose transporter is asymmetrically distributed on brain capillary endothelial lumenal and ablumenal membranes: an electron microscopic immunogold study. *Proc Natl Acad Sci U S A* 88:5779-5783.

9. Lyck R, *et al.* (2009) Culture-induced changes in blood-brain barrier transcriptome: implications for amino-acid transporters in vivo. *J Cereb Blood Flow Metab* 29:1491-1502.
10. Roberts LM, *et al.* (2008) Subcellular localization of transporters along the rat blood-brain barrier and blood-cerebral-spinal fluid barrier by in vivo biotinylation. *Neuroscience* 155:423-438.
11. Roesli C, Mumprecht V, Neri D, & Detmar M (2008) Identification of the surface-accessible, lineage-specific vascular proteome by two-dimensional peptide mapping. *FASEB J* 22:1933-1944.
12. Matsuo H, *et al.* (2000) Expression of a system L neutral amino acid transporter at the blood-brain barrier. *Neuroreport* 11:3507-3511.
13. Franca R, Veljkovic E, Walter S, Wagner CA, & Verrey F (2005) Heterodimeric amino acid transporter glycoprotein domains determining functional subunit association. *Biochem J* 388:435-443.
14. Boulland JL, Rafiki A, Levy LM, Storm-Mathisen J, & Chaudhry FA (2003) Highly differential expression of SN1, a bidirectional glutamine transporter, in astroglia and endothelium in the developing rat brain. *Glia* 41:260-275.
15. Melone M, *et al.* (2004) Localization of the glutamine transporter SNAT1 in rat cerebral cortex and neighboring structures, with a note on its localization in human cortex. *Cereb Cortex* 14:562-574.
16. Cornford EM & Hyman S (2005) Localization of brain endothelial luminal and abluminal transporters with immunogold electron microscopy *NeuroRx* 2:27-43.
17. Ge S, Song L, & Pachter JS (2005) Where is the blood-brain barrier ... really? *J Neurosci Res* 79:421-427.
18. Mackenzie B & Erickson JD (2004) Sodium-coupled neutral amino acid (System N/A) transporters of the SLC38 gene family. *Pflugers Arch* 447:784-795.
19. Broer A, *et al.* (2002) Regulation of the glutamine transporter SN1 by extracellular pH and intracellular sodium ions. *J Physiol* 539:3-14.
20. Chaudhry FA, *et al.* (1999) Molecular analysis of system N suggests novel physiological roles in nitrogen metabolism and synaptic transmission. *Cell* 99:769-780.
21. Broer S & Brookes N (2001) Transfer of glutamine between astrocytes and neurons. *J Neurochem* 77:705-719.
22. Hawkins RA (2009) The blood-brain barrier and glutamate. *Am J Clin Nutr* 90:867S-874S.
23. Smith QR, Momma S, Aoyagi M, & Rapoport SI (1987) Kinetics of neutral amino acid transport across the blood-brain barrier. *J Neurochem* 49:1651-1658.
24. Ennis SR, Kawai N, Ren XD, Abdelkarim GE, & Keep RF (1998) Glutamine uptake at the blood-brain barrier is mediated by N-system transport. *J Neurochem* 71:2565-2573.
25. Agarwal N, Lippmann ES, & Shusta EV (2010) Identification and expression profiling of blood-brain barrier membrane proteins. *J Neurochem* 112:625-635.
26. O'Kane RL, Vina JR, Simpson I, & Hawkins RA (2004) Na+ -dependent neutral amino acid transporters A, ASC, and N of the blood-brain barrier: mechanisms for neutral amino acid removal. *Am J Physiol Endocrinol Metab* 287:E622-629.
27. Verrey F, *et al.* (2004) CATs and HATs: the SLC7 family of amino acid transporters. *Pflugers Arch* 447:532-542.
28. Busque SM & Wagner CA (2009) Potassium restriction, high protein intake, and metabolic acidosis increase expression of the glutamine transporter SNAT3 (Slc38a3) in mouse kidney. *Am J Physiol Renal Physiol* 297:F440-450.

Figure Legends

Figure 1. Confocal microscopy using specific markers for detection of brain vascular membrane localization. **A, B.** Representative image of a capillary stained with anti-Cd71 (green), and anti-Glut1 (blue). **C-F** Representative confocal images of a ~5μm diameter cortical capillary stained with antibodies against Lat1 (green), Glut1 (blue), laminin (red), and the nuclear dye PO-PRO^{TM} (white). Where PO-PRO^{TM} nuclear staining is not shown, the nucleus is indicated (*).

Figure 2. *In vivo* biotinylation of mouse brain vascular luminal membrane proteins preserves BBB integrity and detects known luminal Lat1 expression. Results from a representative blot probed for β-actin (upper panel), laminin (middle panel) and Lat1 (lower panel). Total protein lysate (T), unbound protein (U), and Neutravidin-bound (B) fractions from animals perfused ± biotin as indicated. See Fig. S1A for anti-biotin streptavidin-HRP blot results.

Figure 3. BBB Snat3 localization on both endothelial membranes revealed by confocal microscopy and *in vivo* biotinylation. **A, B.** Representative staining of tissue sections stained with anti-Snat3 (green), and anti-Glut1 (blue), nucleus indicated (*). **C.** Result from representative Western blot of total protein lysate (T), unbound protein (U), and Neutravidin-bound (B) fractions prepared from mice perfused ± biotin as indicated and probed with anti-Snat3 antibody.

Figure 4. Confocal microscopy uncovers expression of Snat1 on large cortical microvessels but not capillaries. Representative confocal images of cortical tissue sections stained as indicated with anti-Snat1 (green), and anti-Glut1 (blue), endothelial nucleus indicated as (*), pericyte as (P). **A, C.** The juncture between two larger microvessels, (>15μm), and **B, D.** a capillary (~5μm) are shown. See Figure S5 for nuclear PO-PRO^{TM} staining. **E.** Mice were perfused ± biotin and total protein lysate (T), unbound protein (U), and Neutravidin-bound (B) luminal fractions analyzed by Western blot for Snat1.

Figure 1

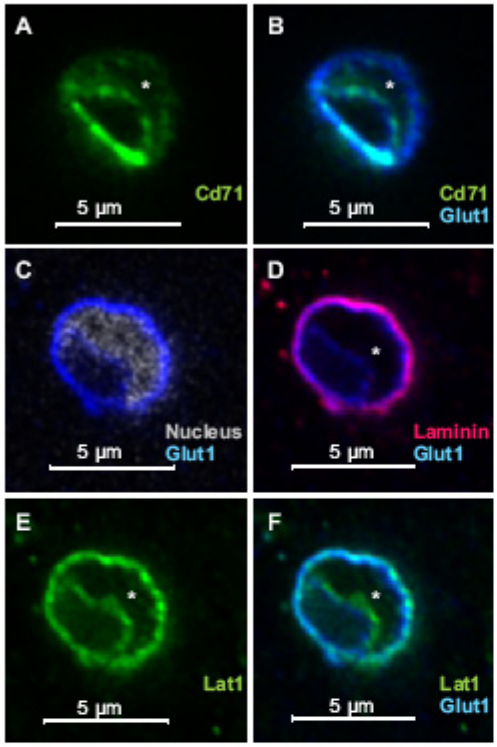
A
Cd71
5 µm
B
Cd71
Glut1
5 µm
C
Nucleus
Glut1
5 µm
D
Laminin
Glut1
5 µm
E
Lat1
5 µm
F
Lat1
Glut1
5 µm

Figure 2

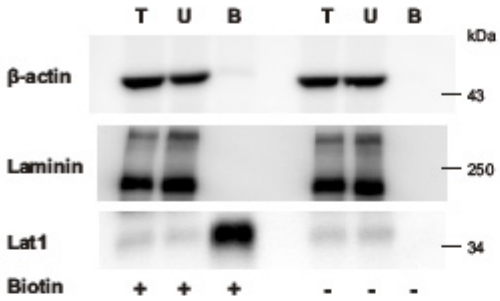

Figure 3

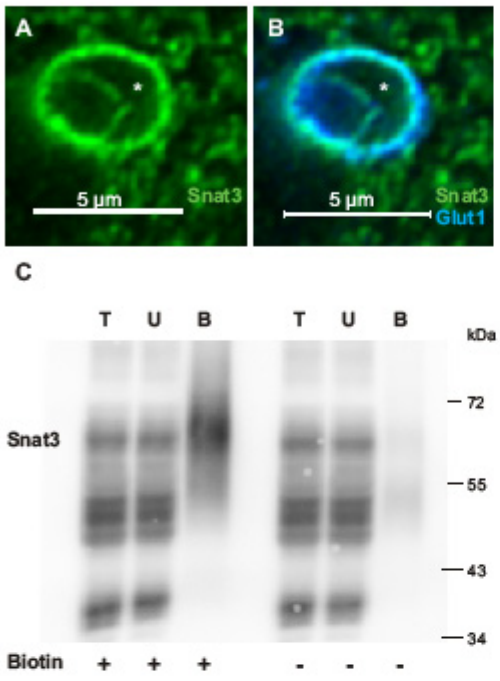
A
5 µm
Snat3
B
5 µm
Snat3
Glut1
C
T U B T U B
kDa
72
55
43
34
Snat3
Biotin + + + - - -

Figure 4

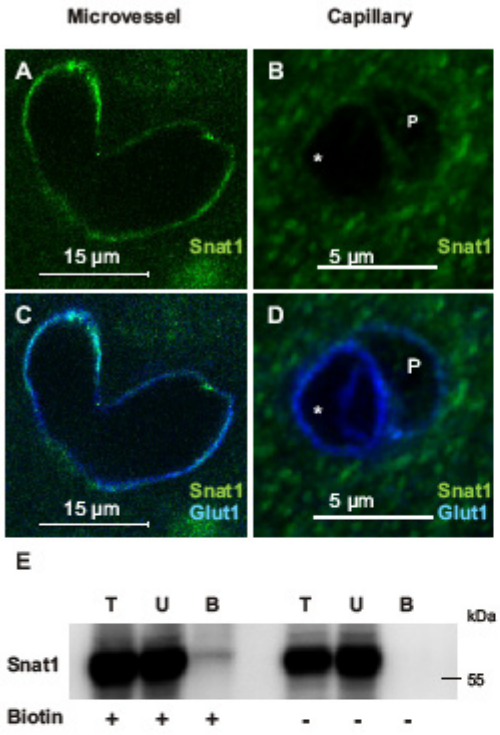
Microvessel
Capillary
A
B
P
*
15 µm
Snat1
5 µm
Snat1
C
D
P
*
15 µm
Snat1
Glut1
5 µm
Snat1
Glut1
E
T U B T U B
kDa
Snat1
55
Biotin
+ + + - - -

Supporting Information

Materials and Methods

Antibodies. The following commercially available primary antibodies were used: mouse-anti-glucose transporter 1 (Glut1), monoclonal ab40084 (Abcam, Cambridge, MA, USA), chicken-anti-laminin polyclonal ab14055 (Abcam), rabbit-anti-laminin polyclonal L9393 (Sigma-Aldrich, St. Louis, MO, USA), rat-anti-Transferrin receptor (CD71) monoclonal NB100-64979 (Novus Biologicals, Cambridge, UK), goat-anti-CD98 (4F2hc) polyclonal sc-7094 (Santa Cruz Biotechnology, Santa Cruz, CA, USA), rat-anti-CD98 (4F2hc) monoclonal 557479 (BD Biosciences, Allschwil, Switzerland); rabbit-anti-L-type amino acid transporter 1 (LAT1) polyclonal KE026 (CosmoBio Co., Tokyo, Japan); rabbit-anti-Claudin-5 polyclonal 34-1600 (Invitrogen, Eugene, OR, USA); mouse-anti-β-actin monoclonal A5316 (Sigma-Aldrich). Polyclonal antisera against mouse Snat1, human SNAT3 and human LAT1 were raised in rabbits using synthetic peptides of the following epitopes: mouse Snat1: MMHFKSGLELTELQNMTVC (Abgent, Bioggio, Switzerland); human SNAT3: MEIPRQTEMVELVPNGKC (Pineda, Berlin, Germany) (1); human LAT1: CTVLCQKLMQVVPQET (2). The following secondary antibodies were used as indicated: Alexa Fluor® 488 goat anti-rabbit / rat IgG (Invitrogen); DyLight™ 549 goat anti-chicken IgY (Jackson ImmunoResearch, Suffolk, UK); Cy5 goat anti-mouse IgG (Jackson ImmunoResearch); Neutravidin, DyLight™ 594 conjugated 22842 (Invitrogen); ECL™ anti-mouse IgG, HRP linked whole antibody (GE Healthcare, Little Chalfont Buckinghamshire, UK); anti-rabbit IgG (Fc) AP conjugate (Promega, Madison, WI, USA); anti-goat IgG AP conjugate (Promega); Streptavidin-HRP conjugate (GE Healthcare).

Protein extraction and purification of biotinylated proteins. Total lysate was prepared as described with minor modifications by Roesli and others (3-4). Briefly, 25 mg per ml of brain tissue was homogenized in lysis buffer (2% SDS, 50 mM Tris, 10 mM EDTA, Complete EDTA-free proteinase inhibitor cocktail (Roche Diagnostics, Mannheim, Germany) in PBS, pH 6.8) using a disperser (Polytron PT 2100, Kinematica AG, Littau, Switzerland). Homogenates were sonicated (Labsonic 1510, B. Braun, Bender + Hobun, Zurich, Switzerland), incubated at 95°C, 20 min and centrifuged at 17,000g, 20 min, 25°C. Total protein concentration was determined using the BCA™ protein assay (Thermo Scientific). Neutravidin-agarose resin (Thermo Scientific, 500 µl/sample) was washed in buffer A (1% Nonidet P-40, 0.1% SDS PBS) and lysis buffer. 15 mg of total protein extract (total protein lysate) was incubated with Neutravidin resin for 2h, RT with mixing. The supernatant was collected (unbound protein fraction) and the Neutravidin-agarose resin washed with buffer A and buffer B (0.1% Nonidet P-40, 1 M NaCl, PBS) and resuspended in solution C (2% SDS, 30 mM biotin (Sigma-Aldrich), 50 mM phosphate, 100 mM NaCl, 6 M urea, 2 M thiourea; pH ~12) (5), incubated 15 min, RT, followed by 15 min, 96°C and the supernatant collected and concentrated with trichloroacetic acid (final concentration 10%) overnight at 4°C. The precipitated proteins were washed 4 times with ice-cold ethanol, lyophilized, and resuspended in Laemmli buffer (Neutravidin-bound fraction).

Gel electrophoresis, Western blot analysis. For SDS polyacrylamide gel electrophoresis (SDS-PAGE), 25% of the total Neutravidin-agarose-bound protein fraction with or without *in vivo* biotinylation vs. 20 µg of the corresponding unbound protein fraction or of total protein lysate, were analysed by Western blotting. Samples from at least 3 independently treated mouse brains were isolated and analysed. Samples were reduced with β-mercaptoethanol and denatured by heating at 95°C, 5 min in Laemmli buffer and fractionated on a 6, 7.5 or 8.5%

SDS-PAGE. Immunoblotting was performed as previously described with minor modifications (6). Fractionated proteins were transferred electrophoretically to PVDF membranes (Immobilon-P; Millipore, Bedford, MA, USA). For Western blot all antibodies except anti-β-actin (1:5,000) were used at 1:500. Antibody binding was detected with Immobilon™ Western Chemiluminescent HRP or AP Substrate (Millipore, Billerica, MA, USA). Chemiluminescence was detected with a Fuji LAS-4000 camera (Bucher Biotec, Basel, Switzerland). The same membranes used to detect SLC proteins were stripped, blocked, and re-probed with Streptavidin-HRP followed by anti-β-actin antibody.

Protein deglycosylation assay. 20 µg of kidney total membranes, prepared as described previously (7), 20 µg of total liver and brain lysates, prepared as described under "protein extraction and purification of biotinylated proteins", and 25% of total Neutravidin-agarose-bound protein fractions with and without *in vivo* biotinylation, were treated with N-Glycosidase F (PNGase F; EC 3.5.1.52; New England Biolabs, Beverly, MA, USA). The samples were denatured at 65°C, 15 min in the provided buffer containing β-mercaptoethanol and SDS, incubated for 1 h at 37°C in reaction buffer with 1% Nonidet P-40 with or without added PNGase F.

References

1. Moret C, *et al.* (2007) Regulation of renal amino acid transporters during metabolic acidosis. *Am J Physiol Renal Physiol* 292:F555-F566.
2. Franca R, Veljkovic E, Walter S, Wagner CA, & Verrey F (2005) Heterodimeric amino acid transporter glycoprotein domains determining functional subunit association. *Biochem J* 388:435-443.
3. Roberts LM, *et al.* (2008) Subcellular localization of transporters along the rat blood-brain barrier and blood-cerebral-spinal fluid barrier by in vivo biotinylation. *Neuroscience* 155:423-438.
4. Roesli C, Neri D, & Rybak JN (2006) In vivo protein biotinylation and sample preparation for the proteomic identification of organ- and disease-specific antigens accessible from the vasculature. *Nat Protoc* 1:192-199.
5. Rybak JN, Scheurer SB, Neri D, & Elia G (2004) Purification of biotinylated proteins on streptavidin resin: a protocol for quantitative elution. *Proteomics* 4:2296-2299.
6. Romeo E, *et al.* (2006) Luminal kidney and intestine SLC6 amino acid transporters of B0AT-cluster and their tissue distribution in Mus musculus. *Am J Physiol Renal Physiol* 290:F376-F383.
7. Nowik M, *et al.* (2008) Genome-wide gene expression profiling reveals renal genes regulated during metabolic acidosis. *Physiol Genomics* 32:322-334.

Supporting Information

Figure Legends

Figure S1. Robust *in vivo* biotinylation of mouse brain vascular lumen. **A.** 20 µg of total protein lysate (T), unbound protein (U), and 25% of total Neutravidin-bound (B) fraction were analysed by Strepavidin-HRP blot. A representative blot following perfusion ± biotin is shown. **B, C.** Immunofluorescence staining of *in vivo* biotinylated brain tissue for Claudin-5 (Cldn5; green) confirmed that exogenous biotinylation (white) was restricted to the vasculature.

Figure S2. *In vivo* biotinylation of cortical vasculature detects luminal localization of 4F2 heavy chain. Representative Western blots are shown. **A**. Mice were perfused ± biotin and 20 µg of total protein lysate (T), unbound protein (U), and 25% of total Neutravidin-bound (B) fraction were analysed for 4F2hc presence. **B.** PNGaseF deglycosylation resulted in detection of a ~65kDa deglycoylated 4F2hc band in both the Neutravidin-bound fraction + biotin (25% of total) (B), and in total kidney membrane lysates (20 µg) (Kidney).

Figure S3. Confocal microscopy verifies expression of Snat3 in cortical microvessels of different sizes and specificity of antibody using $Snat3^{-/-}$ mice. Representative confocal images of tissue sections from 10 day heterozygous ($Snat3^{+/-}$) mice showing **A, C, E,** a large microvessel, and **B, D, F,** a capillary stained with antibodies against Snat3 (green), Glut1 (blue), or nuclear dye, PO-PRO^{TM} (white), as indicated. **G-J.** Confocal microscopy verifies expression of Snat3 in brain parenchyma and cortical microvessels from 10 day wild-type ($Snat3^{+/+}$) but not knockout ($Snat3^{-/-}$) mice. Representative confocal images of: **G, H** overview and **I, J** capillaries stained with Snat3 antibody (green). Endothelial nuclei indicated with (*) and pericyte nucleus designated with (P).

Figure S4. Snat3 antibody specificity was confirmed by Western blot of total brain or liver lysates from 10 day wild-type (+/+), heterozygous (+/-) or Snat3 knockout (-/-) mice. **A.** Representative Western blot of mouse brain or total liver protein lysate probed with anti-Snat3 antibody (upper panel) or β-actin (lower panel). **B.** 25% of Neutravidin-bound fraction (B) and 20 µg total kidney membrane lysates (Kidney) ± PNGaseF deglycosylation were analysed by Western blot and detected ~43 kDa deglycoylated Snat3 band.

Figure S5. Confocal microscopy of cortical capillary shown in Fig. 4 stained with antibodies against Snat1 (green), Glut1 (blue) and nuclear dye, PO-PRO^{TM} (white). Pericyte nucleus indicated as (P), and endothelial nucleus indicated as (*).

Figure S1

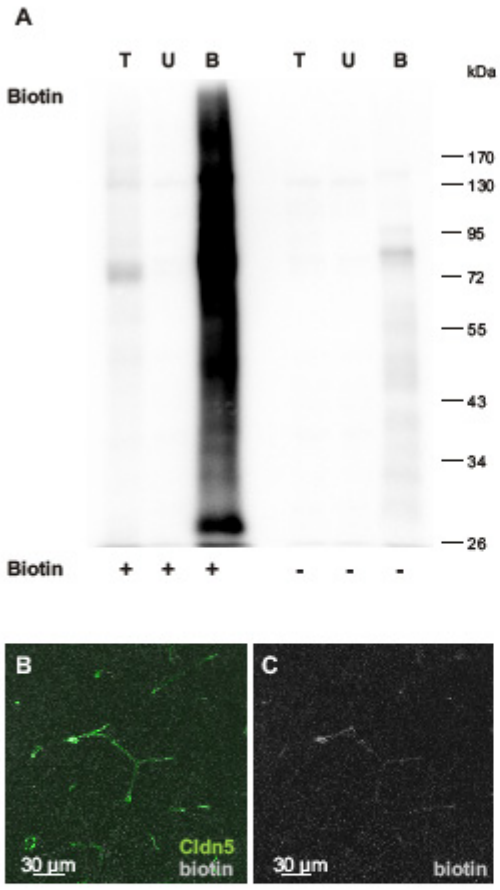
A
T U B T U B
kDa
Biotin
170
130
95
72
55
43
34
26
Biotin + + + - - -
B
Cldn5
biotin
30 µm
C
biotin
30 µm

Figure S2

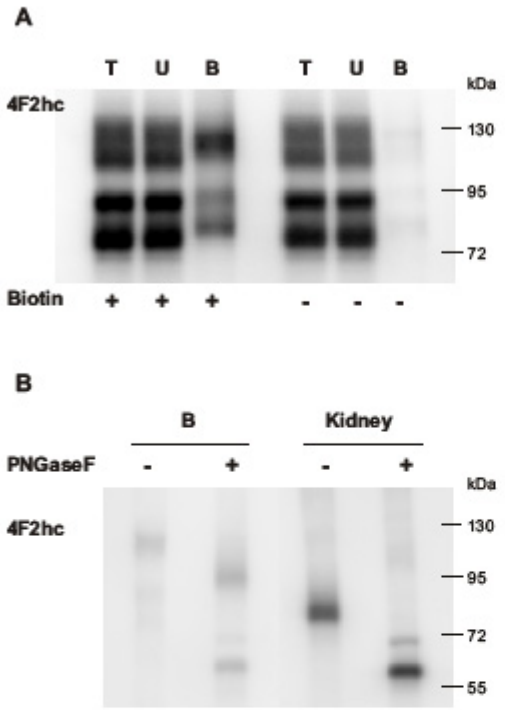
A
T U B T U B
kDa
4F2hc
130
95
72
Biotin + + + - - -
B
B
Kidney
PNGaseF - + - +
kDa
4F2hc
130
95
72
55

Figure S3

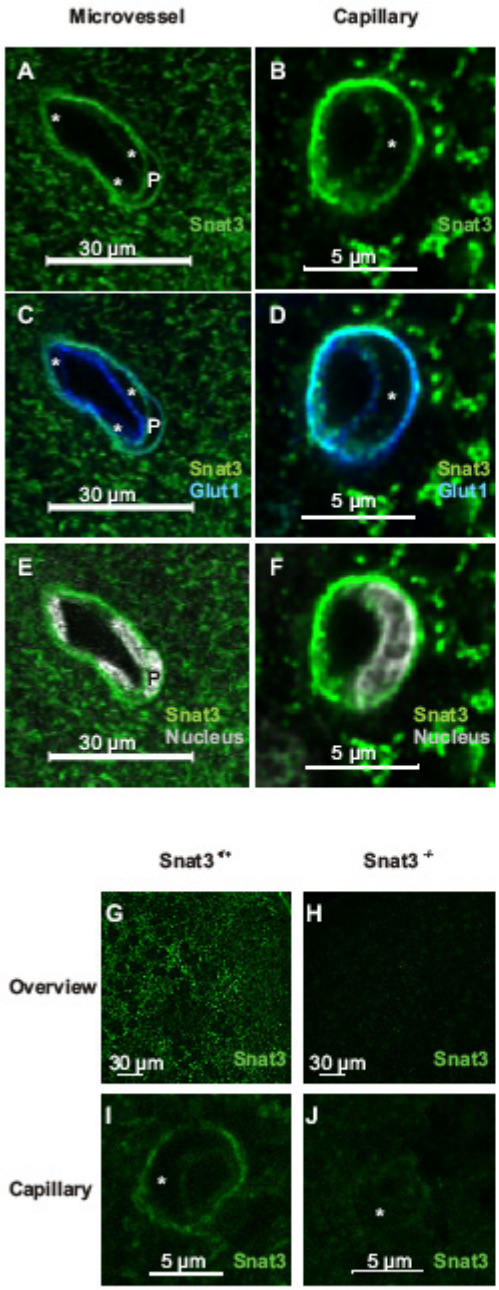
Microvessel
Capillary
A
B
P
Snat3
30 µm
5 µm
C
D
Snat3
Glut1
E
F
Nucleus
Snat3 +/+
Snat3 -/-
Overview
G
H
I
J
Capillary

Figure S4

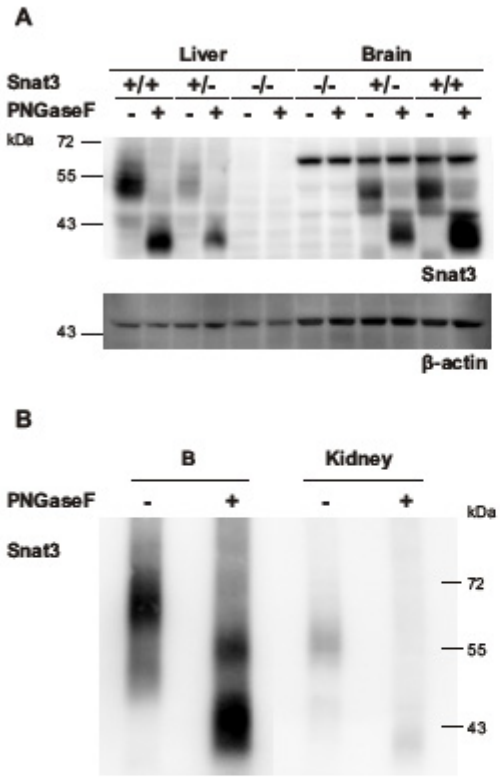
A
Liver
Brain
Snat3
+/+ +/- -/- -/- +/- +/+
PNGaseF
- + - + - + - + - + - +
kDa
72
55
43
Snat3
43
β-actin
B
B
Kidney
PNGaseF
- + - +
kDa
Snat3
72
55
43

Figure S5

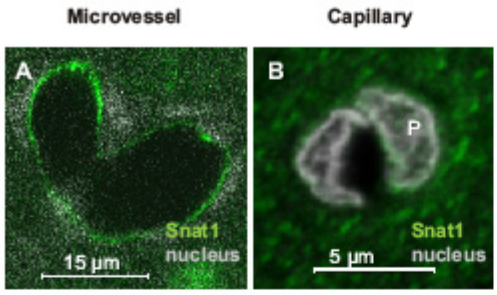
Microvessel
Capillary
A
B
P
Snat1
nucleus
15 µm
Snat1
nucleus
5 µm

6. Discussion and Outlook.

The results presented in this thesis demonstrate that 75% of all known SLC amino acid transporters are expressed by the mouse BBB *in vivo*, the majority of which were not described previously to be present. Furthermore, the 30 transporters expressed on mRNA level by the endothelial cells show differential regulation once dissociated from their *in vivo* microenvironment created by the neurovascular unit. From this differential regulation *in vitro* we hypothesize that transporters such as Lat1-4F2hc and Snat3 are highly expressed specifically in differentiated *in vivo* brain vascular endothelial cells and thus presumably mediate transendothelial transport at the BBB *in vivo*, and that Snat1 expression is linked to intraendothelial metabolism and cell proliferation [2], a function being restricted to larger vessels *in vivo* and microvascular endothelial cells cultured *in vitro*. In addition, our immunohistochemistry and *in vivo* biotinylation experiments show Snat3 being localized to both membranes, luminal and abluminal, indicating that sodium-dependent, secondary active, transport is not an exclusive feature of the abluminal membrane of brain microvascular endothelial cells as previously suggested. This agrees with the contradictory data to this hypothesis on $ATB^{0,+}$ [158] and Taut [155] (see section 3.6.1.1).

Our results show the need to re-examine the proposed mechanisms by which the BBB endothelial cells participate in establishing brain (amino acid) homeostasis, by combining functional data from the literature and current results obtained with the techniques and the knowledge of the postgenomic era.

What and where is the BBB? Localization of the BBB as layer between blood and brain and its high surface area compared to that of the choroid plexus [52] puts the endothelium in position to be the major site for exchange. Also the high number of transporters found to be expressed in our study of BBB endothelial cells supports the importance of this structure. On the other hand, the potential role of the choroid plexus in brain (amino acid) homeostasis may be underestimated since more recent studies suggest that the actual surface area due to the presence of microvilli is greater than estimated, and that the choroid plexus plays an important role in uptake of nutrients [19]. Also, the role of the endothelium in keeping the amino acid levels in brain ISF low may be overestimated and the role of transporters expressed on glial and neuronal plasma membranes underestimated, since they exhibit a higher surface area [3, 5].

The BBB endothelium and the other members of the neurovascular unit [22] may not only contribute to barrier function via cell-cell communication but also via interconnection of their transportomes [23] and by acting as "second line of defence" if the endothelial barrier is dysfunctional [26]. As an example, Snat3 is also expressed in astrocyte endfeet, highlighting their possible involvement in endothelial abluminal membrane transport into or back out of the brain. Furthermore, one has to consider that the brain vasculature shows heterogeneous expression profiles along the vascular tree. This has been shown for P-gp [20] and, in this thesis, for Snat1 (see section 5).

In conclusion, the role of the BBB endothelium in comparison to the other amino acid transporter expressing brain cells, and the role of the single segments of the vascular tree in keeping brain homeostasis, still needs further investigation. This is also true for the interplay of the neurovascular unit and the impact of the other brain barriers in this process. It seems clear that establishing the BBB properties is dependent on a complex interaction network of different cellular and acellular factors with many possible regulation points.

What is the amino acid concentration in the different brain compartments? Keeping amino acid homeostasis actually means to maintain their level at about 10% those of plasma, with exception of glutamine [1]. These values are based on measurements of plasma and CSF samples, as representative fluids facing the two membranes of the brain microvascular endothelial cells.

To equate CSF and brain ISF concentration is a simplification, based on the assumption that they are in equilibrium via diffusion [117] (see section 3.5.4 for details). This assumption on the other hand may underestimate local microenvironmental differences caused by local transport processes and metabolism of brain cells, characteristics of normal brain physiology. Even measuring plasma concentration represents a simplification, since the impact of plasma proteins and of blood flow in establishing a local environment near the luminal membrane may differ from that in the centre of the vasculature. Plasma levels of amino acids are also difficult to interpret since the plasma pool of free amino acids is very small compared with the intracellular pool of free amino acids, which is again small compared with the protein-bound amino acid pool, all three being in equilibrium [122]. Furthermore, the plasma concentration is also subject to high fluctuations, resulting in fluctuations of the gradient across the BBB. This implies that transport across the BBB may not exclusively be regulated via the gradient between blood and CSF.

In conclusion, the composition of the medium at both sides of the endothelial cell membranes is not accurately known [82]. The current assumption that BBB transport occurs according to the gradient between blood and CSF represents a simplification. It does not take into account existing differences between CSF and ISF, local differences in ISF concentrations, and the impact of intracellular amino acid concentration of endothelial and brain cells in regulating transcellular transport processes. Furthermore, the total cytoplasmic amino acid concentration may differ from that directly at the plasma membrane. This information is crucial for understanding the location and quantity of the gradient between blood and brain which drives the transport. It is also important to understand how transporters are localized in response to changes in the amino acid gradient, and how they are regulated to maintain this gradient.

What role does the intraendothelial compartment play in transport processes? The intracellular amino acid concentration is assumed to be generally higher than in ISF and plasma, and transport of amino acids from brain ISF into endothelial cells is highly concentrative, also due to the very small cell volume [32]. Too high cytoplasmic concentrations would impede influx or cause efflux back into brain ISF [32]. The necessary tight regulation of cytoplasmic concentrations can be achieved by transport processes, metabolism [1, 182], compartmentation events like the glutamate-glutamine cycle [1] (details see section 3.5.3.1), and biochemical conversions.

The glutamate-glutamine cycle is described between astrocytes and neurons, but has also been suggested to occur between astrocyte endfeet and brain endothelial cells [32] and even intraendothelial. In this scenario, glutamine would be taken up over the abluminal membrane, converted by the intraendothelial glutaminase to glutamate which than could diffuse into blood by a sodium-independent process. Such a mechanism could be involved in brain to blood transport of glutamate [32]. Glutaminase activity is regulated by end product inhibition, and increased levels of intracellular glutamate result in the accumulation of glutamine [32], the preferred substrate for tertiary active transport processes (see section 3.6 and 3.6.1.3).

Another possible link coordinating transport processes at the luminal and abluminal membranes may be the γ-glutamyl cycle (details see section 3.6.1.4), the regulation of abluminal sodium-dependent transporters via intracellular synthesized pyroglutamate [8, 165]. Transporters are also suggested transceptors [183], integrating extracellular signals with intracellular events, possibly via intracellular amino acid sensors like ATF4 or a member of the TOR pathway. Also the intracellular abundance of amino acid metabolism products, such as ATP, may be involved in amino acid sensing [183].

The endothelial cells are highly metabolic active cells with a high number of mitochondria [52]. Therefore, the endothelial cytoplasm and processes affecting its content may play an important role in determining the gradient over the single membranes and over the whole cell, and in buffering changes in blood as well as brain ISF.

Besides glutaminase, endothelial cells also contain the enzymes required for synthesis and metabolism of serotonin and for catabolism of norepinephrine and dopamine [184]. One example of the impact of these enzymes on BBB transendothelial transport is observed for treatment of patients with neurotransmitter precursors, e.g. L-DOPA used in Parkinson's disease treatment. Large doses of L-DOPA are necessary to achieve a therapeutic effect since it is metabolized in endothelial cells before it reaches the brain parenchyma, the place of action [184].

In conclusion, the role of the intraendothelial compartment in regulating transport processes across the BBB may be underestimated so far. Anatomically it represents the junction between the two endothelial membranes and is therefore in a position to integrate, coordinate and regulate transport processes across the whole endothelial cell. The amino acid transport across the BBB may therefore be divided, in a blood to cytoplasm and a cytoplasm to ISF transport. This would imply that the gradient driving amino acid transport in the first instance, transport across the luminal membrane, would be different from the blood to brain ISF gradient, and that transport over the abluminal membrane would not directly be affected by the plasma amino acid concentrations. This view is supported by findings that the Na^+/K^+-ATPase may be localized on both endothelial membranes [185] and that the sodium gradient (extracellular higher intracellular [1]) driving secondary active transport exists over the abluminal as well as over the luminal membrane. In conclusion, regulation of transport mechanisms over the BBB may have to be re-thought under consideration of these aspects.

What are the different possibilities for polarization of transport? Transport polarity is probably a key feature of BBB function [79], since asymmetrical distribution allows vectorial transport which can create and sustain ionic and metabolite gradients, as seen for amino acids. In this context, asymmetrical expression of Glut1, Snat3 and Cd71 at the two membranes of the BBB endothelium has been shown in this thesis (see section 5). However, heterogeneity in expression and localization of transporters can happen on several levels, between different cell types, between the same cell type according to the environmental input, and in different developmental stages. One example for this is Snat3, which was previously reported to be only transiently expressed in the vascular endothelium during formation of the BBB [163], a

fact disproven in this thesis. Snat1 was found to be expressed at higher levels in the bigger vessels compared to brain capillaries. This highlights that expression heterogeneity seems to be a common feature of many transporters, since also for P-gp, an ABC transporter expressed on the luminal membrane [186], an segmental difference in expression along the brain vascular tree has been shown, with highest expression in capillaries [20]. Furthermore, differences between different vascular segments within the same organ may even be small compared to differences between neighbouring cells. Also within the same endothelial cells, expression and regulation of transporters on the two different membranes may vary since they face different cellular and mechanical environments. There is the possibility of polarized expression on either the luminal or abluminal membrane, and if expressed on both membranes there is the possibility of unequal expression levels, activities, affinities or regulation processes.

Transport processes at the BBB can also be influenced by changing the substrate concentration in one of the compartments involved. It has been shown for example that a reduction of glutamate levels in blood increases the glutamate efflux from endothelial cells into blood and from brain ISF to blood [32]. An increased glutamate efflux is expected to also influence the transport of glutamine from brain ISF into endothelial cells [32]. This is of interest since glutamine can be used to accumulate essential amino acids (details see section 3.5.3.1) and seems to be a possible link between driving and regulating transport processes.

Amino acid gradients over the two membranes may also be influenced by biochemical conversions in the cytoplasm such as transamination, oxidation, hydroxylation, etc [94]. In this way the gradient over the membrane for the original amino acid can be sustained, and its transport further facilitated. Another possibility to influence transport processes are different posttranslational modifications of transporters inserted in the two distinct membranes, as indicated for Snat3 by the *in vivo* biotinylation experiments presented in this thesis (see section 5).

System L1 transport is determined by the plasma concentration and the affinity constants, different for the different neutral amino acids which compete with each other for transport by L1 [5]. Since system L has a reported high exchanging activity, it has been considered certain LNAAs may be effluxed back out of the brain faster than brain cells take them up [184]. An important point that has not been considered adequately yet is the fact that the main neutral essential amino acid transporter expressed in both membranes of BBB endothelial cells, Lat1-4F2hc, does not mediate net amino acid transport (uniport) but mainly amino acid exchange

(see section 3.6.1.1). Thus influx of essential amino acids is always coupled to an equimolar efflux of amino acids that may be nonessential.

The complexity of the system is pointed out by the fact that amino acid transport follows not only concentration gradients, also need, nutritional status, plasma and ISF concentrations of single amino acids and of a group of amino acids transported by the same transporter have to be considered, as well as regional differences [94]. The environmental impact on expression profiles could be shown, e.g. xCT (Slc7a11) and 4F2hc (Slc3a2) expression was found to be upregulated under influence of laminar flow [187]. On the abluminal membrane it has been suggested that gene expression within the neurovascular unit is highly interdependent [23] and that non-endothelial metabolism and transport processes regulating brain ISF concentration may have impact on transport across the abluminal endothelial membrane and therefore participate in the transport from blood to brain via the endothelial cytoplasm [184] (see section 3.6.1).

In conclusion, there are numerous possibilities to coordinate amino acid transport across the BBB. Differences may exist between different organs, within the same organ in different parts of the vascular tree, between neighbouring endothelial cells and within the same endothelial cell. The transportomes of the two membranes may differ, and even if they don't differ on the expression level they may do so by regulation of their function. Polarization may be achieved by substrate conversion, by transport of co-transported substrates, and by asymmetrical distribution of the single transporters. Membrane expression of the transporters may also be influenced by trafficking and protein-protein interactions. Furthermore, transporters often show overlapping properties [122], may depend on amino acid gradients established by other transporters, and some, like SNAT3, can operate in reverse (see section 3.6.1.3.2). In general, uniport mechanisms (facilitated diffusion) seem not to play a major role in establishing brain homeostasis since for instance Tat1, Lat3, and Lat4 expression was found to be very low *in vivo* in this thesis [2].

Interpretation of *in vivo* data is difficult since reports about transporter localization in the literature are often contrary or difficult to interpret (see section 3.6.1.1) and the complexity of the system is far from being understood.

Does sodium-dependent amino acid transport just make sense on the abluminal membrane?

Considering the participation of many amino acids in neurotransmission, together with functional data, and taking into account the existing amino acid gradient from blood to brain, it has been generally postulated that sodium-dependent amino acid transport is a feature of the

abluminal membrane of the BBB, which is absent from the luminal membrane where exclusively facilitative diffusion processes take place (which is of course not true in view of the obligatory exchange mode of Lat1 for instance) [3-6]. The finding of Snat3 presence on the luminal membrane of the BBB challenges this hypothesis and highlights the so far underestimated contribution of this membrane in actively regulating brain amino acid homeostasis.

The hypothesis is based on results obtained from functional studies, like transendothelial transport across the BBB *in vivo*, and transport studies using isolated luminal and abluminal plasma membrane vesicles, a method developed by Betz *et al.* [43]. But, by performing *in vivo* studies, one cannot distinguish between different functions of the luminal and abluminal membrane in the transendothelial transport process [1], and vesicle studies have the disadvantage of working with unpure fractions that are distinguished based on nonspecific marker proteins [87]. In addition, sodium-dependent transport activities observed in luminal membrane-rich fractions was completely accounted for by abluminal vesicle contamination [79] and therefore not investigated further. And, since many amino acid transporters have only recently been cloned, previous functional studies were only able to define transport systems, based on substrate specificity, specific transport inhibiting compounds, and ion dependencies. However, amino acid transporters show overlapping substrate specificities, and the contribution of high-affinity systems with low transport capacities might have remained undetected.

System L, even if not directly coupled to the sodium gradient, is dependent on the amino acid gradient generated by sodium-dependent, secondary active transporters of the System N and System A families [138]. Therefore, Lat1-4F2hc can also be seen as tertiary active transporter, allowing net cellular accumulation or depletion of specific System L substrates like leucine, without any change in the total amino acid concentration on either side of the cell membrane. Glutamine is the best candidate for hetero-exchange via system L, since glutamine is the only amino acid with similar concentrations in plasma and brain, and since it can be accumulated intracellularly by system N and A members. In this way essential amino acids can also be accumulated by Lat1-4F2hc.

The localization of Snat3 on the luminal membrane may indicate a functionally association of Lat1-4F2hc with this secondary active transporter to enhance availability of essential amino acids to brain. Snat3 is not the first secondary-active transporter found to be localized at the luminal membrane, also $ATB^{0,+}$ (Slc6a14) and the serotonin transporter SERT (Slc6a4) have been detected in this membrane (see section 3.6.1.1). The luminal expression was justified by

the fact that serotonin acts as vasoconstrictor and that its clearance from blood is important to maintain cerebral blood flow [188]. Amino acids like aspartate, glutamate, and glycine may exhibit the same function [189] and would offer one explanation for potential luminal localization of EAATs (see addendum) found in this thesis. Another explanation would be that the transported substrate exerts a function in interorgan communication. The need to actively regulate the amino acid clearance from the endothelial cytoplasm may be also one explanation of secondary-active transporters being localized to the luminal membrane like seen in this thesis (see section 5).

Furthermore, amino acid transporters may be involved in other mechanisms than pure transport, opening the possibilities for further regulatory mechanisms affecting localization and function. Amino acid transporters at the plasma membrane represent the first contact between cell and environment, sensing both extracellular and intracellular amino acid concentrations, and are therefore in a position to play a role in nutrient sensing and signalling.

Amino acid transporters have also been shown to change between localization at the plasma membrane and intracellular storage places. Depending on environmental stimuli, like starvation, trafficking from these subcellular localizations to the plasma membrane to guarantee nutrition has been shown.

In conclusion, the gradient driving active transport may be over both membranes and the role of the intraendothelial compartment in transport processes may be underestimated. Therefore the current hypothesis, that sodium-dependent transport is exclusively expressed abluminally, may represent a simplification and needs further investigation. Also the view of blood to brain transport serving nutritional needs and brain to blood transport preventing neurotoxic amino acid levels in the brain ISF may be too simple, highlighting the need to measure brain to blood transport *in vivo* which is less studied. Further, the exact role of facilitated diffusion on the abluminal membrane is not well studied. One has also to consider that efflux, influx and metabolism occur simultaneously and that one can not see the processes separated from each other. Even if no differences can be measured it does not mean that there is no flux existing, it just tells that the sum of all events equals up.

Is it important to study amino acid transport across the BBB? To understand the functional organisation of the BBB and the role of the BBB transportome in physiological and (neuro)pathophysiological states, many of them characterized by impaired brain amino acid concentrations, it is necessary to not only determine which transporters are expressed at the BBB, but also whether these transporters are expressed at the luminal or abluminal

membrane, and how they are regulated. Sodium-dependent transporters expressed on the luminal membrane of vascular endothelial cells may play an important role in situations characterized by limited amino acid supply, like during stroke. Furthermore, luminal expressed amino acid transporters potentially could represent an interesting route for pharmacological interventions due to their easy accessibility. Novel therapeutic approaches, based on the findings how the neurovascular unit communicates to establish the BBB phenotype, may be obtained for improved drug delivery across the BBB [23].
There is a research gap regarding nutrient transporters at the BBB, also since the effort nowadays lies on research of ABC transporters due to their importance for the pharmaceutical industry.

What comes next? Future investigations should aim at determining the molecular nature, subcellular expression, and activity of other, still not characterized, SLC members at the BBB and other brain barriers. Since the basis of normal brain function is not sufficiently understood, the basis of abnormal function is also poorly understood [123]. The BBB transportome, the players presented in this thesis, at least on mRNA level, should be studied by combining expression with functional analysis to give the single players a name and face. *In vivo* studies are necessary to avoid culture induced artefacts [2, 150], also if one keeps in mind that many if not most features of the BBB phenotype can be subject to modulation [14].
One interesting family to examine is system X^-_{AG} (see Table 4). In neurons they have been found to be subject to intracellular trafficking and highly regulated expression. But also the brain vasculature is rich in EAATs, suggesting a role in brain ISF glutamate homeostasis [32]. Preliminary results (see addendum in this thesis and mRNA results in Lyck *et al.* [2]) suggest that the EAATs may play a major role in BBB physiology.
The possibility of differences in regulatory mechanisms on the luminal compared to the abluminal membrane has to be considered and examined, since the two membranes face different biochemical and physical environments. Also, the role of the BBB transportome and single transporters within, in adaptation to regional differences in brain ISF composition, and their developmental and physiological modulations needs further observations. The question of polarity should also be viewed under the light of regulated expression and activity. Localization and activity of a transporter, as well as total expression and functional activity, can be different, highlighting the importance to find a way to characterize brain to blood transport *in vivo*. In general, the methods to examine transport processes should be optimized to be able to measure transendothelial transport of also small hydrophilic solutes like amino

acids. It is difficult to distinguish between unidirectional flux and uptake, since membrane transport processes are very rapid and equilibrium is reached within 1-5 s for glucose or amino acids, and therefore intracellular metabolism may dominate the uptake process [119]. In the past, an inability to measure transendothelial transport of a substance was interpreted in a way that there is no movement of this substance occurring (see section 3.6.1.1). One has also to consider that transport happens not only according to a substrate gradient, also to need, relevance (essential vs. non-), energy-dependency, to plasma and brain ISF concentrations of single amino acids and of a group of amino acids transported by the same transporter. One future focus should also be to identify how amino acids are retained by the brain once they have entered [1].

Furthermore, a functional *in vitro* system would be one of the greatest achievements in BBB research of the last years (see section 3.4.2). With an *in-vivo* like *in vitro* model a high-throughput system would exist allowing to screen for the impact of intraendothelial metabolism on various aspects of barrier physiology. By performing co-culture experiments the interaction of several transporters expressed in the various cells of the neurovascular unit and the impact of compartmentalization events could be studied. Also the measurements of transport processes *in vivo*, e.g. with positron emission tomography (PET), together with the determination of cellular and brain ISF amino acid concentrations over time, would further allow to better understand the gradients driving BBB transport.

In general, the inconsistent use of methodical approaches and transporter nomenclature in the past (see section 3.6.1.1) resulted in difficulties to compare the published data and see them in context to each other. One issue is that characterization of transport systems was mainly performed in the pregenomic era, using bovine and pig material, and that this data was not aligned to the identified and characterized single transporters. One example to mention is the described system Na^+-LNAA, a system not known outside the BBB literature and not described elsewhere. Thus effort should be done to combine the data on expression of single transporters at the BBB with the ones obtained by functional studies describing mainly transport systems.

7. References.

1. Hawkins, R.A., et al., *Structure of the blood-brain barrier and its role in the transport of amino acids.* J Nutr, 2006. **136**(1 Suppl): p. 218S-26S.
2. Lyck, R., et al., *Culture-induced changes in blood-brain barrier transcriptome: implications for amino-acid transporters in vivo.* J Cereb Blood Flow Metab, 2009. **29**(9): p. 1491-502.
3. Betz, A.L. and G.W. Goldstein, *Polarity of the blood-brain barrier: neutral amino acid transport into isolated brain capillaries.* Science, 1978. **202**(4364): p. 225-7.
4. O'Kane, R.L. and R.A. Hawkins, *Na+-dependent transport of large neutral amino acids occurs at the abluminal membrane of the blood-brain barrier.* Am J Physiol Endocrinol Metab, 2003. **285**(6): p. E1167-73.
5. O'Kane, R.L., et al., *Na+ -dependent neutral amino acid transporters A, ASC, and N of the blood-brain barrier: mechanisms for neutral amino acid removal.* Am J Physiol Endocrinol Metab, 2004. **287**(4): p. E622-9.
6. O'Kane, R.L., et al., *Cationic amino acid transport across the blood-brain barrier is mediated exclusively by system y+.* Am J Physiol Endocrinol Metab, 2006. **291**(2): p. E412-9.
7. Hawkins, R.A., *The blood-brain barrier and glutamate.* Am J Clin Nutr, 2009. **90**(3): p. 867S-874S.
8. Lee, W.J., et al., *Role of oxoproline in the regulation of neutral amino acid transport across the blood-brain barrier.* J Biol Chem, 1996. **271**(32): p. 19129-33.
9. Lee, W.J., et al., *Glutamine transport by the blood-brain barrier: a possible mechanism for nitrogen removal.* Am J Physiol, 1998. **274**(4 Pt 1): p. C1101-7.
10. Kandel, E.R. and L.R. Squire, *Neuroscience: breaking down scientific barriers to the study of brain and mind.* Science, 2000. **290**(5494): p. 1113-20.
11. http://www.who.int/mental_health/neurology/chapter_2_neuro_disorders_public_h_challenges.pdf.
12. Boron, W.F.B., E. L., *Medical physiology: a cellular and molecular approach; 2nd edition*. 2009: Saunders Elsevier.
13. Bradbury, M.W., *The concept of a blood-brain barrier.* Chapter 2: The concept of a vascular barrier.; Chapter 3: The ultrastructure of the blood-brain barrier. 1979, Chichester - New York - Brisbane - Toronto: John Wiley & Sons Ltd.
14. Abbott, N.J., L. Ronnback, and E. Hansson, *Astrocyte-endothelial interactions at the blood-brain barrier.* Nat Rev Neurosci, 2006. **7**(1): p. 41-53.
15. Engelhardt, B. and L. Sorokin, *The blood-brain and the blood-cerebrospinal fluid barriers: function and dysfunction.* Semin Immunopathol, 2009. **31**(4): p. 497-511.
16. Ballabh, P., A. Braun, and M. Nedergaard, *The blood-brain barrier: an overview: structure, regulation, and clinical implications.* Neurobiol Dis, 2004. **16**(1): p. 1-13.
17. Smith, Q.R., *Transport of glutamate and other amino acids at the blood-brain barrier.* J Nutr, 2000. **130**(4S Suppl): p. 1016S-22S.
18. Drewes, L.R., *Molecular architecture of the brain microvasculature: perspective on blood-brain transport.* J Mol Neurosci, 2001. **16**(2-3): p. 93-8; discussion 151-7.
19. Rouault, T.A., D.L. Zhang, and S.Y. Jeong, *Brain iron homeostasis, the choroid plexus, and localization of iron transport proteins.* Metab Brain Dis, 2009. **24**(4): p. 673-84.
20. Ge, S., L. Song, and J.S. Pachter, *Where is the blood-brain barrier ... really?* J Neurosci Res, 2005. **79**(4): p. 421-7.

21. Bundgaard, M. and N.J. Abbott, *All vertebrates started out with a glial blood-brain barrier 4-500 million years ago.* Glia, 2008. **56**(7): p. 699-708.
22. Wolburg, H., et al., *Brain endothelial cells and the glio-vascular complex.* Cell Tissue Res, 2009. **335**(1): p. 75-96.
23. Lok, J., et al., *Cell-cell signaling in the neurovascular unit.* Neurochem Res, 2007. **32**(12): p. 2032-45.
24. Nakagawa, S., et al., *A new blood-brain barrier model using primary rat brain endothelial cells, pericytes and astrocytes.* Neurochem Int, 2009. **54**(3-4): p. 253-63.
25. Santaguida, S., et al., *Side by side comparison between dynamic versus static models of blood-brain barrier in vitro: a permeability study.* Brain Res, 2006. **1109**(1): p. 1-13.
26. Abbott, N.J., et al., *Structure and function of the blood-brain barrier.* Neurobiol Dis. **37**(1): p. 13-25.
27. Tam, S.J. and R.J. Watts, *Connecting Vascular and Nervous System Development: Angiogenesis and the Blood-Brain Barrier.* Annu Rev Neurosci.
28. http://www.colorado.edu/intphys/Class/IPHY3430-200/image/09-6.jpg.
29. Sumpio, B.E., J.T. Riley, and A. Dardik, *Cells in focus: endothelial cell.* Int J Biochem Cell Biol, 2002. **34**(12): p. 1508-12.
30. Pries, A.R. and W.M. Kuebler, *Normal endothelium.* Handb Exp Pharmacol, 2006(176 Pt 1): p. 1-40.
31. Zlokovic, B.V., *The blood-brain barrier in health and chronic neurodegenerative disorders.* Neuron, 2008. **57**(2): p. 178-201.
32. Teichberg, V.I., et al., *Homeostasis of glutamate in brain fluids: an accelerated brain-to-blood efflux of excess glutamate is produced by blood glutamate scavenging and offers protection from neuropathologies.* Neuroscience, 2009. **158**(1): p. 301-8.
33. Pardridge, W.M., *Blood-brain barrier genomics and the use of endogenous transporters to cause drug penetration into the brain.* Curr Opin Drug Discov Devel, 2003. **6**(5): p. 683-91.
34. Aird, W.C., *Endothelial cell heterogeneity.* Crit Care Med, 2003. **31**(4 Suppl): p. S221-30.
35. Chi, J.T., et al., *Endothelial cell diversity revealed by global expression profiling.* Proc Natl Acad Sci U S A, 2003. **100**(19): p. 10623-8.
36. Cleaver, O. and D.A. Melton, *Endothelial signaling during development.* Nat Med, 2003. **9**(6): p. 661-8.
37. Hewett, P.W. and J.C. Murray, *Human microvessel endothelial cells: isolation, culture and characterization.* In Vitro Cell Dev Biol Anim, 1993. **29A**(11): p. 823-30.
38. Garlanda, C. and E. Dejana, *Heterogeneity of endothelial cells. Specific markers.* Arterioscler Thromb Vasc Biol, 1997. **17**(7): p. 1193-202.
39. Savidge, T.C., *MIND the gap: an astroglial perspective on barrier regulation.* Neuron Glia Biol, 2007. **3**(3): p. 191-7.
40. Risau, W., S. Esser, and B. Engelhardt, *Differentiation of blood-brain barrier endothelial cells.* Pathol Biol (Paris), 1998. **46**(3): p. 171-5.
41. Pardridge, W.M., *Blood-brain barrier biology and methodology.* J Neurovirol, 1999. **5**(6): p. 556-69.
42. Cornford, E.M. and S. Hyman, *Localization of brain endothelial luminal and abluminal transporters with immunogold electron microscopy.* NeuroRx, 2005. **2**(1): p. 27-43.
43. Betz, A.L., J.A. Firth, and G.W. Goldstein, *Polarity of the blood-brain barrier: distribution of enzymes between the luminal and antiluminal membranes of brain capillary endothelial cells.* Brain Res, 1980. **192**(1): p. 17-28.

44. Correale, J. and A. Villa, *Cellular elements of the blood-brain barrier.* Neurochem Res, 2009. **34**(12): p. 2067-77.
45. Crone, C. and S.P. Olesen, *Electrical resistance of brain microvascular endothelium.* Brain Res, 1982. **241**(1): p. 49-55.
46. Smith, Q.R. and S.I. Rapoport, *Cerebrovascular permeability coefficients to sodium, potassium, and chloride.* J Neurochem, 1986. **46**(6): p. 1732-42.
47. Butt, A.M., H.C. Jones, and N.J. Abbott, *Electrical resistance across the blood-brain barrier in anaesthetized rats: a developmental study.* J Physiol, 1990. **429**: p. 47-62.
48. Furuse, M., et al., *Occludin: a novel integral membrane protein localizing at tight junctions.* J Cell Biol, 1993. **123**(6 Pt 2): p. 1777-88.
49. Nitta, T., et al., *Size-selective loosening of the blood-brain barrier in claudin-5-deficient mice.* J Cell Biol, 2003. **161**(3): p. 653-60.
50. Ohtsuki, S., et al., *Exogenous expression of claudin-5 induces barrier properties in cultured rat brain capillary endothelial cells.* J Cell Physiol, 2007. **210**(1): p. 81-6.
51. Kose, N., et al., *Altered expression of basement membrane-related molecules in rat brain pericyte, endothelial, and astrocyte cell lines after transforming growth factor-beta1 treatment.* Drug Metab Pharmacokinet, 2007. **22**(4): p. 255-66.
52. Nag, S., *Morphology and molecular properties of cellular components of normal cerebral vessels.* Methods Mol Med, 2003. **89**: p. 3-36.
53. Tilling, T., et al., *Basement membrane proteins influence brain capillary endothelial barrier function in vitro.* J Neurochem, 1998. **71**(3): p. 1151-7.
54. Dore-Duffy, P., *Pericytes: pluripotent cells of the blood brain barrier.* Curr Pharm Des, 2008. **14**(16): p. 1581-93.
55. Balabanov, R. and P. Dore-Duffy, *Role of the CNS microvascular pericyte in the blood-brain barrier.* J Neurosci Res, 1998. **53**(6): p. 637-44.
56. Pardridge, W.M., *Molecular biology of the blood-brain barrier.* Mol Biotechnol, 2005. **30**(1): p. 57-70.
57. Peppiatt, C.M., et al., *Bidirectional control of CNS capillary diameter by pericytes.* Nature, 2006. **443**(7112): p. 700-4.
58. Merwin, J.R., et al., *Transforming growth factor beta 1 modulates extracellular matrix organization and cell-cell junctional complex formation during in vitro angiogenesis.* J Cell Physiol, 1990. **142**(1): p. 117-28.
59. Zozulya, A., C. Weidenfeller, and H.J. Galla, *Pericyte-endothelial cell interaction increases MMP-9 secretion at the blood-brain barrier in vitro.* Brain Res, 2008. **1189**: p. 1-11.
60. Choi, Y.K. and K.W. Kim, *Blood-neural barrier: its diversity and coordinated cell-to-cell communication.* BMB Rep, 2008. **41**(5): p. 345-52.
61. Hori, S., et al., *A pericyte-derived angiopoietin-1 multimeric complex induces occludin gene expression in brain capillary endothelial cells through Tie-2 activation in vitro.* J Neurochem, 2004. **89**(2): p. 503-13.
62. Nakagawa, S., et al., *Pericytes from brain microvessels strengthen the barrier integrity in primary cultures of rat brain endothelial cells.* Cell Mol Neurobiol, 2007. **27**(6): p. 687-94.
63. Lee, H.S., et al., *Brain angiogenesis in developmental and pathological processes: regulation, molecular and cellular communication at the neurovascular interface.* FEBS J, 2009. **276**(17): p. 4622-35.
64. Zonta, M., et al., *Neuron-to-astrocyte signaling is central to the dynamic control of brain microcirculation.* Nat Neurosci, 2003. **6**(1): p. 43-50.
65. Rieckmann, P. and B. Engelhardt, *Building up the blood-brain barrier.* Nat Med, 2003. **9**(7): p. 828-9.

66. Simard, M., et al., *Signaling at the gliovascular interface.* J Neurosci, 2003. **23**(27): p. 9254-62.
67. Dronne, M.A., et al., *Role of astrocytes in grey matter during stroke: a modelling approach.* Brain Res, 2007. **1138**: p. 231-42.
68. Siegel, G.J.A., R.W.; Brady, S.T.; Price, D.L., *Basic Neurochemistry: Molecular, Cellular and Medical Aspects; seventh edition*. 2006, Amsterdam - Boston - Heidelberg - London - New York - Oxford - Paris - San Diego - San Francisco - Singapore - Sydney - Tokyo: Elsevier Academic Press.
69. Haseloff, R.F., et al., *In search of the astrocytic factor(s) modulating blood-brain barrier functions in brain capillary endothelial cells in vitro.* Cell Mol Neurobiol, 2005. **25**(1): p. 25-39.
70. Janzer, R.C. and M.C. Raff, *Astrocytes induce blood-brain barrier properties in endothelial cells.* Nature, 1987. **325**(6101): p. 253-7.
71. Hayashi, Y., et al., *Induction of various blood-brain barrier properties in non-neural endothelial cells by close apposition to co-cultured astrocytes.* Glia, 1997. **19**(1): p. 13-26.
72. Joo, F., *Endothelial cells of the brain and other organ systems: some similarities and differences.* Prog Neurobiol, 1996. **48**(3): p. 255-73.
73. Chishty, M., et al., *Glial induction of blood-brain barrier-like L-system amino acid transport in the ECV304 cell line.* Glia, 2002. **39**(2): p. 99-104.
74. Regina, A., et al., *Factor(s) released by glucose-deprived astrocytes enhance glucose transporter expression and activity in rat brain endothelial cells.* Biochim Biophys Acta, 2001. **1540**(3): p. 233-42.
75. Lee, S.W., et al., *SSeCKS regulates angiogenesis and tight junction formation in blood-brain barrier.* Nat Med, 2003. **9**(7): p. 900-6.
76. Sumi, N., et al., *Lipopolysaccharide-activated microglia induce dysfunction of the blood-brain barrier in rat microvascular endothelial cells co-cultured with microglia.* Cell Mol Neurobiol. **30**(2): p. 247-53.
77. Haorah, J., et al., *Oxidative stress activates protein tyrosine kinase and matrix metalloproteinases leading to blood-brain barrier dysfunction.* J Neurochem, 2007. **101**(2): p. 566-76.
78. Lim, J.C., et al., *Neural precursor cell influences on blood-brain barrier characteristics in rat brain endothelial cells.* Brain Res, 2007. **1159**: p. 67-76.
79. Sanchez del Pino, M.M., D.R. Peterson, and R.A. Hawkins, *Neutral amino acid transport characterization of isolated luminal and abluminal membranes of the blood-brain barrier.* J Biol Chem, 1995. **270**(25): p. 14913-8.
80. Terasaki, T., et al., *New approaches to in vitro models of blood-brain barrier drug transport.* Drug Discov Today, 2003. **8**(20): p. 944-54.
81. Cucullo, L., et al., *Immortalized human brain endothelial cells and flow-based vascular modeling: a marriage of convenience for rational neurovascular studies.* J Cereb Blood Flow Metab, 2008. **28**(2): p. 312-28.
82. Sanchez del Pino, M.M., R.A. Hawkins, and D.R. Peterson, *Neutral amino acid transport by the blood-brain barrier. Membrane vesicle studies.* J Biol Chem, 1992. **267**(36): p. 25951-7.
83. Boado, R.J., et al., *Selective expression of the large neutral amino acid transporter at the blood-brain barrier.* Proc Natl Acad Sci U S A, 1999. **96**(21): p. 12079-84.
84. Cecchelli, R., et al., *Modelling of the blood-brain barrier in drug discovery and development.* Nat Rev Drug Discov, 2007. **6**(8): p. 650-61.
85. Smith, Q.R., *A review of blood-brain barrier transport techniques.* Methods Mol Med, 2003. **89**: p. 193-208.

86. Hargreaves, K.M. and W.M. Pardridge, *Neutral amino acid transport at the human blood-brain barrier.* J Biol Chem, 1988. **263**(36): p. 19392-7.
87. Roberts, L.M., et al., *Subcellular localization of transporters along the rat blood-brain barrier and blood-cerebral-spinal fluid barrier by in vivo biotinylation.* Neuroscience, 2008. **155**(2): p. 423-38.
88. Audus, K.L., et al., *The use of cultured epithelial and endothelial cells for drug transport and metabolism studies.* Pharm Res, 1990. **7**(5): p. 435-51.
89. Gumbleton, M. and K.L. Audus, *Progress and limitations in the use of in vitro cell cultures to serve as a permeability screen for the blood-brain barrier.* J Pharm Sci, 2001. **90**(11): p. 1681-98.
90. Youdim, K.A., A. Avdeef, and N.J. Abbott, *In vitro trans-monolayer permeability calculations: often forgotten assumptions.* Drug Discov Today, 2003. **8**(21): p. 997-1003.
91. Hertz, L., *Intercellular metabolic compartmentation in the brain: past, present and future.* Neurochem Int, 2004. **45**(2-3): p. 285-96.
92. Dienel, G.A. and N.F. Cruz, *Neighborly interactions of metabolically-activated astrocytes in vivo.* Neurochem Int, 2003. **43**(4-5): p. 339-54.
93. Smith, Q.R., *The blood-brain barrier and the regulation of amino acid uptake and availability to brain.* Adv Exp Med Biol, 1991. **291**: p. 55-71.
94. Tessari, P. and G. Garibotto, *Interorgan amino acid exchange.* Curr Opin Clin Nutr Metab Care, 2000. **3**(1): p. 51-7.
95. Wu, G., *Amino acids: metabolism, functions, and nutrition.* Amino Acids, 2009. **37**(1): p. 1-17.
96. Fuchs, S.A., et al., *D-amino acids in the central nervous system in health and disease.* Mol Genet Metab, 2005. **85**(3): p. 168-80.
97. Brosnan, J.T., *Interorgan amino acid transport and its regulation.* J Nutr, 2003. **133**(6 Suppl 1): p. 2068S-2072S.
98. Albrecht, J., et al., *Glutamine in the central nervous system: function and dysfunction.* Front Biosci, 2007. **12**: p. 332-43.
99. Hussein, M.A., et al., *Daily fluctuation of plasma amino acid levels in adult men: effect of dietary tryptophan intake and distribution of meals.* J Nutr, 1971. **101**(1): p. 61-9.
100. Yudkoff, M., et al., *Brain amino acid metabolism and ketosis.* J Neurosci Res, 2001. **66**(2): p. 272-81.
101. Banos, G., et al., *Inhibition of entry of some amino acids into the brain, with observations on mental retardation in the aminoacidurias.* Psychol Med, 1974. **4**(3): p. 262-9.
102. www.benbest.com/science/anatmind/anatmd10.html, h.
103. Connors, B.W., *Synaptic transmission in the nervous system.*, in *Medical Physiology: a cellular and molecular approach.*, W.F.B. Boron, E.L., Editor. 2005, Elsevier Saunders: Philadelphia. p. 295-323.
104. Magistretti, P.J. and L. Pellerin, *Cellular mechanisms of brain energy metabolism and their relevance to functional brain imaging.* Philos Trans R Soc Lond B Biol Sci, 1999. **354**(1387): p. 1155-63.
105. Yudkoff, M., et al., *Brain amino acid requirements and toxicity: the example of leucine.* J Nutr, 2005. **135**(6 Suppl): p. 1531S-8S.
106. Mackenzie, B. and J.D. Erickson, *Sodium-coupled neutral amino acid (System N/A) transporters of the SLC38 gene family.* Pflugers Arch, 2004. **447**(5): p. 784-95.
107. Chaudhry, F.A., et al., *Coupled and uncoupled proton movement by amino acid transport system N.* EMBO J, 2001. **20**(24): p. 7041-51.

108. Palmada, M. and J.J. Centelles, *Excitatory amino acid neurotransmission. Pathways for metabolism, storage and reuptake of glutamate in brain.* Front Biosci, 1998. **3**: p. d701-18.
109. Ransom, B.R., *The neuronal microenvironment*, in *Medical physiology: a cellular and molecular approach; 2nd ed.*, W.F.B. Boron, E. L., Editor. 2009, Saunders Elsevier. p. 306.
110. Rocha, J.C. and F. Martel, *Large neutral amino acids supplementation in phenylketonuric patients.* J Inherit Metab Dis, 2009. **32**(4): p. 472-80.
111. Felig, P., *Amino acid metabolism in man.* Annu Rev Biochem, 1975. **44**: p. 933-55.
112. Hutson, S.M., E. Lieth, and K.F. LaNoue, *Function of leucine in excitatory neurotransmitter metabolism in the central nervous system.* J Nutr, 2001. **131**(3): p. 846S-850S.
113. Fernstrom, J.D., *Branched-chain amino acids and brain function.* J Nutr, 2005. **135**(6 Suppl): p. 1539S-46S.
114. Westergren, I., et al., *Concentrations of amino acids in extracellular fluid after opening of the blood-brain barrier by intracarotid infusion of protamine sulfate.* J Neurochem, 1994. **62**(1): p. 159-65.
115. Lerma, J., et al., *In vivo determination of extracellular concentration of amino acids in the rat hippocampus. A method based on brain dialysis and computerized analysis.* Brain Res, 1986. **384**(1): p. 145-55.
116. Segal, M.B., *Extracellular and cerebrospinal fluids.* J Inherit Metab Dis, 1993. **16**(4): p. 617-38.
117. Pardridge, W.M., *Transport of small molecules through the blood-brain barrier: biology and methodology.* Advanced Drug Delivery Reviews, 1995. **15**(1-3): p. 5-36.
118. Roettger, V.R. and M.D. Goldfinger, *Evidence for amino acid concentration gradients between CSF and extracellular fluid.* Neurosci Lett, 1994. **178**(2): p. 197-200.
119. Pardridge, W.M., *Brain metabolism: a perspective from the blood-brain barrier.* Physiol Rev, 1983. **63**(4): p. 1481-535.
120. McGale, E.H., et al., *Studies of the inter-relationship between cerebrospinal fluid and plasma amino acid concentrations in normal individuals.* J Neurochem, 1977. **29**(2): p. 291-7.
121. Lajtha, A., *Transport as control mechanism of cerebral metabolite levels.* Prog Brain Res, 1968. **29**: p. 201-18.
122. Cynober, L.A., *Plasma amino acid levels with a note on membrane transport: characteristics, regulation, and metabolic significance.* Nutrition, 2002. **18**(9): p. 761-6.
123. Kahler, S.G. and M.C. Fahey, *Metabolic disorders and mental retardation.* Am J Med Genet C Semin Med Genet, 2003. **117C**(1): p. 31-41.
124. Tetsuka, K., et al., *The l-isomer-selective transport of aspartic acid is mediated by ASCT2 at the blood-brain barrier.* J Neurochem, 2003. **87**(4): p. 891-901.
125. http://www.bioparadigms.org/slc/menu.asp.
126. Hyde, R., P.M. Taylor, and H.S. Hundal, *Amino acid transporters: roles in amino acid sensing and signalling in animal cells.* Biochem J, 2003. **373**(Pt 1): p. 1-18.
127. Parra, L.A., et al., *The orphan transporter Rxt1/NTT4 (SLC6A17) functions as a synaptic vesicle amino acid transporter selective for proline, glycine, leucine, and alanine.* Mol Pharmacol, 2008. **74**(6): p. 1521-32.
128. Singer, D., et al., *Orphan transporter SLC6A18 is renal neutral amino acid transporter B0AT3.* J Biol Chem, 2009. **284**(30): p. 19953-60.
129. Bohmer, C., et al., *Characterization of mouse amino acid transporter B0AT1 (slc6a19).* Biochem J, 2005. **389**(Pt 3): p. 745-51.

130. Broer, S., *Amino acid transport across mammalian intestinal and renal epithelia.* Physiol Rev, 2008. **88**(1): p. 249-86.
131. Verrey, F., et al., *New glycoprotein-associated amino acid transporters.* J Membr Biol, 1999. **172**(3): p. 181-92.
132. Babu, E., et al., *Identification of a novel system L amino acid transporter structurally distinct from heterodimeric amino acid transporters.* J Biol Chem, 2003. **278**(44): p. 43838-45.
133. Bodoy, S., et al., *Identification of LAT4, a novel amino acid transporter with system L activity.* J Biol Chem, 2005. **280**(12): p. 12002-11.
134. Ramadan, T., et al., *Basolateral aromatic amino acid transporter TAT1 (Slc16a10) functions as an efflux pathway.* J Cell Physiol, 2006. **206**(3): p. 771-9.
135. Battistin, L., A. Grynbaum, and A. Lajtha, *The uptake of various amino acids by the mouse brain in vivo.* Brain Res, 1971. **29**(1): p. 85-99.
136. Ueno, M., *Mechanisms of the penetration of blood-borne substances into the brain.* Curr Neuropharmacol, 2009. **7**(2): p. 142-9.
137. Hediger, M.A., et al., *The ABCs of solute carriers: physiological, pathological and therapeutic implications of human membrane transport proteinsIntroduction.* Pflugers Arch, 2004. **447**(5): p. 465-8.
138. Verrey, F., *System L: heteromeric exchangers of large, neutral amino acids involved in directional transport.* Pflugers Arch, 2003. **445**(5): p. 529-33.
139. Uldry, M. and B. Thorens, *The SLC2 family of facilitated hexose and polyol transporters.* Pflugers Arch, 2004. **447**(5): p. 480-9.
140. Simpson, I.A., et al., *Glucose transporter asymmetries in the bovine blood-brain barrier.* J Biol Chem, 2001. **276**(16): p. 12725-9.
141. Farrell, C.L. and W.M. Pardridge, *Blood-brain barrier glucose transporter is asymmetrically distributed on brain capillary endothelial lumenal and ablumenal membranes: an electron microscopic immunogold study.* Proc Natl Acad Sci U S A, 1991. **88**(13): p. 5779-83.
142. Broer, S., *Adaptation of plasma membrane amino acid transport mechanisms to physiological demands.* Pflugers Arch, 2002. **444**(4): p. 457-66.
143. Broer, S. and N. Brookes, *Transfer of glutamine between astrocytes and neurons.* J Neurochem, 2001. **77**(3): p. 705-19.
144. Meier, C., et al., *Activation of system L heterodimeric amino acid exchangers by intracellular substrates.* EMBO J, 2002. **21**(4): p. 580-9.
145. Christensen, H.N., *Implications of the cellular transport step for amino acid metabolism.* Nutr Rev, 1977. **35**(6): p. 129-33.
146. Ohtsuki, S., *New aspects of the blood-brain barrier transporters; its physiological roles in the central nervous system.* Biol Pharm Bull, 2004. **27**(10): p. 1489-96.
147. Kanai, Y., et al., *Expression cloning and characterization of a transporter for large neutral amino acids activated by the heavy chain of 4F2 antigen (CD98).* J Biol Chem, 1998. **273**(37): p. 23629-32.
148. Mastroberardino, L., et al., *Amino-acid transport by heterodimers of 4F2hc/CD98 and members of a permease family.* Nature, 1998. **395**(6699): p. 288-91.
149. Kageyama, T., et al., *Distribution of the 4F2 light chain, LAT1, in the mouse brain.* Neuroreport, 2000. **11**(17): p. 3663-6.
150. Matsuo, H., et al., *Expression of a system L neutral amino acid transporter at the blood-brain barrier.* Neuroreport, 2000. **11**(16): p. 3507-11.
151. Palacin, M. and Y. Kanai, *The ancillary proteins of HATs: SLC3 family of amino acid transporters.* Pflugers Arch, 2004. **447**(5): p. 490-4.
152. James, J.H. and J.E. Fischer, *Transport of neutral amino acids at the blood-brain barrier.* Pharmacology, 1981. **22**(1): p. 1-7.

153. Cangiano, C., et al., *Brain microvessels take up large neutral amino acids in exchange for glutamine. Cooperative role of Na+-dependent and Na+-independent systems.* J Biol Chem, 1983. **258**(14): p. 8949-54.
154. Sanchez del Pino, M.M., R.A. Hawkins, and D.R. Peterson, *Biochemical discrimination between luminal and abluminal enzyme and transport activities of the blood-brain barrier.* J Biol Chem, 1995. **270**(25): p. 14907-12.
155. Tamai, I., et al., *Na(+)- and Cl(-)-dependent transport of taurine at the blood-brain barrier.* Biochem Pharmacol, 1995. **50**(11): p. 1783-93.
156. O'Kane, R.L., et al., *Na(+)-dependent glutamate transporters (EAAT1, EAAT2, and EAAT3) of the blood-brain barrier. A mechanism for glutamate removal.* J Biol Chem, 1999. **274**(45): p. 31891-5.
157. Takanaga, H., et al., *ATA2 is predominantly expressed as system A at the blood-brain barrier and acts as brain-to-blood efflux transport for L-proline.* Mol Pharmacol, 2002. **61**(6): p. 1289-96.
158. Czeredys, M., et al., *A polarized localization of amino acid/carnitine transporter B(0,+) (ATB(0,+)) in the blood-brain barrier.* Biochem Biophys Res Commun, 2008. **376**(2): p. 267-70.
159. Ohtsuki, S. and T. Terasaki, *Contribution of carrier-mediated transport systems to the blood-brain barrier as a supporting and protecting interface for the brain; importance for CNS drug discovery and development.* Pharm Res, 2007. **24**(9): p. 1745-58.
160. Melone, M., et al., *Localization of the glutamine transporter SNAT1 in rat cerebral cortex and neighboring structures, with a note on its localization in human cortex.* Cereb Cortex, 2004. **14**(5): p. 562-74.
161. Palii, S.S., H. Chen, and M.S. Kilberg, *Transcriptional control of the human sodium-coupled neutral amino acid transporter system A gene by amino acid availability is mediated by an intronic element.* J Biol Chem, 2004. **279**(5): p. 3463-71.
162. Boulland, J.L., et al., *Cell-specific expression of the glutamine transporter SN1 suggests differences in dependence on the glutamine cycle.* Eur J Neurosci, 2002. **15**(10): p. 1615-31.
163. Boulland, J.L., et al., *Highly differential expression of SN1, a bidirectional glutamine transporter, in astroglia and endothelium in the developing rat brain.* Glia, 2003. **41**(3): p. 260-75.
164. Busque, S.M., *The role and regulation of the Slc38a3 (SNAT3) glutamine transporter in the mouse.* Ph.D. thesis, University of Zurich, Faculty of Science, 2009.
165. Hawkins, R.A., et al., *Pyroglutamate stimulates Na+ -dependent glutamate transport across the blood-brain barrier.* FEBS Lett, 2006. **580**(18): p. 4382-6.
166. Garcia, C.M., et al., *Endothelial cell-astrocyte interactions and TGF beta are required for induction of blood-neural barrier properties.* Brain Res Dev Brain Res, 2004. **152**(1): p. 25-38.
167. Meister, A. and M.E. Anderson, *Glutathione.* Annu Rev Biochem, 1983. **52**: p. 711-60.
168. Sweiry, J.H., et al., *A role for gamma-glutamyl transpeptidase and the amino acid transport system xc- in cystine transport by a human pancreatic duct cell line.* J Physiol, 1995. **485 (Pt 1)**: p. 167-77.
169. Bell, J.G., et al., *Studies on the putative role of gamma-glutamyl transpeptidase in intestinal transport of amino acids in Atlantic salmon.* J Comp Physiol B, 1987. **157**(2): p. 161-9.
170. Vina, J.R., et al., *Gamma-glutamyl-amino acids as signals for the hormonal regulation of amino acid uptake by the mammary gland of the lactating rat.* Biol Neonate, 1985. **48**(4): p. 250-6.

171. Vina, J.R., et al., *Role of the gamma-glutamyl cycle in the regulation of amino acid translocation.* Am J Physiol, 1989. **257**(6 Pt 1): p. E916-22.
172. van der Werf, P. and A. Meister, *The metabolic formation and utilization of 5-oxo-L-proline (L-pyroglutamate, L-pyrrolidone carboxylate).* Adv Enzymol Relat Areas Mol Biol, 1975. **43**: p. 519-56.
173. Kamiie, J., et al., *Quantitative atlas of membrane transporter proteins: development and application of a highly sensitive simultaneous LC/MS/MS method combined with novel in-silico peptide selection criteria.* Pharm Res, 2008. **25**(6): p. 1469-83.
174. Lein, E.S., et al., *Genome-wide atlas of gene expression in the adult mouse brain.* Nature, 2007. **445**(7124): p. 168-76.
175. Dahlin, A., et al., *Expression profiling of the solute carrier gene family in the mouse brain.* J Pharmacol Exp Ther, 2009. **329**(2): p. 558-70.
176. Calabria, A.R. and E.V. Shusta, *A genomic comparison of in vivo and in vitro brain microvascular endothelial cells.* J Cereb Blood Flow Metab, 2008. **28**(1): p. 135-48.
177. Enerson, B.E. and L.R. Drewes, *The rat blood-brain barrier transcriptome.* J Cereb Blood Flow Metab, 2006. **26**(7): p. 959-73.
178. Agarwal, N., E.S. Lippmann, and E.V. Shusta, *Identification and expression profiling of blood-brain barrier membrane proteins.* J Neurochem. **112**(3): p. 625-35.
179. Lu, Q., et al., *Analysis of mouse brain microvascular endothelium using immuno-laser capture microdissection coupled to a hybrid linear ion trap with Fourier transform-mass spectrometry proteomics platform.* Electrophoresis, 2008. **29**(12): p. 2689-95.
180. Gonzalez-Gonzalez, I.M., et al., *Immunohistochemical localization of the amino acid transporter SNAT2 in the rat brain.* Neuroscience, 2005. **130**(1): p. 61-73.
181. Hori, S., et al., *Functional expression of rat ABCG2 on the luminal side of brain capillaries and its enhancement by astrocyte-derived soluble factor(s).* J Neurochem, 2004. **90**(3): p. 526-36.
182. Stewart, P.A., R. Beliveau, and K.A. Rogers, *Cellular localization of P-glycoprotein in brain versus gonadal capillaries.* J Histochem Cytochem, 1996. **44**(7): p. 679-85.
183. Hundal, H.S. and P.M. Taylor, *Amino acid transceptors: gate keepers of nutrient exchange and regulators of nutrient signaling.* Am J Physiol Endocrinol Metab, 2009. **296**(4): p. E603-13.
184. deFeudis, F.V., *The brain is protected from nutrient excess.* Life Sci, 1987. **40**(1): p. 1-9.
185. Manoonkitiwongsa, P.S., et al., *Luminal localization of blood-brain barrier sodium, potassium adenosine triphosphatase is dependent on fixation.* J Histochem Cytochem, 2000. **48**(6): p. 859-65.
186. Soontornmalai, A., M.L. Vlaming, and J.M. Fritschy, *Differential, strain-specific cellular and subcellular distribution of multidrug transporters in murine choroid plexus and blood-brain barrier.* Neuroscience, 2006. **138**(1): p. 159-69.
187. Warabi, E., et al., *Effect on endothelial cell gene expression of shear stress, oxygen concentration, and low-density lipoprotein as studied by a novel flow cell culture system.* Free Radic Biol Med, 2004. **37**(5): p. 682-94.
188. Terasaki, T. and S. Ohtsuki, *Brain-to-blood transporters for endogenous substrates and xenobiotics at the blood-brain barrier: an overview of biology and methodology.* NeuroRx, 2005. **2**(1): p. 63-72.
189. Huang, Q.F., et al., *Role of excitatory amino acids in regulation of rat pial microvasculature.* Am J Physiol, 1994. **266**(1 Pt 2): p. R158-63.

8. Curriculum Vitae.

Name	RUDERISCH, Nadine
Date of birth	July 31st 1981 in Schramberg, Germany
Nationality	German
E-Mail	nruderi@physiol.uzh.ch

Education

05/2006-present	**Ph.D. thesis, University of Zurich**, Switzerland in the group of Prof. Dr. Verrey, Institute of Physiology Topic: *Amino acid transport across the murine blood-brain barrier*.
09/2001-04/2006	**Studies of Biology, University of Rostock**, Germany Diploma thesis in the group of Prof. Dr. Lindequist, Institute of Pharmaceutical Biology, Ernst-Moritz-Arndt University, Greifswald Topic: *Investigation of the influence of several stress inducers on the metabolite spectrum of a selected marine fungus.*
08/1988-06/2001	High School Diploma („Abitur"), Luise-Büchner Schule, Freudenstadt, Germany

Publications

Ruderisch N*, Lyck R*, Moll AG, Steiner O, Cohen CD, Engelhardt B, Makrides V*, Verrey F* (2009) Culture-induced changes in blood-brain barrier transcriptome: implications for amino-acid transporters in vivo. *Journal of Cerebral Blood Flow & Metabolism* (2009) **29**, 1491-1502; published online 3 June 2009. PMID: 19491922. **shared authorship*

Fellowships, Prizes and Awards

2009	Travel Grant from 36th International Congress of Physiological Sciences (IUPS), Kyoto, Japan
2008	Poster Prize at the Gordon Research Conference „Barriers of the CNS", Tilton (NH), USA
2001	Kofrányi-Prize in "Nutrition Science with Chemistry"

9. Acknowledgements.

François Verrey, who gave me the opportunity to work in his laboratory where I had the chance to work with great collaborators in- and outside of Zurich, the possibility and support to present my data at conferences around the world, and for the support and fruitful scientific discussions.

The other members of my thesis committee, Britta Engelhardt and Jean-Marc Fritschy, for the interesting discussions and support during and after thesis meetings, and the PhD program in Integrative Molecular Medicine (imMed) for organizing interesting courses and retreats.

Vicky for advise, support and help during the last years.

A special thank also to Ruth Lyck, Daniela Virgintino, and Clemens Cohen from whom I could learn a lot, not just scientifically. I also want to thank all the people from the TKI in Bern, from Bari, and from the Institute of Pharmacology in Zurich, for their support.

Special thanks also to the past, present and future "J-floor" people from all over the world, spicing up lab (and office) work. This life-long lasting and irreversibly connected community has too many members to list, but even if not written down personally, just feel thanked!

Nicola, Brigitte, Simone, Tamara, Katja, Lajos, Nikolay, Sabrina, Steffi, Maja, Chiara, Olga, Soline, Andi, Lisa, Silvia, Markus, Beni, and Martin, thanks for your help, discussions and for simply being around. Thomas and Lorenz, the (blond) boys, who spiced up lab meetings and office life. Tina who was always a great friend and mental support station. The time we shared I don't want to miss. Raphael (one of his countless synonyms) who was a great friend from the beginning on. Dustin, the greatest lab and office partner you can wish for. Marta, thanks for teaching me the important parts of Italian language. I wish we would have met much earlier. Luca, the Swiss, who had always an ear and a smile. Alok for his impact to German language. Nicole and Marija from "the others" for help, support, advise, discussions, and encouraging words. Ilka who was always there for me. Toni for mathematical (and non-mathematical) discussions. Maria, the great sole of the J-floor, who keeps all together and has always two ears and at least three hearts for everyone.

Special thanks to my parents, without whom I could not have gotten this far, to my family and friends, who always supported me. Änni for simply being who you are. I thank you for everything you always do for me and hope that THE long-term aim will become true.

10. Addendum.

1. Introduction.

EAAT3 (SLC1A1), also known as EAAC1, is a member of the SLC1 family of high-affinity glutamate and neutral amino acid transporters. It has been classified as a system X^-_{AG} transporter (see Table 4 in section3.5.4), co-transporting one molecule L-glutamate or D/L-aspartate with three sodium and one proton ions, in exchange for one potassium ion [I]. Due to this stoichiometry it has been calculated that EAAT3 is able to accumulate glutamate $5x10^6$-fold inside cells [I], helping to keep the glutamate concentration in brain ISF low (see section 3.5.3.1 and 3.5.4). Besides substrate uptake, EAAT3 has been shown to also mediate facilitative substrate exchange, with uptake being the predominant transport mechanism [I].
EAAT3 is reported to be highly expressed in brain neurons, in the intestine, kidney, liver and heart [II]. In brain, EAAT3 is predominantly expressed in neurons of hippocampus, cerebral cortex, olfactory bulb, striatum, superior colliculus and thalamus [I]. More precise, in glutamatergic and GABAergic neurons, in cholinergic and aminergic neurons [III], but also in a few astrocytic processes in both gray and white matter and in glial cells other than astrocytes [IV], as well as in ependymal cells and in epithelial cells of the choroid plexus of the four ventricles [V]. EAAT3 is reported to be concentrated in the neuronal cell bodies (somata) and dendrites, avoiding the nerve terminals [VI]. Exceptions are presynaptic GABAergic terminals, where EAAT3 uptake of glutamate contributes to re-synthesis of GABA [VII]. In the kidney, EAAT3 is expressed in the apical membrane of the proximal tubules [I], and the concentration of EAAT3 in the kidneys is reported to be higher than in the hippocampus [V]. EAAT3 shows a developmental expression profile with early expression but rather low expression level in the adult [III]. In addition, EAAT3 is present mainly in the intracellular compartment and only for about 20% at the plasma membrane [III].
It is suggested that the primary physiological function of EAAT3 is to regulate the excitability of postsynaptic neurons [IV] and to protect neurons from excitotoxicity by maintaining the extracellular glutamate concentration low [I] (see Table 2). One condition where glutamate excitotoxicity can be observed is during ischemia, where the insufficient energy supply leads to reversal of the electrochemical gradients and therefore to glutamate release due to reversal of the transport [I]. The detection of EAAT3 protein in all parts of the neurons suggests a function other than solely the uptake of synaptically released glutamate [III]. The role of

EAAT3 in clearing glutamate from the extracellular space is thought to be quantitatively minor compared to the role glial glutamate transporters (EAAT1/SLC1A3, EAAT2/SLC1A2) are playing [VII]. Another suggested function of EAAT3 is the protection of neurons against oxidative stress [III]. This is based on the finding that neuronal cysteine uptake occurs mainly via EAAT3, and that dysfunction leads to impaired glutathione homeostasis and neurodegeneration [VII].

Slc1a1$^{-/-}$ mice develop dicarboxylic aminoaciduria, but no neurodegeneration in a period of over one year [VIII]. However, they have reduced neuronal glutathione levels and, with aging, develop brain atrophy and behavioural changes [VII].

Recently, expression of Eaat3 mRNA in cultured and non-cultured primary MBMECs was examined by us and shown to be lower than the expression of 4F2hc (Slc3a2; see section 3.6.1), Lat1 (Slc7a5; see section 3.6.1), Snat2 (Slc38a2), and Snat5 (Slc38a5), but to be higher than the one of Snat3 (Slc38a3; see section 3.6.1.3.2) and Snat1 (Slc38a1; see section 3.6.1.3.1) [IX]. Surprisingly, the "neuronal" transporter Eaat3 turned out to be the most prominent expressed Slc1 member. Furthermore, Eaat3 expression in cultured and non-cultured primary MBMECs was found to be higher than in whole brain, suggesting an accumulation of Eaat3 in endothelial cells of the brain vasculature. This stands in contrast to the view that Eaat3 is mainly expressed in neurons, shown to be involved in the glutamate-glutamine cycle (see section 3.5.3.1). On the other hand, functional data using isolated bovine brain endothelial membrane vesicles supported the view of Eaat3 being expressed at the BBB, with restricted localization to the abluminal membrane and suggested based on inhibitor studies a relative activity of 1:3:6 for EAAT1:EAAT2:EAAT3, respectively [X].

In the following section an overview on data generated during this PhD thesis is presented, supporting the view that Eaat3 is an important player in the BBB endothelial cell transportome and that it may be expressed on both membranes, luminal and abluminal.

2. Material and Methods.

Animals. Female C57BL/6JOlaHsd mice were purchased from Harlan Laboratories B.V. (Venray, Netherlands). The mice were housed in standard conditions and fed a standard diet. All animal procedures were according to the Swiss Animal Welfare laws and approved by the Kantonales Veterinäramt Zurich (permission number 119/2008).

Primary cortical neurons. Primary cortical neurons isolated from embryonic rat brains were a kind gift of Thomas Grampp and Corinne Sidler, Institute of Pharmacology and Toxicology, University of Zurich.

Antibodies. The following commercial available primary antibodies were used: mouse-anti-glucose transporter 1 (Glut1) monoclonal ab40084 (dilution 1:200; Abcam, Cambridge, MA, USA); chicken-anti-laminin polyclonal ab14055 (1:200; Abcam); rabbit-anti-EAAC1 polyclonal cat#EAAC11-A (1:200; Alpha Diagnostic, San Antonio, TX, USA); mouse-anti-microtubule associated protein-2 (MAP2) monoclonal MAB3418 (Millipore); mouse-anti-P-glycoprotein, mAB (C219) monoclonal ALX-801-002-C100 (1:100; Alexis Biochemicals, San Diego, CA, USA); guinea-pig-anti-Mrp1 polyclonal (1:3,000; kind gift of Jean-Marc Fritschy, Institute of Pharmacology and Toxicology, University of Zurich [XI]); mouse-anti-β-actin monoclonal A5316 (Sigma-Aldrich, Steinheim, Germany). The following secondary antibodies were used as indicated: Alexa Fluor® 488 goat anti-rabbit IgG (1:400/500; Invitrogen, Eugene, OR, USA); Alexa Fluor® 568 goat anti-guinea pig IgG (1:500; Invitrogen); DyLight™ 549 goat anti-chicken IgY (1:400; Jackson ImmunoResearch, Suffolk, UK); Cy5 goat anti-mouse IgG (1:400/500; Jackson ImmunoResearch); Texas Red®-X phalloidin T7471 (1:500; Invitrogen); PO-PRO™-1 iodide (1:400; Invitrogen); ECL™ anti-mouse IgG, HRP linked whole antibody (1:10,000; GE Healthcare, Little Chalfont Buckinghamshire, UK); anti-rabbit IgG (Fc) AP conjugate (1:5,000; Promega, Madison, WI, USA); Streptavidin-HRP conjugate (1:20,000; GE Healthcare).

Immunohistochemistry. The cellular localization of EAAT3 was assessed by quadruple immunofluorescence staining with antibodies against specific markers, raised in different species (specifications and dilutions described under “antibodies”). Five-week-old female mice were anesthetized and perfused through the left cardiac ventricle with PBS, pH 7.4, followed by 2% paraformaldehyde (PFA), 0.2% glutaraldehyde in PBS. The brains were harvested and postfixed by immersion in fixative for 2 h at 4 °C. After an overnight washing step in PBS at 4 °C, they were stored in 0.02% PFA at 4 °C. For staining, 20-µm thick tissue sections were prepared using a vibrating microtome (Leica VT 1000S; Leica, Heerbrugg, Switzerland). Fluorescence triple immunolabeling was carried out on free-floating sections at RT. The sections were immersed and gently agitated in 0.5% Triton X (TX)-100 in PBS for 30 min, followed by 10 min blocking (Protein Block Serum-Free; Dako, Carpinteria, CA, USA), and incubation with the primary antibodies overnight at 4 °C. Sections were then

incubated for 45 min with the appropriate secondary antibodies, followed by 10 min in 4% PFA. Between each step, sections were washed three times 5 min in PBS. Nuclear counterstaining was performed by incubation in PO-PRO™-1 iodide (Invitrogen). The sections were transferred onto Polysine™ slides (Kindler, Freiburg, Germany), drained, and mounted in Vectashield mounting medium (Vector Laboratories) for imaging.

Alternatively, unperfused brains were rapidly excised and frozen with powdered dry ice. Sections were cut at 14 µm with a cryostat (Leica CM 1850, Leica Microsystems, Nussloch, Germany), mounted onto Polysine™ slides, fixed in ice-cold methanol for 10 min at -20 °C and rinsed with PBS. Sections were then immersed in 0.1% SDS for 5 min, rinsed in PBS and blocked in blocking solution (PBS containing 2% BSA, 0.02% TX-100) for 15 min at RT. After, sections were incubated overnight at 4 °C with a mixture of primary antibodies raised in different species and diluted in blocking solution. They were then rinsed with PBS and incubated with the corresponding fluorophore-conjugated secondary antibodies diluted in blocking solution for 1 h at RT. Sections were washed three times for 10 min with PBS and coverslipped in Dako® fluorescent mounting medium (Dako Corporation, Carpinteria, CA, USA).

Control experiments were always performed by omitting the primary antibodies. The secondary antibodies alone did not produce any significant staining in all tissues tested (data not shown).

Immunocytochemistry. Cultures of rat primary neuronal cells were washed with PBS, fixed with PFA (3%) in PBS containing 0.2% TX-100 for 15 min at RT. The cells were rinsed in PBS and further processed as described under “immunohistochemistry on methanol-fixed mouse brain tissue sections”.

Control experiments were performed by omitting the primary antibodies. The secondary antibodies alone did not produce any significant staining in all tissues tested (data not shown).

Data analysis. The sections were viewed with a Leica TCS SP2 confocal laser scanning microscope (Leica) using a 63x objective lens (numerical aperture of 1.4, pinhole set to 1.0 airy unit) with different zoom factors (5-8). A sequential scan procedure was applied during image acquisition of the fluorophores and acquisition parameters were adjusted to use the full dynamic range of the photomultipliers. Typically, stacks of four to eight images (512 x 512 pixels) were taken and analysed at 122-nm intervals through the z-axis of the section. Representative images from the examined samples were chosen for figure editing. Digital

images were processed using the software Imaris® (Imarisx64 7.1.1, Bitplane, Zurich, Switzerland) and Huygens (CMLE algorithm; SVI, The Netherlands).

Surface biotinylation of rat primary neurons. Experiments were performed as described elsewhere [XII], with minor modifications. Shortly, neurons have been isolated and plated in 12-well plates. After eleven days, cells were placed on ice at 4 °C, washed in HBSS (14025-050; Invitrogen / Gibco, Paisley, UK), and incubated in HBSS containing 1 mg/mL EZ-Link® sulfo-NHS-LC-biotin (Thermo Scientific, Rockford, IL, USA) or, as control, in HBSS without biotin, for 30 min. After a washing step in TBS (20 mM Tris pH 7.4, 150 mM NaCl) containing 5 mg/mL glycine, cells were extracted by adding 100 µL TE (5 mM Tris pH 8, 5 mM EDTA) containing 1% NP40 and 1x PIC and placed for 30 min on a shaker. Cells were scraped, the wells washed with 100 µL TE, and the extracts of two wells pooled. After storing the samples at -80 °C, the extract has been drawn several times through a 23-gauge needle, followed by heating at 70 °C for 5 min, and drawing several times through a 27g-needle. The resulting extract has been centrifuged (13,000xg, 10 min, RT), and the supernatant (= T) separated from the pellet. The next steps included to add IP (100 mM NaCl, 20 mM sodium borate, 15 mM EDTA, pH 8.5) containing 1.2% TX-100 and 1x PIC) (300 uL) to the supernatant, to wash the Neutravidin-agarose twice in IP containing 0.17% SDS, 0.85% TX-100, to add the diluted extract to the washed agarose resin (Thermo Scientific, 60 µl / sample), and to incubate with mixing overnight at 4 °C. After centrifugation (1,000xg, 2 min, 4 °C), the supernatant containing non-biotinylated proteins was collected (= U) and the Neutravidin-agarose resin washed four times with chilled IP containing 0.1% SDS, 0.5% TX-100, and once with chilled PBS. The biotinylated proteins were released by adding 60 µL 4x Laemmli buffer / DTT to the Neutravidin-agarose, then incubated with mixing 2 h at 4 °C, followed by 5 min at 90 °C, and the supernatant (= B) collected by centrifugation (1,000xg, 2 min, RT).

Total membrane protein and whole cell lysate preparation. Whole nonperfused mouse brains and kidneys were snap frozen in N_2(l), sonicated with 200 µL RB (200 mM mannitol, 80 mM HEPES, 41 mM KOH, pH 7.5, along with 1x Complete EDTA-free proteinase inhibitor cocktail (Roche Diagnostics, Mannheim, Germany)) on ice, and subsequently centrifuged for 20 min at 2,000 rpm at 4 °C. The supernatant was aspirated (= whole cell lysate), centrifuged (41,000 rpm, 1 h, 4 °C), the resulting supernatant containing cytosolic proteins was removed, whereas the pellet (= total membrane proteins) was resuspended in RB and sonicated briefly

to evenly distribute proteins. Protein concentration was measured using the BioRad D_C protein assay (Bio-Rad Laboratories, Hercules, CA, USA). Samples were mixed with Laemmli sample buffer, and further processed as described under "Gel electrophoresis and Western blot analysis".

In vivo biotinylation. In vivo biotinylation experiments were performed as described elsewhere [XII, XIII], with minor modifications, using perfusion conditions to maintain the integrity of the BBB. Shortly, five-week-old female mice were anesthetized, the abdominal aorta clamped, and the brain perfused through the left cardiac ventricle with PBS (Invitrogen, Paisley, UK) containing 10% (wt/vol) dextran 40 (Sigma-Aldrich). Drainage was from the right atrium. Perfusion of the prewarmed solutions (38 °C) was performed applying a pressure of 100 mm Hg. Immediately afterwards, the mice were perfused with 5 ml of freshly prepared biotinylation solution, containing 3 mg/ml EZ-Link® sulfo-NHS-LC-biotin (Thermo Scientific) in PBS and 10% (wt/vol) dextran 40. The biotinylation solution was incubated for 5 min at RT, before non-reacted biotin was quenched by perfusion with 50 mM Tris in PBS, 10% (wt/vol) dextran 40. As non-exogenously biotinylated negative control, mice were perfused as above with PBS and 10% (wt/vol) dextran 40, but without added biotin. Immediately after perfusion, the brain was excised, the cerebellum removed, and the brain snap-frozen in liquid nitrogen.

Protein extraction and purification of biotinylated proteins. Experiments were performed as described elsewhere [XII, XIII], with minor modifications. Shortly, perfused brains were resuspended in lysis buffer (2% SDS, 50 mM Tris, 10 mM EDTA, Complete EDTA-free proteinase inhibitor cocktail (Roche Diagnostics) in PBS; pH 6.8; 25 mg brain per ml of lysis buffer) and homogenised using an disperser (Polytron PT 2100, Kinematica AG, Littau, Switzerland). Homogenates were sonicated (Labsonic 1510, B. Braun, Bender + Hobun, Zurich, Switzerland), incubated at 95 °C for 20 min and centrifuged at 17,000g for 20 min at 25 °C. Total protein concentration was determined using the BCA™ protein assay (Thermo Scientific). Neutravidin-agarose resin (Thermo Scientific, 500 µl / sample) was washed three times in buffer A (1% Nonidet P-40 and 0.1% SDS in PBS) and once in lysis buffer. 15 mg of total protein extract (total protein lysate) were added to the washed resin, and incubated with mixing for 2 h at RT. The supernatant containing non-biotinylated proteins was collected (unbound protein fraction) and the Neutravidin-agarose resin washed four times with buffer A and two times with buffer B (0.1% Nonidet P-40 and 1 M NaCl in PBS). The biotinylated

proteins were released by resuspending the Neutravidin-agarose in solution C (2% SDS, 30 mM biotin (Sigma-Aldrich), 50 mM phosphate, 100 mM NaCl, 6 M urea, 2 M thiourea; pH ~12) [XIV], incubated 15 min at RT, followed by 15 min at 96 °C, and the supernatant collected. The supernatant containing biotinylated proteins was concentrated with trichloroacetic acid (final concentration 10%) overnight at 4 °C, the precipitated proteins washed four times with ice-cold ethanol, lyophilized, and resuspended in Laemmli buffer (Neutravidin-agarose-bound protein fraction).

Gel electrophoresis and Western blot analysis. For SDS polyacrylamide gel electrophoresis (SDS-PAGE) fractionation, 25% of the total Neutravidin-agarose-bound protein fraction from mouse brains with and without *in vivo* biotinylation vs. 20 µg of the corresponding unbound protein fraction and total protein lysate, were analysed by Western blotting. Samples from independently perfused and processed mouse brains were isolated and analysed in at least triplicate. Samples were reduced by heating at 95 °C for 5 min in Laemmli buffer and fractionated on a 7.5 or 8.5% SDS-PAGE. For immunoblotting, proteins were transferred electrophoretically from unstained gels to PVDF membranes (Immobilon-P; Millipore, Bedford, MA, USA). After being blocked with Tris-buffered saline supplemented with 2% Topblock^{TM} powder (VWR, Dietikon, Switzerland) and 0.1% TX-100 for 2 h at RT, the blots were incubated with the primary antibodies overnight at 4 °C. All primary antibodies were used at a 1:500 dilution, except β-actin (1:5,000). After being washed, blots were incubated with the corresponding secondary antibody for 1 h at RT. Antibody binding was detected with Immobilon^{TM} Western Chemiluminescent HRP or AP Substrate (Millipore, Billerica, MA, USA). Chemiluminescence was detected with a Fuji LAS-4000 camera (Bucher Biotec, Basel, Switzerland). The same membrane first used to detect Eaat3 was stripped, blocked, and re-probed with Streptavidin-HRP and β-actin.

Whole cell and total membrane preparations from mouse kidney and brain have been diluted in Laemmli buffer (25-100 µg protein) and further processed as described.

Surface biotinylated neuronal membrane proteins (total fraction obtained), as well as the corresponding non-biotinylated and total protein lysates (20 µg each), were analysed by Western blot as described.

3. Results.

3.1 Characterization of the antibody against Eaat3 (Eaac1; Slc1a1) used.

The antibody directed against a C-terminal antigen of EAAT3 was previously successfully used in several publications (see manufacturer's data sheet). Also the experiences in the laboratory of C.A. Wagner, Institute of Physiology, University of Zurich, have been positive (personal communication). Therefore we have chosen to use this antibody to test the expression and localization of Eaat3 in the mouse endothelial cells comprising the BBB.

First, by performing Western blot analysis using total kidney and brain lysates and kidney membrane preparation, we could detect one band of the expected size in all samples tested (~69 kDa, according to the manufacturer) (see Figure I). Furthermore, the signal was dependent on the amount of protein loaded and of the antibody dilution used. The signal intensity in the kidney membrane preparation was higher than in the kidney total lysate, and in both cases higher than in the total brain protein lysate.

Figure I: Expression of Eaat3 in mouse kidney and brain samples.

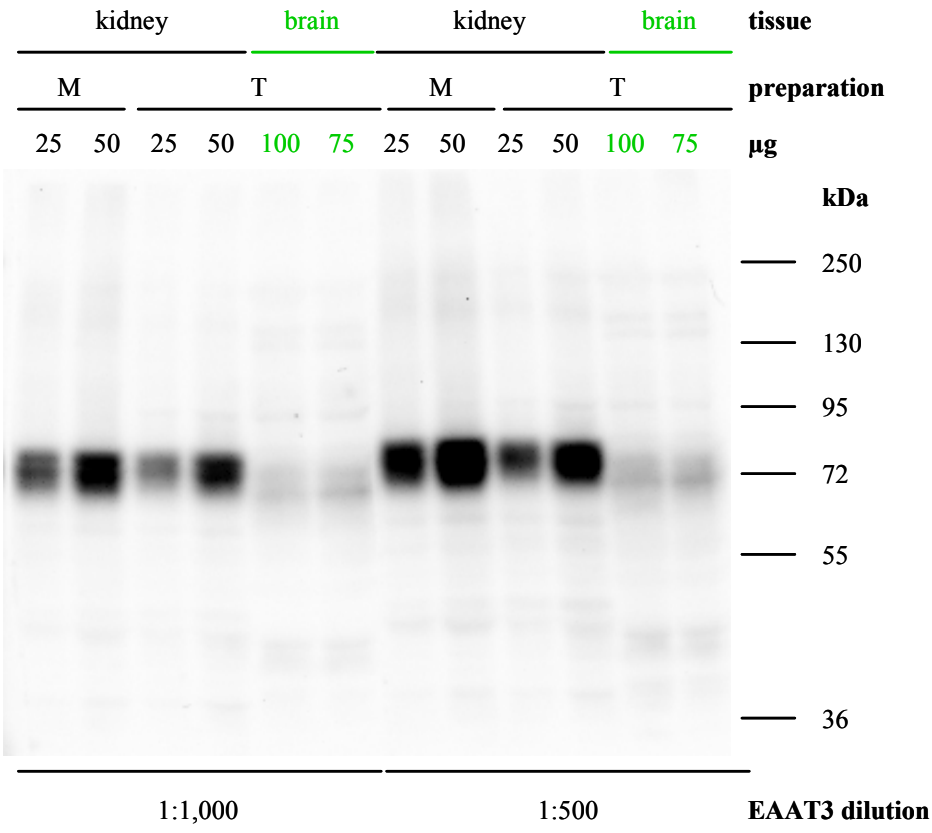

Western blot analysis of total protein and membrane fractions of mouse kidney and brain. Different protein concentrations (25/50/75/100 µg) have been loaded on a gel, SDS-PAGE performed, transferred to a PVDF membrane, and subsequently stained for Eaat3 using different antibody concentrations (1:500/1,000). A band of expected size (~69 kDa) could be detected in all cases. Eaat3 expression in brain is low, lower than in kidney. M, total membrane preparation; T, whole cell preparation. *Picture can be found under 160208_SNAT1_EAAT3_010.*

In brain, Eaat3 has been described to be mainly expressed in neurons, in all their parts of the neurons. Therefore, immunocytochemistry on primary cortical neurons has been performed (see Figure II). The signal of Eaat3 showed the expected cellular distribution excluding the nuclear region, and a colocalization with the neuronal marker Map2. The Eaat3 staining pattern shown is consistent with more than one neuronal cell stained (see also nuclear staining, Figure II) and with the cells being grown in different planes.

Figure II: Localization of Eaat3 in cortical neurons.

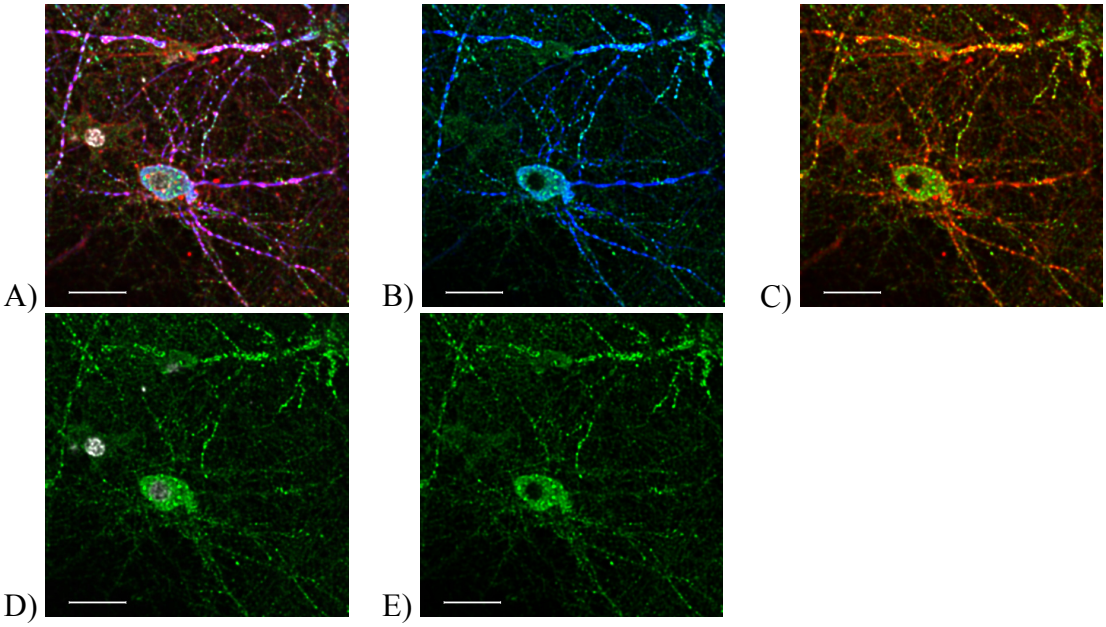

Immunocytochemistry on PFA fixed rat cortical neurons. **A)** Staining for Eaat3 (green), nucleus (white), Map2 (blue), and phalloidin (red). Map2 (microtubule associated protein) is an established neuronal marker, phalloidin binds to F-actin; **B)** Colocalization of Map2 (blue) with Eaat3 (green); **C)** Staining for Eaat3 (green) and phalloidin (red); **D)** Staining for Eaat3 (green) and nucleus (white); **E)** Eaat3 (green) staining alone, showing the reported broad distribution of Eaat3 in the whole neuronal body and possibly intracellular storage vesicles. Scale bar = 5 µm. *Pictures can be found under neurons_151009_Eaat3_series011.*

The specificity of the antibody was further tested by surface biotinylation of primary cultures of cortical neurons. After subsequent purification of the exogenously labeled proteins, Western blot analysis of the different fractions obtained during the purification procedure has been performed (total protein lysate, biotinylated proteins captured by Neutravidin and proteins of the total lysate not binding to Neutravidin) (see Figure III). The staining for Eaat3 showed a band of the expected size (see Figure I) in all fractions, with low expression in the Neutravidin-bound fraction of exogenously biotinylated samples. In the control without exogenously biotinylation, the Eaat3 signal was below the detection limit in the Neutravidin-bound protein fraction, like expected.

Figure III: Expression of Eaat3 on the membrane of surface biotinylated cortical neurons.

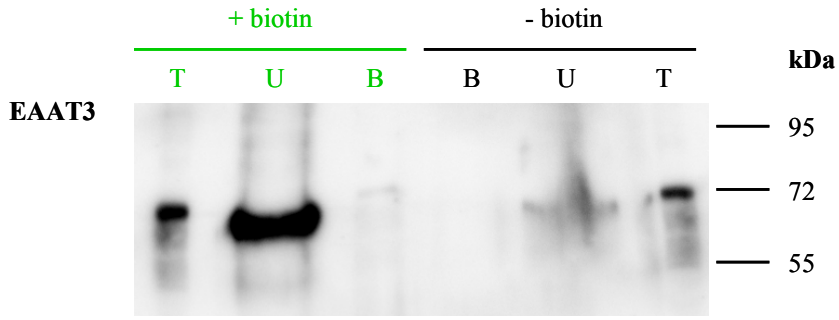

Western blot analysis of surface biotinylated rat cortical neurons. Fractions in different stages of purification show expression of Eaat3 (~69 kDa), with highest expression in the exogenously biotinylated protein fractions. Control experiments without added biotin show a less strong signal. The results suggest a detectable amount of Eaat3 being expressed at the membrane of cortical neurons. T, total protein (non- and biotinylated proteins); U, Neutravidin-unbound, non-biotinylated proteins; B, Neutravidin-bound, biotinylated proteins. *Pictures can be found under WB from 211009_221009_gel 3_Eaat3_30 sec; WB from 211009_221009_gel 3_biotin_30 sec.*

3.2 Expression of Eaat3 on both membranes of mouse brain vascular endothelial cells.

The high expression of Eaat3 mRNA in MBMECs [IX] suggested an important role of this transporter on the protein level. Therefore, two independent approaches have been chosen to examine the expression and localization of Eaat3 in the mouse brain *in vivo*.

First, immunohistochemistry on fresh frozen, methanol fixed, tissue and tissue fixed by perfusion with a PFA/glutaraldehyde mixture has been performed. By using the former method, the signal for Eaat3 was shown to colocalize with that of the ABC-transporter Mdr1, a known marker of the luminal membrane of the BBB (see Figure IVC). On the abluminal membrane the signal for Eaat3 was shown to colocalize with the one of the abluminal expressed ABC-transporter Mrp1 (see Figure IVD). To improve the tissue quality, perfusion and fixation of the mouse brain with PFA/glutaraldehyde was chosen. By staining of in this way processed tissue sections the expected localization of the sodium-dependent transporter Eaat3 on the abluminal membrane of brain vascular endothelial cells could be shown by colocalizing the signal with the one of Glut1 (see Figure VC/G/K). The endothelial cell specific staining was further shown by localizing it luminally relative to the signal of the extracellular matrix marker laminin (see Figure VD/K). Also the luminal localization of Eaat3 could again be shown by colocalizing it with the luminal signal of Glut1 staining (see Figure VC/G). The obtained staining pattern highlights the possibility of Eaat3 being localized in intracellular storages like shown in neurons.

Figure IV: Localization of Eaat3 on the luminal and abluminal membrane of BBB endothelial cells.

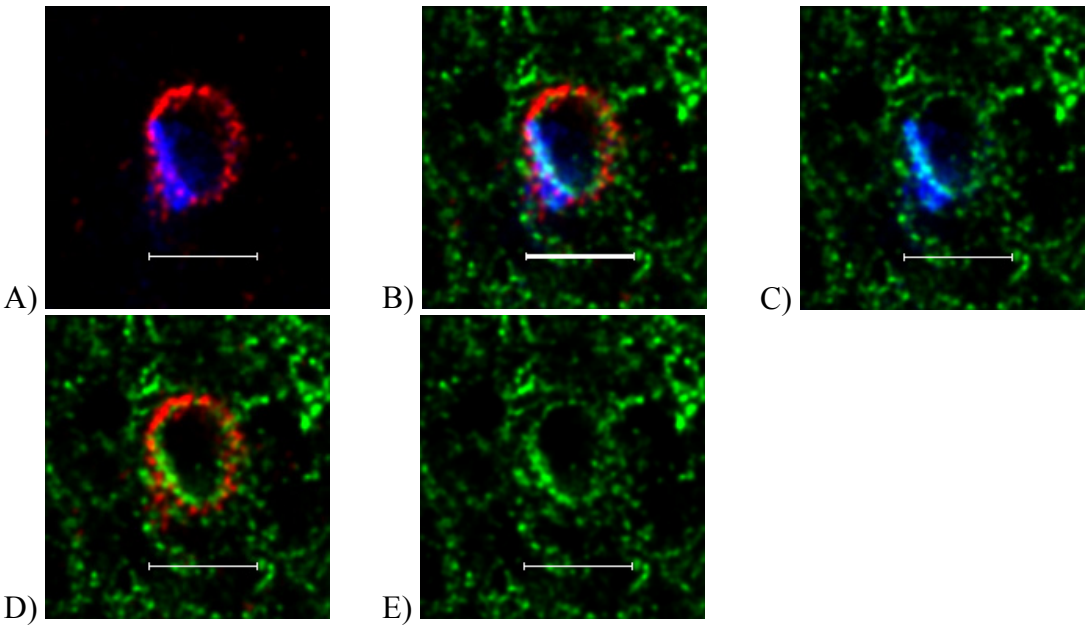

Immunohistochemistry on methanol fixed mouse brain tissue sections. **A)** Colocalization of Mdr1 (blue) with Mrp1 (red). Like previously shown [XI], the ABC transporter Mdr1 can be used as marker for the luminal membrane of BBB endothelial cells, Mrp1 as marker for the abluminal membrane; **B)** Colocalization of Eaat3 (green) with Mdr1 (blue) and Mrp1 (red); **C)** Colocalization of Eaat3 (green) with Mdr1 (blue) on the luminal membrane of BBB endothelial cells; **D)** The luminal signal of Eaat3 (green) does not colocalize with the abluminal signal of Mrp1 (red); **E)** Eaat3 (green) staining alone. Scale bar = 5 µm. *Pictures can be found under slide31_63x_Series014.*

Figure V: Localization of Eaat3 on the luminal and abluminal membrane of BBB endothelial cells.

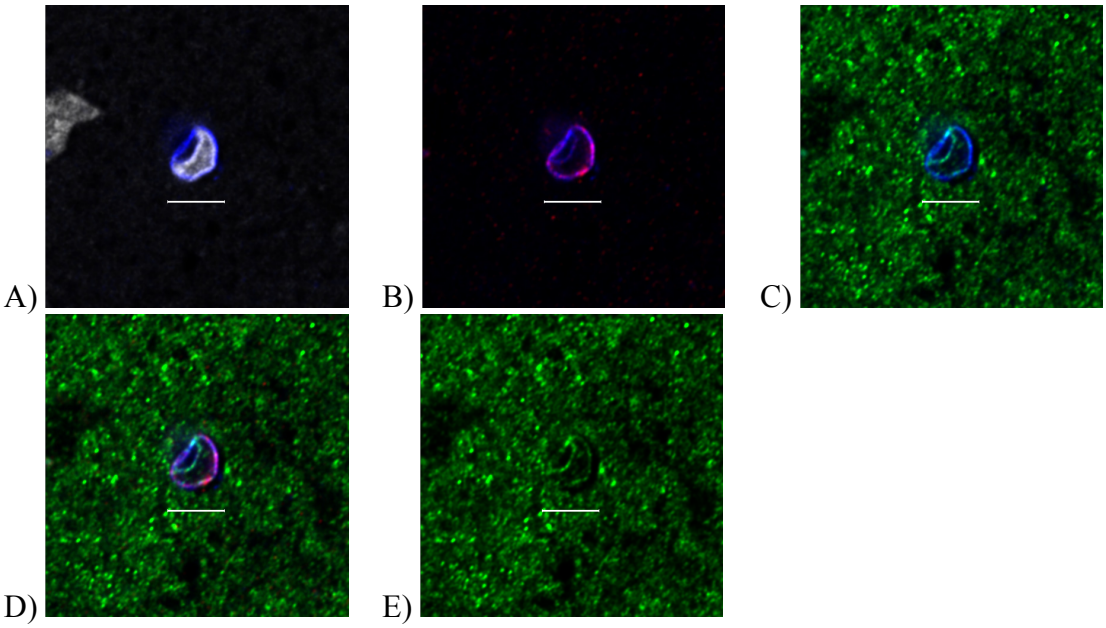

Figure legend see next page.

Figure V: Localization of Eaat3 on the luminal and abluminal membrane of BBB endothelial cells.

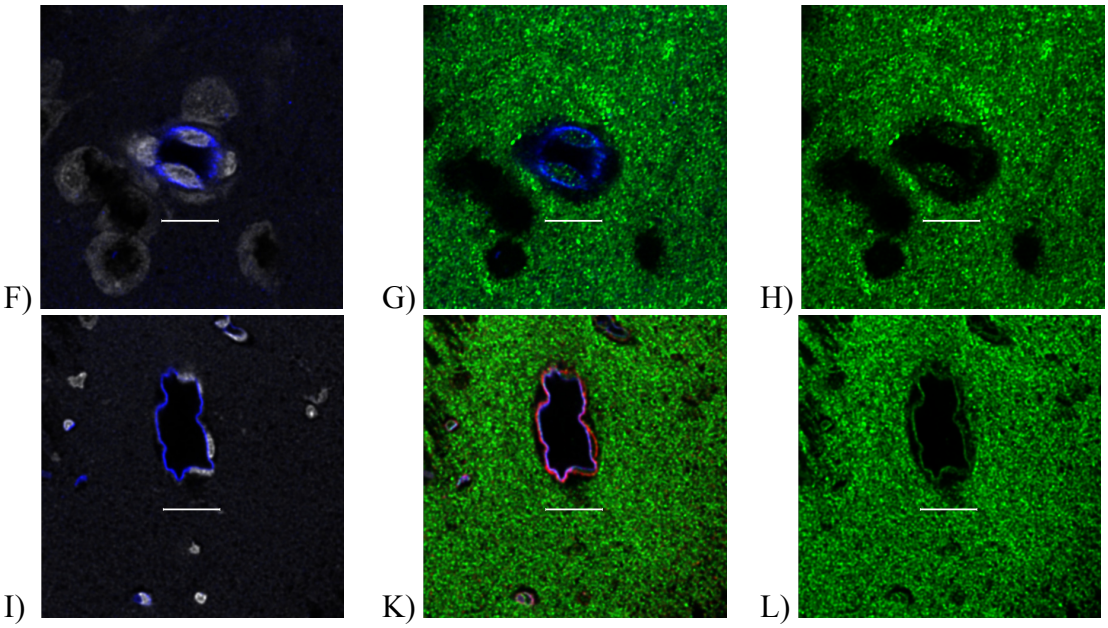

Immunohistochemistry on PFA/glutaraldehyde fixed mouse brain tissue sections. **A)**, **F)** and **I)** Colocalization of Glut1 (blue) and nucleus (white), showing that Glut1 can be used as marker for the luminal and abluminal membrane of BBB endothelial cells; **B)** Staining for Glut1 (blue) and laminin (red), showing that Glut1 staining is specific for BBB endothelial cells and does not stain brain parenchymal cells; **C)** and **G)** Colocalization of Eaat3 (green) and Glut1 (blue) on the luminal and abluminal membrane of BBB endothelial cells; **D)** and **K)** Eaat3 (green), Glut1 (blue), and laminin (red) staining, showing Eaat3 being localized to vascular endothelial cells, as well as to brain parenchymal cells; **E)**, **H)** and **L)** Eaat3 (green) staining alone, highlighting the possibility of Eaat3 being localized in intracellular storages like shown in neurons. **A)-E)** small cortical vessel with one nucleus; **F)-H)** small cortical vessel with two nuclei; **I)-L)** bigger cortical vessel. Scale bar = 5 µm. *Pictures can be found under 270110_Snat1 etc_Eaat3_series 068; 270110_Snat1 etc_Eaat3_series 044; EAAT3_050110_slide2_series031.*

Second, to probe for proteins expressed at the luminal surface of the vasculature, the brains of anesthesized mice were perfused with the membrane-impermeable biotinylation reagent sulfo-NHS-LC-biotin. The total protein lysate (input) out of one mouse brain, containing both labeled luminal proteins and non-*in vivo* biotinylated proteins (unbound protein fraction), was purified using Neutravidin-coated agarose. As expected, by Western blot analysis a strong biotin signal of multiple diffuse bands was detected in the Neutravidin-agarose-bound protein fractions, absent or only weakly found in the total protein lysates and unbound protein fractions (see Figure VI). Further, consistent with a lack of intracellular protein labeling, β-actin was almost not detected in the Neutravidin-agarose-bound protein fractions, but was present in all other fractions (see Figure VI). Taken together, the data is consistent with the preservation of the BBB integrity during the *in vivo* biotinylation procedure and the restriction of the labeling by *in vivo* biotinylation to proteins expressed on the luminal cell surface of the vasculature. To probe for possible luminal localization of Eaat3, Western blot analysis of the different fractions obtained after *in vivo* biotinylation of the brain vascular lumen was performed. A weak band corresponding to the expected molecular weight of Eaat3 (~69 kDa)

was found in the Neutravidin-agarose-bound protein fraction from *in vivo* biotinylated mice and to a lesser extent in the corresponding fraction from the non-exogenously biotinylated negative control brains (see Figure VI).

Taken together, Eaat3 shows endothelial expression, that is suggested to be also on the luminal membrane of brain vascular endothelial cells comprising the BBB.

Figure VI: Possible expression of Eaat3 in the lumen of mouse brain vascular endothelial cells.

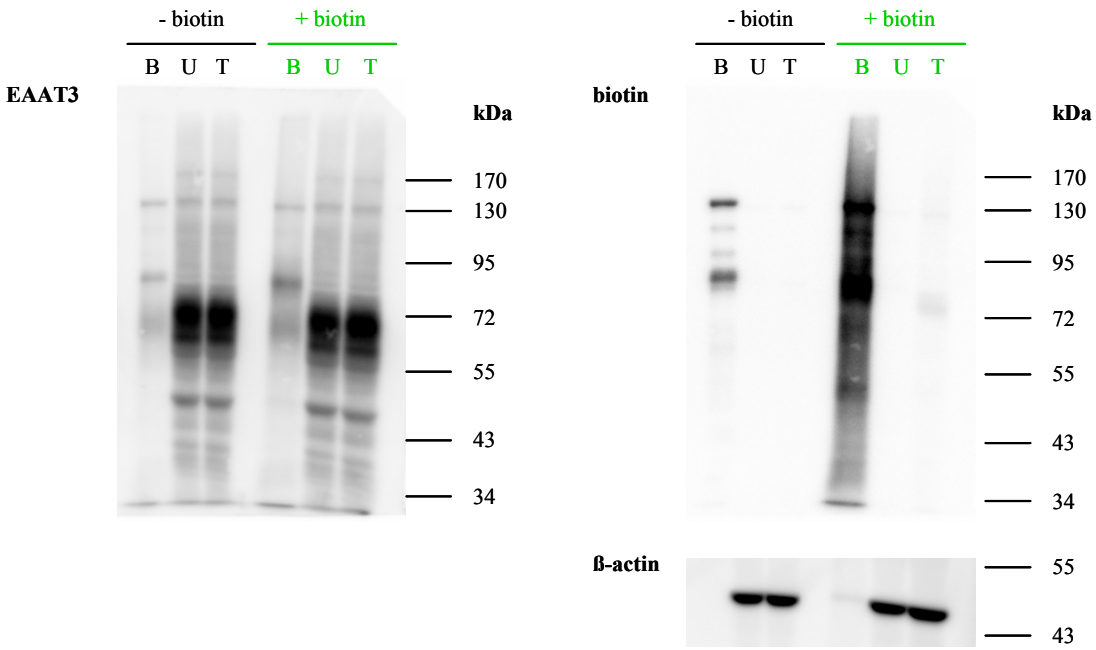

Western blot analysis of *in vivo* biotinylated mouse brain vascular endothelial cells. Different fractions obtained after exogenously biotinylating proteins expressed on the luminal membrane of brain vascular endothelial cells were loaded on a SDS-PAGE gel, transferred to a PVDF membrane and subsequently stained for Eaat3, biotin, and β-actin. In all fractions a signal for Eaat3 at the expected size could be detected. The signal in the exogenously biotinylated protein fraction was stronger than the one in the control without added biotin in the perfusion solution. The controls showing effective exogenously biotinylation (biotin) of the luminal membrane (β-actin) show the expected pattern. T, total protein (non- and biotinylated proteins; 20 µg loaded); U, Neutravidin-unbound, non-biotinylated proteins (20 µg); B, Neutravidin-bound, biotinylated proteins (25% of total fraction). *Pictures can be found under WB from 200110_210110_Eaat3_gel 3_30 sec; WB from 200110_220110_biotin_gel 3_30 sec; WB from 200110_220110_actin_gel 3_30 sec.*

4. Discussion.

The results on Eaat3 expression and localization presented in this thesis show the potential significance of this high-affinity glutamate transporter in the endothelial cells of the BBB. Eaat3 was shown to be highly expressed on mRNA level in MBMECs and not to be subject to culture-induced changes [IX]. The observed stable and high expression in non-cultured and primary cultured MBMECs and the expression below detection limit in the endothelial cell-line b.End5 points up the possibility that Eaat3 may play an important role in cell nutrition as well as in transendothelial transport *in vivo*.

Due to the proposed importance of Eaat3 in BBB endothelial cells, its expression and localization on the protein level was further studied. By using different methods, it appeared that Eaat3 localizes to both luminal and abluminal membranes of brain vascular endothelial cells along the vascular tree. This is analogous to the results presented in this thesis concerning the localization of Snat3, another sodium-dependent amino acid transporter unexpectedly found also at the luminal endothelial membrane (see section 5). These results are not compatible with the current hypothesis that sodium-dependent transporters are exclusively localized to the abluminal membrane, a hypothesis that is based on physiological considerations regarding the existing amino acid gradient between plasma and ISF / CSF (see section 3.5.4) and on functional *in vivo* and *in vitro* data (see sections 3.6.1.1/2 and literature cited therein).

One possible pitfall in studying the expression and localization of Eaat3 might be the specificity of antibodies used [VI]. The antibody used in the present study was raised against a C-terminal, cytoplasmic 14 amino acid long peptide, that is 100% identical in mouse, rat, rabbit, and human. Previously, it has been reported that only by using EAAT3 antibodies to C-terminal peptides strong and specific signals can be obtained [VI]. Its specificity can be assumed, also based on the expected labeling pattern obtained in different tissues and cell types (see Figure I and II), and under use of different methododical approaches (see Figure I and III). However, the proposed luminal localization of Eaat3 has nonetheless to be validated by a different, non-antibody based, method like for instance the analysis of the Neutravidin-captured surface protein fractions using mass spectrometry.

In the BBB endothelial cells, Eaat3 may play a role in the suggested intraendothelial glutamate-glutamine cycle (see section 3.5.3.1 and 6), and may be involved in clearing brain ISF and therefore in preventing glutamate excitotoxicity. In this context it is important to mention that, contrary to the rather low expression of EAAT3 in the brain (see Figure I), the

expression in brain vascular endothelial cells was shown to be the highest of all Slc1 members [IX], and that the relative activity of EAAT3 in bovine cerebral capillaries was reported to be higher than that of EAAT1/2 [X]. Therefore one can hypothesize that Eaat3 expressed at the abluminal membrane of brain vascular endothelial cells may play an important role in keeping the brain ISF glutamate concentration low. Furthermore, since BBB endothelial cells do express all system X^-_{AG} members together, and also system A and N members at high levels [IX], the requirements for an intraendothelial glutamate-glutamine cycle are given.

One should also consider the potential of Eaat3 as important site of regulation. Eaat3 in neurons has been shown to be expressed mainly intracellularly, similar to our observation in endothelial cells of the BBB (see Figure V), and to be rapidly trafficked to the membrane on demand. Another important role of Eaat3 is the transport of cysteine that may influence the endothelial glutathione homeostasis and suggests an important role of the BBB in the oxidative stress response protecting the brain from effects of low oxygen, radicals, and low energy. Especially luminal expressed Eaat3 may be important in this context if one considers that the vasculature represents a first barrier between circulation and brain parenchyma. Therefore, especially the luminal membrane may act as buffer, as metabolic and oxidative security system. The presence of Eaat3 at the luminal membrane may also suggest a participation of this transporter in brain nutrition and vascular reaction to brain events. Possibly, luminal expressed Eaat3 may be important to clear blood from the vasoconstrictors glutamate and aspartate to maintain cerebral blood flow (see section 6).

Further studies should include functional analysis of Eaat3 at the BBB and verify the proposed importance of this “neuronal” transporter at the BBB.

5. References.

[I] Kanai, Y. and Hediger M.A., *The glutamate/neutral amino acid transporter family SLC1: molecular, physiological and pharmacological aspects.* Pflugers Arch, 2004. **447**(5): p. 469-79.

[II] http://www.bioparadigms.org/slc/menu.asp.

[III] Nieoullon, A., et al., *The neuronal excitatory amino acid transporter EAAC1/EAAT3: does it represent a major actor at the brain excitatory synapse?*. J Neurochem, 2006. **98**(4): p. 1007-18.

[IV] Conti, F., et al., *EAAC1, a high-affinity glutamate transporter, is localized to astrocytes and gabaergic neurons besides pyramidal cells in the rat cerebral cortex.* Cereb Cortex, 1998. **8**(2): p. 108-16.

[V] Danbolt, N.C., *Glutamate uptake.* Prog Neurobiol, 2001. **65**(1): p. 1-105.

[VI] Holmseth, S., et al., *Specificity of antibodies: unexpected cross-reactivity of antibodies directed against the excitatory amino acid transporter 3 (EAAT3).* Neuroscience, 2005. **136**(3):p. 649-60.

[VII] Aoyama, K., et al., *Neuronal glutathione deficiency and age-dependent neurodegeneration in the EAAC1 deficient mouse.* Nat Neurosci, 2006. **9**(1): p. 119-26.

[VIII] Peghini, P., et al., *Glutamate transporter EAAC-1-deficient mice develop dicarboxylic aminoaciduria and behavioural abnormalities but no neurodegeneration.* EMBO J, 1997. **16**(13): p. 3822-32.

[IX] Lyck, R., et al., *Culture-induced changes in blood-brain barrier transcriptome: implications for amino-acid transporters in vivo.* J Cereb Blood Flow Metab, 2009. **29**(9): p. 1491-502.

[X] O`Kane, R.L., et al., *Na(+)-dependent glutamate transporters (EAAT1, EAAT2, and EAAT3) of the blood-brain barrier. A mechanism for glutamate removal.* J Biol Chem, 1999. **274**(45): p. 31891-5.

[XI] Soontornmalai, A., et al., *Differential, strain-specific cellular and subcellular distribution of multidrug transporters in murine choroid plexus and blood-brain barrier.* Neuroscience, 2006. **138**(1): p. 159-69.

[XII] Roberts, L.M., et al., *Subcellular localization of transporters along the rat blood-brain barrier and blood-cerebral-spinal fluid barrier by in vivo biotinylation.* Neuroscience, 2008. **155**(2): p. 423-38.

[XIII] Roesli, C., et al., *In vivo protein biotinylation and sample preparation for the proteomic identification of organ- and disease-specific antigens accessible from the vasculature.* Nat Protoc, 2006. **1**(1): p. 192-9.

[XIV] Rybak, J.N., et al., *Purification of biotinylated proteins on streptavidin resin: a protocol for quantitative elution.* Proteomics, 2004. **4**(8): p. 2296-9.

[XV] Masuoka, J., et al., *Complications in cell-surface labelling by biotinylation of Candida albicans due to avidin conjugate binding to cell-wall proteins.* Microbiology, 2002. **148**(Pt 4): p. 1073-9.

[XVI] Haugland, R.P. and You, W.W., *Coupling of antibodies with biotin.* Methods Mol Biol, 2008. **418**: p. 13-24.